



TECHNISCHE
UNIVERSITÄT
WIEN
Vienna | Austria

DISSERTATION

Timber-Steel Hybrid Beams for Multi-Storey Buildings

**ausgeführt zum Zwecke der Erlangung des akademischen Grades eines
Doktors der technischen Wissenschaften unter der Leitung von**

o. Univ. Prof. Dipl – Dipl. Ing. Wolfgang Winter

E259/2 - Abteilung Tragwerksplanung und Ingenieurholzbau

Institut für Architekturwissenschaften

und

Univ. Prof. Arch. Francisco Javier Estévez Cimadevila

Departamento de Tecnoloxía da Construcción

Universidade da Coruña

**eingereicht an der Technischen Universität Wien
Fakultät für Architektur und Raumplanung**

von

M. Arch. Felipe Riola Parada

Matrikelnummer 1128622

Goldschlagstraße 69/6/34, 1150 Wien

.....
Wien, im Dezember 2016

KURZFASSUNG

Die technischen Möglichkeiten für Holzgebäude sind in den letzten Jahren stark vorangeschritten. Die Entstehung neuartiger Holzprodukte und das steigende Umweltbewusstsein treiben die Entwicklung von Holzkonstruktionen stetig voran. Eine wesentliche Zielsetzung für die nähere Zukunft ist die Errichtung mehrgeschossiger Gebäude im städtischen Raum. Es gibt mittlerweile zahlreiche Forschungsprojekte auf dem Gebiet der Holz- und Holzverbundbauweise, die zunehmend an gebauten Beispielen Anwendung finden. Im Zuge vieler gegenwärtiger Projekte wird der Werkstoff Holz durch andere Materialien ergänzt, um bestimmte strukturelle Erfordernisse erfüllen oder hinsichtlich der Kosten wirtschaftlicher werden zu können.

Der zentrale Fokus dieser Arbeit liegt in der Betrachtung und Diskussion eines möglichen Potentials bei der Kombination von Stahl und Holz (siehe Kapitel 2). In Kapitel 3 werden bisherige Forschungsergebnisse zu diesem Thema zusammengefasst. Das Material wird entsprechend der kombinierten Nutzung von Holz und Stahl beschrieben. Die vorgeschlagenen Klassifikationen werden ausgehend von den strukturellen Leistungsmerkmalen der Stahlteile (passiv oder aktiv) und der geometrischen Anordnung vom Stahl eingeteilt. Das bauliche Ziel der Kombinationen von Stahl und Holzquerschnitten wurde für jeden einzelnen Fall näher bezeichnet (siehe 3.1). Besondere Aufmerksamkeit wurde der Kennzeichnung des Designs, der Konstruktion und der Umsetzung von ökonomischen Problemstellungen bei den vorgeschlagenen Lösungen gewidmet. Der praktische Erfolg von jeder Holz-Stahl-Kombination-Strategie ist in einer Liste reflektiert, wenn vorhanden auch in Form von gebauten Beispielen. Dieser gesamte Überblick und die damit verbundenen Analysen dienen zur Kennzeichnung und somit Berücksichtigung von wichtigen Konstruktionskennwerten, wenn Holz-Stahl-Trägerlösungen entworfen werden (siehe 3.5 und 3.6).

Unter Einsatz des erworbenen Wissens wurden Holz-Stahl-Hybridträger konstruiert, welche kaltgeformte Stahlprofile mit Holz kombinieren und so auch vorgeschlagen werden. Die Hybridlösung wurde basierend auf Kombinationen von den Elementen entwickelt, ohne Übertragung der horizontalen Scherkräfte zwischen den Stahl- und Holzkomponente. Zwei Vorschläge, eine symmetrische und eine im Querschnitt symmetrische Anordnung werden vorgeschlagen (siehe 4.3). Bedingungen, welche zu berücksichtigen sind und vorgegebene Ziele sind angeführt, sowie der beschriebene Entwicklungsprozess einer Querschnittskonstruktion für Einfeld-Balken (siehe 4.4. und 4.5). Die Besonderheiten der Querschnittsdimensionierung von statisch unbestimmten Systemen wurden ebenso analysiert und zugehörige Bemessungskriterien vergeben (siehe 4.8.)

Teile der bisher erwähnten theoretischen Arbeit wurden geprüft und getestet. Kurzzeitbelastungstests für die Holz-Stahl-Balken wurden durchgeführt (siehe Kapitel 5), ebenso ein Langzeitbelastungstest (siehe Kapitel 6).

In einer ersten Testreihe wurde die symmetrische Hybridanordnung, welche kaltgeformten Stahl verwendet, getestet und mit anderen möglichen und statisch ähnlichen Balken verglichen. Die Stahlkonstruktion, das Umsetzungsverfahren und die strukturelle Leistung wurden getestet und validiert. Eine totale Anzahl von 10 Hybridbalken mit unterschiedlichen Querschnittsanordnungen aber immer mit einer Spannweite von sechs Metern wurden gebaut und getestet (siehe 5.3). In einem zweiten Testdurchgang wurden nur kaltgeformte Stahlelemente für die hybriden asymmetrischen Anordnungen verwendet. Hybridbalken mit einer strukturellen/baulichen Tiefe von $L/17$ und $L/20$ wurden konstruiert, berechnet und getestet. Besondere Aufmerksamkeit wurde den Untersuchungen zum Einfluss von unterschiedlichen Unterstützungsbedingungen auf die strukturelle Leistung der Balken. Eine endgültige Anzahl von zwölf Hybridbalken mit einer Spannweite von sechs Metern und acht Metern wurden gebaut und getestet.

Eine Langzeitbelastungsprüfung wurde über einen Zeitraum von einem Jahr durchgeführt. Die Leistungsfähigkeit von zwei Balken wurde mit zwei Brett-schichtholzbalken verglichen. Der

Verhaltenstrend war sehr klar und die Vorteile der Hybridsysteme, wenn Langzeitverformungen bedeutend sind, konnte bestätigt werden (siehe Kapitel 6).

Eine Zusammenfassung der zukünftigen Richtungen für die Forschung wurde gemacht (siehe Kapitel 7). Teile der Bereiche wurden vorgeschlagen, teilweise schon studiert oder initiiert, mit dem Hintergrund, als Autor der Doktorarbeit, gleichzeitig auch dem Forschungsteam zugehörig zu sein.

Holz-Stahlstrukturelemente allgemein und im spezifischen die Balken, werden hier als eine Alternative für die Entwicklung von ganzheitlichen Konstruktionskonzepten präsentiert, bei einer Optimierung von beiden Materialien, beginnend beim strukturellen Niveau. Deren Entwicklung für die Anwendung in mehrgeschossigen architektonischen Lösungen ist das endgültige Ziel und Hauptanwendungsgebiet.

ABSTRACT

The technical possibilities for building with timber experienced a big advance in the last years. The development of new timber and timber-based products together with growing environmental concerns are pushing the research and study on timber construction. One objective is the construction of multi-storey buildings in urban environment. Urban timber and timber-based building proposals are emerging, as many research projects and built examples illustrate. Many present day projects propose the combined use of timber elements with other materials for specific structural purposes difficult or costly to fulfil with an only-timber solution.

In this work the potential of combining steel and timber in beams is identified and discussed (see chapter 2). A review of the studies carried out until now was compiled (see chapter 3). This material was summarized and classified depending on the timber-steel combination strategies used. The proposal of classification is based on the structural performance of the steel components (passive or active) and the steel geometrical arrangement. The structural purpose of combining the steel with the timber cross sections was identified for each case (see 3.1). Special attention was devoted to the identification of the design, construction, implementation or economical problems of the proposed solutions. The practical success of each timber-steel combination strategy is reflected in a list, when existing, of built examples. All this review and analysis was used for the identification of important design parameters to take into account when designing timber-steel beams solutions (see 3.5 and 3.6)

Using the knowledge gained a design of timber-steel hybrid beams combining cold-formed steel profiles with timber is proposed. The hybrid solution developed is based on the combination of the elements without the transmission of horizontal shear forces between the steel and timber components. Both a symmetrical and a asymmetrical cross-section arrangement are proposed (see 4.3). Conditions to take into account and objectives were stated and a cross-section design procedure developed for the case of single span beams (see 4.4 and 4.5). The particularities for the cross-section arrangement and application of these beams forming part of statically undetermined systems were also analysed and related design criteria given (see 4.8).

Part of the theoretical work mentioned until now was proofed and tested. Short term loading tests of the timber-steel beams were carried out (see chapter 5) as well as a long-term loading test (see chapter 6)

In a first testing series the hybrid symmetrical arrangement using cold-formed steel was tested and compared to other possible and statically equivalent beams. The steel design, assembly procedures and structural performance were tested and validated. A total of ten hybrid beams with different cross-section arrangements but always with a span of six metres were built and tested (see 5.3). In a second testing series only cold-formed steel elements were used for the hybrid asymmetrical arrangement. Hybrid beams with a structural depth of $L/17$ and $L/20$ were designed, calculated and tested. Special attention was paid to the study of the influence of different support conditions on the structural performance of the beams. A total of twelve hybrid beams with spans of six and eight metres were built and tested.

A long-term loading test was carried out for the duration of one year. The performance of two hybrid beams was compared to two only-glulam beams. The behavioural trend was very clear and the advantages of hybrid systems when long-term deflections are relevant could be confirmed (see chapter 6).

A summary of open future lines of research was made (see chapter 7). Part of the topics proposed were already partially studied or initiated, being the author of this doctoral thesis part of the researching teams.

Timber-steel structural elements in general and beams in particular are therefore presented as an alternative for developing a holistic construction concept making the most of the properties from both materials starting at the structural element level. Its optimization for their application in multi-storey architectural solutions is the final objective and main application field.

ACKNOWLEDGMENT

I gratefully acknowledge the supervisors of this doctoral thesis, Prof. Wolfgang Winter, from the Vienna University of Technology, and Prof. Javier Estévez Cimadevila, from the University of A Coruña, for all their ideas, advices, hours of discussion, criticism and support during the years that were spent on this work.

A very special mention deserves Dr. Kamyar Tavoussi, for all the intensive discussions and exchange of ideas we had, for his continuous input to the research project, his enthusiasm and, last but not least, his good mood and supporting attitude in any situation.

I would also like to thank all the colleagues that in any moment, and in very different ways, were involved around this project. Discussions, suggestions, proposals, help during the tests and many other inputs came from Andrew Bradley, Balazs Joo, Tamir Pixner, Hagop Shahakian, Matthias Rinnhofer, Christoph Radlherr and Atsuko Tani. Thanks also to Dr. Alireza Fadaei for answering so many questions.

Thanks to all my other colleagues, present and past ones, of the Institute of Structural Design and Timber Engineering of the Vienna University of Technology who were responsible of a friendly, collaborative and great work environment. Thanks to our secretary Alena Üblein for all the paper work and many other things, to Andrea Borska, Joachim Nackler, Aída Santana Sosa, Khaled Saleh Pascha, Baris Cokçan and Fabian Gasser. Thanks also to our student assistants Lara Bettinelli, Alex Müllner, Sladjana Petrusic and Thomas Sicay.

The tests described in this doctoral thesis were carried out at the testing facilities of the Camillo Sitte Lehranstalt in Vienna. I would like to thank Prof. Hans Baumgartner, director of the testing laboratory, for all his help, availability, knowledge and valuable suggestions.

A key role at the testing facilities was played by Mr. Franz Tanzberger, employee of the testing laboratory who assisted in the practical preparation of the tests and suggested many practical and fine solutions. Dankeschön, Franz!

I do not forget all the teachers, employees and numerous students from the Camillo Sitte Lehranstalt who assisted to the tests. Without their help and collaboration these would not be the same. Thanks to all of you.

The experimental work of this doctoral thesis was funded by the Austrian Sparkling Science National Research Programme. The author gratefully acknowledges the financial support provided by the Austrian Federal Ministry of Science, Research and Economy (BMFWF) project number SPA 04/107.

The first three years of work on this doctoral thesis (August 2011 – August 2014) were funded by a scholarship from the Grant Programme for Postgraduate Study Abroad from the Pedro Barrié de la Maza Foundation (A Coruña – Galicia), awarded to the author in the year 2010. The author gratefully acknowledges the financial support provided by the foundation, the trust of the selection committee and all the help and support received through the foundation employees.

This work is dedicated to my parents, family and friends, who accompanied and supported me in many different ways in Galicia and in Vienna during all these years.

TABLE OF CONTENTS

KURZFASSUNG	ii
ABSTRACT	iv
ACKNOWLEDGEMENT	v
1. INTRODUCTION: GLOBAL FRAME OF RESEARCH	
1.1 Research topic: building towards resource efficiency	2
1.1.1 Increasing the capacity of utilization of buildings	3
1.1.2 Reducing the resources used in and during building processes	3
1.1.3 Conclusions	4
2. THE POTENTIAL OF THE COMBINATION OF TIMBER AND STEEL	
2.1 Improving timber performance with steel	5
2.1.1 Physical properties	5
2.1.2 Mechanical properties	7
2.2 Improving steel performance with timber	11
2.2.1 Physical properties	11
2.2.2 Mechanical properties	12
2.2.3 Environmental and economical considerations	14
2.3 Compatibility of timber and steel: potential and risks	17
2.3.1 Physical properties	17
2.3.2 Technological considerations	18
2.4 The potential of the combination of timber and steel in beams from a structural performance point of view	19
3. STATE OF THE ART: TIMBER AND STEEL COMBINATION IN BEAMS	
3.1 Proposal of a systematic classification	20
3.2 Combinations with passive steel	22
3.2.1 Horizontal steel arrangements	22
3.2.2 Vertical steel arrangements	32
3.2.3 Combination of horizontal and vertical steel arrangements	50
3.3 Combinations with active steel	56
3.3.1 In grain direction: pre- and post-tensioning	56
3.3.2 Perpendicular to grain	64

3.4 Amount of existing research and number of built examples	66
3.5 Critics and lessons learned	68
3.6 Conclusions: Where is the potential?	70
3.7 Addendum: Timber-steel approaches in the research projects “8+” and “Das erdbebensichere Holzhaus”	71

4. TIMBER-STEEL HYBRID BEAMS

4.1 Introduction: the hybrid strategy	73
4.1.1 Terminology	73
4.2 The potential of the hybrid strategy: design conditions and objectives	76
4.2.1 Material combination towards resource efficiency	76
4.2.2 Reduction of costs	76
4.2.3 Reusability and recyclability	77
4.2.4 Structural performance	78
4.2.5 Reduction of variability	79
4.2.6 System strength	80
4.2.7 Self-fire protection	81
4.2.8 Allowable structural depth	81
4.3 Description of the proposed cross-sections	83
4.3.1 Cold formed steel technology	83
4.3.2 Cold formed steel production	85
4.3.3 Symmetrical arrangement	87
4.3.4 Asymmetrical arrangement	87
4.4 Cross-section design criteria	88
4.4.1 Basic structural concept	88
4.4.2 Structural depth allowable	90
4.4.3 Fire design strategy	90
4.4.4 Optimization of the mechanical performance. Elastic analysis	97
4.4.5 Total bending stiffness required	106
4.4.6 Timber-steel stiffness balance	106
4.4.7 Verification of the shear capacity	110
4.4.8 Influence of the long term performance for the cross-section optimization	112
4.5 Summary: Cross-section design in seven steps	122
4.6 Calculation of single span beams	123
4.6.1 Simplified methods for single span beams	123
4.6.2 Matrix based calculation model	123
4.6.3 Ultimate limit state verifications	124
4.6.4 Serviceability limit state verifications	124
4.7 Single span beams performance	125
4.7.1 Conclusions: structural performance, economical and ecological considerations	125
4.8 Statically undetermined systems performance	132
4.8.1 Performance of single span beams. Influence of shear flexibility	132
4.8.2 The performance of statically indeterminate systems. Influence of shear flexibility	133
4.8.3 Statically indeterminate systems performance	135
4.8.4 Conclusions	140

5. SHORT-TERM LOADING TESTS

5.1 Load definition and pre-dimensioning	141
5.2 Calculation of single span beams	142
5.2.1 Calculation of deflection, moment of inertia for steel and elastic modulus of timber	142
5.2.2 Effective width of flanges	143
5.3 First testing series	144
5.3.1 Specimens	144
5.3.2 Production, delivery and assembly	146
5.3.3 Test set-up, testing procedures and measuring techniques	148
5.3.4 Testing series A – Assessment of the global modulus of elasticity of glulam beams	151
5.3.5 Testing series B – Cross-sections and results	152
5.3.6 Testing series C – Cross-sections and results	154
5.3.7 Testing series D – Cross-sections and results	157
5.3.8 Testing series E– Cross-sections and results	161
5.3.9 Interpretation and conclusions	164
5.4 Second testing series	168
5.4.1 Specimens	168
5.4.2 Design and dimensioning	168
5.4.3 Production, delivery and assembly	169
5.4.4 Test set-up, testing procedures and measuring techniques	170
5.4.5 Load implementation and support conditions	172
5.4.6 Testing series G – Cross-sections and results	174
5.4.7 Testing series H – Cross-sections and results	178
5.4.8 Testing series I – Cross-sections and results	183
5.4.9 Testing series J– Cross-sections and results	186
5.4.10 Interpretation and conclusions	189
5.5 Global Conclusions – Short term loading tests	191

6. LONG-TERM LOADING TESTS: CREEPING

6.1 Introduction	197
6.2 Assessment following Eurocode 5	198
6.3 Objectives of the tests	199
6.4 Design criteria of specimens	200
6.5 Calculation of the desired stress level	202
6.6 Testing procedures	203
6.7 Results	209
6.8 Interpretation and conclusions - Long term loading tests	211

7. FUTURE LINES OF RESEARCH

7.1 Joint design, modelling and testing	216
7.2 Floor system design, modelling and testing	217
7.3 Frame design, modelling and optimization	217
7.4 Advanced fire design, modelling and testing	218
7.5 Detailed economical evaluation and life cycle assessment	218

8. CONCLUSION

8.1 Timber-steel hybrid systems as an alternative for timber-based multi-storey buildings	219
--	-----

LIST OF REFERENCES	220
---------------------------	-----

LIST OF FIGURES	236
------------------------	-----

LIST OF TABLES	244
-----------------------	-----

LEBENS LAUF

Timber-Steel Hybrid Beams for Multi-Storey Buildings

1. INTRODUCTION - GLOBAL FRAME OF RESEARCH

1.1 RESEARCH TOPIC: BUILDING TOWARDS RESOURCE EFFICIENCY

Being able to offer a good quality of life for a growing worldwide population is one of the most important global challenges faced by the society at the beginning of the 21st century. The complexity of this problem is reflected in political, economical, scientific and ecological discussions.

The comparison of quality of life levels among different parts of the globe shows a totally unbalanced situation (1). At the same time the extremely different quantity of natural resources used and consumed at different parts of the globe is also a fact.

We are therefore in front of a problem of balance, i.e. how to offer an enough quality of living for the whole world population, but also of efficiency because the quantities of resources at our disposition for this task are limited and therefore should be used carefully.

This global point of view should be used and taken as a reference for evaluating almost all the design processes we can imagine, from product engineering to urban planning.

Friedrich Schmidt-Bleek tackled this problem stating it as the question:

“Could technology provide goods and services that offer undiminished end-use satisfaction with substantially less natural resources than is the case today?”(2)

In order to analyse, evaluate and compare different design solutions he introduced the “Material Input pro Unit of Service” or MIPS concept. It assesses how much material input is needed for producing any item and compares it with the performance offered by the solutions measured in “unit of services”.(2) (3) (4)

This way the answer to the question stated can be “yes” if:

- the capacity of utilization of an item (unit of service) is improved and/or
- the material input needed for producing the item is reduced

We can use Schmidt-Bleek approach for the particular case of architectonic solutions re-stating the question as:

Could architecture provide building solutions that offer undiminished end-use satisfaction with substantially less use of natural resources than is the case today?

Again, the answer would be “yes” if:

- the capacity of utilization of buildings is increased and/or
- the quantity of resources needed in and during building processes is reduced

Analysing these two issues we can look for influencing parameters that will guide us to design solutions fulfilling the objective of building with resource efficiency.

1.1.1 Increasing the capacity of utilization of buildings

The capacity of utilization of buildings can be increased “in a given time” and/or “during time”.

In this first case the objective are the usually referred as “flexible buildings”, capable of housing different programs, like housing, offices and commercial uses at the same time, in the same or different storeys.

Some conditions have to be fulfilled in order to offer a sound and wide enough base where the different uses could find place. Namely:

- The ceilings should be high, at least providing 3 metres free height.
- Medium to high free spans should be provided (6-12 m)
- The capacity of supporting medium to high live loads (3-5 kN/m²) shall be guaranteed.
- The fire resistance of the solutions provided should reach the REI60-REI90 requirements.
- A free façade configuration should be allowed.

The case of increasing the capacity of utilization of buildings “during time” points to the design of architectonic solutions which allow the increase of the life span thanks to easy-to-carry and affordable adaptations. These will lead to economically affordable changes of use after a determined time lapse, when the originally planned uses are no longer necessary or desirable.

It should be pointed out that this a case more and more frequent in recent times. The so-called “economical life” of an architectonic solution (understood as the time a built object stays useful as originally designed) has the tendency to be shorter meanwhile the “technical life” of the materials and components used (understood as the time during which the used materials can offer a full performance) stays constant or even increases. Both facts point to the necessity of designing for allowing changes of uses after a given time, as well making maintenance and repair procedures as easy as possible.

Frame systems composed of supports and beams, or supports and plates, offer good solutions for both cases of increasing the capacity of utilization of buildings, especially when compared with massive or wall-based solutions which are much more difficult and costly to adapt to new or different uses, both in a given or during time.

1.1.2 Reducing the resources used in and during building processes

The second objective of reducing the resources needed and used in and during building processes can be assessed from different points of view, at urban, building and component levels.

At urban level the infrastructure needed per square meter built should be minimized. This deals with the quantity of piping, wiring, roads and so on needed for guaranteeing an adequate building use and performance. Building in an urban environment where the same infrastructure can be used or designed for several neighbouring buildings helps to optimize the quantity of resources needed.

At building level the optimization of resources to be used pushes to build multi-storey in order to minimize the quantity of buildings services per square meter built. In this case where several storeys are built one over another a low structural depth (thickness of the structural solutions) is desirable to minimize the square meters of façade needed per square meter built.

At component level the objective is the minimization of the total resource consumption, materials and energy, needed for a building solution. This leads to the efficient use of materials and at the same time, and thinking about easy changes in use, to the design taken into account processes of reusing, disassembling, recovering and recycling of the materials used.

1.1.3 Conclusions

As a general conclusion of the previous analysis it can be stated that, in order to increase the capacity of utilization of buildings, flexible multi-storey buildings making use of frame structural solutions could be an effective strategy, both for a given time as well as for allowing transformations during time.

On the other hand, and in order to reduce the quantity of resources used in and during building processes, the focus should point to urban multi-storey buildings making an efficient use of the materials used.

Both conclusions point together to the research field where this work finds its place: the resource efficient design of frame structural solutions for urban multi-storey buildings.

In this case, and as the starting point, the research will be focused on one frame structural element, the beam, stating the hypothesis of combining timber and steel for achieving the resource efficiency goal stated.

2. THE POTENTIAL OF THE COMBINATION OF TIMBER AND STEEL

Timber and steel are two very different materials regarding origin, manufacturing processes and both physical and mechanical properties. Even though the potential of their combination is high due that both of them are widely used worldwide and there is enough experience and knowledge about their practical use.

Moreover, their very different physical and mechanical properties should be considered as a potential, not a problem. Both materials, if well combined, can offer the best of their own, complementing and improving each other performance precisely because they have very different properties to offer.

2.1 IMPROVING TIMBER PERFORMANCE WITH STEEL

Timber natural properties are well fitted for a big amount of structural purposes. Nevertheless, a good number of improvement or reinforcement strategies with other materials (such as modified wood, steel, glass and carbon fibres and others) were studied, researched and used.

It can be distinguished between the cases where a structural piece or timber is improved punctually, because the existence of some localized problem and those where the improvement is general and affects the whole timber piece or structure.

Regarding the first case, localized reinforcements are common in joints because of high shear stresses or in changes of direction of beams because of the apparition of tensions perpendicular to the grain. The reasons behind the second strategy are very varied but most of them look for combinations with other materials to improve the overall structural behaviour.

In any case both situations point out that timber can reach its natural limits because of some particular weak performance regarding one or several response parameters. The conclusion is that in many cases it would be desirable to improve its performance under these structural demanding situations.

In the next points a series of properties, that make the timber performance comparatively weaker that the steel one, are listed and explained.

2.1.1 Physical properties

Variability

Timber is a natural material and therefore the variability of their properties is much higher than other artificial or industrial materials like the case of steel. The natural and high variability inside a random group of timber pieces can be reduced thanks to several strategies. One is the selection of the material, the classification of the pieces inside different strength classes, as can be seen in *Figure 1*.

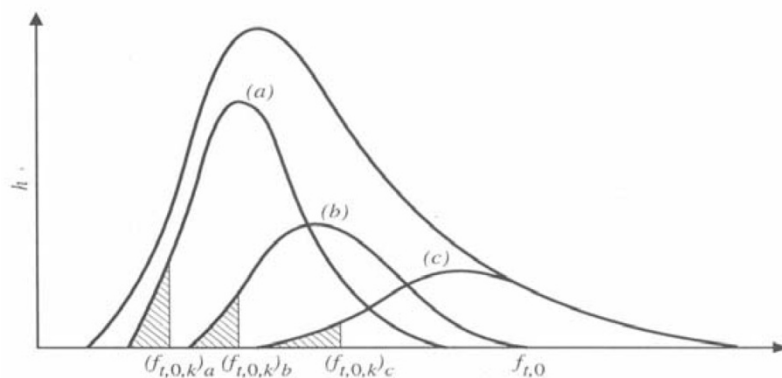


Figure 1: Tensile strength distribution of structural timber assigned to three grades a, b, c (5)

Other options are manufacturing processes. In this case new timber-based products (glulam, plywood) are produced controlling the quality of the individual timber pieces (boards, sheets) used for their production.

This variability affects the determination of the characteristic and mean values used for structural calculations following semi-probabilistic methods. In practice it is also responsible for the fact that the partial security factors for the material properties and resistance used in structural calculations are higher for structural timber and timber-based products than the case of steel.

As an example, the current timber Eurocode 5 establish values for the partial security factor for the material as $\gamma_M=1,3$ for solid timber and many timber-based boards and $\gamma_M=1,25$ for glued laminated timber (6) . On the other hand the steel Eurocode 3 recommends values of $\gamma_{M0}=1,00$ for the resistance of cross-sections whatever the class is.(7)

In the case of the transition from solid timber to glulam, the glulam variability is reduced thanks to the selection and treatment (removing of knots) of boards used for its manufacturing. Following the same principle, the combination of glulam with other materials with even smaller variability (steel, fibre reinforced plastics, carbon fibres and others) could yield even further improvement as some authors proposed (8) and can be observed in *Figure 2*. The improvement would not only affect the variability itself but also the level of middle and characteristic values of a particular property.

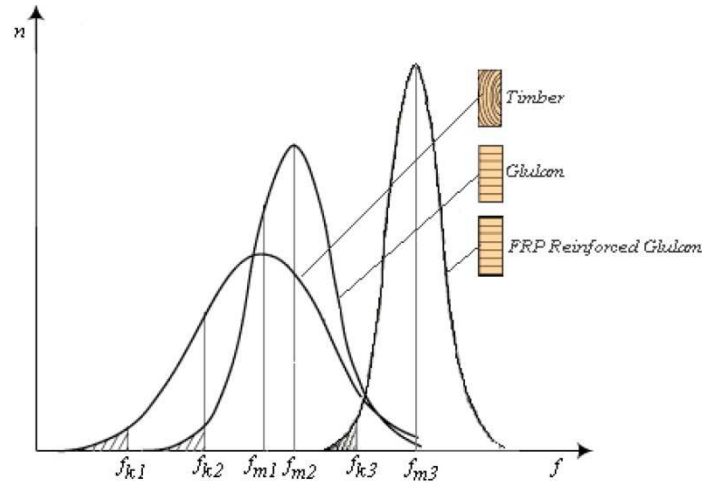


Figure 2: Variability, middle and characteristic values of timber, glulam and FRP reinforced glulam (8)

Homogeneity

Timber, as almost all natural materials, is non-homogeneous. This non-homogeneity has its roots in the wood growing processes. The presence of knots, resin cavities, growing irregularities and others can provoke that different parts of the same piece can offer different structural capacities under the same applied loads.

On the other hand steel is a completely homogeneous material. In sound steel no defects appear, the performance and properties of every part of a piece is the same. It is also an isotropic material, and that means that it performs always in the same way, it does not matter in which direction the forces are applied.

Combustibility

The reaction to fire is defined as the response of a product in contributing by its own decomposition to a fire to which it is exposed under specified conditions (9).

Timber is a combustible material. It is classified as *D-s2, d0* following the EN 13501-1 (9). That means that timber is a combustible material with a medium contribution to fire (*D*), its smoke emission level during combustion is of an average intensity (*s2*) and it doesn't produce flaming droplets or particles during fire (*d0*).

This classification is valid for timber, glulam, cross-laminated timber, medium density fibreboards (MDF), oriented strand boards (OSB) and particleboards. Only some timber-based products, where wood is combined with other mineral components like cement or magnesite, can reach a classification of *B-s1, d0*. That means they are combustible materials but with a very limited contribution to fire (*B*), an absent or weak intensity of smoke emission during combustion (*s1*) and they do not produce flaming droplets or particles during fire (*d0*). This is the case, for example, of cement bonded particle boards.

On the other hand steel is a non combustible material. It is classified as *A1* following the EN 13501-1 (9). That means that steel is a non-combustible (*A1*) and therefore it does not produce smoke, flaming droplets or particles during fire.

The reaction to fire is an important parameter taken into account inside many building codes in order to allow, limit, condition or prohibit the use of certain materials for building purposes. This is due that combustible materials not only suffer the effects of fire themselves, but they also contribute with their presence to increase the total fire load of a building.

Malleability

An object or material is "malleable" when it is "capable of being stretched or bent into different shapes" (10).

Timber is a material with a natural low-malleability and usually considered as stiff and unyielding. But it can be bent. The possible radius of bending depends on the timber thickness and should be limited for not damaging the timber pieces.

During history different methods for bending wood were developed and the use of heat and/or vapour can make easier many forming processes. Examples of this can be found in processes used for building furniture, musical instruments or boats (11).

Steel is a material which has a very good malleability, both in warm and cold states. It can be bended, stretched and deformed in almost any imaginable shape.

2.1.2 Mechanical properties

Anisotropy / Isotropy

Timber is an anisotropic material, their properties are directionally dependent. That means that wood, because of its physical arrangement, which could be simplified as a bunch of longitudinal tubes (wood fibres) grouped together, performs in very different ways depending on the direction we consider. More precisely it is an orthotropic material. Three perpendicular axes define the longitudinal, radial and tangential directions which offer very different mechanical properties.

Steel is an isotropic material, and that means that it performs always in the same way, it does not matter in which direction forces are applied.

Ductility

Timber is a brittle material when subjected to tension. Its deformation is proportional to the loads applied until reaching one point when the material, suddenly, fails.

In the case of compression, timber presents a ductile behavior and its failure is no more sudden. After an initial and proportional load-deformation behavior the material plasticizes, being deformations not proportional to loads anymore. A clearly-defined rupture point does not occur.

In the case of a timber element under bending these two performances find place at the same time inside one piece, inside the different tension and compression areas. But at the end it is the brittle rupture in tension the one which governs the failure of the whole piece. That is why in overall terms timber can be considered as a brittle material also for the bending case.

Steel is ductile under tension, compression and therefore also under bending. After elastic deformations the material plasticizes and deformations grow not proportionally to the loads applied. The failure is not sudden.

Creeping

Timber presents a viscoelastic behaviour. A loaded timber piece, and after an initial deformation, increases during time its deflection if the load stays without change, reaching values that can be comparable or even bigger than the initial one. This phenomenon is known as creeping. It provokes an increasing deformation during time without change of the load level.

Creeping is a very complex phenomenon and is conditioned by factors like the magnitude of loads and related stress levels, load history, timber quality and Young Modulus, timber humidity content and its variation during time and temperature (12).

Indirectly this means that timber is very well-suited for short-time loads that provoke instant or short term deformations that can be recovered, totally or partially, when the original loads disappear or vary in intensity. But in the case of heavy permanent loads, the long-term deformations could be a limiting factor for the structural design of a piece.

Steel does not creep. A certain load causes deformation and this remains constant, it does not matter how much time the load stays. This deformation can be completely recovered if the load goes away when the steel that was performing under its elastic limit. On the contrary, if the steel reached a certain degree of plasticization, some residual deformation will remain when the load disappears. But in no case will the deformation change, increase or recover, without any variation of load.

Modulus of Elasticity

As already explained, and as it is the case for almost all physical and mechanical properties of timber, its modulus of elasticity in the grain direction is variable and depends on a variety of factors like species and quality.

Middle ($E_{m,0,mean}$) and characteristic ($E_{m,0,k}$) values of the E-Modulus for bending in the grain direction and for different structural grades are collected in building codes and norms like the EN 338:2009 (13) or EN 14080:2013 (14).

In order to have some references, the middle value of the Young modulus of timber structural grades of common use like, for example sawn timber C24 is 11.000 N/mm² (13) or 12.500 N/mm² for the case GL28c (14).

Lower grades like C16 present values of $E_{m,0,mean}=8.000$ N/mm² (13) and the best one of the best grades available nowadays in the market like GL32h presents a value of $E_{m,0,mean}=14.200$ N/mm² (14).

That means that in the most habitual cases the middle value of the E-Modulus ranges from 8.000 to 14.200 N/mm², being a value approximately of 12.000 N/mm² a very common situation.

The E-modulus of steel depends on its chemical composition. For the structural steels covered by the Eurocode 3 the design value of the modulus of elasticity should be taken as 210.000 N/mm² (7).

It can be seen that the ratio between the timber Young modulus and the steel one can range from 26 to 15, being a value of around 17,5 a quite common situation. This means that steel is 17,5 times stiffer than timber, that is a much more deformable material. This is reflected in the tension-strain deformation diagrams of both materials as can be seen in *Figure 3*.

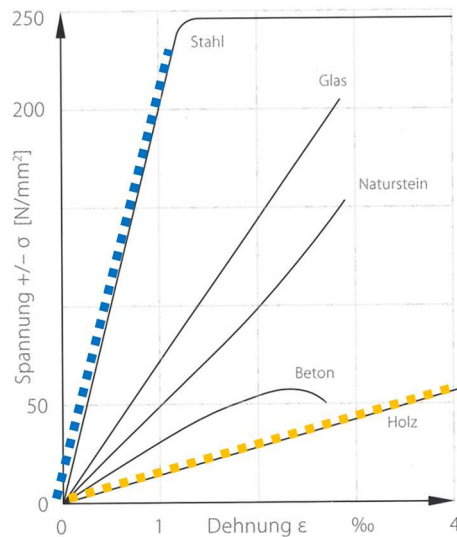


Figure 3: Tension-Strain diagrams of different materials. Steel in blue and timber in yellow. (15)

Shear resistance

The shear strength of timber is reduced. Its characteristic value range from $f_{v,k} = 3,2$ N/mm² for a strength class C16 (13) to the value of $f_{v,k} = 4,0$ N/mm² for a C24. The values for the glulam strength classes are $f_{v,g,k} = 3,5$ N/mm² (14).

It can be seen that the variability is small in this cases, being for all of the grades really low values. Timber is weak against shear stresses. In the best cases strength classes of timber from deciduous trees can reach values of $f_{v,k} = 5,0$ N/mm², like it is the case of strength classes D65 or higher.

In comparison the shear strength of steel is very high. The shear strength of steel is related to the yield strength f_y , being its value equal to $\frac{f_y}{\sqrt{3}}$ (7). This means that for common structural steels grades S355, with a $f_y = 355$ N/mm² (7), its value is of 205 N/mm². For a S235 grade, with a $f_y = 235$ N/mm² (7), its value is of 136 N/mm².

In any case these values are much higher than the timber ones, being from around 40 to 60 times bigger. In the cases where the shear resistance could be a limiting factor timber is a not well suited material meanwhile steel can withstand this type of stresses without major problems.

Time dependent strength

The strength of timber is load-time dependent. Timber is capable of withstanding high values of stresses under short-term or instantaneous actions, but these values are smaller if the loads are permanent.

This fact is addressed by most building codes introducing a modification factor which multiplies the characteristic strength values in order to obtain the design values.

This is the case of the modification factor k_{mod} used Eurocode 5 (6), also dependent on the material type and service class. For a given material type, for example sawn timber or glulam, and if we consider a particular service class, for example service class 1, we can observe that the values of the modification factor vary from $k_{mod} = 0,6$ for permanent actions to $k_{mod} = 1,1$ for instantaneous actions. That means that the timber characteristic strength values, obtained from standardised five minutes duration tests, can be increased a 10% for the case of instantaneous actions but should be reduced in a 40% if the actions are permanent. In all cases, and in order to find the final design values, the calculation must take into account also the partial security factor for the material.

For a graded glulam GL28c, for example, the bending design stress would be $f_{m,g,d} = 13,44 \text{ N/mm}^2$ for permanent actions, but of $f_{m,g,d} = 24,64 \text{ N/mm}^2$ for instantaneous actions, that is 1,83 times bigger. Therefore timber is a very well suited material, as was the case regarding deflection and creeping, for short and instantaneous duration loads but not so for the permanent ones.

The strength of steel is not time dependent. Their strength properties are not affected by the duration of load.

Ratio from E-Modulus to G-Modulus

The ratio of the modulus of elasticity (E) to the shear modulus (G) is a useful parameter for measuring the relevance of the shear deformation contribution to the total deformation of a structural element under bending. Most classic manual calculation methods do not take into account the shear deformation contribution due to its low relevance for the most common cases.

In the case of steel the modulus of elasticity is $E = 210.000 \text{ N/mm}^2$ meanwhile the shear modulus has a value of $G = 81.000 \text{ N/mm}^2$ (7). This means a ratio $E/G = 2,6$. This is one of the reasons why in the case of steel structures the contribution of the shear deformation to the total deflection of an element under bending is really small.

But in the case of timber this ratio has a much higher value and therefore the contribution of the shear deformation is more relevant. For example for a strength class C16 the values are $E_{m,0,mean} = 8.000 \text{ N/mm}^2$ and $G_{mean} = 500 \text{ N/mm}^2$ (13) and the ratio $E/G = 16$. For GL28c the values are $E_{0,g,mean} = 12.500 \text{ N/mm}^2$ and $G_{g,mean} = 650 \text{ N/mm}^2$ (14) and the ratio $E/G = 19$.

Even though, the shear deformation in usual timber structures is not responsible for more than approximately a 5% of the total deformation and it is in many cases negligible, like is the case for steel. But under more demanding or special conditions, like high load values, point loads, continuous or short beams it could be important to take this fact into account for obtaining precise results.

We can conclude that in the case of steel structures the contribution of the shear deformation does not play a role, meanwhile in the timber ones it should be taken into account for obtaining precise results.

2.2 IMPROVING STEEL PERFORMANCE WITH TIMBER

The list of characteristics explained in the previous points seems to communicate the idea that timber is comparatively not so well suited for structural purposes like steel. But this is not the case, they are only two very different materials, with different properties, each one offering different possibilities and raising up also different limits and design problems.

Cases where the steel performance can be considered inferior or at least not so well-suited as the timber one can also be found. Steel has also its limits and weak points.

In the next points a series of properties, that make the steel performance comparatively weaker than the timber one, are listed and explained.

2.2.1 Physical properties

Performance under fire

As already explained steel is a non combustible material, but its mechanical properties are highly temperature-dependent. Its yield strength and slope of the linear elastic range are reduced when steel reaches high temperatures (16).

The norm ISO 834 (17) establishes rules for the fire resistance tests for elements of building construction. It defines a time-temperature curve that models the temperature developed during a fire situation. This curve reaches values of 1000 °C after 90 minutes fire, being the temperature after 30 minutes higher than 800 °C (17).

Following Eurocode 3 (16) the reduction factor (relative to f_y) for the design yield strength of hot rolled and welded class 4 sections, or the reduction factor (relative to f_{yb}) for the design yield strength of cold formed class 4 sections, has a value of 0,03 for a temperature of 1000 °C (after 90 minutes following ISO 834) and 0,07 for a temperature of 800°C (after 30 minutes following ISO 834). Following ISO 834 the temperature after only 10 minutes fire would be almost 700 °C and this would mean a reduction factor of already 0,13 (16).

All this data reflect the poor performance of unprotected steel under fire. In practical terms this means that the steel structural elements should be protected with other temperature isolating materials. An excessive increasing in temperature of the steel structural components should be avoided or it will become a decisive and very limiting factor. After few minutes of fire steel structural elements can lose a good amount of their original cold-state structural capacity.

The performance of timber under fire is very different. Timber mechanical properties are, as in the case of steel, also temperature dependent. Its compression, tension, and shear strength parallel to grain and the modulus of elasticity are reduced when the temperature increases (18). But in this case this fact is much less relevant than in the steel one because of the very particular way that timber performs under fire.

It is not until the temperature is in excess of 250 °C that there is a sufficient build-up in volatile gases in timber to cause ignition in the presence of a pilot flame. Then timber undergoes thermal decomposition with subsequent removal of mass, leaving behind enough material to preserve structural integrity (12). This process describes the formation of an external char layer (charcoal) which protects the unburnt timber and allows it to keep a low temperature, therefore maintaining its cold-state mechanical properties.

This fact is taken into account by structural design codes in order to prescribe calculation methods for the case of a fire situation. In the case of Eurocode 5 (16) , and among other more advanced methods, it proposes a reduced cross-section method where the part of sound timber not affected by fire remaining after a defined time can be easily evaluated. If this reduced cross-section is enough for withstanding the loads for a fire situation the structure can be considered safe from a structural point of view.

In general the timber structural elements performance during fire can be described as easy to predict and therefore very reliable. The opposite is valid for the steel ones. Their join performance under fire can be observed in *Figure 4*.

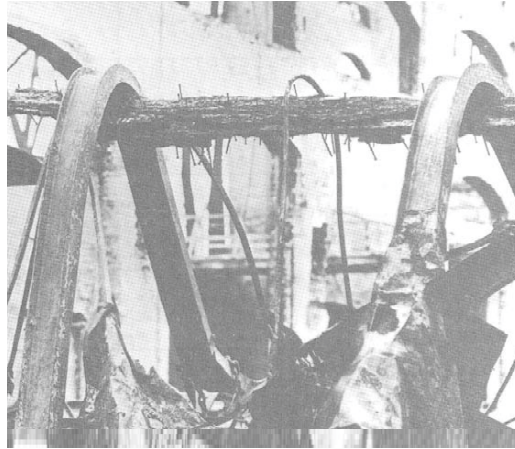


Figure 4: Damage resulting from a large building fire. Steel members yielded by the heat are supported by a charred wood beam (19).

Thermal conductivity

The thermal conductivity measures the rate of heat flow (W/m^2) through a material subjected to unit temperature difference (K or $^{\circ}\text{C}$) across unit thickness (m).

The thermal conductivity of timber is affected by factors like density, moisture content, grain direction, structural irregularities and temperature.

The conductivity of structural softwood at 12% moisture content is in the range of 0,10 to 0,14 W/m K , meanwhile the value for steel is 0,9 W/m K (20). This is a ratio from steel to timber from 9 to 6,4, and it means that timber is a much more insulating material than steel.

This is a very important property for designing building details where different materials are combined. Materials with a high thermal conductivity, like steel, are the source of thermal bridges when in contact with both exterior and interior environments. Materials with low thermal conductivities, like timber, minimize these problems in the same situation.

2.2.2 Mechanical properties

Stiffness to weight ratio / Strength to weight ratio

Structural elements support not only applied loads but also their own weight. A resistant material could be not interesting for structural purposes if at the same it is very heavy. Its own structural capacity could be exhausted, or considerably consumed, only by its own weight. This is why the ratios stiffness to weight and strength to weight are interesting for comparing the structural performance of different materials.

Both timber and steel have very good ratios stiffness to weight, especially when compared when other common construction materials like concrete.

In the case of timber C24, with an $E_{m,0,mean} = 11.000 \text{ N/mm}^2$ and $\rho_{mean} = 420 \text{ kg/m}^3$ (13) this ratio is of 26,19. For the case of GL28c, with an $E_{m,0,mean} = 12.500 \text{ N/mm}^2$ and $\rho_{mean} = 420 \text{ kg/m}^3$ (14) the ratio is 29,76. Structural steel presents very similar values. Being its $E = 11.000 \text{ N/mm}^2$ and $\rho = 7.850 \text{ kg/m}^3$ (7), the ratio is 26,75.

In the case of concrete with an strength class C25/30, with an $E = 31.000 \text{ N/mm}^2$ and a $\rho = 2.500 \text{ kg/m}^3$ following Eurocode 2 (21) the factor is of only 12,4. This means that, per unit of weight, both timber and steel offer more than double stiffness as concrete. This leads to considerably lighter structural solutions.

In the case of the strength to weight ratios it is necessary to define which type of strength we consider, tensile, compressive, bending or shear. Some authors like Christopher Mettem (22) studied some of these factors, namely stiffness and tensile strength, for timber, steel and other materials in order to argue which type of timber reinforcements would be reasonable. The “relative values” are calculated taking the C24 case as a reference. His results can be seen in *Table 1*.

Table 1. Non-wood materials – potential reinforcements – specific performance relative to timber

Materials families	Specific properties*			
	Modulus of elasticity	Relative value†	Tensile strength	Relative value†
Timbers	<i>specific</i>	<i>relative</i>	<i>specific</i>	<i>relative</i>
C24	26	1.0	0.033	1.0
D60	20	0.8	0.043	1.3
GL36	33	1.2	0.058	1.8
Steels				
S275	26	1.0	0.035	1.1
S355	26	1.0	0.045	1.4
Glasses				
E	28	1.1	1.3	39
S-2	36	1.4	1.9	56
Aramids				
K29	40	1.5	2.5	76
K49	86	3.3	2.5	76
Carbon fibres				
T300	130	5.0	2.0	61
T1000-G	160	6.2	3.5	107

* Indicative values only. Units are derived from normal SI properties for structural design. Timber strengths are characteristic lower 5%iles. Moduli are mean values.
† Relative values use Strength Class C24 softwood timber as datum. D60 is a hardwood Strength Class; GL36 is high-grade glulam. European LVL properties are similar the latter.

Table 1: Specific performance relative to timber (22)

From these comparisons Mettem (22) states that reinforcing C24 timber for stiffness with steel does not bring benefits at all, because both materials have a very similar specific modulus of elasticity. In the case of reinforcing timber with steel for tensile strength the conclusions are very similar, because both relative values are again very close to each other.

It should be pointed out that the calculations provided (22) were made with middle values for the modulus of elasticity and characteristic values for the tensile strength, being $f_{t,0,k} = 14 \text{ N/mm}^2$ for C24, $f_{t,0,k} = 36$ for D60 (13), $f_y = 275 \text{ N/mm}^2$ for steel S275 and $f_y = 355 \text{ N/mm}^2$ for steel S355 (7). This is of course correct from a pure material point of view, but in real calculations following Eurocode 5 (6) the tensile strength of timber would be affected by the factors k_{mod} and γ_M , reducing its value, meanwhile the steel calculation following Eurocode 3 (7) would in normal cases not affect at all the considered numerical value for the steel tensile strength, due that the material security factor would be 1.

A new calculation taking into account these factors is presented in *Table 2*, adding the results for the case of timber GL28c and for the bending situation. The relative values are calculated again taking the C24 case as the benchmark value.

The partial material security factors of $\gamma_M = 1,25$ for glulam and $\gamma_M = 1,30$ for sawn timber (6) are already included, as well as a value of $k_{mod} = 0,8$. This last one was chosen for corresponding to a *Service Class 1* and to a medium-term *Load-duration class*, which is one of the most common limiting situations for the design of timber structures for multi-storey buildings. Of course these relationships would change and should be corrected for other specific situations.

	Specific properties					
	Modulus of elasticity specific	Relative value relative	Tensile strength specific	Relative value relative	Bending strength specific	Relative value relative
Timber						
C24	26,19	1,00	0,021	1,00	0,035	1,00
D60	20,24	0,77	0,026	1,29	0,044	1,25
GL28c	29,76	1,14	0,030	1,45	0,043	1,21
Steel						
S275	26,75	1,02	0,035	1,71	0,035	1,00
S355	26,75	1,02	0,045	2,21	0,045	1,29

Table 2: Specific performance relative to timber a $k_{mod} = 0,8$ and material security factors γ_M .

In comparison to the results obtained by Mettem (22) it can be seen that the relative tensile strength of steel is significantly improved. The affirmation that is not worth reinforcing timber with steel for tensile strength is not under this new perspective questionable.

The stiffness results are not affected, both materials present a good a very similar stiffness to weight ratio, and this is the case also for the bending situation, where steel S355 offers the best performance, but really close to timber alternatives like GL28c.

As a summary it can be stated that both steel and timber present very good and similar values of stiffness to weight ratios, especially when compared to steel. Regarding strength the steel performance is slightly better than the timber one in the tension case meanwhile both materials offer very similar values for the bending situation. After all this it can be inferred that the “reinforcing timber with steel” concept looks only reasonable for the tension case. In other situations an alternative concept, using both materials with an equal level of structural responsibility, looks more promising.

2.2.3 Environmental and economical considerations

Renewability and recyclability

Timber is a renewable material. Its source, trees and forests, if well managed and exploited, can offer a continuous supply of timber for structural and other purposes without exhausting the available resources. Almost any timber product can be reused or recycled when reaching its end of life point. These recycling procedures, depending on the product under consideration, range from using the old timber for manufacturing new timber-based boards to burning the timber for obtaining energy.

Steel is not renewable. The existing reserves of iron needed for producing steel are limited and they cannot be produced or grown again. That means that they should be used carefully.

On the other hand steel is a highly recyclable material. If recovered after its use, it can be transformed again for obtaining recycled steel.

Meanwhile for timber the challenge ranges from the sustainable management of forests to the optimization of reusing and recycling procedures, in the case of steel reusing and recycling is the only strategy that can guarantee a future undiminished supply of the material. These facts focus the attention on the importance of designing for making the recovery of materials easy and economically viable. If the recovery procedures are complicated and expensive no recycling will be economically competitive.

Energy production demand

The primary energy content (PEC) is the overall consumption of energy resources required to manufacture a product or a service. It is divided into renewable and non-renewable energy resources (23).

The concept of Cumulative Energy Demand (CED) is used for determining and comparing the energy intensity of processes. Timber presents a comparatively low energy demand for its production.

In the IBO – Richtwerte für Materialien (24) , and for the case of spruce sawn timber, naturally dried, the *Total CED non renewable (Ho)* value is of 1,86 MJ per kg. In comparison, and using the same source, the value for non-alloyed steel is of 19,23 MJ. That is 10 times bigger. If we consider the case of timber products which require more manufacturing like standard glulam the *Total CED non renewable (Ho)* value is of 7,95 MJ per kg and the ratio is reduced 2,4. In any case the energy demand of steel is considerably bigger than the timber one.

It should be pointed out that the comparison must be done between equally performing structural elements or solutions, and not between 1 kg of timber against 1 kg of steel like was the case in the previous paragraph. But this first raw comparison can offer a qualitative first approximation to the problem and concepts involved.

Price

As already stated in the previous point, the manufacturing process of steel is very energy demanding. This makes the steel production very dependent on the energy and oil markets and both influence strongly its final price.

In the last decades this was characterized by a strong instability with steep up and downs of the prices tendency. Although also dependent on the location of the steel production, the average steel price shows the tendency to rise.

As can be seen in *Figure 5* for the period between 2001 and 2016, the evolution of the standard steel plates price was very unstable, offering a global increase in the steel price of almost 60% in 15 years for the United States produced steel, after a series of sudden price changes.

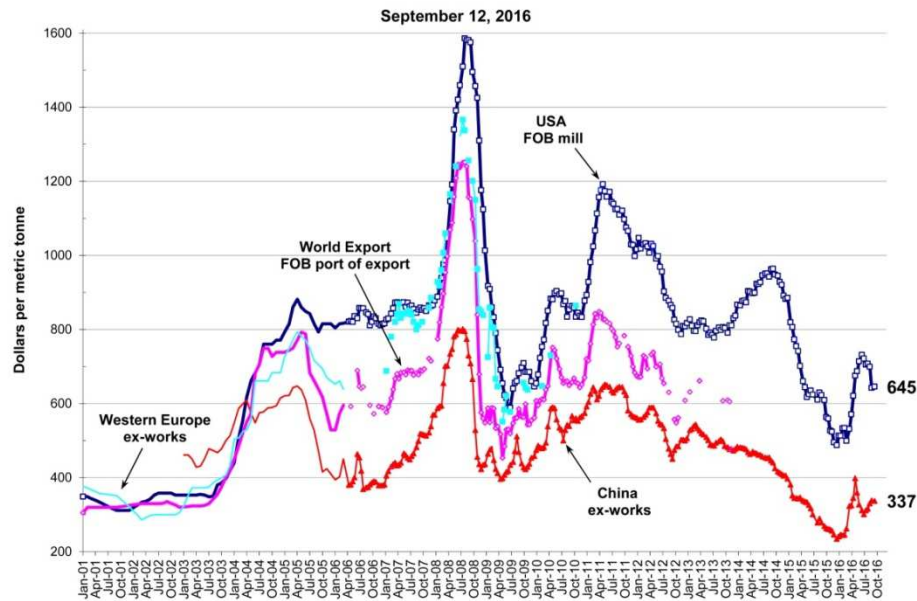


Figure 5: Evolution of standard steel plates prices from 2001 to 2016 (25).

Timber requires much less energy for its production and therefore it is comparatively much less dependent on the energy and oil markets. This fact indirectly protects it until some extent from fast reactions to changes in these markets.

As it can be seen in *Figure 6*, for the Austrian case and between the period of 1995 and 2016, the evolution of spruce and fir sawn timber prices was much more stable, being the global increase in price of around only 15% in 21 years.



Figure 6: Evolution of spruce and fir sawn timber in Austria from 1995 to 2016 (26)

2.3 COMPATIBILITY OF TIMBER AND STEEL: POTENTIAL AND RISKS

As already seen timber and steel are two very different materials. Stating as an objective the structural use of both materials for structural purposes in multi-storey buildings, steel could offer better properties under some situations, timber could do the same under others. But for their jointly use, and in order to make the most of both of them, the question of compatibility is a main one.

Some physical properties should be examined and taken into account not for finding which material, timber or steel, could perform better, but because they are relevant for allowing both of them to work and be used together without being the source of problems.

2.3.1 Physical properties

Coefficient of thermal expansion (parallel to grain)

The coefficient of thermal expansion is a measure of the relative change of dimension caused by temperature change. Timber expands on heating and contracts on cooling. In tests of both hardwoods and softwoods, the parallel-to-grain values range from about 0,0000031 to 0,0000045 m/m °C (20).

The coefficient of linear thermal expansion of structural steel is 0,000012 m/m °C for temperatures inferior to 100 °C (7). That means it is about 3,9 to 2,7 times bigger than the timber one.

As an example, if we take two pieces of steel and timber, both of them eight meters long, and the temperature varies in 30 °C, the steel piece would increase its length almost 3 mm, meanwhile the timber one only around 1 mm.

Coefficient of thermal expansion (perpendicular to grain)

For timber thermal expansion coefficients across the grain (radial and tangential) are proportional to specific gravity. These coefficients range from about 5 to more than 10 times greater than the parallel-to-grain ones (20). Taken 7,5 as a middle value that would mean values from around 0,000023 m/m °C to 0,000034 m/m °C.

The comparison with the steel one would now yield very different results, because in direction perpendicular to grain timber expands more than steel, from two to almost three times more.

As an example, if the same timber and steel pieces of the previous example would be 50 cm high and again subjected to a temperature variation of 30 °C, the steel piece would expand around 0,2 mm, meanwhile the timber one from 0,4 to 0,6 mm.

This difference in movement behaviour, although for this particular cases not very relevant, should be taken into account when connecting pieces of both materials with long dimensions which would expand differently if temperature changes occur.

Shrinkage and swelling

Below a moisture content corresponding to the fibre saturation point timber changes dimension as it gains moisture (swells) or loses moisture (shrinks). It does this in an anisotropic way. It shrinks and swells most in the direction of the annual growth rings (tangentially), about half as much across the rings (radially), and only slightly along the grain (longitudinally) (20).

In the case of red spruce, for example, the shrinkage from green to oven-dry moisture content, expressed as a percentage of the green dimension is around 3,8 % in the radial direction, 7,1 in the tangential direction and 11,8% volumetrically (20).

More useful are the values of dimension change depending on the variation of humidity content of the timber piece. The contraction value is for softwoods around 0,16%/ % in the radial direction and around 0,32%/ % (27).

Applying these relations to the example of a timber beam with a height of 50 cm would yield the result that a change of only 5% in the timber humidity content would be responsible of a change of dimension of 4 mm, if the beam has horizontal annual rings in the cross section (radial deformation). If the annual rings would be vertical the change of dimension would be in the tangential direction and reach the value of 8 mm.

Steel does not change its dimensions at all because of these reasons. That is why, as in the case of changing dimensions because of increasing of temperature, the different behaviour of the two materials should be taken into account when used together in order to avoid any type of pathology.

Humidity

The timber humidity content and its change are not only the cause of changing dimension of timber pieces, but also an important factor for the deterioration of wood.

Organisms that can degrade wood need minimum amounts of humidity for being able of attacking it. These are principally fungi, insects, bacteria and marine borers (20). Keeping timber dry, or allowing it to dry easily after being in contact with water, is the best strategy for avoiding this type of problems.

In the case of steel water and water vapour are also important factors to take into account, because when in contact with steel they facilitate and accelerate corrosion processes.

As a conclusion and as a general rule it should be stated that the contact of both timber and steel pieces with water should be avoided. If not possible, at least it should be controlled carefully, with designs that facilitate the structural pieces to dry and not to retain water which could stay in permanent contact with the materials.

2.3.2 Technological considerations

Tolerances and precision

Modern timber construction products, procedures and technologies offer a high precision. The tolerances needed nowadays are much smaller than before. Thanks to the control of the humidity content of the timber components and timber-based products their dimensional accuracy can reach the precision range of +/- 1 mm.

The steel industry offers also products with an extremely high precision. Their dimensional accuracy reaches also the +/- 1 mm range.

This agreement of precision between both materials facilitates their combination. The small tolerances needed for combining components of both materials can be easily fulfilled and controlled from both parts. No demanding special elaboration or controlling processes are needed which would lead to price increases.

Workability

Working on timber is very easy with simple tools. Moreover, nowadays the use of Computer Numeric Control (CNC) machines and robot are state-of-the-art techniques. With either traditional tools or modern ones timber is an easy workable material. Complex geometries can be produced (28).

Steel offers a very high warm and cold malleability. Almost any shape can be produced possible. On the other hand its workability at the construction site is much more reduced than the timber one. Construction elements can be modified on-site but with much more effort than in the timber case.

Modern production techniques and automated processes allow high degrees of prefabrication. The tendency to prefabricate structural elements as much as possible under controlled conditions in the factory and assemble them at the construction site is facilitated by the characteristics and technological possibilities offered by these two materials.

2.4 THE POTENTIAL OF THE COMBINATION OF TIMBER AND STEEL IN BEAMS FROM A STRUCTURAL PERFORMANCE POINT OF VIEW

In the previous points a series of timber and steel properties were cited and analysed. First the attention was paid to situations where steel offers a comparatively better performance. Later the focus was laid on topics where the timber performance overcomes the steel one. At the end compatibility issues were presented. All this can be applied now to the particular case of structural elements, and particularly to beams. From a structural performance point of view it can be stated that for every relevant situation (ultimate limit states, serviceability limit states, normal or extraordinary situations) timber and steel can complement, support and/or reinforce each other in a variety of ways. Their combined use looks very promising because together they are able of addressing and offering answers to all these situations and they can do it in a better way than both materials on their own. A theoretic beam which could profit at the same time from both steel and timber properties would be able to offer optimal solutions against all structural relevant situations.

In Ultimate Limit States (ULS), under a normal situation, both timber and steel offer good properties for withstanding bending moments. Steel would offer a good performance against shear stresses and cases of compression in direction perpendicular to the grain. Under a fire situation timber could offer resistance and reliability. Under a seismic situation both timber and steel offer globally light solutions, a fact interesting in order to reduce the magnitude of seismic actions, and steel would provide ductility. In the case of Serviceability Limit States (SLS) both timber and steel present good stiffness to weight ratios, being a good option for limiting instant deformations. Finally steel, which does not creep, would be a good option for limiting long-term deformations. A summary of these facts under different situations is presented in *Table 3*.

Situation	Problem	Suitable Material
ULS Normal Situation	Bending	Timber + Steel
	Shear	Steel
	Compression (perpendicular)	Steel
ULS Fire Situation	Fire resistance	Timber
ULS Seismic Situation	Lightness	Timber + Steel
	Ductility	Steel
SLS	Instant deformation (w_{inst})	Timber + Steel
	Final deformation (w_{fin})	Steel

Table 3: The potential of combination of timber and steel in beams.

3. STATE OF THE ART: TIMBER AND STEEL COMBINATION IN BEAMS

The research on combining timber and steel in beams is relatively recent.

“Metal reinforced timber dates back to the 1940s (29) and some patent exists from the 1920s (30). The flitch-beam, where a metal plate is sandwiched between two joists so that the three act as a composite, was known in the last century” wrote Bulleit (31) in 1984.

Although relatively recent, there is already a good amount of research on the topic. In the last 65 years numerous authors looked for the structural possibilities that the combination of the two materials opened from very varied points of view and looking as well to very varied objectives.

In the next points an overview of all this research is carried out, paying special attention to the different strategies approached in order to combine the two materials, the objectives pursued, the problems found and to the built examples existing with the studied solutions.

Some other type of metal reinforcement, like the aluminium ones, will be also cited because of the interest of the particular solution or knowledge gained, that could be useful for the study of steel-timber combinations.

3.1 PROPOSAL OF A SYSTEMATIC CLASSIFICATION

As already mentioned, it already exists a big quantity of research work on the topic of timber-steel structural elements, and in particular for the case of beams. But very few authors tried to systematize all this existing information.

As it is the case with any attempt to classify a wide research topic, very different approaches would be possible. A classification of the combinations of timber and steel for beams could be based on the characteristics of the materials used, the geometry of the arrangements, the objectives pursued, the means used for connecting the materials and many others.

One of the few examples existing is the proposal from Isoda et al (32). This system focus only on the geometry of the possible solutions, i.e. “position of the reinforcement, etc” as shown in *Figure 7*. The result is that for every defined category there is still a big number of variations possible.

Table 2 Classification of timber-based hybrid members


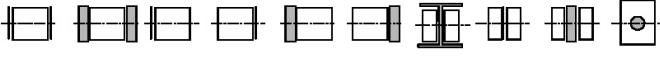
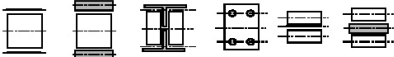
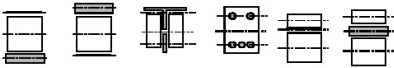
Class	Position of Reinforcement, etc	Example of member section
1	Neutral axes of timber and reinforcement are not at the same position	
2	Neutral axes of timber and reinforcement are at the same position	
3	More than one piece of reinforcement, positioned symmetrically.	
4	More than one piece of reinforcement, positioned asymmetrically	
5	Pre-stressed	(Many variations)
6	Assembled member	(Many variations)
7	Others	(Many variations)

Figure 7: Classification of timber-based hybrid members (32).

As an alternative and with the objective of organizing all the research information found a new classification is proposed as show in *Figure 8*.

Two big groups are defined, depending on if the steel elements are used in a passive or in an active way. The second division recognizes if the steel elements run, in relation to timber, in grain direction (like is very usual) or in direction perpendicular to the grain.

The classification system makes also use of geometry parameters, like if the steel elements are horizontally (H), vertically (V) or both horizontally and vertically (H+V) arranged, or if they remain out or inside of the timber section.

And at the end, and very relevant for structural purposes, it can be recognized for which structural task the steel pieces were used. If they are used mainly for working under tension (T), compression (C) or they withstand shear stresses (S) or any combination of these three main stresses.

This way, the classification helps to identify, to look for or to choose a particular solution depending of the particular problem under consideration. It is also useful for identifying problems for which the particular solution is not well fitted.

In the following pages all the research contributions found on the topic of timber-steel beams will be listed, summarized and commented in the corresponding classification cell. This way the process of finding authors that worked making use of similar strategies is easy. It also allows the comparison of the different solutions proposed for addressing a common structural issue.

		PASSIVE					ACTIVE		
		In grain direction					In grain direction	Perp. to grain	
		T	C	S	T+C	T+C+S	T	T+S	T (p.g.)+S
H	Outer								
	Inner								
V	Outer								
	Inner								
H+V	Outer								
	Inner								

Figure 8: Systematic classification of timber-steel combination in beams.

3.2 COMBINATIONS WITH PASSIVE STEEL

3.2.1 Horizontal steel arrangements

		PASSIVE				
		In grain direction				
		T	C	S	T+C	T+C+S
H	Outer					
	Inner					
V	Outer					
	Inner					
H+V	Outer					
	Inner					

References:

Borgin et al (1968) _(33)

Krueger (1973) _(30)

Krueger and Eddy (1974) _(34)

Krueger and Sandberg (1974) _(35)

Kobetz and Krueger (1976) _(36)

Uzielli (1995) _(37)

Isoda et al (2000) _(32)

Hansson & Karlsson (2007) _(38)

Kliger et al (2008) _(39)

Kliger & André (2013) _(40)

Borri & Corradi (2011) _(41)

Summary:

Borgin et al (33), cited in Dorey & Cheng (42), used continuous steel strips.

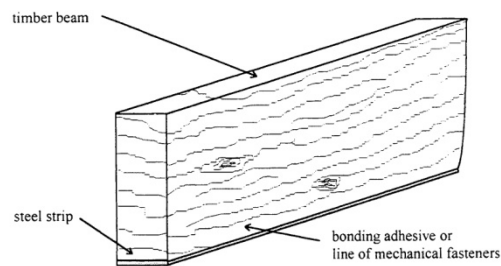


Figure 9: Bonded steel strip specimen (33) in Dorey & Cheng (42).

Krueger and his associates (30), (34), (35), (36), as cited in Bulleit (31), have examined the reinforcing of wood with a composite of epoxy resin and woven steel wire with a bronze coating. The beams were reinforced removing sections in tension and replacing them with the epoxy-steel composite. The goal was to determine methods and criteria for ultimate strength design of reinforced timber (31).

Uzielli (37) focuses on the reinforcement and reparation of existing structures. Among other methods he cites glued steel bars with epoxy resin inside grooves in the tension side of the beams. The failure is now not determined by irregularities in the tension side but because of compression failure. He reports improvements in structural capacity and stiffness, as well as increases in ductility.

Isoda et al (32) tested four metres span glulam beams with glued steel plates on the tension side as a part of a bigger project on hybrid structural members.

Table 3 Planning of experiments for hybrid timber structural members

Type of member		Section of glulam (mm)	Section of reinforcement (mm)	Fastener or adhesive (mm)	Span length of 3-point bending (mm)
Glulam beam with steel plate at top and bottom		100×200	6×65	2-LS*(d=9, l=75) @70	4,000 and 2,000
				LS (d=9, l=75) @70	4,000
				LS (d=9, l=75) @140	4,000 and 2,000
Glulam beam with steel plate at tension side		100×200	6×65	2-LS (d=9, l=75) @70	4,000
				LS (d=9, l=75) @70	
				LS (d=9, l=75) @140	

Table 4: Part of the timber-steel specimens reported by Isoda et al (32)

Kliger and his teams (38), (39), (40) studied timber beams enhanced with bonded steel plates and carbon-fibre-reinforced polymers (CFRP) in different arrangements, in the tension or both tension and compression sides. All specimens showed an increase in stiffness and ultimate moment capacity. Four point bending tests until failure and creeping tests were carried out. The arrangement of reinforcement can be used to control the failure mode and the mechano-sorptive creep was reduced.

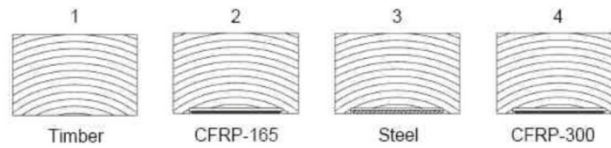


Figure 10: Different strengthening schemes and a reference for creep tests specimens (39).

Borri and Corradi (41) used high steel strength cords. The external bonding of steel fibres produced high increases in flexural stiffness and capacity.

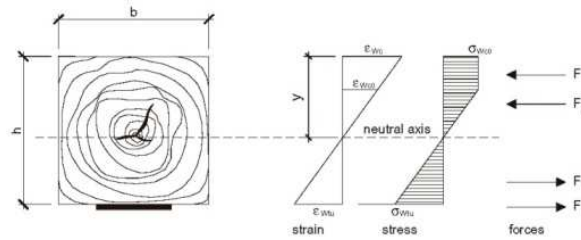


Figure 11: Distribution of strain, stress and forces in the cross section of a strengthened beam with high steel strength chords (41).

References:

Isoda et al (2000) _(32)

Sakamoto et al (2004) _(43)

González-Bravo (2007) _(44)

González-Bravo et al (2008) _(45)

González-Bravo (2009) _(46)

González-Bravo et al (2010) _(47)

González-Bravo et al (2011) _(48)

		PASSIVE				
		In grain direction				
		T	C	S	T+C	T+C+S
H	Outer					
	Inner					
V	Outer					
	Inner					
H+V	Outer					
	Inner					

Summary:

Isoda et al (32) and Sakamoto et al (43) report about solutions with bonded steel plates on the upper part of beams among many other timber-based hybrid structures. The objectives of the global project were the development of high-performance timber-based composite members and timber-based hybrid structures. Structural and fireproof performances were the main points to focus on.

González-Bravo and his collaborators (44), (45), (46),(47), (48) studied the reinforcement of existing timber beams with steel profiles connected with screws to the upper side of the beam. Glue laminated, sawn and old timber beams specimens were reinforced and tested. Increases in stiffness (from 45 to 98%) and load bearing capacity (from 27 to 58%) were reported.

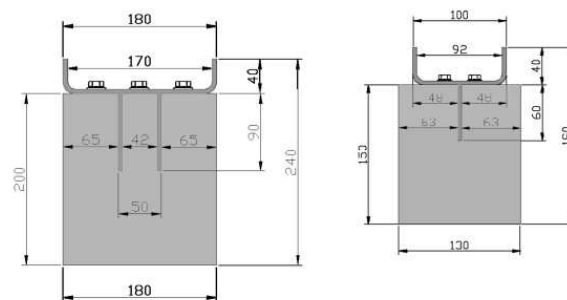


Figure 12: Steel cross-section reinforcement in timber sections of 180x200 mm and 130x150 mm (45).

Built examples:

The reinforcing system proposed by González-Bravo was used at least for the refurbishment of a building in Madrid (46).

References:

Granholm (1954) _(49)

Mark (1961) _(50)

Isoda et al (2000a) _(32)

Isoda et al (2000b) _(51)

Nakajima et al (2004) _(52)

		PASSIVE				
		In grain direction				
		T	C	S	T+C	T+C+S
H	Outer					
	Inner					
V	Outer					
	Inner					
H+V	Outer					
	Inner					

Summary

Granholm (49), cited in Bulleit (31), used square rods placed in grooves that had been cut in the bottom and top surfaces of both rectangular and I-cross section timber beams.

Mark (50), cited in Dorey & Cheng (42) and Kirilin (53), investigated the use of aluminium plates for reinforcement along the compressive and tensile faces of timber. Increased stiffness and strength were observed.

Isoda et al tested four metres span glulam beams with glued steel plates on both the tension and compression side as a part of a bigger project on hybrid structural members (32). Solutions with bolted specimens were also designed (51).

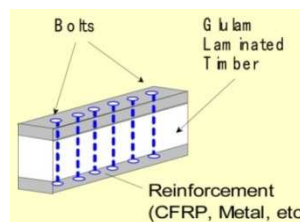


Figure 13: Image of hybrid timber members (51).

Nakajima et al (52) studied the creep performance of timber beams reinforced with steel plates on both tension and compression faces. The steel plates were mechanically fastened with go-through bolts to the timber. The creep performance was not affected. The slip between glulam and the steel plates was supposed to be the causing responsible of this bad performance.

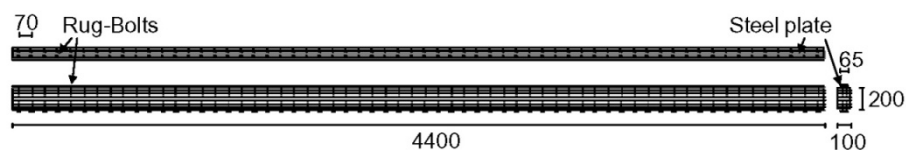


Figure 14: Test specimens type A (52)

		PASSIVE				
		In grain direction				
		T	C	S	T+C	T+C+S
H	Outer					
	Inner					
V	Outer					
	Inner					
H+V	Outer					
	Inner					

References:

- Shchuko (1969) _(54)
- Anon. (1964)_(55)
- Lantos (1964a)_(56)
- Lantos (1964b) _ (57)
- Lantos & Harvey (1964) _(58)
- Lantos & Wellner (1966) _(59)
- Dziuba (1980) _(60)
- Dziuba (1985) _(61)
- Candowicz & Dziuba (1989) _(62)
- Bulleit et al (1989) _(63)
- Fabris (1999) _ (64)
- Jorissen & Fragiaco (2010) _(65)
- Lu et al (2012) _(66)
- Kaestner et al (2014) _(67)

Summary:

Shchuko (54), cited in Alam (68), reinforced timber with steel rods situated at the outermost tensile fibres of the beam. He measured the cross section strains within the linear elastic range as being linearly distributed. Outside this range however, deviation from linear strain behavior was observed. He also reported the phenomenon of initial compression failure as a consequence of reinforcing beams on only the tensile face (68).

Bulleit (31) cites that The Timber Research and Development Association in Great Britain (55), (56), (57), (58), (59) examined the reinforcement of timber with steel rods. Both square and round cross-sections were used to reinforce laminated timber. The bars were placed in grooves prior to the laminating process in either the tension zone or the tension and compression zones. The bond between steel and wood was achieved with phenol-resorcinol formaldehyde resin or using serrated rods pressed in undersized grooves (31).

Dziuba (61), cited in Candowicz & Dziuba (62) and Alam (68), tested timber beams reinforced with steel rods bonded into the tensile face. Three reinforcement series comprised progressively increasing quantities of reinforcement and exhibited different failure modes. These were an outermost tension fibers break, tension fibers break when the compression area is partially yielding and compression failure. The failure on the compressive side was noted in each series. The tensile failure was reduced increasing the tensile reinforcement.

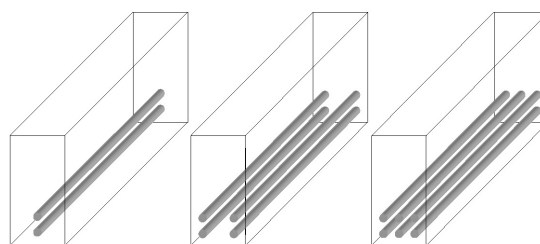


Figure 15: Geometric arrangement of Dziuba's experiments cited in (68).

Candowicz & Dziuba (62) continued the previous work and found that an increase in the amount of reinforcement causes an increase of the ultimate strength mean value and a decrease of standard deviation.

Bulleit et al (63) embedded concrete-reinforcing steel in oriented flakeboard. Beams were tested in dry (50% relative humidity) and wet (90% relative humidity) conditions. Dry beams showed increases in stiffness (24% to 32%) and in ultimate moment capacity (29% to 30%). The wet beams increased their stiffness also around 30% but did not show significant increases in strength. The lack of reinforcing effect is attributed to the reduction in the wood modulus of elasticity and flakeboard internal bond strength caused by increased moisture content.

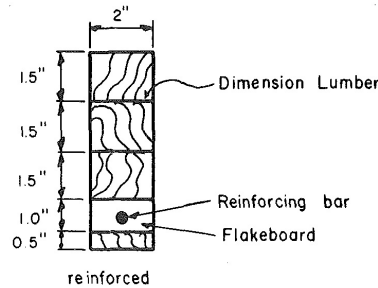


Figure 16: Typical beam cross sections in Bulleit (63)

Fabris (64) studied the reinforcement of the tension area of laminated veneer lumber (LVL) beams with corrugated steel bars of different qualities. The bonding material was epoxy resin. It was found that in the cases where the yielding strain of the steel corresponds approximately to the point of timber rupture the addition of the capacity of both materials is possible.

Jorissen & Fragiacomio (65) refer to glued-in reinforcements in the tension area as a way of increasing the ductility of timber, that is to ensure that plasticization in compression occurs before brittle failure in tension. This way stress redistribution in members subjected to bending would be possible.

Lu et al (66) found improvements in the creeping behavior of glulam beams reinforced with reinforcing steel bars in the tensile area.

Kaestner et al (67) developed several prototypes of the High-Tech Timber Beam® (HTTB), composed of glulam strengthened in the tension zone with steel bars or reinforced polymers with carbon or glass fibers. The compression zone is reinforced with polymer mortar. Shear reinforcement using polymer concrete casted steel rods is also used. Improvements in the flexural strength and stiffness are reported.

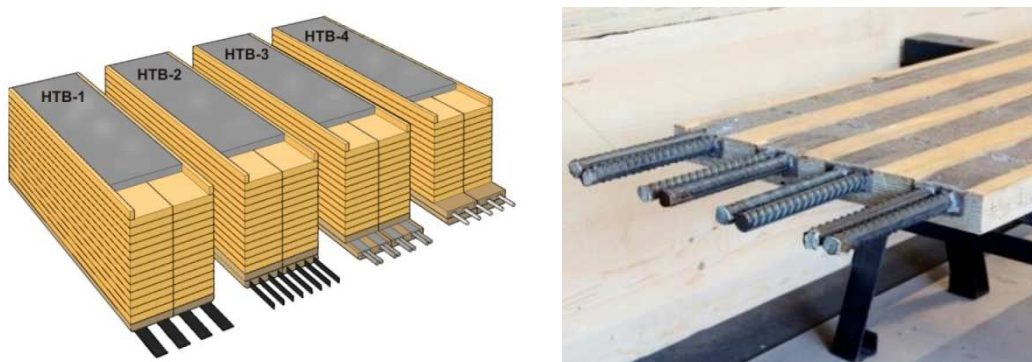


Figure 17: Prototypes of HTTB (left) and tension zone reinforcement with steel and LVL (right) (67)

References:

Lu et al (2012) _(66)

		PASSIVE				
		In grain direction				
		T	C	S	T+C	T+C+S
H	Outer					
	Inner					
V	Outer					
	Inner					
H+V	Outer					
	Inner					

Summary:

Lu et al (66) studied the bending creeping behavior of reinforced glulam beams. They tested 2,85 meters long beams reinforced with fiber-reinforced polymers (FRP) and steel bars under a four-point bending arrangement during six months. The reinforcements were located in the tensile area, tensile and compression areas or only compression area. They found improvements in the creeping behavior of glulam beams reinforced with reinforcing steel bars in the compression area, although not so good as with reinforcements on the tensile side.

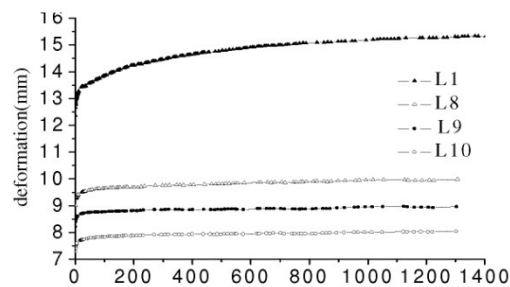


Figure 18: Creep deformation of glulam beams reinforced with steel bars. Specimens: L1- pure glulam beam; L8- 1Ø6 in the compression area; L9 - 1Ø6 in the tensile area; L10 - 1Ø8 in the tensile area (66).

References:

- Sliker (1962) _(69)
- Anon. (1964) _(55)
- Lantos (1964a) _(56)
- Lantos (1964b) _(57)
- Lantos & Harvey (1964) _(58)
- Lantos & Wellner (1966) _(59)
- Lantos (1970) _(70)
- Coleman (1974) _(71)
- Gardner (1991) _(72)
- Oiger (1997) _(73)
- Tasbeam(TM) _(74)
- Aralam (TM) _(74)
- Shioya et al (2016) _(75)
- Uchimura et al (2016) _(76)
- Kusumoto et al (2016) _(77)
- Yagi et al (2016) _(78)
- Subic et al (2016) _(79)

		PASSIVE				
		In grain direction				
		T	C	S	T+C	T+C+S
H	Outer					
	Inner					
V	Outer					
	Inner					
H+V	Outer					
	Inner					

Most important concepts:

Sliker (69), cited in Bulleit (31) and Alam (68), “reinforced both horizontally and vertically laminated wood beams with aluminium sheeting placed between selected laminations. Wood-to-wood bonding was accomplished using a resorcinol resin; and wood to aluminium bonds were made with an epoxy resin. Increases in stiffness were reported, but ultimate moment capacity showed only slight increases. Generally, as the amount of reinforcing was increased, the mode of failure shifted from compression or tension to shear” (31).

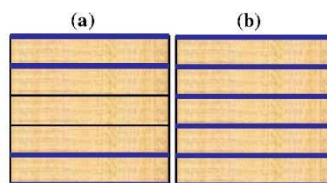


Figure 19: Cross sectional arrangement of beams tested by Sliker (69) with laminates of aluminium (in blue) as timber reinforcements cited by Alam (68).

Bulleit (31) cites that The Timber Research and Development Association in Great Britain (55), (56), (57), (58), (59) examined the reinforcement of timber with steel rods. Both square and round cross-sections were used to reinforce laminated timber. The bars were placed in grooves prior to the laminating process in either the tension zone or the tension and compression zones. The bond between steel and wood was achieved with phenol-resorcinol formaldehyde resin or using serrated rods pressed in undersized grooves (31). Kirilin (53) cites also the work of Lantos (70), who continued the investigation using phenol-resorcinol formaldehyde adhesive to fix the square or round steel rods placed between the two outer laminations along the full length of the beam in both the tensile and compressive zones.

Coleman (71), cited in Kirilin (53), used three laminations of wood, with two U shaped sections surrounding the compressive and tensile zones of the central lamination. Coleman used the U-shaped reinforcement in the central fifty percent of moment members and steel plates in the high shear regions of a shear beam (53).

Gardner (72), cited in Dorey and Cheng (42), developed a system which located a steel reinforcing bar inside of a glulam sample. Some mechanical properties were enhanced by as much as 208% when compared with unreinforced specimens. Moreover the steel reinforcing in the tested glulam beam had significantly reduced the creep of the member to an almost negligible level.

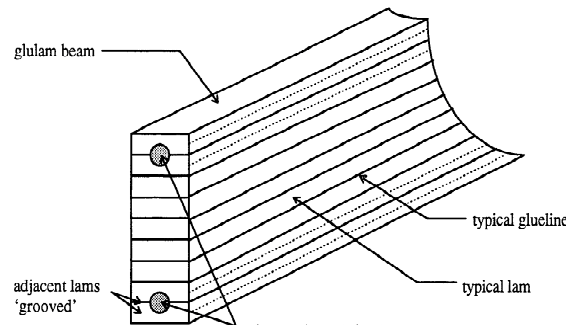


Figure 20: Rebar-glulam beam by Gardner (72) cited by Dorey and Cheng (42).

Oiger (73) investigated reinforced and prestressed glulam beams. The reinforced bars were symmetrically arranged in the cross section without or with prestress. He concludes that relatively simple methods could be used to analyse unstressed reinforced beams. The reduced (equivalent) section method offers sufficient accuracy. He also points out that the load carrying capacity and stiffness depend on the intensity of reinforcement, but the shear capacity of the beam, which sometimes tends to be unsatisfactory, should be observed carefully in the design process.

Schober et al (74) review the possibilities of timber with passive reinforcement and make reference to two commercial systems, i.e. the Tasbeam® and the Aralam®. They present them as an alternative to the high-performance fibres using instead common and less expensive rebars. Steel rebars are inserted into longitudinal holes and, after being in place, adhesive is injected under pressure through small holes in the top surface of the timber element. At the same time it is pointed out that some preliminary studies cast doubt over if the increase in strength compensates the cost, because the manufacturing process is even more complex than bonding fibre reinforcement strips to the tensile face of timber beams.

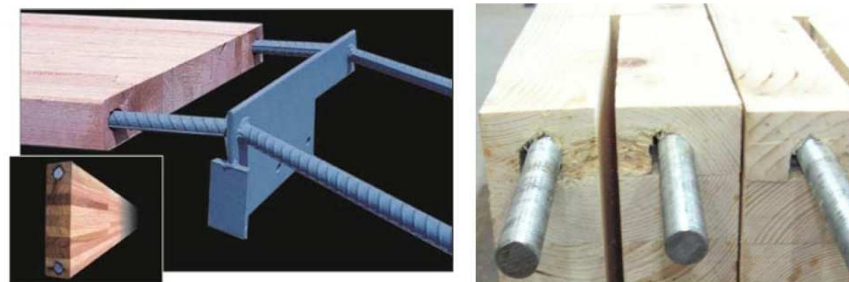


Figure 21: Steel reinforcement systems, Tasbeam® (left) and Aralam® (right) in Schober et al (74)

The Department of Architecture and Architectural Engineering of the Kagoshima University in Japan developed a hybrid timber system using glulam, deformed steel bars and epoxy resins adhesives. The objective was to improve flexural stiffness and strength in glulam of rapid grown Japanese cedar. They studied both beams and columns (75), beam-to beam moment resisting joints (77), the long-term behaviour of beams (76), and the bending performance of the reinforced beams connected to CLT plates (78). Stiffness and strength were increased meanwhile creeping reduced.



Figure 22: Interface and jointing bars for the moment resisting joints of the RGTSB system (77)

Subic et al (79) studied aluminium-wooden hybrid beams in order to improve bending stiffness and load-bearing capacity of wooden beams for big-sized windows.

Built examples:

Gardner (72), cited in Dorey and Cheng (42), reports that the developed rebar-glulam beams are in use in many structures in Australia.

The studies of the Department of Architecture and Architectural Engineering of the Kagoshima University in Japan lead to the building of the “Samurai” Prototype Building in the year 2014.

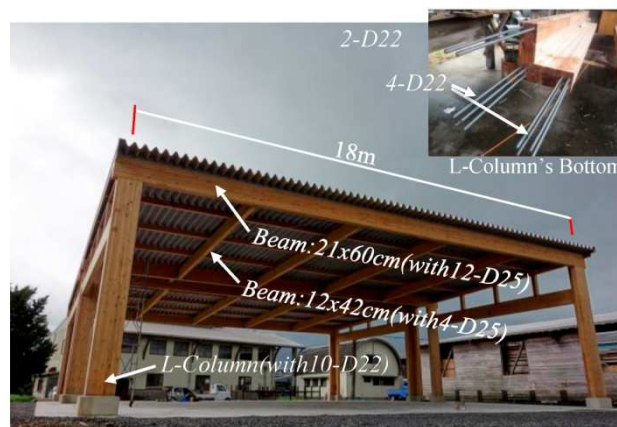


Figure 23: The first prototype building, “Samurai”, utilizing glulam timber reinforced using deformed steel bars and epoxy resin adhesives (RGTSB)(75)

3.2.2 Vertical steel arrangements

References:

Nielsen (1999) _(80)

		PASSIVE				
		In grain direction				
		T	C	S	T+C	T+C+S
H	Outer					
	Inner					
V	Outer					
	Inner					
H+V	Outer					
	Inner					

Summary:

Nielsen (80) analysed the behaviour of timber reinforced with punched metal plate fasteners. The focus of the study was trusses which joints were already built with punched metal fasteners. Therefore the idea of using the same product for reinforcing the trusses where peak moments appear. Failure load and stiffness were increased by 20% to 30%

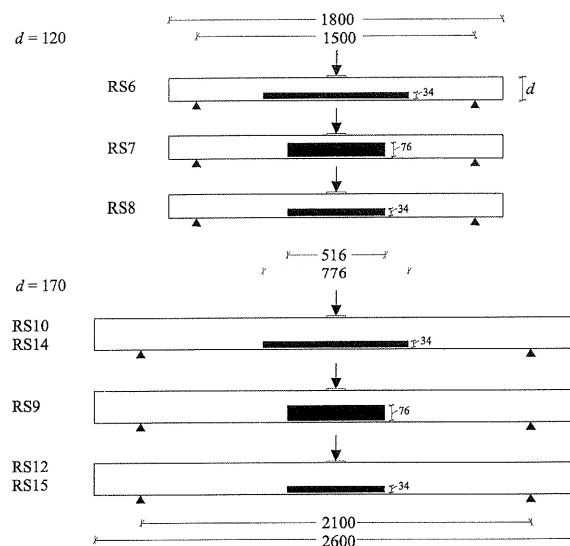


Figure 24: Test specimens with plate reinforcement by Nielsen (80)

References:

Tanaka et al (2006) _(81)

		PASSIVE				
		In grain direction				
		T	C	S	T+C	T+C+S
H	Outer					
	Inner					
V	Outer					
	Inner					
H+V	Outer					
	Inner					

Summary:

For this particular case of timber-steel combination no examples of beams were found. Nevertheless at least an example of timber columns reinforced with steel plates and carbon fibre sheets exist in the literature. Its inclusion in this review is due to the focus of the research on the buckling strength of columns with reinforcement about the buckling axis, which, although a different structural problem, in some aspects offer points of connection with the performance of bending beams.

Tanaka et al (81) reinforced timber columns attaching steel plates to the outside surface about the buckling axis. Steel plates were attached using lag screws. Following the authors it is generally understood that the hybrid timber columns have a high performance in terms of stiffness, strength and deformation capacity. The buckling strength of hybrid timber columns reinforced with steel plates resulted larger than unreinforced glulam at a large slenderness ratio. The authors also reported different failure mechanisms depending on slenderness: compressive failure of glulam for colums with an small slenderness, tensile failure at the mid-height of the column during buckling deformation for the specimens with high slenderness. Also the local buckling of steel for the steel-reinforced columns with a direct axial force at the end of the column was observed.

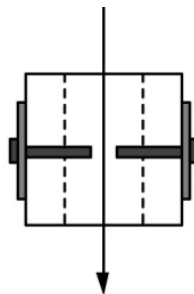


Figure 25: Cross section of column reinforced with steel plates (81)

References:

Dolby (1990) _(82)

Echavarría et al (2014) _(83)

		PASSIVE				
		In grain direction				
		T	C	S	T+C	T+C+S
H	Outer					
	Inner					
V	Outer					
	Inner					
H+V	Outer					
	Inner					

Summary:

Dolby (82) studied wooden laminated beams joined with nail-plates as a cheap alternative to glulam. The nail plates were placed on the outside of the beam joining the laminations to a structural composite. The size and spacing of the nail-plates should be designed depending on the shear. Experiments with four metres long beams were carried out. The mode of failure was characterized by teeth withdrawals in the most-stressed nail plates. Long-term loading tests were carried out during 170 days.

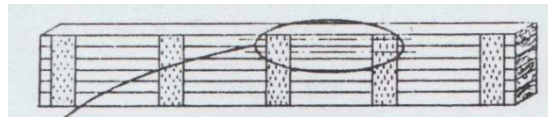


Figure 26: Wooden laminated beam joined with nail-plates (82)

Echavarría et al (83) investigated the mechanical performance of glulam beams also reinforced by punched metal plates. The local reinforcement is proposed for improving the flexural strength in areas with a moment peak. Apart from the increased of strength and stiffness a more uniform behaviour that not reinforced specimens was also reported. This leads to a decreasing in the coefficient of variation and shows that the failure load is less sensitive to weak timber sections.

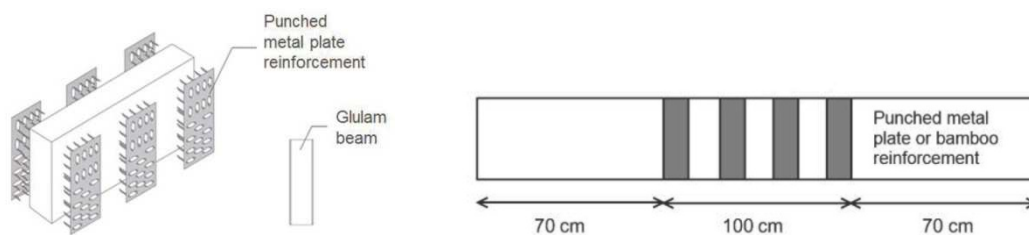


Figure 27: Punched metal plate reinforced glulam beams (83)

References:

Steurer (1999) _(84)

Kliger et al (2007) _(85)

Jacob & Garzón Barragán (2007) _(86)

Alam (2004) _(68)

De Melo Moura et al (2008) _(87)

		PASSIVE				
		In grain direction				
		T	C	S	T+C	T+C+S
H	Outer					
	Inner					
V	Outer					
	Inner					
H+V	Outer					
	Inner					

Summary:

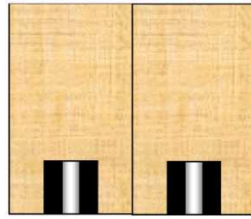
Steurer (84) studied possibilities of reinforcement with steel or different glass, aramid or carbon fibres. Asymmetric reinforcements were also tested in six metres long beams, being the reinforcing steel plates vertically arranged and glued inside grooves in the bottom part of the beam. Comparisons with the not reinforced reference cross-sections showed improvements in the bending stiffness.

Kliger and his team (85), (86) tested four metres span beams with steel and carbon fibres reinforcements only in tension or in both the tension and compression sides. The steel plates were glued to the timber in vertical grooves using the adhesive SikaDur®-330. The results of the laboratory tests and theoretical analyses showed that all interventions resulted in higher stiffness and higher ultimate moment capacity and the arrangement or reinforcement can be used for controlling the failure mode.



Figure 28: Reinforcement configuration with 4x(4mm x 30 mm) steel plates (85)

Alam (68) also studied similar reinforcements but for LVL beams with steel and glass or fibre reinforced polymers. The reinforcements are adhesively bonded. He also studied similar systems for the reparation of fracture spruce beams.



TENSION FACE REINFORCEMENT

Figure 29: Tension face reinforcement specimens (68)

De Melo Moura et al (87) researched metal reinforcements for improving the behavior of fast-grown pine and eucalyptus with the idea of turning them competitive for structural applications. Cantilever metal profiles were inserted and glued. They tested reinforcements on compression or the tension side, being the last ones more efficient. Reinforced beams offered a better behavior than the not reinforced ones and the metal reinforcement proved to be more efficient as the wood has low mechanical properties.

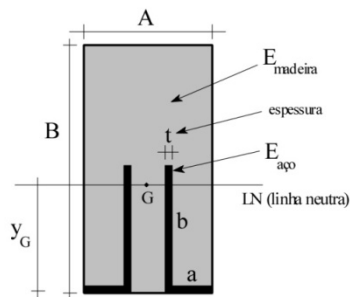


Figure 30: Geometric parameters and cross-section of reinforced beams (87)

		PASSIVE				
		In grain direction				
		T	C	S	T+C	T+C+S
H	Outer					
	Inner					
V	Outer					
	Inner					
H+V	Outer					
	Inner					

References:

Borgin et al (1968) _(33)

Uzielli (1995) _(37)

Jones (1997) _(88)

Fontana (1999) _ (89)

Alam (2004) _(68)

De Melo Moura et al (2008) _(87)

Summary:

Borgin et al (33), cited in Bulleit (31) and Alam (68), used vertically oriented steel strips to reinforce horizontally laminated wood beams. The beams were reinforced by bonding steel strips into vertical grooves using an epoxy resin. Reinforced was placed on either the compression side or both the compression and the tension sides. Increases in both strength and stiffness were reported. Beams reinforced on the compression side failed from either wood tension failure or horizontal shear failure and were found to yield lower flexural stiffness values compared to beams reinforced on both faces (31),(68).

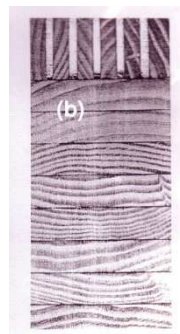


Figure 31: Vertically laminated steel-timber composite beam by Borgin (33). The steel reinforcement comprises 5% of the total cross sectional area. Cited in (68)

Uzielli (37) focuses on the reinforcement and reparation of existing structures from the upper part of the original beams. Among other methods he cites glued steel plates with epoxy resin inside vertical grooves all along the length of the beam. The steel plates, protected by wood against fire and corrosion, take almost the whole load of the original beams.

Jones (88), cited in Alam (68), reinforced solid timber beams from the compressive side down to the tensile face with steel rods. The specimens failed in tension. It was reported that the use of an adhesive with a low modulus of elasticity significantly reduced the strength and stiffness enhancement and

therefore a good quality and stiff adhesive appears to be essential for achieving superior mechanical performance for rod reinforcements.

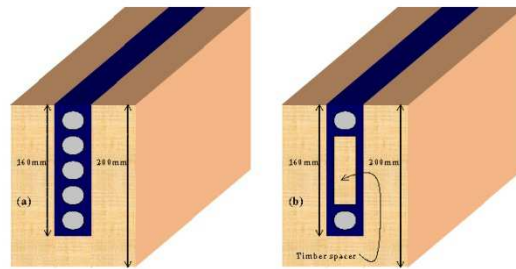
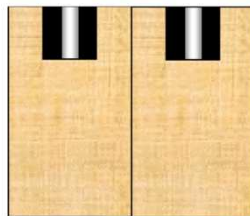


Figure 32: Geometric arrangement of tests by Jones (88) cited in Alam (68)

Fontana (89) makes reference to beams reinforced with glued steel strips on the upper side for obtaining timber-steel composite performance.

Alam (68) propose, among others, upper side steel strip reinforcements for the reparation of fractured spruce beams.



COMPRESSION FACE REINFORCEMENTS

Figure 33: Compression face reinforcements for the reparation of beams by Alam (68)

De Melo Moura et al (87) researched metal reinforcements for improving the behavior of fast-grown pine and eucalyptus with the idea of turning them competitive for structural applications. Cantilever metal profiles were inserted and glued. They tested reinforcements on compression or the tension side, being the last ones more efficient. Reinforced beams offered a better behavior than the not reinforced ones and the metal reinforcement proved to be more efficient as the wood have low mechanical properties.

References:

Robinson (1987) _(90)

Guan & Gendall (2008) _(91)

Nail Web® _(92)

TecBeam® _(93)

Posi-Joist® _(94)

		PASSIVE				
		In grain direction				
		T	C	S	T+C	T+C+S
H	Outer					
	Inner					
V	Outer					
	Inner					
H+V	Outer					
	Inner					

Summary:

Robinson (90) studied space joists with irish timber, a system composed of two timber chords separated by a metal lattice. The idea appears because of the considerable quantity of small sawlogs produced in Irish forest, which otherwise would not normally be used in building construction.

Guan and Gendall (91) researched the buckling behaviour of steel webbed timber joists. This type of product is interesting because it offers low self-weight and uses timber of small sections from fast-grown trees. But the thin-walled nature of the steel web and the slenderness of the cross sections are weak point which could be limiting, especially in the case of lateral buckling.

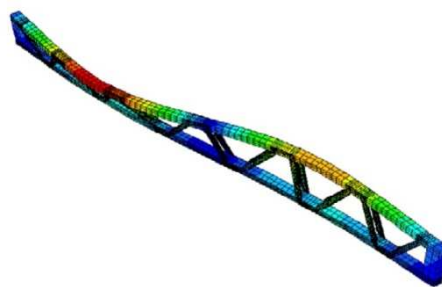


Figure 34: Out of plane buckling of steel webbed joist with centre restraint (91)

There exist a series of commercial products like Nail Web® (92), TecBeam® (93), Posi-Joist® (94) and others, which share quite common characteristics. Two timber chords of small dimensions are connected thanks to a light steel web. This web can be a lattice or a thin folded steel plate. The result is a very light joist, where the timber elements withstand compression and tension forces, meanwhile the steel web resists the shear forces. The timber chords make easy their combination with other common light framing construction elements which can be nailed or screwed to the joists.

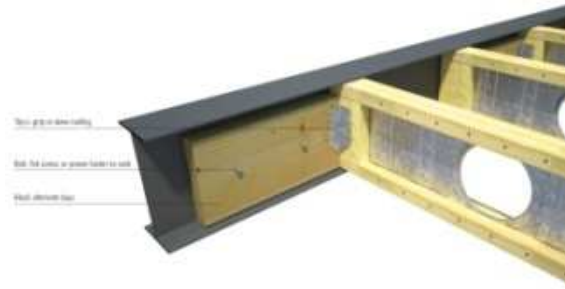


Figure 35: TecBeam® (93)



Figure 36: Posi-Joist® (94)

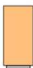


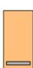






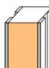



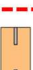
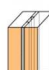






Figure 37: Nail Web® (92)

Built examples:

As already mentioned, timber-steel joist are a successful commercial product due to its simplicity, lightness and cost-competitiveness. They are used for roofs and floors, especially as an alternative or combined with light timber framed structures. Examples of buildings where these elements were used are very numerous, mainly in countries where the light timber frame structures are widely used like Australia, New Zealand, the United States of America and Great Britain.

Some Australian examples are the Luxury Residential, the East Timor Embassy Fund –in Canberra, the Cecil Saint Multi-Townhouse in South Melbourne, and the Duke St Refurbishment in Windsor.

		PASSIVE				
		In grain direction				
		T	C	S	T+C	T+C+S
H	Outer					
	Inner					
V	Outer					
	Inner					
H+V	Outer					
	Inner					

References

- Borgin et al. (1968) _(33)
- Hoyle (1975) _(95)
- Usuki et al (2000) _(96)
- Usuki et al (2002) _(97)
- Usuki et al (2003) _(98)
- Kiss et al (2005) _(99)
- Kiss et al (2006) _(100)
- Honda et al (2006) _(101)
- Kiss et al (2008) _(102)
- Gotou et al (2008) _(103)
- Chida et al (2010) _(104)
- Alam (2004) _(68)
- Alam et al (2004) _(105)
- Alam et al (2012) _(106)
- Kliger et al (2007) _(85)
- Jacob & Garzón Barragán (2007) _(86)
- Kliger & André (2013) _(40)
- Lawson et al (2008) _(107)
- Negrao et al (2011) _(108)
- Wenighofer et al (2016) _(109)

Summary:

Borgin et al (33), cited in Bulleit (31) and Alam (68), used vertically oriented steel strips to reinforce horizontally laminated wood beams. The beams were reinforced by bonding steel strips into vertical grooves using an epoxy resin. Reinforced was placed on either the compression side or both the compression and the tension sides. Increases in both strength and stiffness were reported. Beams reinforced on both sides failed in the reinforcement lamina in either tension or compression (31).

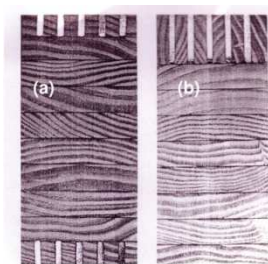


Figure 38: Vertically laminated steel-timber composite beams by Borgin (33). The steel reinforcement comprises 5% of the total cross sectional area. Cited in Alam (68)

Hoyle (95), cited in Alam (68), connected two toothed steel plates to surrounding timber members pressing the four elements together. Hoyle found that the specimens under flexural load and taken to failure suffered buckling of the plates in the compressive side of the beam, although this was not so marked for causing the timbers members to separate.

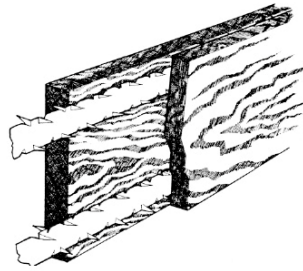


Figure 39: The “Steelam” beam form Hoyle (95) is composed from two plates with protruding toothed connectors mechanically sandwiched between two timber members. Cited in Alam (68)

Teams from the Akita University in Japan (96), (97), (98), (99), (100), (101), (102), (103), (104) studied the reinforcement of glulam beams with inserted vertical upper and lower steel plates. The idea came for reinforcing the jointing areas and the steel plates were bonded with epoxy resin. The reinforcement of both upper and lower sections of the beam makes that the shear stresses could become limiting for the structural performance of the pieces.

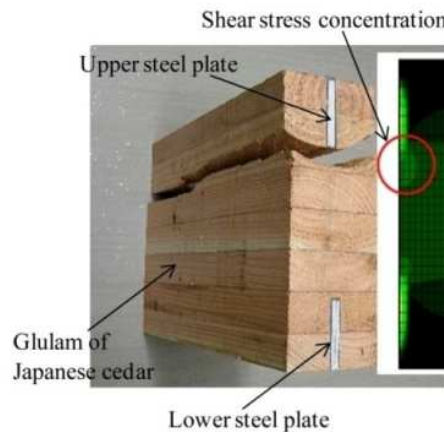


Figure 40: Shear fracture of Japanese cedar glulam beam reinforced with steel plates (104)

Alam and collaborators (68), (105), (106) reinforced LVL beams with bonded-in plates and rods, studying the effects of the placement of reinforcement with different configurations. Improvements in strength and stiffness were reported. The yield strength increased linearly as a function of increasing the reinforcement volume fraction meanwhile the flexural modulus followed more closely a power law regression.

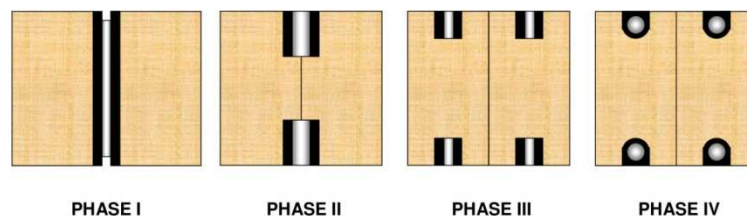


Figure 41: Composite beam reinforcement configurations by Alam et al (106)

Kliger and his teams (85), (86), (40) tested four metres span beams with steel and carbon fibres reinforcements only in tension or in both the tension and compression sides. The steel plates were glued to the timber in vertical grooves using the adhesive SikaDur®-330. The results of the laboratory tests and theoretical analyses showed that all interventions resulted in higher stiffness and higher ultimate moment capacity and the arrangement or reinforcement can be used for controlling the failure mode.

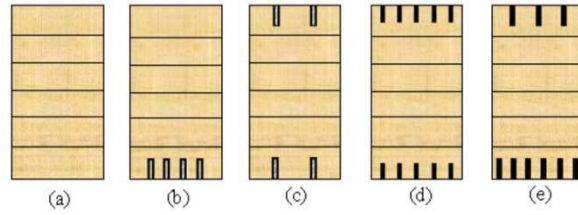


Figure 42: Reinforcement configurations studied by Kliger et al (40); (b) and (c) steel, (d) and (e) CFRP

Lawson et al (107) combined cold-formed steel sections as chords with plywood webs to create composite joists. The elements were connected with countersunk screws. Floor arrangement composed of two joists and a floor boards metres were tested under bending. The double web box-shaped “plyweb” joist with ballistically nailed plywood to C section flanges is reported as having optimum characteristics and minimum shear deformation. The effective flexural rigidity of the composite floor joist may be calculated as 70% of the flexural rigidity of an equivalent I beam, ignoring the web, which takes account of slip in the fixings.

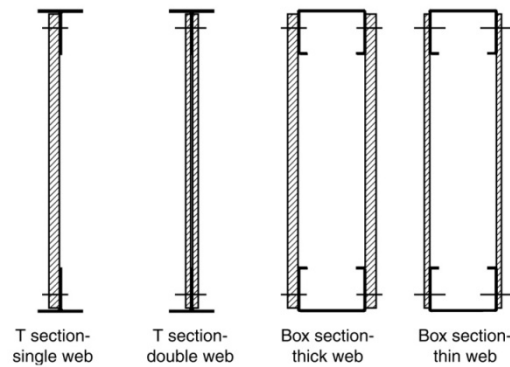


Figure 43: Steel-timber joist configurations using T and C section flanges (107)

Negrao et al (108) studied theoretically the reinforcement of glulam with inner steel plates. The objective was the development of a fire resistance cross section where the steel plate, protected against fire with the surrounding timber, would take more percentage of the existing load as the timber is consumed. A parametric study yielded the result that the reinforced system could double the fire resistance time of a non reinforced beam.

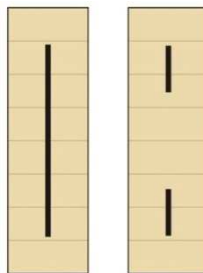


Figure 44: Reinforced section studied by Negrao et al (108)

Wenighofer et al (109) developed a timber hybrid beam with glued aluminium profiles in the spruce flanges, the Doka formwork I tec pro. The new design of the beam, designed as a component of a formwork system, increased the load bearing capacity allowing at the same time the connection of other system components in the integrated aluminium rails. Extensive research was carried out for finding appropriate gluing systems. Pre-treatment of aluminium in combination with 1-K PUR offered the best performance in tests.

Built examples:

The research of the teams from the Akita University was developed around the project and construction of the Bouchu Bridge in Japan in the year 2010, a king-post type structure where the steel plate reinforcing technique, among other innovations, was applied.

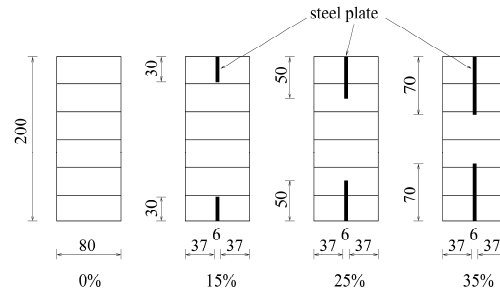


Figure 45: Image of the Bouchu Bridge(101) and reinforced beams tested before its construction (103)

		PASSIVE				
		In grain direction				
		T	C	S	T+C	T+C+S
H	Outer					
	Inner					
V	Outer					
	Inner					
H+V	Outer					
	Inner					

References:

- Sliker (1962) _(69)
- Kumar et al (1972) _(110)
- Stern & Kumar (1973) _(111)
- Coleman & Hurst (1974) _(71)
- NAHB (1981) _(112)
- DeStefano & MacDonald (1997) _(113)
- DeStefano (2007) _(114)
- Steurer (1999) _ (84)
- Ban et al (1999) _(115)
- Hart & Fast (2000) _(116)
- Alam (2004) _(68)
- Alam & Ansell (2012) _(117)
- Isoda et al (2000) _(51)
- Sakamoto et al (2004) _(43)
- Koshihara et al (2005) _(118)
- Isoda et al (2010) _(119)
- Koshihara (2014) _(120)
- Trada (2006) _(121)
- Gotou et al (2012) _(122)
- Gang-Nail Manual (2007) _(123)
- Pryda (2013) _(124)

Summary:

Sliker (69), cited in Bulleit (31) and Alam (68), bonded aluminium laminates to timber with a rigid epoxy system. He tested both horizontal and vertical laminates and found that laminating timber horizontally is more effective than vertically when equal volume fractions of reinforcing material are used. Tensile fracture was reported as the governing failure mode for vertically laminated specimens.

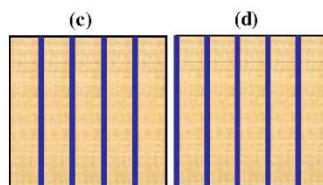
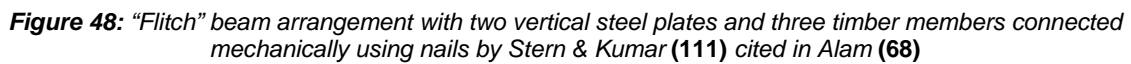
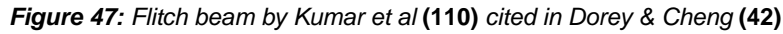


Figure 46: Vertical laminates of aluminium (in blue) tested by Sliker (69), cited in Alam (68)

Kumar et al (110), cited in Dorey & Cheng (42), and Stern & Kumar (111), cited in Alam (68), developed beams with internal vertical steel plates known as flitch beams. The connection between elements is made with nails. The specimens tested by Stern & Kumer (111) yielded on average 48% increase in flexural stiffness and a 45% increase in flexural strength relative to un-reinforced beams.



The National Association of Home Builders (NAHB) of the USA published in 1981 a Manual of Fitch Plate and Steel I-Beams (112) with design tables taking into account design loads, plate thickness and spacing of connector nails.

Steurer (84) studied cross-sections similar to flitch beams but gluing the steel plates to the timber pieces.

46

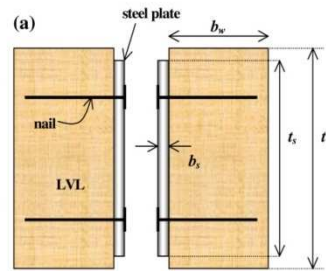


Figure 50: Schematic cross-section of a beam pair showing the arrangement of steel plates and nailing direction (117)

Flitch beams or timber beams reinforced with internal vertical steel plates are referenced also by teams of Japanese researchers in their studies of hybrid structures (32), (43), (118), (119), (120).

Other flitch beams calculation manuals or rules were published by TRADA (121) or companies like Pryda (124) or MiTek (123).

Gotou et al (122) use a variation of flitch beams for a less common use like a bridge deck. In this case the combination is made between a stress-laminated deck that has vertical perforated steel plates on the outer borders. The authors report about bending stiffness of several tens of times larger than those of one-deck stress-laminated deck bridges.



Figure 51: One-box test model (plate) of timber-steel hybrid deck bridge (122)

Built examples:

The use of flitch beams was quite popular and used in combination with timber frame structures in countries like New Zealand, Australia and the USA. This reinforced beams were used for allowing bigger spans or carrying more loads in specific parts of conventional timber frame constructions. Apart from this particular and practical use, with numerous built examples, there exist other type of buildings where several variations of this structural element were used as an integral part of the structural design.

Ban et al (115) report the design and construction of the Nagano Olympic Memorial Arena in Japan in 1998 with a hanging roof composed of “composite beams” from glulam with inserted steel plates.

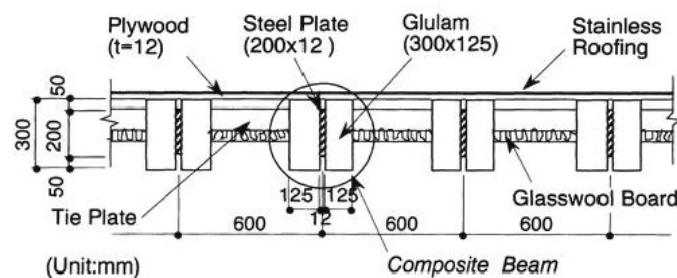


Figure 52: Section of the hanging roof of the Nagano Olympic Memorial Arena (115)

Hart & Fast (116) offer several examples of material combinations incorporating wood. One of them is the Rupert Station in Vancouver, Canada, from the year 2000. In this structure timber beams are connected to an inner steel plate.



Figure 53: Visualization of the Rupert Station in Vancouver (116)

Other example is the District of North Vancouver Municipal Hall Atrium, also from the year 2000, where the same design principle is applied to a grid of roof beams.

Other built examples with flitch beams exist in Japan, like the Saitama Prefectural Budokan from the year 2003 cited by Isoda et al (32). In this cases steel plates are placed inside glulam beams and studs forming a tridimensional framed roof structure.

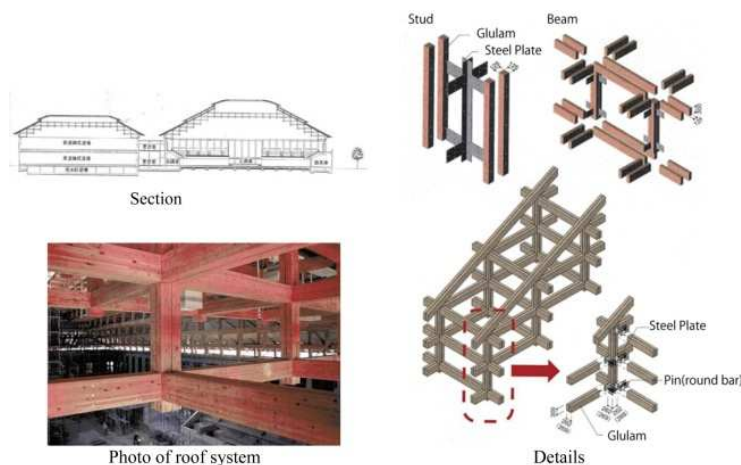


Figure 54: Roof system of the Saitama Prefectural Budokan (32)


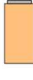
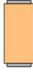

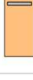















The Kanazawa M Building in Japan built in the year 2005 (119), (118), (120) is a five storey building with a timber-steel structure. The floor beams are composed by a glulam cross-section with a vertical steel plate inserted in it.



Figure 55: Kanazawa M Building (2005). Façade, interior view and cross section of the floor beams (120)

References:

Radford et al (2002) _(125)

		PASSIVE				
		In grain direction				
		T	C	S	T+C	T+C+S
H	Outer					
	Inner					
V	Outer					
	Inner					
H+V	Outer					
	Inner					

Summary:

Radford et al (125), cited in Alam (68), proposed the “shear spikes” concept for the repair of beams. The spikes are inserted at intervals along the length of two timber beams stacked on top of each other. This way the two beams are connected creating a semi-composite cross section, but less effectively than other procedures like gluing.

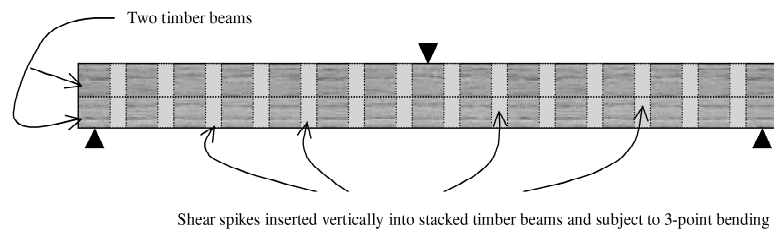


Figure 56: “Shear spike” concept by Radford et al (125) cited in Alam (68)

3.2.3 Combination of horizontal and vertical steel arrangements

References

Mark (1963) _(126)

		PASSIVE				
		In grain direction				
		T	C	S	T+C	T+C+S
H	Outer					
	Inner					
V	Outer					
	Inner					
H+V	Outer					
	Inner					

Summary:

Mark (126), cited in Bulleit (31), “reinforced small rectangular and trapezoidal beams with aluminium. Beams with a trapezoidal cross section were reinforced with aluminium facings that enclosed all four sides and had an extended aluminium flange on the wider base of the trapezoid. The wide flange was placed in compression. Beam failure was generally initiated by tension failure of the aluminium facings in the tension zone.” (31) .

		PASSIVE				
		In grain direction				
		T	C	S	T+C	T+C+S
H	Outer					
	Inner					
V	Outer					
	Inner					
H+V	Outer					
	Inner					

References

Tharmabala & Bakht (1986) _(127)
Bakht & Tharmabala (1987) _(128)

Taylor & Ritter (1990) _(129)

Krisciunas (1996) _(130)

Ma & He (2012) _(131)
He et al (2014) _(132)

Loss et al (2014) _(133)
Loss et al (2015) _(134)

Hassanieh et al (2016) _(135)
Hassanieh et al 2 (2016) _(136)
Keipour et al (2016) _(137)

Zimmer & Augustin (2016) _(138)

Summary:

Tharmabala & Bakht (127), (128) developed steel-wood composite bridges composed of a transversely prestressed laminated wood deck connected to steel girders with a bulkhead shear connector. This shear connector was developed though experimental studies. They tested a half-scale model of the bridge system statically and dynamically for confirming the feasibility of the system.

Ma & He (131) and He et al (132) proposed a prototype timber-steel hybrid structure composed of steel moment-resisting frames, timber-steel hybrid diaphragms and infill wood-frame shear walls. The hybrid diaphragms are composed by ribs of two cold-formed thin-walled C steel sections joined with bolts screwed to a dimension lumber deck covered with a mortar layer. One main point of the research was the evaluation of the in-plane rigidity of the floor plates, important condition for they use as part of the global system in seismic situations. The in-plane stiffness and load carrying behaviour of these diaphragms was obtained by tests. Results showed that the in-plane deformation of the diaphragm is governed by shear deformation.

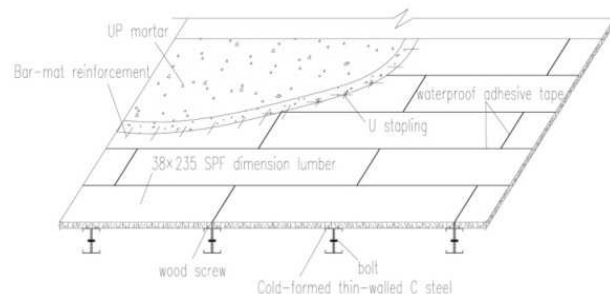


Figure 57: Timber-steel hybrid diaphragm by He et al (132)

Loss et al (133), (134) proposed a steel frame with hot-rolled sections and CLT panels placed over them and mechanically fixed to the beams.

Hassanieh et al (136), (135) and Keipour et al (137) proposed steel-timber composite (STC) beams. In this case laminated veneer lumber (LVL) panels are connected to the steel girders by mechanical shear connectors (screws or bolts) or glue. Push-out tests were carried out for investigating the load-slip behavior of the different connections proposed. Four point bending tests were carried out for investigating the load-deflection response, short-term stiffness, peak load capacity and failure modes. The glued specimens reached almost full composite action. The comparison with conventional steel-concrete composite floors showed that this have higher loading capacity (around 20%) compared with steel-timber composites with identical slab and shear connector size and spacing. However the construction of STC beams is less demanding in terms of labor force and time.

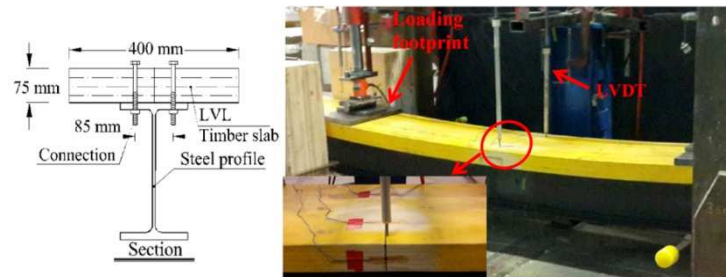


Figure 58: Geometrical outline and four-point bending tests on steel-timber composite beams (136)

Zimmer & Augustin (138) combined trapezoidal steel plates glued to CLT elements for studying a hybrid possibility for long span timber floors. The bending stiffness required can be adjusted depending of the project demands and placing the steel part on the tension side a ductile failure mode can be achieved. This alternative is proposed as a way for saving timber in long span floors, where the thickness of CLT needed is considerable.

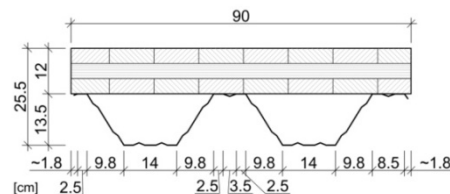


Figure 59: Dimensions of the cross section of the version I of timber-steel composite plates (138)

Built examples:

Taylor & Ritter (129) report about a prototype bridge built in North Dakota, USA, in the year 1988 by Wheeler Consolidated Inc using similar techniques as the ones proposed by Tharmabala & Bahkt (127). Krisciunas (130) reports about several composite wood-steel bridges built in Ontario following the research by Tharmabala & Bahkt (127). Three bridges were built from 1991 to 1994: the North Pagwachuan River Bridge built in 1991 and the Aubinadong River Bridge and the Hoiles Creek Bridge from the year 1994. These examples connect steel girders to a stress laminated wood deck with grout filled shear bulkheads.

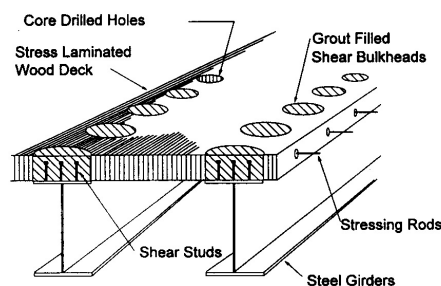




















Figure 60: The concept of composite steel-wood bridge deck (130)

References:

Lim et al (2010) _(139)

		PASSIVE				
		In grain direction				
		T	C	S	T+C	T+C+S
H	Outer					
	Inner					
V	Outer					
	Inner					
H+V	Outer					
	Inner					

Summary:

Lim et al (139) proposed small hybrid beam sections composed of aluminium or steel pipes inserted into hollow pine timber beams for their use as guardrails. Static bending tests were carried out. The performance of the steel specimens was better than the aluminium ones; the bending moment withstood by the hybrid sections was higher than the comparison hollow timber beams. The failure of all the specimens occurred because of rupture in the tension side.

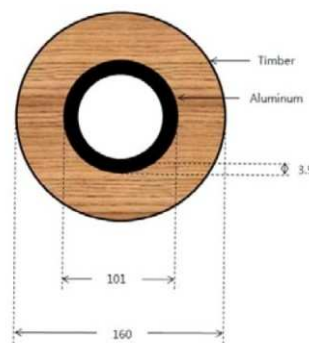


Figure 61: Hybrid beam consisting of hollow timber section and inner aluminium or steel pipe (139)

References:

Ito et al (2012) _(140)

		PASSIVE				
		In grain direction				
		T	C	S	T+C	T+C+S
H	Outer					
	Inner					
V	Outer					
	Inner					
H+V	Outer					
	Inner					

Summary:

Although it is not a beam case, here a proposal by Ito et al (140) is referenced due to the interest of the timber-steel combination. A plywood panel – steel composite member was proposed. In this case a slender steel column is sandwiched between two sheets of plywood and was tested under compression. The maximum strength was determined by the flexural buckling. The plywood panel was used as a stiffener for the slender steel member. The concept looks for reducing the volume of steel needed for lightweight building structures and a simple construction process.

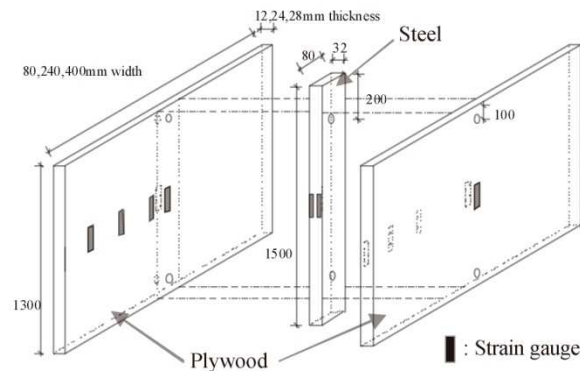


Figure 62: Elements of the plywood-steel panel composite (140)

References:

- Kimura et al (1990) _(141)
 Sakamoto et al (2004) _(43)
 Yamaguchi et al (2008) _(142)
 Koshihara (2014) _(120)
 Izumi (2008) _(143)
 Izumi et al (2008) _(144)

		PASSIVE				
		In grain direction				
		T	C	S	T+C	T+C+S
H	Outer					
	Inner					
V	Outer					
	Inner					
H+V	Outer					
	Inner					

Summary:

Kimura et al (141) designed and studied experimentally composite beams combining LVL and steel. A steel lattice composed from C cold-formed steel channels and welded round bars is connected laterally with bolts to two LVL beams. Flexural rigidity tests and creeping tests were carried out, the last one using 1:2 scaled beams. The results showed that the combination of LVL and steel provided a very high degree of composite action. The creep deflection of the composite beams was reduced, compared to a pure timber beam, because the existence of the metal lattice decreased the stress level of the timber members.

Several Japanese researchers (43), (142), (120) make reference to buildings solutions where commercial steel profiles remain embedded in timber pieces, mainly for getting fire protection. Izumi et al (143), (144) studied similar type of solutions in the case of fire.

Built examples:

The research of Kimura et al (141) was carried out for verifying the constructive solutions adopted for a two storey wooden office building. Other built examples that use steel profiles covered by timber elements in Japan are the GC Osaka Office and the Marumi Sangyo Building in Nagoya, both built in the year 2000, and the “Wood Square” Building of the year 2002 (120).



Figure 63: “Wood Square” building in Japan (120)

3.3 COMBINATIONS WITH ACTIVE STEEL

3.3.1 In grain direction: pre- and post-tensioning

References

Peterson (1965) _(145)

Turkovsky et al. (1991) _(146)

Pletz & de Melo Moura _(147)

ACTIVE		
In grain direction	Perp. to grain	
T	T+S	T (p.g.)+S

Summary:

Peterson (148), cited by Bulleit (31) and Alam (68), bonded stressed steel plates to the tension side of laminated beams. The bending strength and stiffness were significantly increased and the variability in the bending strength was reduced.

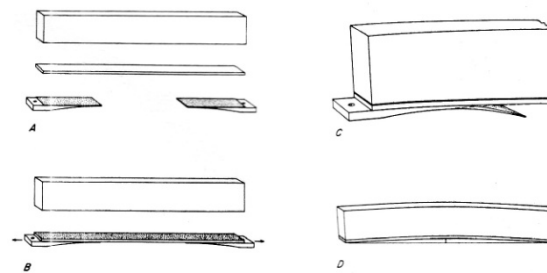


Figure 64: Horizontal lamination of the tensile face of a wooden beam using pre-stressed steel by Peterson (148) cited in Alam (68)

Turkovsky et al (146), cited in Dorey & Cheng (42), developed a bracket structure embedded into the beam to support external reinforcing rods. This system is reported as being successful at providing a suitable joint between the timber member and the metallic reinforcement and it was used in many structures in the former Soviet Union. Production costs limited its use to reparation interventions.

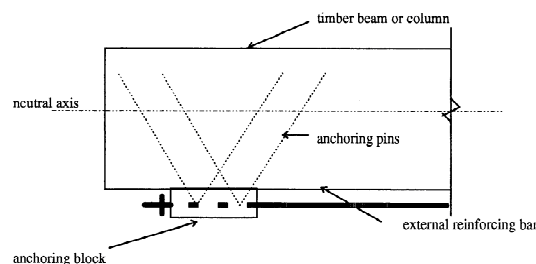
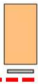







Figure 65: Reinforcing anchor bracket by Turkovsky et al (146) cited in Dorey & Cheng (42)

Pletz & de Melo Moura (147) applied pre-stressing forces to trussed timber beams, that is, they applied an external pre-stressing to the timber component. The load capacity was enhanced, larger spans are possible and the total deformation was reduced. Long-term tests were carried out for evaluating the loss of pre-stressing by creep and shrinkage.



Figure 66: *Proposal of pre-stressed beams by Pletz & de Melo Moura (147)*

ACTIVE		
In grain direction		Perp. to grain
T	T+S	T (p.g.)+S
		
		

References:

- Bohannon (1962) _(149)
 Bohannon (1964) _(150)
 Bohannon (1974) _(151)
 Oiger (1997) _(73)
 Mischler (1999) _(152)
 Negrao et al (2008) _(153)
 Negrao (2012) _(154)
 Sigrist & Lehman (2012) _(155)
 Leyder et al (2014) _(156)
 Wanninger et al (2014) _(157)
 Leyder (2015) _(158)
 Wanninger (2015) _(159)
 Ogrizovic et al (2016) _(160)
 Leyder et al (2016) _(161)
 Estévez-Cimadevila et al (2016) _(162)
 Pampanin et al (2006) _(163)
 Buchanan et al (2008) _(164)
 Fragiaco & Davies (2008) _(165)
 Davies & Fragiaco (2008) _(166)
 Iqbal et al (2008) _(167)
 Smith et al (2008) _(168)
 Carradine et al (2009) _(169)
 Newcombe et al (2010) _(170)
 van Beerschoten et al (2011) _(171)
 van Beerschoten et al (2012a) _(172)
 van Beerschoten et al (2012b) _(173)
 Carradine et al (2012) _(174)
 Curtain et al (2012) _(175)
 Holden et al (2012) _(176)
 John & Buchanan (2012) _(177)
 Morris et al (2012) _(178)
 Newcombe et al (2012) _(179)
 Ponzo et al (2012) _(180)
 Smith et al (2012) _(181)
 Spellman et al (2012) _(182)
 Armstrong et al (2014) _(183)
 Buchanan (2014) _(184)
 Ponzo et al (2014) _(185)
 Sarti et al (2014) _(186)
 Smith et al (2014) _(187)
 Smith et al (2016) _(188)
 Granello et al (2016) _(189)

Summary:

Bohannon (149), (150), (151) studied prestressed laminated wood beams. He compared post-tensioned beams with high strength steel strands in the tension zone of the beams to not prestressed ones. He found that an increase in 30% of strength and a decrease in 50% of variability can be obtained with prestressing. He studied also the time-dependent characteristics of this system testing during eight years prestressed specimens and not prestressed ones. The time-deflection performance was consistently similar and there was no significant loss in the prestressing force.

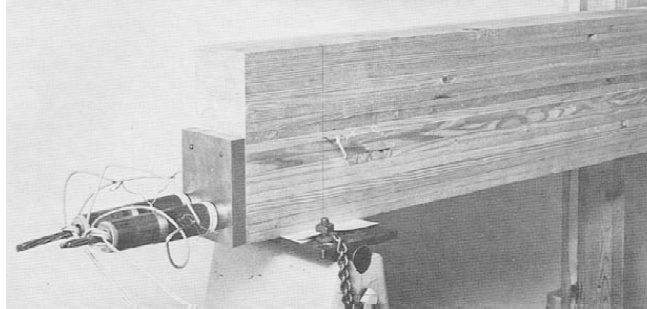


Figure 67: View of a beam reinforced with steel cables showing bearing plates (150)

Oiger (73) investigated several reinforcement and prestressing schemes for glulam beams. For the prestressing he used straight steel bars in the tension zone of the beam or curved high-tension cables. He reported that prestressed glulam beams are applicable (in particular by post-tensioning) and interesting for heavy loaded slender beams, though a relatively large portion of initial prestress disappears with time.



Figure 68: Halves of tested beam with grooves for steel bars (73)

Michsler (1999) proposed the pre-stressing of timber pieces on the tension area for timber-concrete composites.

Negrao and collaborators (153), (154) studied the pre-stressing of timber beams using pre-tensioning and post-tensioning approaches. In both cases the steel bars were placed inside the tension side of the beam, being glued in the first case and anchored with a steel base plate and nuts in the second one. The authors report about the possibility of adding a production step to the common glulam production lines for allowing the mass production of timber pre-stressed elements. Benefits regarding increased bending strength and reduction of deflections are achieved.

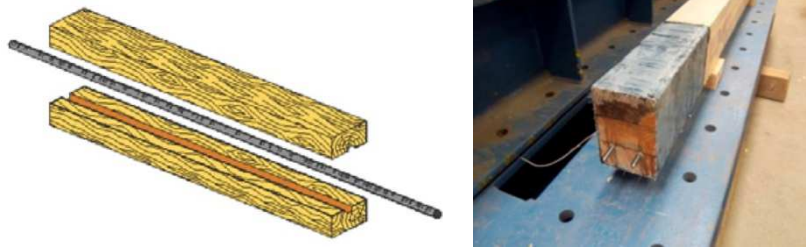


Figure 69: Specimens for adhesion tests (left) and post-tensioned beams (right) (154)

Sigrist & Lehmann (155) applied the pre-stressing techniques to cross laminated timber (CLT) bridge decks in the longitudinal direction. The post-tensioning of CLT plates in their tension side with steel strands lead to the reduction of deformations and additional benefits regarding strength. The system is proposed also as effective for the lateral distribution of high point loads.

Teams of the Swiss Federal Institute of Technology and collaborators (156), (157), (158), (159), (160), (161) developed a post-tensioned solution for timber frames of beech-LVL components. The novelty in their solution is that they apply the pre-stressing to a grid of timber beams post-tensioned in both perpendicular directions.

Estévez Cimadevila et al (162) developed a force-multiplying device for the self-tensioning of long-span wooden structural floors. The efficient redistribution of bending stresses achieved makes the system interesting for its use in long-span structural floors with reduced structural depths.

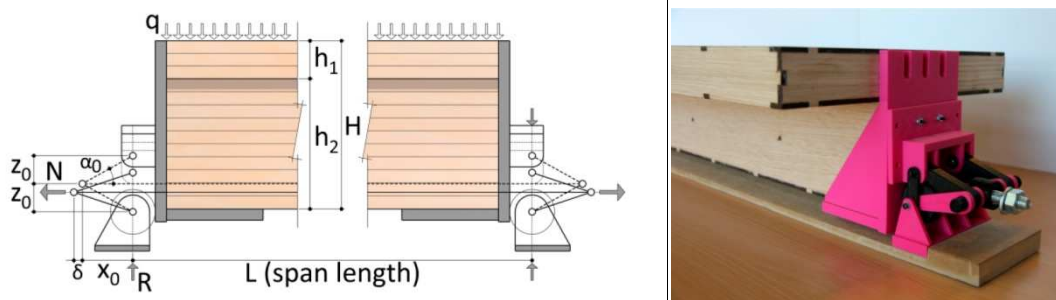


Figure 70: Force-multiplying device (left) and its 3D-printer prototype by Estévez Cimadevila et al (162)

Several timber pre-stressing solutions were extensively studied in New Zealand at the University of Canterbury, in collaboration with other universities and researchers, using post-tensioned timber frames, sometimes combined with other structural systems like post-tensioned timber walls. Several buildings were constructed using the developed solutions and they are referenced in the next point (163), (164), (165), (166), (167), (168), (169), (170), (171), (172), (173), (174), (175), (176), (177), (178), (179), (180), (181), (182), (183), (184), (185), (186), (187), (188), (189).

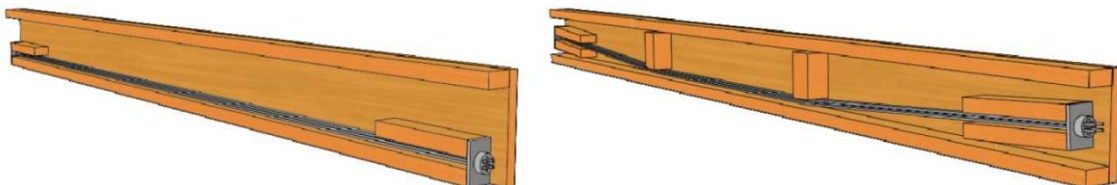


Figure 71: Longitudinal section of a timber-box beam with straight post-tensioning (left) and draped post-tensioning tendons (right) (172)

Built examples:

The engineer Jürg Conzett and his partners used the technique of prestressed timber in different projects (190). For the Murau Bridge in Austria, built in the year 1995, a timber Vierendeel structure was proposed. The lower glulam timber chord was post-tensioned with central cables.



Figure 72: Pedestrian bridge in Murau, Austria (190)

The Looby Roof of the building of the Swiss Re company in Rüschlikon, built in 1999, is composed of glulam beams that cantilever more than 13 meters from the building façade. In this case the tensioning cables remain not always in the centre of the cross-section, as was the case of the Murau bridge. Instead they move across the beams cross section balancing the tension stresses were they reach their maximum values along the length of the beam.

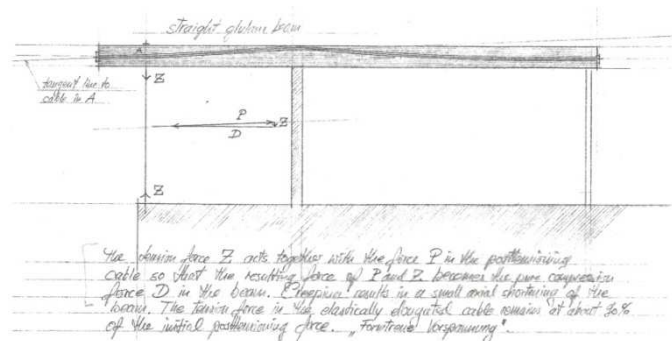


Figure 73: Sketch of the structural solution for the Swiss Re Lobby Roof (190)

The Benau Footbridge in Schwyz in Switzerland, finished in the year 2002, was built with a glulam hollow beam prestressed with five central cables.

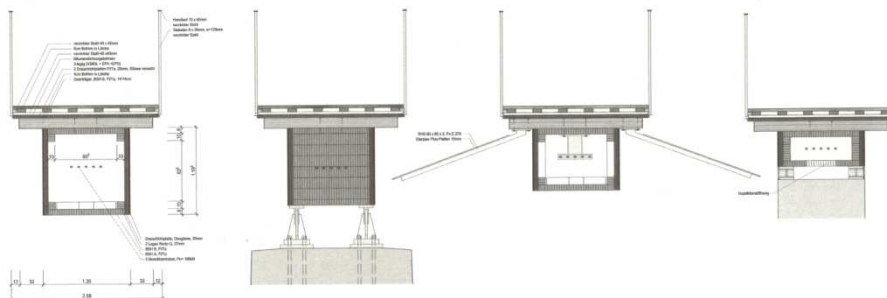


Figure 74: Several cross sections of the Benau footbridge (190)

Several buildings were built in New Zealand following structural designs tested by teams of the University of Canterbury, in collaboration with other universities and researchers, using post-tensioned timber frames, sometimes combined with other structural systems like post-tensioned timber walls.

The university of Canterbury Expan building was originally a test specimen used in the University's laboratories. The building consists of lateral resisting post-tensioned timber frames in one direction and post-tensioned coupled shear walls in the other one (188).



Figure 75: Expan building in Christchurch (188)

The Massey University's CoCA "Te Hara Hihiko Building" built in New Zealand in 2012 used post-tensioned timber beams with draped tendons.

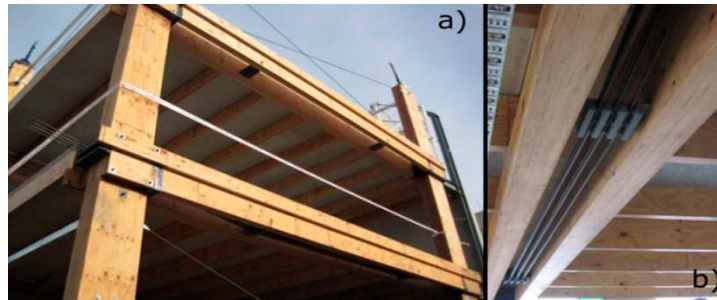


Figure 76: lateral view of the post-tensioned frame (left) and draped tendon detailing (right) of the Massey University in Wellington (189)

The Merritt Building is a three storey office building in Christchurch. The use of one way, single bay frames challenged the designers due to the very large gravity loads and post-tensioned frames were used (183).



Figure 77: Exterior and frame (left) (183) and view of the post-tensioned frame (right) of the Merritt Building in Christchurch (189)

The Diocesan School for Girls Aquatic Centre is another Christchurch example with post-tensioned timber beams.



Figure 78: View of the post-tensioned beams of the Diocesan School for girls aquatic centre (189)

The Trimble Navigation Offices building is a two-storey building. The building uses Pres-Lam walls in one direction and Pres-lam frames in the other. The two storey frames are horizontally post-tensioned at the first floor level but not at the roof (188) (183).



Figure 79: Trimble Navigation Offices in Christchurch (188)

St Elmo Courts is an office and retail building built in Christchurch. It uses concrete columns with post-tensioned timber beams (183).

The studies of teams from the Swiss Federal Institute of Technology and collaborators (156), (157), (158), (159), (160), (161) were applied for the “ETH House of natural Resources”, a three storey building with the two top storeys constructed with post-tensioned timber frames.

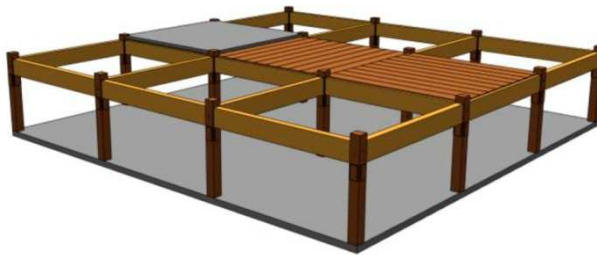





Figure 80: Visualization of the first timber storey of the ETH House of natural Resources. Post-tensioned timber frames made of ash and composite floor of beech-LVL and concrete (156).

3.3.2 Perpendicular to grain

ACTIVE		
In grain direction	Perp. to grain	
T	T+S	T (p.g.)+S
		

References:

Ritter (1990) _(19)

Wacker & Smith (2001) _(191)

Crews & Bakoss (1996) _(192)

Crews (2000) _(193)

Crews (2001) _(194)

Crews (2002) _(195)

Crews (2006) _(196)

Crews_(197)

Cheung et al (2008) _(198)

Karlsson et al (2009) _(199)

Karlsson et al (2010) _(200)

Ekholm (2013) _(201)

Ekholm & Kliger (2014) _(202)

Gotou et al (2012) _(122)

Summary:

Stress-laminated deck superstructures for bridges consist of a series of lumber laminations that are placed edgewise between supports and are compressed transversely with high-strength prestressing elements (19). It is a successful technique used for building bridge decks in numerous countries around the world. In Europe design, calculation and construction rules are defined in the Eurocode 5 – Part 2 (203).

Ritter (19) reports about the development of this structural solution, prestressing systems, time-related stress loss, construction methodology and design procedures.

Wacker & Smith (191) gathered up a collection of standard plans for timber bridge superstructures with design tables. Nail-laminated, spike-laminated, stress-laminated sawn lumber and stress-laminated glulam decks are included. Also longitudinal glulam panel, glulam stringer and transverse glulam decks.

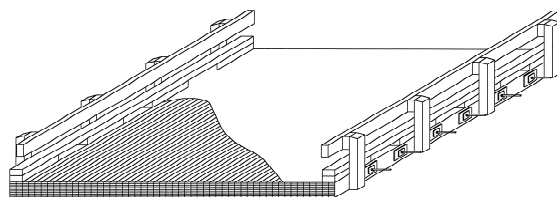


Figure 81: Stress-laminated sawn lumber deck (191)

Crews and collaborators (192),(193),(194),(195),(196),(197) studied extensively this type of structural solutions for its application in Australia. Different variations, like the stress laminated timber cellular deck were object of the analysis. The research indicated that the technology is structurally and economically viable.

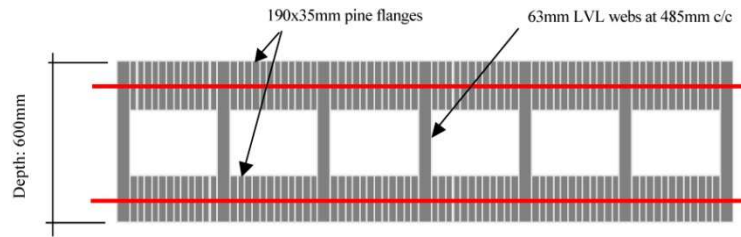


Figure 82: Section detail of the cellular deck utilising Radiata pine flanges and pine LVL webs (195)

Cheung et al (198) investigated the structural reliability with special focus on bending strength and stress losses for the use of the system in Brazil.

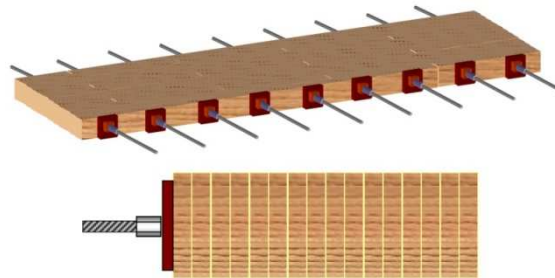


Figure 83: Typical stress-laminated deck (198)

Karlsson et al (199), (200) and Eckholm et al (201), (202) focused on the ultimate limit state and pointed out that phenomena that generally do not occur in serviceability limit state should be taken into account. These are the slip in the interlaminar surface and stress redistribution.

Gotou et al (122) combined stress-laminated decks with steel members for the development of hybrid bridges. They proposed two different types, both of them using upper and lower stress-laminated decks connected by steel members with steel bars. One of the types utilized vertical steel trusses at the outer border of the laminations and the second one a perforated steel plate with triangle holes in the same position. The authors report that the proposed hybrid bridges have bending stiffness several tens of times larger than those of the one-deck stress-laminated deck bridge. An important issue and objective of the research is that the deck and steel parts are easy to assemble and disassemble in order to build bridge or replace decayed ones at the construction site and also in case of disasters.



Figure 84: One-box test model with lateral perforated steel plates (122)

Built examples:

As already mentioned the stress-laminated deck superstructure for bridges is a successful technique used for building bridge decks in numerous countries around the world.

3.4 AMOUNT OF EXISTING RESEARCH AND NUMBER OF BUILT EXAMPLES

A visual summary of the previous state-of-the-art review can be seen in the *Figure 85*. The “Proposal of a systematic classification of timber-steel combination in beams” of the *Figure 8* is reproduced again with additional information in order to offer a fast overview of the quantity of existing research and building examples cited.

It should be pointed out that this review could be in some points incomplete. Of course it is possible, and even highly probable, that worldwide there exist more research references and built examples than the mentioned ones. Even though, it is thought that the carried out review offers a quite wide and representative outlook of the topic under study. Due to this fact, the identification of which material combination strategies were more extensively studied and which of them found more numerous applications in real buildings seems interesting.

In the *Figure 85* the red lines accentuate those material combination strategies which count with more than ten research references inside the state-of-the-art review. The green figures count the number of built examples making use of the respective solution.

The first noticeable fact is that, apart from three exceptions, most timber steel combinations were until now not successful in terms of practical applications. Very few built examples exist apart from those that use steel-web joist, flitch beams or transversely stressed timber decks. From all the combinations studied these are the only three that count with more than fifty built examples and can be considered as widely widespread. The other solutions remain until now in the field of experimental or singular solutions.










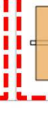
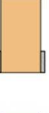

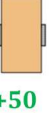
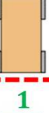


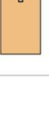

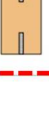





		PASSIVE					ACTIVE		
		In grain direction					In grain direction	Perp. to grain	
		T	C	S	T+C	T+C+S	T	T+S	T (p.g.)+S
H	Outer								
	Inner								
V	Outer								
	Inner								
H+V	Outer								
	Inner								

Figure 85: Summary of amount of existing research and number of built examples. Red: combinations with more than ten references in the state-of-the-art review. Green: number of already built examples using the respective technique.

Moreover, it can be seen that the most researched solutions are not always the most used in the practice. Strategies like horizontal and in grain direction passive reinforcements were extensively studied but very few used. On the other side we can find solutions like the steel-web joist that, although counting with not many research references are a quite successful product in practical terms.

Another important fact is that the best solutions from a pure structural performance point of view are also not always the most successful ones in the practice. Price issues, simplicity of manufacturing and the address of multiple problems at the same time (structural performance, fire protection, cost competitiveness of materials, amount and cost of the connections between materials needed) play also a very relevant role.

3.5 CRITICS AND LESSONS LEARNED

The previous overview of the existing amount of research and number of built examples rises the question of why the situation is so, that is, why so few strategies were until now commercially successful, although the structural improvements studied are in many cases remarkable.

A good number of researchers which studied timber-steel combinations for their application in beams pointed out factors and problems which can be determinant for the successful development of structural elements. Some of the most interesting ones are cited in the next paragraphs.

Bulleit (1984) _ (31)

“Reinforced wood materials are generally expensive to fabricate, usually because the reinforcing process requires at least one additional manufacturing step. [...] Reinforced laminated timber is not a cost-effective material. The cause of this seems to be the amount of labour involved in the fabrication in combination with the cost of the reinforcing material.”

Dorey & Cheng (1996) _ (42)

“Despite the moderate increase achieved in the engineering properties of the wood, the majority of these researches were not taken beyond the experimental stage. There are a variety of reasons for this. [...] First and foremost has been the economics. Current large scale manufacturing costs of these products have not outweighed the structural advantages achieved. Secondly, the difficulty of developing a successful connection between the different components has also limited commercial production.”

Kirilin (1996) _ (53)

“Numerous successful reinforcement schemes have been developed over the past 35 years, and most technologies offered enhanced static strength and stiffness. None of the technologies has yet to be used on a wide-scale basis. [...] The economic practicability and feasibility was not realized until recently.”

Dagher (2006) _ (204)

“While significant increases in strength and stiffness have been achieved, the problems encountered were generally related to incompatibilities between the wood and the reinforcing material. [...] The differences in hygro-expansion and stiffness between the wood and reinforcing materials can lead to a separation at the glue line, or tension failure in the wood near the glue line.”

Nielsen (2007) _ cited in Leckie (2007) _ (205)

“The big problem from a structural point of view is the different expansion/contraction coefficients when you have dissimilar materials.”

Schober et al (2008) _ (74)

“One cannot help wondering whether the increase in strength compensates for the cost, because this process (steel rebars inserted in longitudinal holes and injection of adhesive) seems to be even more complex than that of bonding fibre reinforcements to the tensile face of the timber beam. Some preliminary studies indicate that the answer is no, for reasons similar to those pointed out for the new engineered materials.”

Larsen (2011) _ (206)

“In analogy to steel reinforced concrete, many researchers have suggested to reinforce timber with steel or fibre materials (glass fibres or carbon fibres) although there is a vital difference: As opposed to concrete timber has excellent tension properties in the fibre direction. All the same there are numerous papers on the topic. Generally improvements are reported, mostly because of a reduction of variability,

but in all cases the improvements are small and the production costly and it would have been much more effective and cheaper to use wood as reinforcement. An exception is repair of damaged structures by gluing on reinforcement. The same applies to the proposals to pre-stress timber beams. An exception is timber bridge decks, where pre-stressing perpendicular to grain because of low tensile strength perpendicular to grain may be effective or necessary.”

Kliger & André (2013) _ (40)

“One problem with using reinforcement is the incompatibility between the wood and the reinforcement, most notably the differences in hygro-expansion and creep that resulted in failure in the bond line between timber and steel leading to delamination. Modern adhesives has minimised this problem and reinforcing timber beams are now a real opportunity to improve the performance of timber structures.”

It can be seen that some points are repeatedly mentioned by the different authors as the causes why the different timber-steel combinations namely: cost of reinforcing material, labour cost involved in the fabrication, cost of the connections between the different components, economic practicability and feasibility, incompatibilities between the wood and the reinforcing material, different expansion/contraction coefficients. They all should be considered as important conditions for approaching any timber-steel design combination.

After this and although all the precedent combination proposals opened very interesting lines of research and reported relevant structural improvements, a general critic can be posed.

Most of these proposals focused purely on structural performance issues and forgot to address production costs problems or other important issues as the performance under a fire-situation.

In some cases these absences are justified because of a focused reinforcement criteria, which makes a punctual increasing in costs not so relevant and the fire protection easy to solve in a reduced area of the structure. But when the combination strategy is devised as general approach, affecting the whole structural element is when addressing all the problems at once becomes really important. Otherwise one of the problems not addressed could invalidate the whole design or approach.

The situation could be summarized as a lack of a “comprehensive design” approach. Most proposals, although interesting, are still too complex or costly to be used by the real building industry. They are good first steps, but in preliminary stages needed of being perfected and simplified, both in costs and implement procedures, before its mass use.

The proposals based of combining different materials lead always to the important issue of how they are connected. If the number of connection devices needed is important for an appropriate structural performance the rising of costs, both of materials and of assembling, is immediate. In some cases, like with an excessive quantity of nailing, their effect could be even negative, due that an excessive number of nails could weaken the original timber pieces. Alternatives as gluing are not always possible and in cases have the drawback of not allowing an easy future disassembling.

A proof of all these drawbacks is that in reality, even when most of these options were started to be researched already decades ago, few of them had real success as feasible options for the construction industry.

As a final conclusion, it could be stated that any combination strategy should address all the design issues comprehensively, not only the structural performance ones.

Good mechanical performance, self-fire protection, easiness of assembling and disassembling, good performance regarding ecologic parameters and reasonable costs are key points to be fulfilled for reaching a good overall design of timber-steel structural elements.

3.6 CONCLUSIONS: WHERE IS THE POTENTIAL?

As mentioned in the second chapter “The potential of the combination of timber and steel” it is clear that both materials could and should be used making the most of the specific properties that each of them has to offer. In the point “The potential of the combination of timber and steel in beams from a structural performance point of view” it was analysed how depending on the design situation timber, steel or both materials together could offer answers to the different structural designs conditions. It could be detected how steel could act not as a “timber-reinforcement” but as an integral structural component, using its capacities against tension, compression and shear stresses depending on the particular situation.

In the *Figure 86* the “Proposal of a systematic classification of timber-steel combination in beams” of the *Figure 8* is reproduced again and used for detecting which timber-steel combination strategies could make the most of both timber and steel properties. The vertical green box surround those options where steel is used with a most comprehensive strategy (T+C+S). The horizontal green boxes those when steel, because of fire protection and corrosion issues remains inside the cross section, protected by timber. The crossing areas in red show therefore those options with theoretically more potential to offer a global solution to all the design problems faced. But this will be possible and would lead to successful solutions if and only if some important problems which proved to be limiting for timber-steel structural development, as already mentioned in the previous point, are taken into account and offered adequate answers and design strategies. The cost of the combined material should be kept low as possible, also the labour costs and cost of connections. The compatibility between materials, allowing their different movements should be also guaranteed.

		PASSIVE					ACTIVE		
		In grain direction					In grain direction	Perp. to grain	
		T	C	S	T+C	T+C+S	T	T+S	T (p.g.)+S
H	Outer								
	Inner								
V	Outer								
	Inner								
H+V	Outer								
	Inner								

Figure 86: The potential of combination of steel and timber

3.7 ADDENDUM: TIMBER-STEEL APPROACHES IN THE RESEARCH PROJECTS “8+” AND “DAS ERDBEBENSICHERE HOLZHAUS”

In the year 2008 the research report “*Möglichkeiten eines vielgeschossigen Holzbaus im urbanen Raum mit Zielrichtung auf acht oder mehr Geschosse*” (207) was published, shortly known as “8+ Research Project”

The research team was composed by members of the architectural office Schluder Architektur ZT GmbH, of the Institute of Structural Design and Timber Engineering of the Vienna University of Technology, Holzforschung Austria, Wiehag Holding, Vasko+Partner Ingenieure ZT GmbH, UNIQA Sachversicherung, brand Rat ZT, PE CEE GmbH, Rhomberg Bau GmbH and Arsenal Research.

This interdisciplinary research team studied the possibility of building timber-based multi-storey structures with the objective of reaching the eight or more stories. Determining and design factors to take into account were the possible architectonic solutions, fire protection design, structural engineering solutions and market and cost analysis.

Several design prototypes were studied, making use of different architectonic and structural configurations, up to 20 storeys with timber-based systems. Due to the structural challenges faced by this type of building, this was one of the first research projects where a solution combining steel and timber in beams and supports was proposed for some of the prototypes studied.

The timber-steel beams proposed can be seen in the *Figure 87*.



Figure 87: Hybrid construction combining timber and steel beams (207)

One of the objectives of the combined use of timber and steel for the structural elements (beams, supports and broad bracing supports) was the attempt to design semi-rigid connections as can be seen in *Figure 88*.

The overall design concept of one of the building prototypes studied was to work with rigid and semi-rigid frames for avoiding as much as possible the necessity of using massive cores for bracing the overall structure.

Although these structural elements were not analyzed and detailed in depth or experimentally tested, this research project can be considered as the starting point of some structural ideas that will be developed in the following chapters of this doctoral thesis.

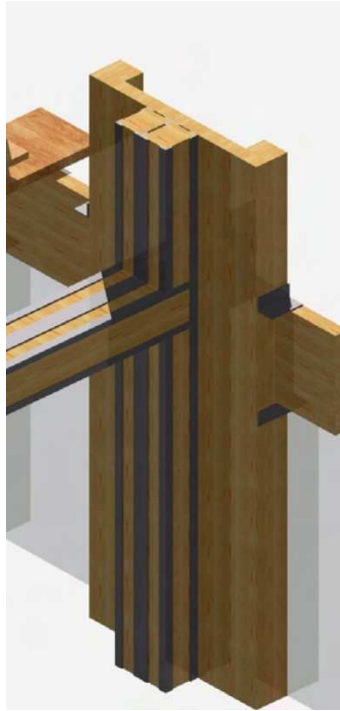


Figure 88: Sketch of the detail connection between timber-steel beams and supports (207)

In another related research project “Das Erdbebensichere Holzhaus” (208) (translation: “The earthquake-safe timber building”) from the year 2010, some of the suggested structural concepts of “8+” were developed, specifically the combination of steel and timber for the broad bracing supports located at the façade of one of the 8+ prototype buildings.

In this case this particular structural configuration of bracing support and steel anchoring was developed and tested as can be seen in *Figure 89*.



Figure 89: Anchoring system (left) and test set-up for wall and anchoring system (right) (208)

4. TIMBER-STEEL HYBRID BEAMS

4.1 INTRODUCTION: THE HYBRID STRATEGY

4.1.1 Terminology

In the existing literature dealing with structures or structural elements composed of different materials the words “reinforced”, “mixed”, “composite” and “hybrid” are used commonly.

In all cases these words make reference to the combined use of two or more materials with structural purposes, but the criteria about what is exactly each one differs among different authors.

The terms “composite” (128), (42), (61), (136), (209), (140), (137), (141), (130), (127), (138) and “reinforced” (31), (53), (68), (33), (63), (62), (71), (87), (60), (83), (72), (45), (38), (95), (36), (57), (66), (80), (73), (74), (54), (69), (146) are used mainly for referring to different arrangements of structural elements or pieces, and the word “hybrid” for structural systems (104), (122), (132), (101), (51), (102), (77), (133), (131), (43), (78), (142). But not always. “Hybrid” is used also for structural elements composed of different materials (51), (139), (52), (79), (81), (109), the same happens with the word “mixed” and the difference among the different terms becomes blurred. Sometimes the terms “composite” or “mixed” are used as well for both elements or structural systems in an indeterminate manner adding confusion to the use of all this terminology.

In any case several overall tendencies can be detected. “Reinforced” is mostly used for structural elements (beams, supports) of one material with additions of another one. There is a “principal” material which is reinforced with the second one. “Composite” is mostly used for structural elements composed of two different materials whose connection achieves a certain degree of composite structural action. Both materials are at the same level, combined, but there is no a “main” material and a “secondary one” “Hybrid” is mainly used for structural systems which combine structural elements of different materials, for example a building with steel columns and concrete slabs. But the use of the term “hybrid” for structural elements is much less clear. Some authors use the word for combinations of two materials achieving some degree of composite action, which other authors would call “composite” or “reinforced”.

Eisert et al. (210) proposed in the year 1999 a definition for “hybrid structural system” due that the term, as already mentioned, is used in different ways by different authors. A hybrid structural system should fulfil five conditions, namely:

- Be composed of two or more individual structural elements that together can support loads.
- Each component is capable of supporting loads on its own.
- The structural performance of each element is different, determined by geometry and/or material
- Inside their combination each element conserves its characteristic structural performance.
- The load distribution between the elements and their deformation can be influenced actively, for example with prestressing.

Although good for structural systems, this definition would not be adjusted to the case of structural elements. Most structural elements referred as “composite” by many authors would fulfil also the five “hybrid” requirements.

Due to all of this it is therefore necessary to define accurately in which sense the words “Reinforced”, “Composite” and “Hybrid” will be used as of now referring to structural elements, and a definition taking into account the mechanical performance and properties of the final element is proposed in the following points.

Reinforced:

The material-combined cross-section is not necessarily constant in all the length of the structural element. There is a main material with additions of another one.

There is horizontal shear transmission between the main material and the reinforcement one in the case of horizontal elements (beams or slabs), or vertical shear transmission in the case of vertical elements (supports or walls), and the connection system between them have to guarantee it. In the cross-section where the reinforcement is used a certain degree of composite action between the two materials is achieved.

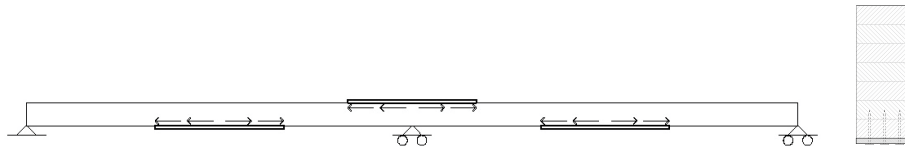


Figure 90: Example of a reinforced timber beam with steel plates

Composite:

The material-combined cross-section is constant along the structural element.

There is horizontal shear transmission between the two materials in the case of horizontal elements (beams or slabs), or vertical shear transmission in the case of vertical elements (supports or walls), and the connection system between them has to guarantee it. A certain degree of composite action between the two materials is achieved.

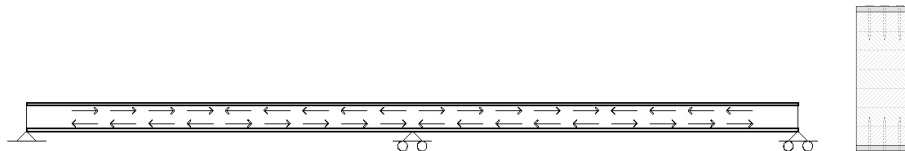


Figure 91: Example of a composite timber-steel beam with nailed steel plates.

Hybrid:

The material-combined cross-section is constant along the structural element.

There is no horizontal shear transmission between the two materials in the case of horizontal elements (beams or slabs), or vertical shear transmission in the case of vertical elements (supports or walls), and therefore the connection system between them doesn't have to guarantee it. No composite action between the two materials is achieved.

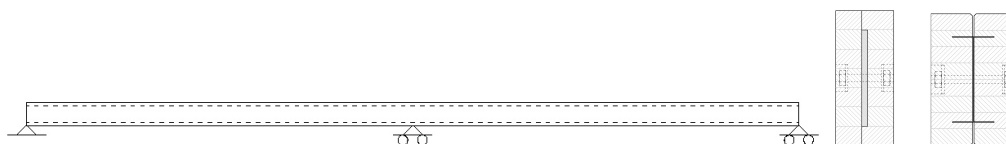


Figure 92: Example of a timber- steel hybrid beam

It is worth noting that in a structural arrangement like the one represented in the beam of *Figure 92* the decision of how to arrange the connection system among pieces could lead to get a hybrid or a composite performance. For example, if the steel core elements are completely glued to the wood it will result a composite beam, meanwhile if the connection elements are limited to punctual bolts inside holes with enough tolerance to avoid a horizontal shear transmission between materials a hybrid performance will be achieved.

The hybrid option looks promising if kept simple. On one hand well designed timber-steel hybrid structural elements would be able to make the most of both the steel and timber properties and, on the other hand, the not necessity of structural connection elements would make them easy and fast of assembling and disassembling and would reduce both material and manufacturing costs.

4.2 THE POTENTIAL OF THE HYBRID STRATEGY: DESIGN CONDITIONS AND OBJECTIVES

The development of hybrid beams from the structural performance and technical production points of view should take a series of important points into account for making the most of the timber and steel natural material properties. Fundamental design concepts for their planning are:

Regarding structural performance:

- The achievement of the required static performance, fulfilling the requirements for both Ultimate Limit States (ULS) and Serviceability Limit States (SLS)
- Both cross-section components, timber and steel, should provide a relevant carrying capacity.
- The protection of the steel elements with the timber components should provide enough self-fire protection for the cross-section performance in a fire situation.
- Long-term deformations should be taken into account.

Regarding structural design:

- The structural depth should be kept small in comparison to only-timber solutions.
- Rigid and semi-rigid joints should be possible.

Regarding economical and ecological parameters:

- The beams should be easy to assemble and to disassemble. This would allow easy, fast and economic building procedures and the eventual recovering and reuse of building elements.
- A reduced weight of the individual components should allow an easy and fast assembly.
- The number of joint elements should be kept to a minimum.
- The solutions should be competitive from an economical point of view.

The overall goal is the design of beams making use of all the potential of the combination of timber and steel in beams from a structural point of view, as explained in the point 2.4, and at the same time taking into account the factors and lessons learned from other timber-steel proposals as enumerated in the point 3.5

Some of these design conditions and objectives are explained with more detail in the following points.

4.2.1 Material combination towards resource efficiency

The objective of developing a beam solution combining two different materials is focused not only on making use of the best properties of each material, but also in offering an alternative which improves the performance of the only-one-material alternatives. This should be reflected in the amount of materials used and necessary for fulfilling a determined structural task.

Resource efficiency should be understood in this case as a global saving in the overall material input needed for fulfilling a determined goal.

4.2.2 Reduction of costs

Resource efficiency leads to the reduction of materials needed for performing a determined task. This should be reflected in a reduction of costs, but this would only be true if the joining methods used for their combination do not increase the material and manufacturing costs in more than the savings achieved.

The hybrid strategy, which does not need of structural connection elements for guarantying an appropriate structural performance, is a promising alternative to this problem.

Moreover, quoting Julius Natterer in his article “*A way to Sustainable Architecture by new technologies for engineered timber structures*” (211):

“ Today, ecological concerns become more and more important and wood, under the double aspect of the energy necessary to its production and its aptitude to store CO₂, could be the best-suited building material of XXIst century. However, if these ecological concerns take more amplitude and influence, there is another aspect, the economic concern. Thus each project must present not only one ecological or architectural value, but also an economical one.

It is necessary to promote the different possibilities where wood as timber can be used. Besides the utilization of high quality wood for high-tech constructions of halls, wide span covers and bridges, one should further develop the possibilities of using medium to low quality for massive-timber construction for floors, walls and roofs, also in association with other materials like steel, concrete, glass or fiber glass.” (211)

Following some of these ideas the hybrid strategy could be used for improving standard or even low quality timber pieces. An idea would be to be able of building high demanding structures by means of simple and standardized elements, as less sophisticated as possible.

From another point of view, keeping at a low level the costs and complexity of the elements to be assembled, makes the production possible for any medium-sized timber company without the necessity of major changes in its production line.

As already stated, a good number of attempts of combining timber with steel failed in their commercial implementation because of their excessive complexity or too high material costs of high-performance components. They remain as interesting research approaches but without practical use.

Inside this conceptual frame, with the hybrid approach the use of standard or even low quality timber should not to be seen as a problem, but as an opportunity. The opportunity of reducing the material costs and of guaranteeing an easy supply of the source components.

4.2.3 Reusability and recyclability

State-of-the-art techniques and research regarding life cycle analysis (212), provide several criteria and ideas which can be used for assessing the necessity of reusability and recyclability of constructive elements.

Life cycle costing is defined as “the total cost of a building or its parts throughout its life, including the costs of planning, design, acquisition, operations, maintenance and disposal, less any residual value” (212). Life cycle costing calculation methods are devised for making comparative studies among different options, not for getting an accurate value of the real monetary cost.

A “technical” life duration and an “economical” life duration of buildings can be distinguished. The first one refers to the period of time during which the constructive elements or services can fulfil their requirements without being renovated. The second refers to how much time passes until the change in functions or use of the building (or parts of a building) makes it to be refurbished in some degree.

There is a tendency that shows that, meanwhile the “technical” life didn’t change relevantly in the last fifty years, the “economical” life got shorter (212). This fact urges us to pay attention to two important issues: the possibility of recovering of the materials used and the design of structural systems for buildings which would allow enough spatial flexibility for undertaking these probable changes during their lifetime. All of this with as reduced costs as possible.

A growing importance of paying attention to the disassembling, reusing and recycling costs, from both environmental and monetary point of views, has been greatly driven by new global economic and environmental concerns in the last years.

After a whole life costs analysis of a building with “long life” (this excludes average industrial buildings), it can be stated that the costs of demolition reach an average of 10% of the total life cycle costs. “Demolition” includes the demolition itself, but also waste disposal and site clearance.

Construction is responsible of 15%, planning 1,5%, and the main part remains for operational costs, 73,5% , in which there are included also reparations and changes of elements (212).

Concepts like “urban mining”, developed after analysis that show that, for example, in Europe there is more copper stored in buildings than in the reserves in the lithosphere, push for an increasing concern about the way of an easy and not costly recovering of any material used, especially the not renewable ones. Composite materials like wood-plastics for example, are very difficult and costly of recycling.

The “storage of materials” in buildings will become an interesting economic asset if, after their life use, they can be easily recovered without higher costs than their material value. This will be achieved if and only if from now on the procedures and costs of dismantling and disassembling are taken into account at the same level as the ones of building.

These approaches will affect the whole architectural and engineering design. Exhaustive and accurate documentation about which materials are stored in buildings and the way to recover them will be necessary.

The European Union Resource Strategy establishes a legal recycling target to improve resource efficiency, being of 70% in the case of construction and demolition (213).

Timber-steel hybrid structural systems are designed for fulfilling these new worries and requirements, which in the near future will probably become compulsory.

4.2.4 Structural performance

The use of two materials in the cross-section of structural elements opens the possibility to arrange them in different ways, influencing both its structural performance and cost-production.

In the case of beams a good hybrid design strategy can allow the maximization of bending stiffness without the necessity of complex or expensive horizontal shear-resistant connection devices. The key point is how the different elements composing the beam are combined in the cross-section of the piece.

An easy example using a simple cut timber piece can be used for proving how the way of “recomposing” the original section affects the overall performance. In *Figure 93* a glulam block is cut horizontally and later recomposed using both “hybrid” (no existence of horizontally shear-resistant connection) and “composite” (guaranteeing horizontal shear transmission) strategies. The difference value in the final bending stiffness is relevant, being the hybrid option four times less stiff.

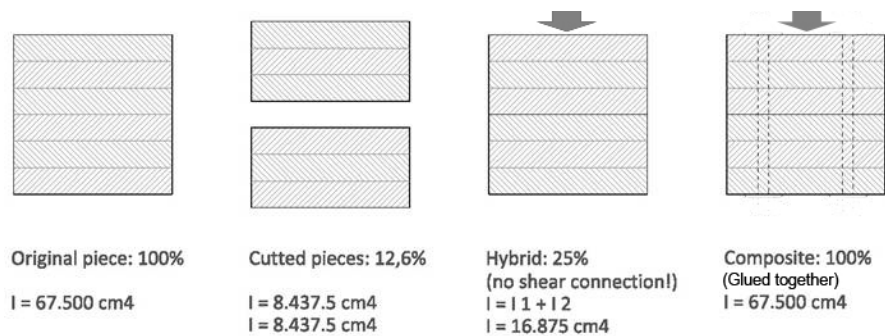


Figure 93: Bad hybrid design for bending stiffness. Comparison of glulam-glulam hybrid and composite options.

But if the original piece is cut vertically, as shown in *Figure 94*, and later recombined following the hybrid strategy, the final bending stiffness will be exactly the same as the previous composite option.

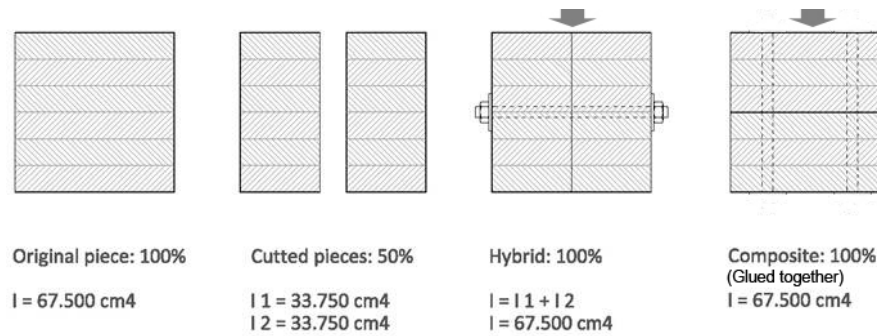


Figure 94: Good hybrid design for bending stiffness. Comparison of two glulam-glulam hybrid and composite options.

Moreover, meanwhile the composite option needs connection devices able of guaranteeing the horizontal shear forces transmission, in the hybrid case they do not play any relevant structural role and can be reduced to a minimum number for only constructive purposes.

This basic concept explained with only timber pieces for simplicity, is also valid if any of the wooden pieces is changed for other structural material.

If one of the timber pieces is substituted by a steel plate, the decision of how to assemble it will lead to the necessity of a bigger or smaller number of screws, nails or bolts.

It is easy to see then how for getting an almost “same performance beam” this design decisions could affect significantly the costs involved regarding material, costs of assembling and disassembling and time needed for these procedures.

4.2.5 Reduction of variability

In the already cited article “A way to Sustainable Architecture by new technologies for engineered timber structures”(211), Natterer discusses the benefits of using massive timber floors or walls, composed by a big number of connected elements, in comparison to the use of single pieces.

One of the benefits is that with these systems, a hypothetical defect in one plank will not lead to a failure of the whole structure, another is getting a reduction in variability, as shown in *Figure 95*.

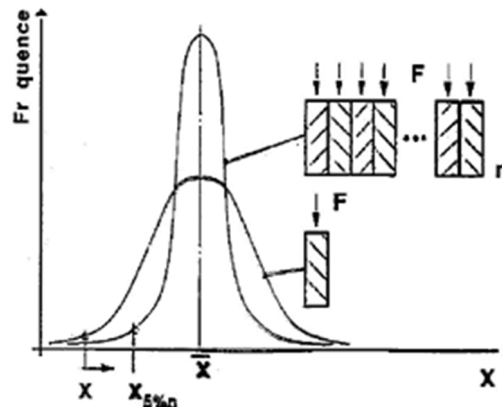


Figure 95: System effects diagram following Natterer (211).

A series of bending tests of single wood planks provides the mean value for their strength, but also the distribution, or variability, of this property. A series of bending test of boards made from a connected number of the same wood planks will show a higher loading capacity because of their increasing stiffness value, but also a reduction in the variability of their properties due to this system effect.

This concept is interesting because a reduction in variability means that the coefficient needed to obtain characteristic values, usually 5% percentile, from mean values is smaller in the second case than in the first. Therefore security factors can be smaller.

This same effect appears if we compare glulam and structural timber. Following the explanation of Kjell Arne Malo and Vanessa Angst in Kuklík et al (214) :

“This “lamination effect” is usually explained as follows:

Critical for the strength of structural timber is the strength of the weakest cross-section – usually at a knot or similar. The difference between boards is, therefore, considerable. In a glulam beam, however, laminations with different strengths are mixed and the risk that several laminates with major flaws should occur in the same beam is minimal. The load sharing between laminations in the glulam allows for locally weak zones to redistribute stress to adjacent stronger regions.

This fact is often recognized in safety or material factors used in design. In Eurocode 5, the material factor accounting for model uncertainties and dimensional variations is reduced to 1.25, while it is set to 1.3 for solid timber.”

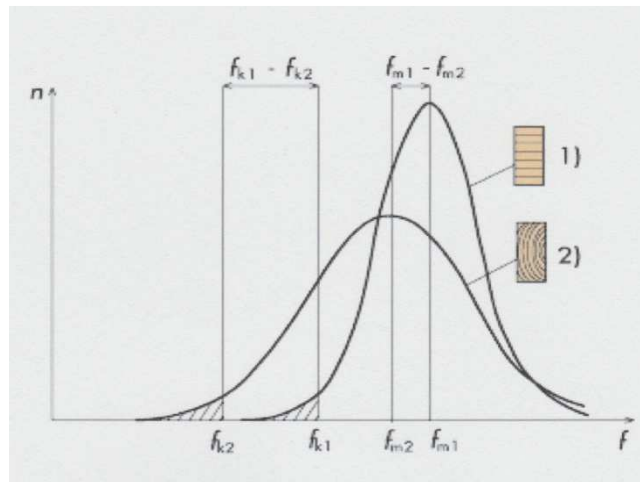


Figure 96: Frequency distribution of the ultimate strength of glulam and structural timber following P. Kuklík et al (214).

This idea can be applied to the design of hybrid elements. In this case, the design of a compound cross-section, for example composed by two different steel pieces and two different timber pieces, would lead to a reduction in variability of the mechanical performance of timber.

This approach questions if the security factors for the material properties and resistances as stated in codes Eurocode 5 (6), $\gamma_M = 1,3$ for solid timber and $\gamma_M = 1,25$ for glued laminated timber , could be changed when they do not perform on their own, but inside the structural arrangement of a hybrid structural element.

4.2.6 System strength

Building codes approach this issue through the definition of the factor k_{sys} in Eurocode 5 (6). This factor is defined for the cases of “equally spaced similar members” and “laminated decks or floors”.

One open question is that if, in the case of hybrid structural systems this factor could be used twice, and with which values.

It could be used at first for the global structural system, for example frames, if they fulfil the requirements specified in codes, i.e. “when several equally spaced similar members, components or assemblies are laterally connected by a continuous load distribution system” Eurocode 5 (6) with the value $k_{sys} = 1,1$.

As an alternative to the definition of a new security factor for hybrid elements, this factor could be used secondarily for the sub-structural system that the hybrid elements form themselves.

For laminated timber decks or floors Eurocode 5 (6) provides the following graphic:

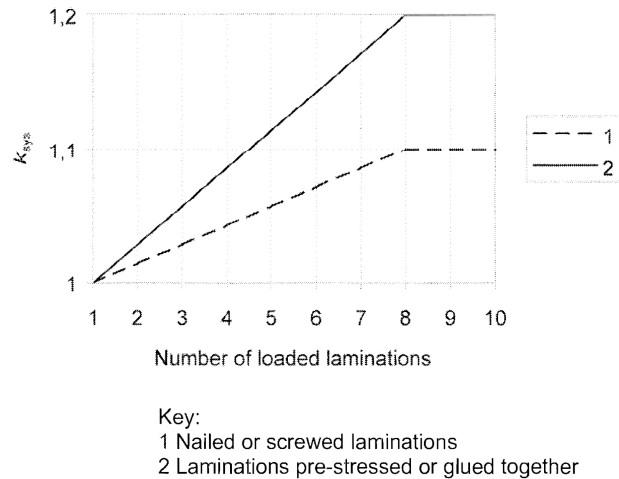


Figure 97: System strength factor k_{sys} , for laminated deck plates of solid timber or glued laminated members. From Eurocode 5 (6)

The exact values that should be adopted for hybrid structural elements should be researched because the codes figures' field of application is only pure timber elements. That means that it does not take into account the smallest variability of steel components.

In any case the value of k_{sys} will be not higher than 1,25 for glulam and 1,30 for sawn timber based elements, because these are the limit values which would counteract completely the original security factors for the material properties.

4.2.7 Self-fire protection

The hybrid beam design should make use of the good properties of timber against fire. Timber can be used for protecting the steel elements if these are covered by the first one. Timber would act then as an insulating material avoiding that the steel would reach high temperatures during fire. The timber covering should be designed for being enough for the fire-resistance time needed.

4.2.8 Allowable structural depth

The allowable structural depth for horizontal structural elements, beams and slabs, is an important factor in the design of multi-storey buildings. These structural solutions are usually repeated for every storey, and when this repetition reaches a considerable amount of storeys a small difference can be the source of relevant cost increases.

For example, a difference of ten centimetres in the structural depth between two floor solutions could mean the possibility of building an extra level in a thirty floor multi-storey building. Apart from that

bigger structural depths are in any case the cause of needing more square metres for the façade elements and the related costs for their construction.

For all of this the structural depth should be kept as small as possible, especially in the case of multi-storey buildings.

4.3 DESCRIPTION OF THE PROPOSED CROSS-SECTIONS

The hybrid beams proposed are composed of two symmetrically arranged glulam or cross-laminated timber beams and two cold-formed steel U profiles that placed back to back, form an I cross-section, as can be seen in *Figure 98*.

The four cross-section components are hold together without horizontal shear connection thanks to four threaded rods that connect the individual pieces transversally. These connections are used only for guaranteeing the geometrical arrangement of the cross section. Moreover, it is assumed that the laterally compressed timber will prevent the web buckling of the steel pieces, allowing a high slenderness for the steel elements. For the practical use of beams, and for fire protection reasons, the end bolts, washers and threaded rods should be kept inside holes in the timber cross-section and covered with a thick-enough timber or fire resistant material closing piece.

4.3.1 Cold formed steel technology

For the manufacturing of the steel components the folding technology is proposed. The question about why is this folded steel arrangement proposed, instead of using other standard or common steel products, is important and needs to be answered. The main concept is the search for efficiency in use of materials.

The pros and cons of other possible steel arrangements were studied in order to look for the better option and are summarized in the next list.

On one hand commercial rolled steel profiles (IPE, IPN, HEB, etc) are price competitive. But on the other hand they show a flange width/structural depth ratio ($b:h$) for providing enough lateral fire protection for the flanges of the steel component. Moreover they are not divided, so the weight of the steel component cannot be halved. A single steel component is too heavy for allowing an easy assembling.

Castellated beams, with both Peiner and Litzca cutting arrangements, have a better geometry arrangement, with not so broad flanges. They could be suitable from this point of view, but their production procedures require cutting and welding, increasing production costs. They have to be custom-made. The problem of weight for assembling is the same as for IPE profiles.

In the case of using flat steel plates, like the ones inside flitch beams, a low yield (W/A) is achieved in comparison with I arrangements. This type of plates are cheap and easy to use, as already demonstrated by flitch beams, but using the same amount of steel they generate much lower improvements compared with the other steel designs considered. This amount of improvement could be enough in the scope of light-frame wood structures (flitch beams), but not for structural heavy-frames under demanding conditions like the objective of these research.

Custom-made welded profiles could be an optimum option. The steel thicknesses and dimensions could be arranged to fit perfectly the structural problem. They present two problems: the first and more important one is the necessity of welding and following important increasing in costs. The second is the tolerance dimension: welding optimized, slender and thin steel plates provokes remaining thermal deformations in the steel pieces that make them more difficult for fitting within the wood. The problem of weight of a single I piece could be avoided proposing two U, but this would increase the dimensional tolerance problem already stated, warping and bending the steel beams.

On the other hand folding is a versatile, simple, clean and easy technology which, if used for market-oriented quantities of components, until a thickness of 4 mm, would provide flexible cross-section designs and be price competitive.

Using this technology custom-made inner profiles can be fast and very easily produced, the ratio flange width/structural depth is flexible and profiles with a good yield (W/A) can be obtained. And from the

very important aspect of assembling and disassembling these profiles allow the division of the elements self-weight and its manufacturing process offer an extremely good dimensional accuracy.

The great advantage of the cold-formed profiles is their geometric flexibility. The light weight of the individual two U components is also an advantage for the assembly in comparison to a statically equivalent welded I profile. The option of cold-formed steel profiles, until a plate thickness of 4 mm, could be a multi-purpose, clean, simple and price adjusted possibility.



Figure 98: Hybrid beam cross-section and detail of cold-formed steel elements

In the case of the timber components, two possibilities were studied. One with glulam and the other with cross laminated timber, which could be advantageous in the case of high transversal pressure at the support areas.

It is important not to weaken excessively the timber components when designing the grooves needed for receiving the steel flanges. The grooves reduce the shear capacity of the timber pieces. Due that the grooves are placed far away from the neutral axis, where the shear stresses reach their maximum values in the cross-section, they are not an important problem. It can be calculated how much timber should be left in place for avoiding any shear problem. Moreover, the grooves weaken the best quality boards in C-grades glulam, i.e. combined glulam. This could cause reductions in the theoretical beam capacity and stiffness and should be taken into account.

In any case, these two points were examined and studied during the testing series, and the problems guessed and explained proved not to be relevant for the timber and hybrid beams performance.

The four elements are connected by bolts with the only task of providing lateral pressure to the pieces in order to make not possible their dismantling under load. In the case of fire these bolts are laterally introduced inside the wood pieces, and their assembling hole covered by a wooden cap. Therefore the bolts are provided with the same wood thickness for fire protection as the inner structural steel pieces.

Inside the structural frames, the steel pieces will be designed for being capable of withstanding and transmitting the shear forces. Buckling problems of the web are avoided thanks to the restraining action of the surrounding wood, therefore the minimum dimension of web is conditioned only because of the shear and supply possibilities.

4.3.2 Cold formed steel production

Nowadays two industrial procedures are available for the production of cold formed steel profiles: roll-forming and cold-pressing.

The first procedure is a continuous process where the steel from a coil follows a continuous path and is gradually deformed within steel rollers.

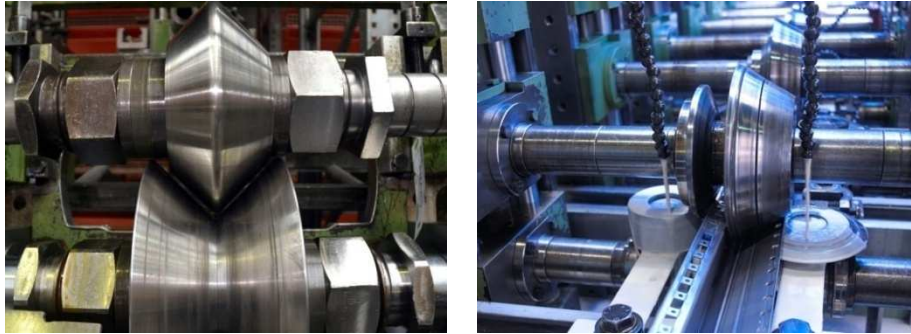


Figure 99: Steel plates being deformed between rollers in a continuous process (215)

Almost all imaginable cross-sections are possible. The drawback of using this technology is that a relevant quantity of the desired profile must be produced for making it competitive from an economical point of view. The process is almost fully automated, but the quantity of the specific cross-section to be produced must be enough for making the specific disposition of rollers and adaptation of the production line competitive. Nowadays it is possible to produce with roll-forming cold-formed steel profiles until a total length of 27 metres (215).



Figure 100: Example of complex cold-formed steel profile manufactured with roll-forming (215)

A well-known product manufactured with this procedure is the corrugated sheet steel profile, as it can be seen in Figure 101.



Figure 101: Corrugated sheet steel profile manufactured with roll-forming(216)

On the other hand the second technology, cold-pressing, makes use of bending presses. The steel plates should be cut in advanced to the desired length, and then pressed for producing the desired geometry of the cross-section.

This is a not so automated procedure as the roll-forming one. Steel plates have to be previously cut and then manipulated by qualified workers in the bending press. The cross-section geometry that can be produced are more limited that the ones using the roll-forming procedure. But in this case the production flexibility is higher. Specific cross-sections can be produced in smaller quantities, compared to roll-forming, and still be economically competitive.



Figure 102: Image of a steel bending press (217)



Figure 103: Image of a big-size cold-formed profile (217)

Nowadays there exist bending presses capable of cold-form until 21 metres long pieces, a thickness of 60 mm using until 3.000 Tons of pressure (217). Smaller presses are usually widely available, with bending lengths of up to eight meters, although the most common bending lengths at are six and four metres.



Figure 104: Production (left) of cold-formed steel profiles manufactured with bending presses (right) (217)

As a summary it can be said that both procedures offer the possibility of producing cold-formed steel elements for structural purposes. The current state-of-the-art capabilities are more than enough for the range of dimensions, and cross-section geometries needed for timber-steel hybrid beams. The decision of using one or other option is an economical one, dependent mainly on if the quantity and complexity of the cross-sections to be produced compensates the costs of a roll-forming production or not.

4.3.3 Symmetrical arrangement

The hybrid beams are composed by two wooden beams, sawn wood or glulam, with two lateral grooves. Two U pieces made from cold-folded steel sheets are placed in the middle, introducing their flanges inside the grooves. These steel elements are produced by folding and making it double in flanges, see *Figure 105*.

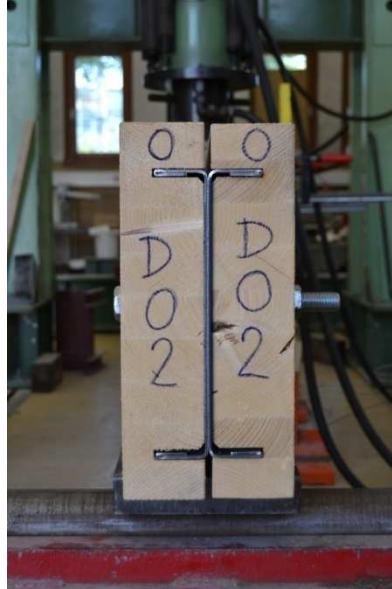


Figure 105: Example of symmetric timber-steel hybrid beam

4.3.4 Asymmetrical arrangement

The hybrid beams are composed by two wooden beams, sawn wood or glulam, with one lateral groove. Two U pieces made from cold-folded steel sheets are placed in the middle, introducing their flanges inside the grooves. These steel elements are produced by folding and making it double in flanges, see *Figure 106*.



Figure 106: Example of asymmetric timber-steel hybrid beam

4.4 CROSS-SECTION DESIGN CRITERIA

4.4.1 Basic structural concept

The basic structural concept of a hybrid beam is a very simple one. Two beams, a timber and a steel one, share the load and experience the same deformation. Each individual beam, as already described, is formed by two steel or timber pieces joined laterally together.

A structural diagram is shown in *Figure 107*. A hybrid beams is represented by the connection of two different beams, the superior a steel one and the inferior a timber one. The connection between beams is represented by vertical pinned bars with infinite stiffness and no weight. This way the two beams will have the same vertical deformation under load, but there is no horizontal shear transmission among the different components.

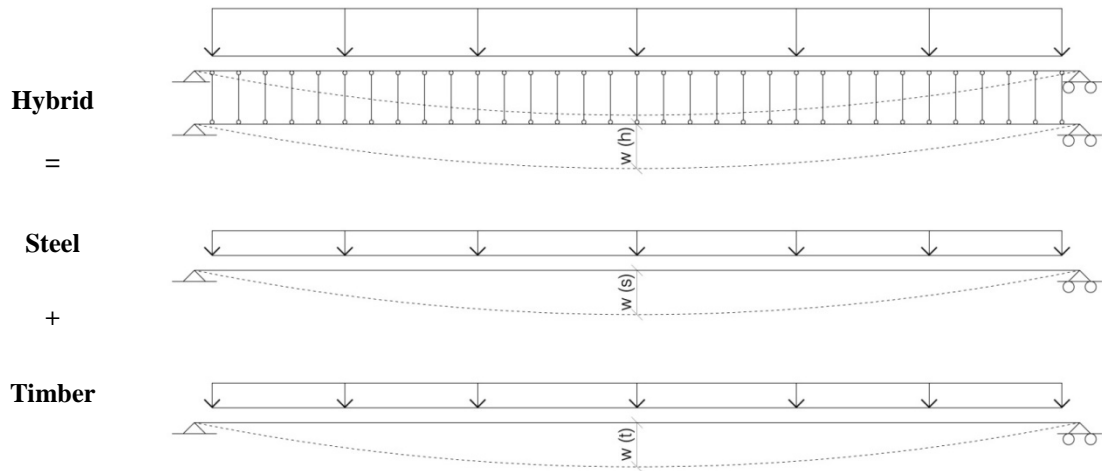


Figure 107: Basic structural concept of a timber-steel hybrid beam

“The deflection of straight beams that are elastically stressed and have a constant cross section throughout their length is given by:

$$w_{inst} = k_b \cdot \frac{W \cdot l^3}{E \cdot I} + k_s \cdot \frac{W \cdot l}{G \cdot A'}$$

where “ w_{inst} ” is the instant deflection, “ W ” the total beam load acting perpendicular to the beam neutral axis, “ l ” the beam span, “ I ” the beam moment of inertia, “ A' ” the modified beam area, “ E ” the beam modulus of elasticity, “ G ” the shear modulus and k_b and k_s constants dependent upon beam loading, support conditions and location of the point whose deflection is going to be calculated.” (20)

For the particular case of uniformly distributed load “ q ” and a simply supported beam, the factors are $k_b = \frac{5}{384}$ and $k_s = \frac{1}{8}$, and the equation can be written as:

$$w_{inst} = \frac{5}{384} \cdot \frac{q \cdot l^4}{E \cdot I} + \frac{1}{8} \cdot \frac{q \cdot l^2}{G \cdot A'}$$

The first term of both equations represents the bending deformation, meanwhile the second one the shear one.

It is a well-known fact that the contribution of the shear flexibility to the overall deformation depends on several factors like type of load, the supporting conditions, the ratio of span to structural depth and the ratio of modulus of elasticity to shear modulus. For the case of simply supported beams and continuous

load this contribution is usually very small and is not taken into account for manual or simplified calculation methods.

The influence of the shear flexibility in the hybrid beams performance will be studied with more detail in the chapter 4.8.1. , but accepting is low influence for simply supported beams under uniformly distributed loads the simplified deformation equation of the beam would be:

$$w_{inst} = \frac{5}{384} \cdot \frac{q \cdot l^4}{E \cdot I}$$

Putting into practice this equation for the structural problem sketched in the *Figure 107* it can be seen that the deformation of a hybrid beam w_h has to be equal to the deformation of the beams which compose it, that is w_s for the steel beam and w_t for the timber one

$$w_h = w_s = w_t$$

But the load supported by the hybrid beam is the total one, q_{tot} , meanwhile the individual steel beam support a fraction of the load q_s , and the timber one a fraction q_t . This two added two fraction should logically be equal to the total load carried by the hybrid beam.

$$q_{tot} = q_s + q_t$$

Due that the deformations of the steel and timber beams also follow the equations:

$$w_s = \frac{5}{384} \cdot \frac{q_s \cdot l^4}{E_s \cdot I_s}$$

$$w_t = \frac{5}{384} \cdot \frac{q_t \cdot l^4}{E_t \cdot I_t}$$

It is easy to prove, using the previous equations, that the fractions of load that the individual steel and timber components have to withstand are proportional to their bending stiffness ($E \cdot I$).

$$q_s = q_{tot} \cdot \frac{E_s \cdot I_s}{E_{tot} \cdot I_{tot}}$$

$$q_t = q_{tot} \cdot \frac{E_t \cdot I_t}{E_{tot} \cdot I_{tot}}$$

Using this method it is easy to calculate how much load has to carry each of the elements composing a hybrid beam and carry out the necessary structural verifications for steel or timber.

In the following points a design process is proposed for the design of geometrically optimized timber-steel hybrid cross sections for single span beams.

There are many determining and interconnected factors involved in the design of a hybrid beam. The design process proposed can be seen as a guide composed of several steps tackling the different design conditions to take into account. It is a “step by step” method for defining the cross-section of hybrid beams. Although the design rules follow a quite simple order of succession, in some cases the complexity and interdependence among the design parameters could lead to revisions of decisions made in previous steps. In any case the structural analysis of the final beam element has to comply with all the requirements detailed during the proposed design process.

4.4.2 Structural depth allowable

The first step for the design of a timber-steel hybrid cross section is the definition of the structural problem to be solved. This means the definition of structural system and/or building type and design conditions.

That the beam to be designed is a single span beam, a continuous beam or a beam inside a frame plays also a relevant role. The cross-section design process detailed here is applicable to single span beams. The adaptation of the design rules to continuous beams or beams forming part of a structural frame will be discussed in the point 4.8.

With the determination of the building and structural type, beam design conditions like the span, loads, spacing and fire resistance required must be defined.

Moreover the structural depth allowable plays a very important role, especially in the case of multi-storey buildings. This allowable dimension will be established as a starting point for the geometric definition of the beam cross-section, fixing the maximum depth the timber pieces can have, as shown in *Figure 108*.

Usual structural depths allowable defined by the division of the span length by a factor between 17 and 20, $L/17$ and $L/20$, are recommended for getting economical designs and were studied experimentally (see chapter 5). In any case any, other structural depths can be used and designed following the next points. Its results should be compared to any other alternatives from the design, structural performance and economical point of views in order to choose the best option for each particular case.

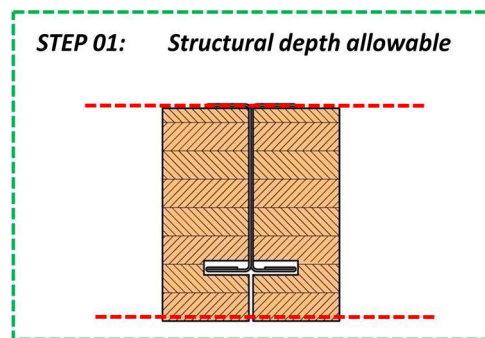


Figure 108: Cross-section design. Step 01 – Structural depth allowable

4.4.3 Fire design strategy

In order to assess the performance of any material or structural element under a fire situation, it is important to notice the difference between the developing phase of a fire and its fully developed phase.

For the developing phase characteristics such as combustibility, ease of ignition and speed of fire spread are of the utmost importance, meanwhile for the fully developed phase the integrity and heat insulation (for separating elements) and carrying load capacity (for separating and non-separating elements) supplied by the different elements are the key factors to be taken into account.

The capacity to withstand the effects during a fully developed fire is known as fire resistance, and it is the main point to be assessed inside this chapter.

The fire resistance required for structural elements are established by national building codes depending on a variety of factors like the number of floors, the fact of these floors are above or underground, evacuation height, gross area of the building, use of the building and formal typology. In the case of multi-storey buildings fire resistances of R60 and R90 are common (218), (219)

The ambient temperatures to be experienced during a fully developed fire are characterised in tests by the standard time-temperature curve from ISO 834 (17), following the equation:

$$\Theta_g = 20 + 345 \log_{10} (8 t + 1)$$

being Θ_g the gas temperature and t the time since the beginning of the fire.

This curve-temperature describes gas temperature values of approximately:

Time of fire (minutes)	30	60	90
Temperature of gas (°C)	840	950	1000

This range of temperatures should be withstood by the timber and steel of a hybrid beam.

Timber is a combustible material; nevertheless it performs better than steel regarding the maintenance of stiffness and strength when exposed to increasing temperatures during time.

A range of several “critical” temperatures defining different behavioural borders should be observed in order to understand timber behaviour in a fire situation. Following Dinwoodie (12), these temperatures are, approximately:

100 °C – above this surface temperature volatile gases begin to be emitted as thermal degradation starts

250 °C – above this temperature there are enough gases in the affected heated material and they allow the ignition of timber if a pilot flame is present

500 °C – without the presence of a pilot flame the surface temperature can reach values above this temperature before the gases become self-igniting.

Other authors (214), (20) establish these values around 300 °C for the presence of a relevant quantity of flammable gases and 400°C for the approximate temperature level where the gases become self-igniting, but in any case it is important to notice that thermal degradation of wood and its ignition is not only related to the absolute temperature values, but also to the time of exposure to those temperatures.

At temperatures above ignition level a quasi-steady state is reached with a balance between the rate of loss of surface and the rate of recession of the undamaged wood. For most softwoods and medium-density hardwoods the rate at which the front recedes is about 0,64 mm/min, whereas for high-density hardwoods the value is about 0,5 mm/min. The formation of the char therefore protects the unburnt timber which may be only a few millimetres from the surface (12).

The still unaffected by pyrolysis inner timber parts maintain is normal temperature and, therefore its mechanical properties intact.

P. Kuklík et al. (214) explain this last effect as:

“In case of solid timber, the core section remains cool only a short distance behind the burning zone. As a consequence, the temperature of the residual section is cool and the construction does not have to accommodate damaging thermal expansions. Also, because the core remains cool, all of the cold state physical properties of the timber are retained and any loss of load bearing capacity is as result of the reduced cross-section, rather than a change in the physical properties.” (214)

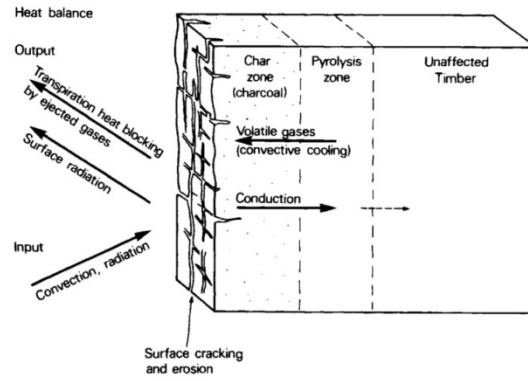


Figure 109: Representation of the thermal decomposition of timber by Dinwoodie (12)

The analysis of this behaviour allows the drawing of “temperature profiles” for a piece of timber burning, where the approximately temperature from the burning surface to the core can be represented. One is proposed by P. Kuklík et al (214) as it follows:

“The temperature for the actual charline is of a magnitude of about 300 °C. The charline derived from β_0 can be put at 200 °C. For a fire exposure more than 20 minutes, ambient temperatures are reached at a distance below the charline which remains constant for the remaining exposure time. This distance is about 30 mm from the charline and for the charline related to β_0 about 25 mm.” (214)

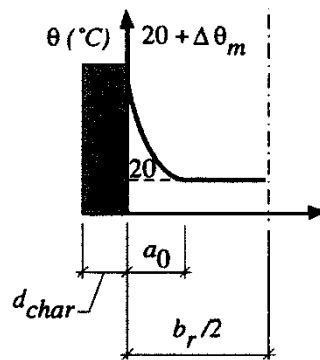


Figure 110: Temperature profile for $br > 2 a_0$ following P. Kuklík et al (214)

β_0 is the one dimensional design charring rate under standard fire exposure following Eurocode 5 (18), i.e. without including the effect of corner roundings and fissures that is included in the *notional charring rate* β_n .

On the other hand steel the performance of steel in a fully developed fire is much more problematic. The critical temperature of a structural steel element is defined in Eurocode 3 “for a given load level, the temperature at which failure is expected to occur in a structural steel element for a uniform temperature distribution” (16). The structural properties of steel, effective yield strength, slope of the linear elastic range and proportional limit, are strongly temperature dependent. Eurocode 3 (16),(220) propose the use of reduction factors for these properties that are graphically gathered up in *Figure 111* and *Figure 112* for the particular case of cold-formed and hot-rolled class 4 steel sections.

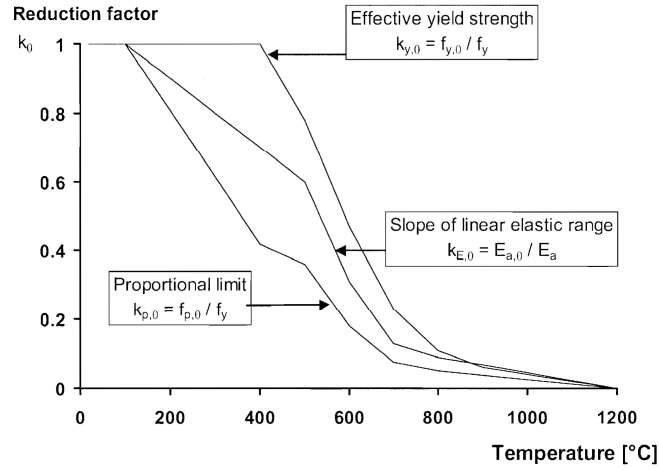


Figure 111: Reduction factors for stress-strain of carbon steel at elevated temperatures. Eurocode 3 (16)

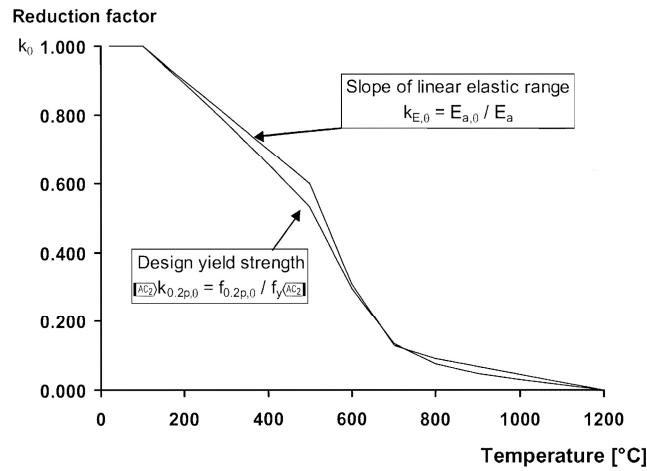


Figure 112: Reduction factors for carbon steel for stress-strain relationship of cold formed and hot rolled class 4 steel sections at elevated temperatures. Eurocode 3(220) .

It can be observed that there is no reduction for effective yield strength $f_{y,0}$ until more than 400 °C (or 100 °C for class 4 cross-section elements), although we will find reduction factors for both proportional limit and the slope of the linear elastic range (i.e. reduction of Young Modulus) for more than 100 °C. But the values of the reduction factors for temperatures of 840, 950 and 1000°C, correspondent to 30, 60 and 90 minutes fire of the ISO curve (17) are extremely low. That means, at this temperatures the structural performance of steel is very poor and it should be protected.

The fire design strategy will, therefore, to keep the steel inside timber pieces at a low temperature.

In order to assess the maximum temperature that could affect the inner steel pieces of a hybrid beam during a fire situation is necessary to pay attention to the different way of calculating the position (and therefore different real temperatures) of the charring line of a timber piece.

For example, and for a 60 minutes fire:

<u>Design charring depth:</u>	<u>Notional charring depth:</u>	<u>Effective charring depth:</u>
$d_{char,0} = \beta_0 \cdot t$	$d_{char,n} = \beta_n \cdot t$	$d_{ef} = d_{char,n} + k_0 \cdot d_0$
$d_{char,0} = 0,65 \cdot 60 = 39 \text{ mm}$	$d_{char,n} = 0,70 \cdot 60 = 42 \text{ mm}$	$d_{ef} = 42 + 1 \cdot 7 = 49 \text{ mm}$
		with:
		$d_0 = 7 \text{ mm}$
		$k_0 = 1,0 \text{ (} t \geq 20 \text{ minutes)}$

Accepting as approximate values, as already stated before following (214), that the *real charring depth* present a temperature of around 300 °C, that the one correspondent to the *design charring depth* is 200 °C, and than 25 mm from it the inner timber core maintains its normal ambient temperature (20°C), we can draw the temperature profile of the whole piece, as show in *Figure 113*.

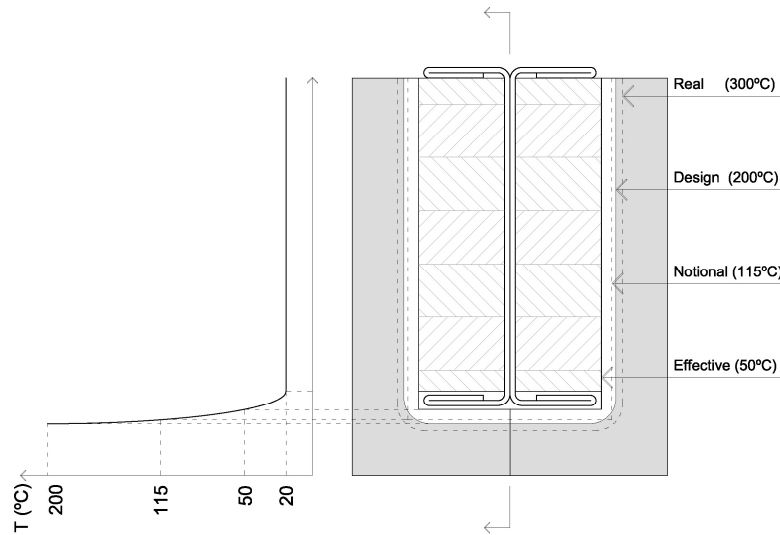


Figure 113: Temperatures through the cross section of a hybrid beam in function of charring depths.

It can be seen how theoretically the steel piece and effective timber cross-section keep a temperature under approximately 50 °C. Therefore all the mechanical properties of the steel piece remain unchanged and we can consider its full section without any properties change for the calculation in a fire situation.

The cross section design strategy will provide enough fire protection for the steel pieces thanks to the timber covering them. The objective is that, during the fire duration, the steel will not be affected by direct flames or relevant change of temperature. At the final point the structural cross section will be composed by the full steel section and the remaining, not burned, timber pieces. For the calculation of the thickness of timber protection needed the reduced cross-section method proposed in Eurocode (18) is used, because, as already seen, it guarantees that the steel pieces remain cool in the interior of timber.

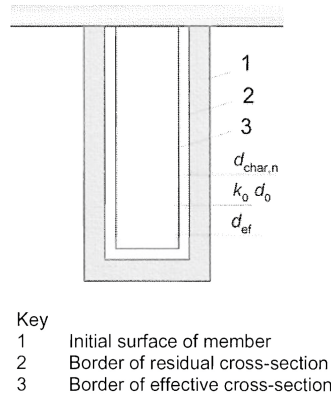


Figure 114: Definition of residual cross-section and effective cross-section, following Eurocode (18)

The method defines a carbonized thickness of wood on the exposed faces of the elements during the fire, which will be subtracted from the original cross-section of the piece. The calculation of this thickness follows the equation:

$$d_{ef} = d_{char,n} + k_0 \cdot d_0$$

with the following related parameters:

$$d_{char,n} = \beta_n \cdot t$$

$$d_0 = 7 \text{ mm}$$

$$t \geq 20 \text{ min} \quad \rightarrow \quad k_0 = 1$$

$$t < 20 \text{ min} \quad \rightarrow \quad k_0 = t/20$$

being t the time the wood is exposed to the fire and β_n the notional charring rate, which is variable depending on the type of wood, and the magnitude of which includes for the effect of corner surroundings and fissures. The values of β_n for each type of wood, and their correspondence with structural grading, are stated in the following table.

Species: Softwood and beech

Glulam	$\delta_k \geq 290 \text{ kg/m}^3$	\rightarrow	$\beta_n = 0,70 \text{ GL24c/h – GL36c/h}$
--------	------------------------------------	---------------	--

Sawn timber	$\delta_k \geq 290 \text{ kg/m}^3$	\rightarrow	$\beta_n = 0,80 \text{ C14 – C50}$
-------------	------------------------------------	---------------	------------------------------------

Species: Hardwood

Glulam or sawn timber	$\delta_k = 290 \text{ kg/m}^3$	\rightarrow	$\beta_n = 0,70$
-----------------------	---------------------------------	---------------	------------------

Glulam or sawn timber	$\delta_k \geq 450 \text{ kg/m}^3$	\rightarrow	$\beta_n = 0,55 \text{ D18 – D70}$
-----------------------	------------------------------------	---------------	------------------------------------

Table 5: Values of β_n in function of type of wood and correspondence with structural grading.

Taking all these parameters into account the thickness of wood needed for providing enough protection during the different duration of fire specified in the codes can be calculated and are stated in the *Table 6* for the cases of glulam, sawn coniferous and sawn deciduous timber.

GLULAM GL24c/h - GL36c/h			SAWN CONIFEROUS C14 - C50		
Protection required (mm)			Protection required (mm)		
	(min)	(mm)		(min)	(mm)
R15	15	15,75	R15	15	17,25
R30	30	28	R30	30	31
R60	60	49	R60	60	55
R90	90	70	R90	90	79
R120	120	91	R120	120	103
R180	180	133	R180	180	151

SAWN DECIDUOUS D18 - D70		
Protection required (mm)		
	(min)	(mm)
R15	15	13,5
R30	30	23,5
R60	60	40
R90	90	56,5
R120	120	73
R180	180	106

Table 6: Thickness of protection wood required depending on type of wood and fire duration.

In this second cross-design step a border limiting the position area that the steel element can occupy inside the cross section is defined.

It should be mentioned that for a good fire performance the gap existing between timber pieces in the bottom part of the beam should be closed. This can be done with an extra glued timber piece or adjusting the geometry of the inner sides of timber components for receiving the thickness of the steel webs. In many drawings in this doctoral thesis and in the real tested beams (see chapter 5) this fact was not addressed due that the fire testing was not a pursued objective.

In any case, this constructive solution is very simple and was already successfully tested. A group of Japanese researchers, with the assistance of members of the Institute of Structural Design and Timber Engineering of the Technical University of Vienna, studied and tested this fact, among other research questions, in a related project designed as a continuation of the works started in this doctoral thesis. More detailed information can be found in Izumi et al (221).

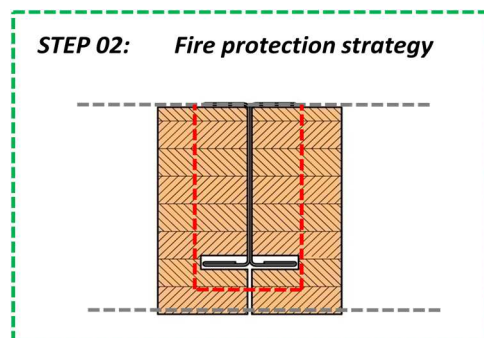


Figure 115: Cross-section design. Step 02 – Fire protection strategy

4.4.4 Optimization of the mechanical performance. Elastic analysis

A way of optimizing a timber-steel hybrid cross section is to design it for making both materials reach their maximum allowable stresses under bending at the same moment. These allowable stresses should be defined for each material and can be taken, for an elastic analysis, as the elastic limit f_y for steel and bending design strength $f_{m,d}$ for timber. For particular cases or other types of analysis other limits can be chosen.

With this limits defined and due to the different elastic modulus of timber and steel each component can reach a different maximum allowable strain “ ϵ ”.

In the case of beams, and as already mention not taking into account the contribution of the shear flexibility, it can be considered that both materials perform together sharing the load under bending. Both materials have the same vertical deformation and that means that their radius of curvature is also the same. Moreover a flat section remains flat after the deformation, according to the Bernoulli hypothesis.

Following the explanation and diagram in *Figure 116* by Timoshenko (222)

“The following theory of bending is based on the assumption that not only such lines as mm remain straight but that the entire transverse section of the beam, originally plane, remains plane and normal to the longitudinal fibres of the beam after bending. [...] From the above assumption it follows that during bending the cross sections mm and pp rotate with respect to each other about axes perpendicular to the plane of bending, so that longitudinal fibres on the convex side suffer extension and those on the concave side compression. [...] The elongation $s's_1$ of any fibre, at a distance y from the neutral surface, is obtained by drawing the line n_1s_1 parallel to mm . Denoting by r the radius of curvature of the deflected axis of the beam and using the similarity of the triangles non_1 and s_1n_1s' , the unit elongation of the fiber ss' is” (222)

$$\epsilon_x = \frac{s' \cdot s_1}{n \cdot n_1} = \frac{y}{r}$$

Therefore:

$$\frac{1}{r} = \frac{\epsilon_x}{y} = \tan \alpha$$

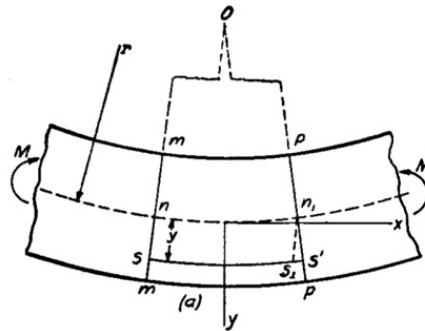


Figure 116: Diagram of a bending beam by Timoshenko (222)

For the particular case of a hybrid beams the two components have the same deformation and radius of curvature:

$$r_t = r_s$$

Therefore, and for timber-steel cross sections like the proposed ones, it is easy to draw the stress and strain diagrams of the cross-sections and find a geometrical arrangement that makes that both materials will reach their allowable stresses under the same vertical deformation.

This leads to an optimum placement of one material in relation to the other. That is, there is an optimum ratio of structural depth (D.R.) for the structural depth required for each of the materials. Finding the optimum ratio of structural depth between different steel qualities and different types of timber is therefore possible, and can be used for designing the hybrid beams cross-section.

In order to explain in a simple way the design concept an example with steel S355 and glulam GL28h is carried out. The design strength of glulam $f_{m,d}$ depends on the characteristic strength, partial material security factor γ_M and the modification factor k_{mod} . In order to simplify the example the allowable stress for timber will be defined as the characteristic strength $f_{m,k}$ in this example. In following points the influence of this factors will be taken into account.

Defining the allowable limit in steel as its elastic limit f_y and for glulam as its characteristic strength $f_{m,k}$:

Material Properties of Steel S355

Young modulus: $E = 210.000 \text{ N/mm}^2$

Elastic limit: $f_y = 355 \text{ N/mm}^2$

Material properties of Glulam GL28h

Young modulus: $E_{0,m} = 12.600 \text{ N/mm}^2$

Characteristic strength: $f_{m,k} = 28 \text{ N/mm}^2$

Maximum strain allowable:

$$\sigma = E \cdot \varepsilon \quad \rightarrow \quad \varepsilon = \sigma / E$$

$$\varepsilon_{\text{steel}} = 355 / 210.000 = 1,69 \cdot 10^{-3}$$

$$\varepsilon_{\text{glulam}} = 28 / 12.600 = 2,22 \cdot 10^{-3}$$

Ratio of Structural Depth:

$$R_{S,D} = \varepsilon_g / \varepsilon_s = 2,22 \cdot 10^{-3} / 1,69 \cdot 10^{-3} = 1,31$$

The physical meaning of these parameters can be easily visualized for the case of a symmetric timber-steel hybrid beam in *Figure 117*.

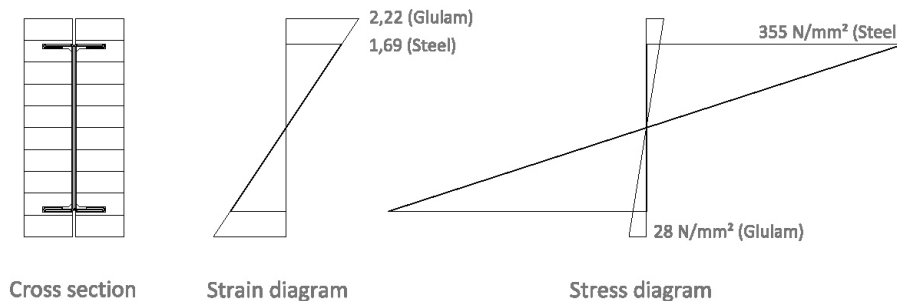


Figure 117: Timber-steel cross-section and strain (10^{-3}) and stress diagrams

The ratio of structural depth represents a geometrical relation between both materials. For this particular case timber should be 1,31 times deeper than steel. If the allowable structural depth, that is, the structural

depth of timber is known, see point 4.4.2, it is easy to calculate how deep the steel pieces should be. That is timber depth divided by 1,31.

This structural depth ratio is influenced by the properties and grading of the materials combined. Different material grades have different properties, elastic modulus and/or characteristic bending strength, that allow for more or less relative deformation

This fact can be observed in *Figure 118* for the case of steel and glulam. Steel grades S235 and S355 have the same elastic modulus $E = 210.000 \text{ N/mm}^2$ but different elastic limits $f_y = 355 \text{ N/mm}^2$ for S355 and $f_y = 235 \text{ N/mm}^2$ for S235. Their maximum possible elastic strains are therefore $\epsilon_{\text{steel-355}} = 1,69 \cdot 10^{-3}$ and $\epsilon_{\text{steel-235}} = 1,12 \cdot 10^{-3}$ respectively. Meanwhile glulam GL24h and glulam GL36h have different values of both elastic modulus $E_{0, m}$ and characteristic bending strength $f_{m,k}$.

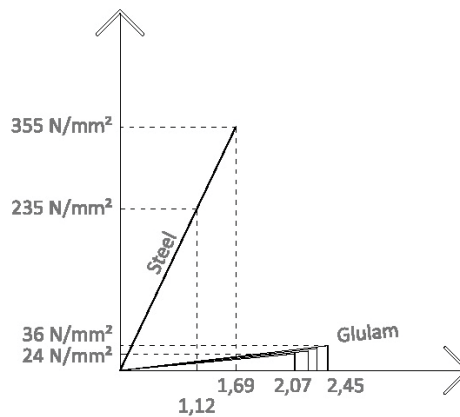


Figure 118: Stress-strain ($\cdot 10^{-3}$) diagrams of different steel and glulam grades in elastic range

It is interesting to notice that the maximum elastic strains of steel are smaller than the glulam ones. This indirectly means that the steel components should remain inside the timber pieces for getting this kind of allowable stress-optimized structural performance. And this fact makes this cross-design step compatible with other conditions like the fire protection that timber has to provide to steel, as stated in the point 4.4.3

Due that there is no horizontal shear connection between the steel and timber components the previous reasoning can be also applied to the proposed asymmetric timber-steel hybrid cross-section. The structural depth ratio can be expressed as the timber structural depth divided by the steel one or, as seen in *Figure 119*, the half o these values. That is $d(s)$ as half of the steel structural depth and $d(t)$ as half of the timber structural depth.

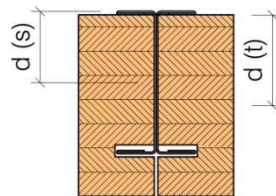


Figure 119: Structural depth ratio $R=d(t)/d(s)$ for a asymmetric timber-steel hybrid beam

The stress and strain diagrams of two equivalent symmetric and asymmetric timber-steel hybrid cross-sections combining glulam GL24c and steel S355 can be seen in *Figure 120*.

Material Properties of Steel S355

Young modulus: $E = 210.000 \text{ N/mm}^2$

Elastic limit: $f_y = 355 \text{ N/mm}^2$

Maximum strain allowable:

$$\sigma = E \cdot \varepsilon \quad \rightarrow \quad \varepsilon = \sigma / E$$

$$\varepsilon_{\text{steel}} = 355 / 210.000 = 1,69 \cdot 10^{-3}$$

Material properties of Glulam GL24c

Young modulus: $E_{0,m} = 11.000 \text{ N/mm}^2$

Characteristic strength: $f_{m,k} = 24 \text{ N/mm}^2$

$$\varepsilon_{\text{glulam}} = 24 / 11.000 = 2,18 \cdot 10^{-3}$$

Ratio of Structural Depth:

$$R_{S,D} = \varepsilon_g / \varepsilon_s = 2,18 \cdot 10^{-3} / 1,69 \cdot 10^{-3} = 1,29$$

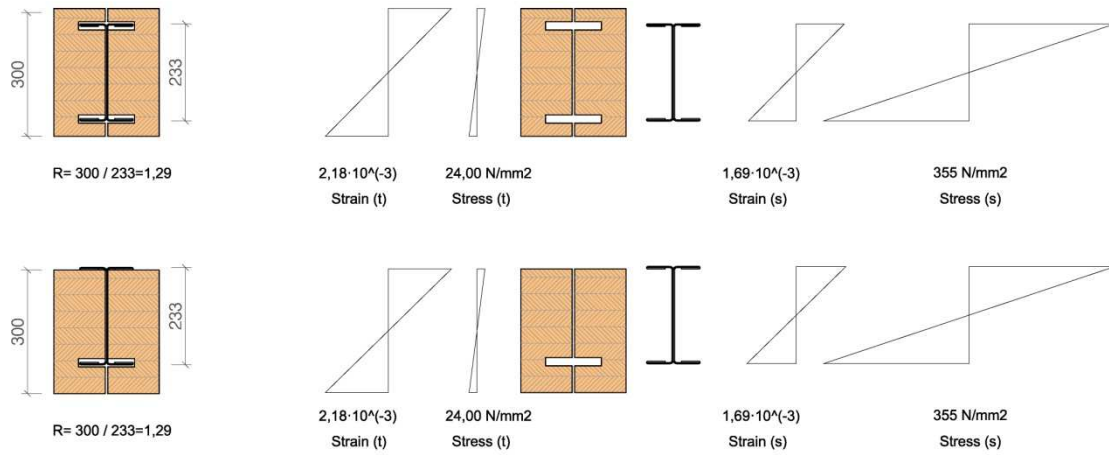


Figure 120: Strain and stress diagrams for two equivalent symmetric (top) and asymmetric (bottom) timber-steel hybrid cross-sections

This structural depth ratio is also influenced by other factors which affect the decision until which point of the stress-strain diagram should the materials be allowed to perform, i.e. the decision of if the steel should be kept in the elastic range or some plasticization is allowed, the different partial security factors for the materials or the coefficient k_{mod} for timber pieces.

For the cases of designing the cross-section taking the strength characteristic values for timber as the design limit, that is $\gamma_{\text{steel}} = 1$, $\gamma_{\text{timber}} = 1$ and $k_{\text{mod}} = 1$, the depth ratios for combinations of steel and combined glulam can be seen in *Table 7*, and the depth ratios for the combinations of steel and sawn timber (from coniferous or deciduous trees) can be seen in *Table 8*

	S235	S275	S355	GL24c	GL28c	GL30c	GL32c
E ; E _{0,m} (N/mm ²)	210000	210000	210000	11000	12500	13000	13500
f _y ; f _{m,k} (N/mm ²)	235	275	355	24	28	30	32
ε max	0,00112	0,00131	0,00169	0,00218	0,00224	0,00231	0,00237

Assumptions				D.R.	GL24c	GL28c	GL30c	GL32c
γ steel	1			S235	1,95	2,00	2,06	2,12
γ glulam	1			S275	1,67	1,71	1,76	1,81
k mod	1			S355	1,29	1,33	1,37	1,40

$D.R. = d(t) / d(s)$

Table 7: Depth ratios calculation for combined glulam; $\gamma_{steel}=1$; $\gamma_{glulam}=1$; $k_{mod}=1$

As already mentioned, it is important to notice that those material combinations where the calculated depth ratio is bigger than one are the most interesting ones, because this indirectly means that the steel components should remain inside the timber pieces for getting this kind of allowable stress-optimized structural performance. And this fact makes this cross-design step compatible with other conditions like the fire protection that timber has to provide to steel.

For a cross-section design optimized for calculations following the prescriptions of Eurocode 5 (6) this depth ratios should be take into account the reduction in strain allowable caused by the material partial security factor for timber and the modification factor k_{mod} . The partial security factors are $\gamma_{glulam}=1,25$ for glulam and $\gamma_{timber}=1,30$ for sawn timber.

The value of k_{mod} to take into account should be defined for each particular case, depending on the material chosen, the service class and the load-duration class of the combinations of loads studied. This leads to a big variety of possible depth ratios, and the correct should be chosen attending to all these factors in.

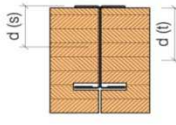
This problem can be simplified for the most common cases in multi-storey buildings with elements composed of glulam or solid timber and performing in service class 1. For this cases the limiting design condition is usually the combination of the permanent actions (load-duration class *permanent*) and live loads (load duration class *medium term*). For this cases the modification factor $k_{mod} = 0,8$.

The calculation of depth ratios for this cases, that is taking into account $\gamma_{steel} = 1$, $\gamma_{glulam} = 1,25$ or $\gamma_{timber} = 1,30$ and $k_{mod} = 0,8$, are shown in *Table 9* and *Table 10*, for glulam and sawn timber respectively.

Any other special case or combination of loads which could be limiting would lead to different depth ratios that can be easily calculated following the procedures explained. The method could also be applied with other values of the modification and security factors prescribed by other construction codes different from Eurocode 5 (6).

	S235	S275	S355	GL24c	GL28c	GL30c	GL32c
E ; E 0,m (N/mm2)	210000	210000	210000	11000	12500	13000	13500
f y ; f m,k (N/mm2)	235	275	355	24	28	30	32
f y,d ; f m,d (N/mm2)	235	275	355	15,36	17,92	19,2	20,48
ϵ max	0,00112	0,00131	0,00169	0,00140	0,00143	0,00148	0,00152

Assumptions							
γ_{steel}	1						
γ_{glulam}	1,25						
k_{mod}	0,8						



D.R.	GL24c	GL28c	GL30c	GL32c
S235	1,25	1,28	1,32	1,36
S275	1,07	1,09	1,13	1,16
S355	0,83	0,85	0,87	0,90

Table 9: Depth ratios calculation for combined glulam; $\gamma_{steel}=1$; $\gamma_{glulam}=1,25$; $k_{mod}=0,8$

Studying this problem graphically or analytically we can find that the depth ratio varies between 0,83 and 1,36 among the combinations possible with steel S235, S275 and S355 and combined glulam.

Other combinations of steel with soft and hardwood sawn timber lead to other relations. High grades of softwoods (coniferous C27-C50) allow much more maximum relative deformation due to its lower Young Modulus than hardwoods (deciduous) or glulam pieces.

As an example combining steel S235 and hardwood timber D18 we could reach a value of 1,04, with steel having almost the same structural depth as glulam.

Anyway this ratio of structural depth from a mechanical point of view should be balanced also with other requirements such as the fire protection that timber should provide to the inner steel pieces. This could lead to adopt depth ratios that are not “optimum” from an structural performance point of view.

In ideal cases the combination of materials should be chosen in order to make compatible an optimum depth ratio with the fire protection requirements. That means depth ratios bigger than 1 and allowing the needed timber protection for steel. This could be in some situations not possible because of the materials commercially available. In these cases, and keeping the steel pieces inside the timber cross-section, not “optimum” ratios usually lead to steel components that are still not performing at their elastic limit when the timber components reach their maximum stresses.

Situations like that can be reasonably justified. For example a cross-section combining GL28c and steel S235 with a depth ratio 1,28 offers the pursued performance. If the same cross section is finally built with steel S355 because the difference of price with S235 is small or even negligible, the final solution will perform also correctly but with an extra structural reserve in the steel part, fact that can be of interest in many cases.

We will come back to this point again because taking into consideration long-term effects could affect again the calculation of the depth ratios, as it will be explained in the point 4.4.8.

In any case, and at this point, a decision must be made referring to the combination the materials and depth ratio to be used. Following considerations (point 4.4.8) can later affect this initial decision and cause adjustments or changes in the cross-section design.

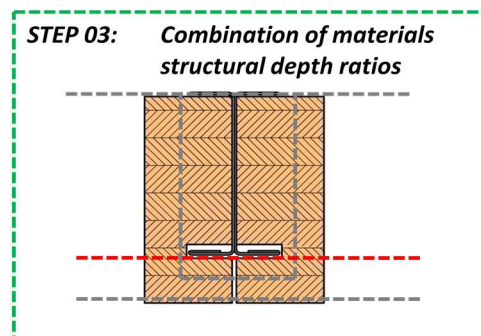


Figure 121: Cross-section design. Step 03 – Combination of materials. Structural depth ratios

4.4.5 Total bending stiffness required

Paying attention again to the basic structural concept of a hybrid beam, as shown in *Figure 107*, it is easy to calculate the total bending stiffness required.

$$w_{\text{tot}} = \frac{5}{384} \cdot \frac{q_{\text{tot}} \cdot l^4}{E_{\text{tot}} \cdot I_{\text{tot}}}$$

$$E_{\text{tot}} \cdot I_{\text{tot}} \geq \frac{5}{384} \cdot \frac{q_{\text{tot}} \cdot l^4}{w_{\text{tot}}}$$

It is necessary to define the deformation limit. In Eurocode 5 (6) the limiting value for the instant deflection of beams is determined as:

$$w_{\text{inst,tot}} \leq \frac{L}{300} \text{ to } \frac{L}{500}$$

Fixing a value according to this and the pertinent National annex it is easy to calculate how much total bending stiffness is necessary for fulfilling this requirement.

The total bending stiffness required should be supplied by the steel and the timber components of the hybrid beam. The proportion in which this bending stiffness should be divided between both materials can be only determined by an iterative process taking into account the total bending stiffness required, as explained in this point, and the timber-steel stiffness balance necessary due to the calculation in a fire situation, which will be detailed in the following point 4.4.6 .

As a first approximation it is useful to consider that the timber part of the hybrid beam should supply around 50% of the total bending stiffness. According to this the width of the timber cross-section can be defined.

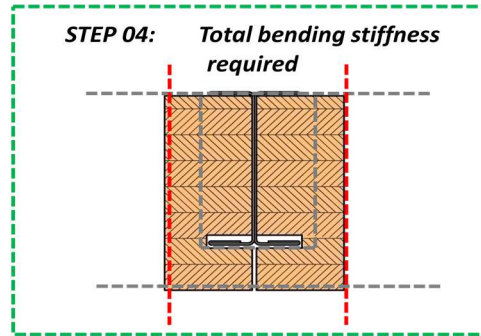


Figure 122: Cross-section design. Step 04 – Total bending stiffness required

4.4.6 Timber-steel stiffness balance

Eurocode 5 (18) prescribes rules for the calculation of timber beams in the case of a fire situation. The calculation concept is based on the fact that the remaining structural cross-section after fire should be able to withstand the load combination of a fire situation.

In the case of a hybrid beam this cross-section would be composed of the fully performing steel element and the effective timber cross-section after the duration of fire.

For determining the load combination in a fire situation, and following Eurocode 5 (18), the effect of actions $E_{d,fi}$ may be obtained from the analysis for normal temperature as:

$$E_{d,fi} = \eta_{fi} E_d$$

where E_d is the design effect of actions for normal temperature design for the fundamental combination of actions (223) and η_{fi} is the reduction factor for the design load in fire situation.

The reduction factor η_{fi} for load combination in EN 1990:2002 (223) should be taken as:

$$\eta_{fi} = (G_k + \psi_{fi} \cdot Q_{k,1}) / (\gamma_G \cdot G_k + \gamma_{Q,1} \cdot Q_{k,1})$$

Eurocode 5 (18) shows the graphic of *Figure 123* as an example of the variation of the reduction factor η_{fi} versus the load ratio $Q_{k,1}/G_k$ for different values of the combination factor ψ_{fi}

ψ_{fi} is the combination factor for frequent values of variable actions in the fire situation, given by $\psi_{1,1}$ (223) that in the case of domestic or residential areas (Category A) or office areas (Category B) has a value of 0,5.

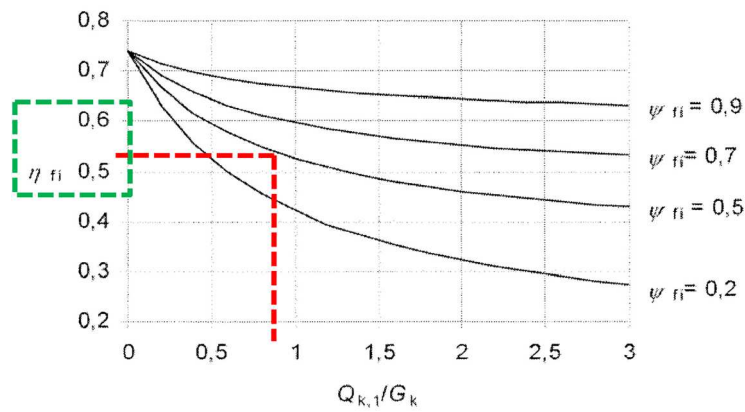
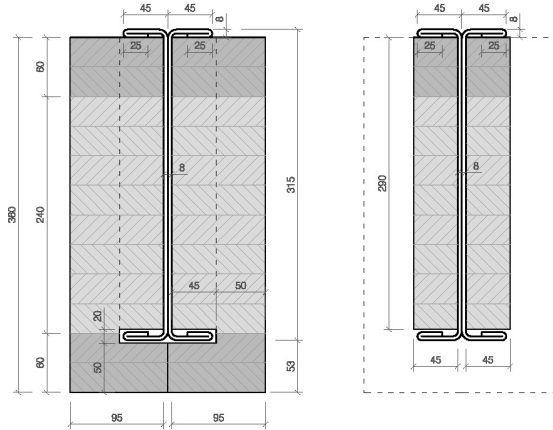


Figure 123: Examples of reduction factor η_{fi} versus load ratio $Q_{k,1} / G_k$

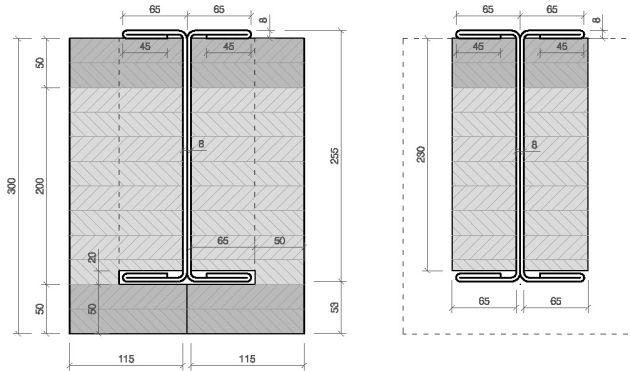
Therefore it can be seen that for usual cases in multistory buildings with residential or office use, where $Q_{k,1}/G_k$ has a value of around 0,8, and if ψ_{fi} the reduction factor η_{fi} should be at least between 0,5 and 0,6. This indirectly means that the cross-section performing in a fire situation should supply at least for 0,5 to 0,6 times the bending stiffness of the original cross-section.

Four examples fulfilling this condition can be seen from *Figure 124* to *Figure 127*. After sixty minutes fire the effective cross-section should provide at least 55% of the original bending stiffness, according to *Figure 123*.



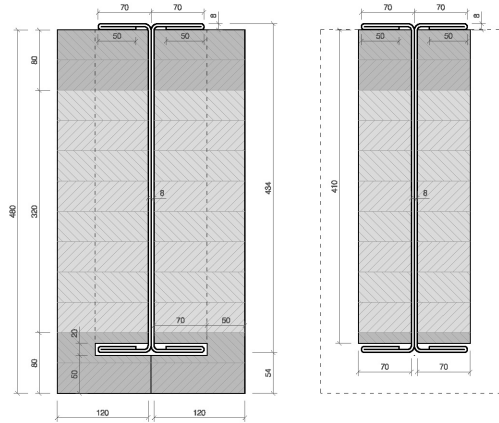
Hybrid G			Hybrid G – 60 minutes fire		
Steel	S355MC		Steel	S355MC	
E	210.000 N/ mm ²		E	210.000 N/ mm ²	
I _s	44.051.400 mm ⁴		I _s	44.051.400 mm ⁴	
E _s · I _s	9,25 · 10 ¹² N · mm ²	51 %	E _s · I _s	9,25 · 10 ¹² N · mm ²	
Glulam	GL28c		Glulam	GL24h-fire	
E	12.600 N/ mm ²		E	10.810 N/ mm ²	
I _g	708.782.400 mm ⁴		I _g	182.917.500 mm ⁴	
E _g · I _g	8,93 · 10 ¹² N · mm ²	49 %	E _g · I _g	1,98 · 10 ¹² N · mm ²	
Total	Hybrid G		Total	Hybrid G	
E _h · I _h	1,818 · 10 ¹³ N · mm ²	100 %	E _h · I _h	1,123 · 10 ¹³ N · mm ²	61,8%

Figure 124: Hybrid beam type G before and after 60 minutes fire



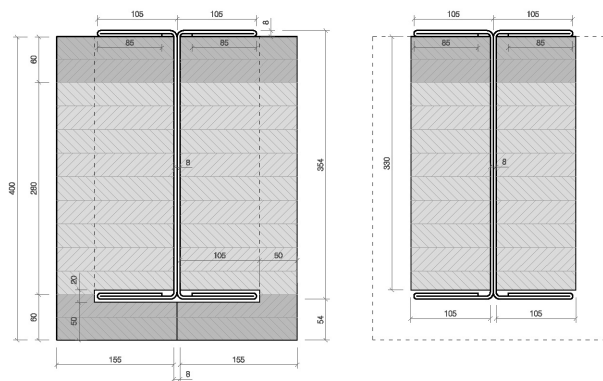
Hybrid H			Hybrid H – 60 minutes fire		
Steel	S355MC		Steel	S355MC	
E	210.000 N/mm ²		E	210.000 N/ mm ²	
I _s	35.864.600 mm ⁴		I _s	35.864.600 mm ⁴	
E _s · I _s	7,53 · 10 ¹² N · mm ²	55 %	E _s · I _s	7,53 · 10 ¹² N · mm ²	
Glulam	GL28c		Glulam	GL24h-fire	
E	12.600 N/ mm ²		E	10.810 N/ mm ²	
I _g	495.450.000 mm ⁴		I _g	131.809.167 mm ⁴	
E _g · I _g	6,24 · 10 ¹² N · mm ²	45 %	E _g · I _g	1,42 · 10 ¹² N · mm ²	
Total	Hybrid H		Total	Hybrid H	
E _h · I _h	1,377 · 10 ¹³ N · mm ²	100 %	E _h · I _h	8,95 · 10 ¹² N · mm ²	65 %

Figure 125: Hybrid beam type H before and after 60 minutes fire



Hybrid I			Hybrid I – 60 minutes fire		
Steel	S355MC		Steel	S355MC	
E	210.000 N/mm ²		E	210.000 N/ mm ²	
I _s	135.433.500 mm ⁴		I _s	135.433.500 mm ⁴	
E _s · I _s	2,84 · 10 ¹³ N · mm ²	52 %	E _s · I _s	2,84 · 10 ¹³ N · mm ²	
Glulam	GL28c		Glulam	GL24h-fire	
E	12.600 N/ mm ²		E	10.810 N/ mm ²	
I _g	2.118.758.400 mm ⁴		I _g	804.078.333 mm ⁴	
E _g · I _g	2,67 · 10 ¹³ N · mm ²	48 %	E _g · I _g	8,69 · 10 ¹² N · mm ²	
Total	Hybrid I		Total	Hybrid I	
E _h · I _h	5,51 · 10 ¹³ N · mm ²	100 %	E _h · I _h	3,71 · 10 ¹³ N · mm ²	67 %

Figure 126: Hybrid beam type H before and after 60 minutes fire



Hybrid J			Hybrid J – 60 minutes fire		
Steel	S355MC		Steel	S355MC	
E	210.000 N/mm ²		E	210.000 N/ mm ²	
I _s	116.518.600 mm ⁴		I _s	116.518.600 mm ⁴	
E _s · I _s	2,447 · 10 ¹³ N · mm ²	55 %	E _s · I _s	2,447 · 10 ¹³ N · mm ²	
Glulam	GL28c		Glulam	GL24h-fire	
E	12.600 N/ mm ²		E	10.810 N/ mm ²	
I _g	1.567.466.700 mm ⁴		I _g	628.897.500 mm ⁴	
E _g · I _g	1,975 · 10 ¹³ N · mm ²	45 %	E _g · I _g	6,80 · 10 ¹² N · mm ²	
Total	Hybrid J		Total	Hybrid J	
E _h · I _h	4,422 · 10 ¹³ N · mm ²	100 %	E _h · I _h	3,127 · 10 ¹³ N · mm ²	71 %

Figure 127: Hybrid beam type H before and after 60 minutes fire

This relationship between the bending stiffness needed before fire and in a fire situation provides, together with the timber width defined in the point 4.4.5, the parameters needed for determining the thickness needed for the steel components of the hybrid beam.

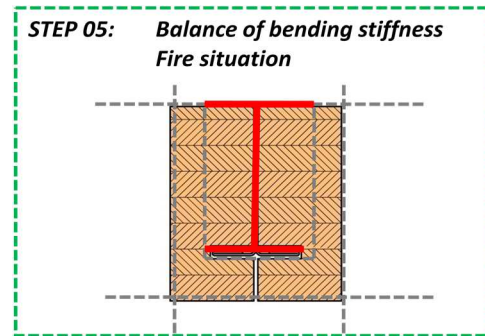


Figure 128: Cross-section design. Step 05 – Balance of bending stiffness. Fire situation

4.4.7 Verification of the shear capacity

Regarding the timber components it is important to proof that the grooves, designed with a proper depth for receiving the steel flanges, will not have any negative effect on the structural performance.

From a structural point of view it is important to maintain an enough amount of wood in the proximity of the grooves in order to withstand and transmit properly the shear forces. Timber has a low shear capacity and the problem has to be taken into account.

It should be examined that for the beams proposed the position of the grooves keep an enough distance to the neutral axis of the timber pieces for making the shear stress values in these areas not causing any problems, as seen in *Figure 129*.

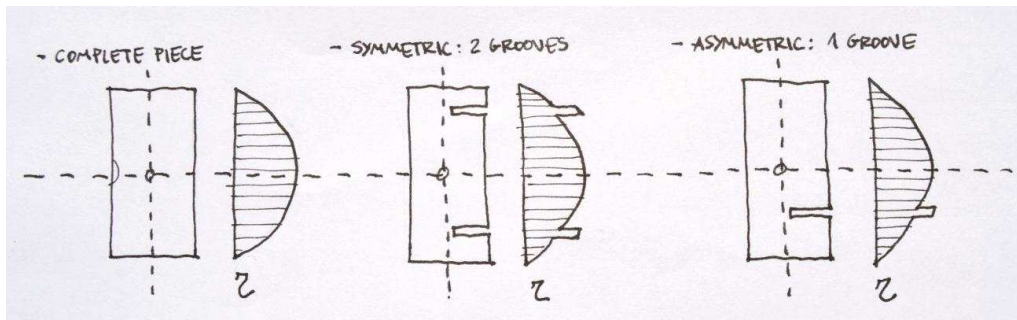


Figure 129: Influence of the position of grooves for the distribution of shear stresses

It should be mentioned that the timber lateral cover is conditioned by the fire protection strategy, as mentioned in 4.4.3. The thickness of protection wood required depending on type of wood and fire duration can be found in *Table 6*, and for usual fire resistance requirements in multi-storey buildings, R60 and R90, is for glulam around 50 and 70 mm, for sawn timber from coniferous species 55 and 80 mm, and for sawn timber from deciduous species 40 and 57 mm.

This range of dimensions for the lateral timber thickness beside the grooves, and taking into account the structural depth of the beam, around $L/17$ to $L/20$, is enough for withstanding the shear stresses of fully loaded beams. The value of the shear stresses in those sections of the beams can be easily calculated using the classic equations of resistance of materials, taking into account the shear forces that the timber components have to withstand and limiting the shear stress value according to Eurocode 5 (6) or other design codes:

$$\tau_d = \frac{Q_d \cdot S_{nn}}{b \cdot I_{nn}}$$

$$\tau_d \leq f_{v,d}$$

This assumption was experimentally verified during the different testing series carried out (see 5.3 and 5.4). No single specimen suffered any problems, cracks or rupture due to this fact.

In any case it is necessary to calculate and verify this condition for any particular case under study.

On the other hand these grooves can have a positive effect and can be used for addressing other kind of problems.

One of the objectives of developing the hybrid system is the improvement of the capacity of medium or even low quality timber pieces. In the particular case of sawn wood, some species show high dimensional changes because of swelling and shrinkage effects. This change in dimensions happens when the wood dries but also with any change of humidity content. The effects become bigger as the size of the piece increases and can produce undesirable warping or cracks. Usually the cracks are not big enough for causing any structural problems, but can affect durability because they are placed where water can be accumulated or insects establish their nests. Dimensional changes, if big enough, can cause a variety of constructive problems, particularly if the straightness of the piece is lost.

The so-called “relieving grooves” have been used traditionally for avoiding this kind of problems. The strategy consists in providing the wood piece, even in green condition, with an already manufactured “crack” for allowing these effects in a controlled way.

Using the grooves proposed for the hybrid beams also for this purposes would be a good strategy for improving the performance of medium or big pieces of sawn wood of certain species, and make them able of addressing demanding structural purposes.

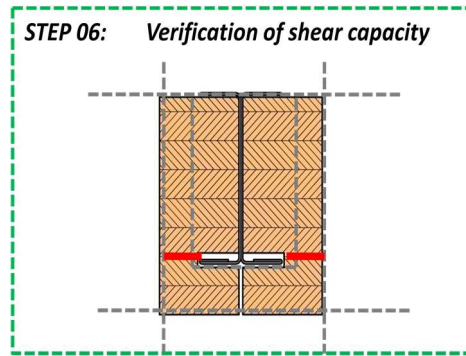


Figure 130: Cross-section design. Step 06 – Verification of shear capacity

4.4.8 Influence of the long term performance for the cross-section optimization

One property of hybrid structural elements is if that the combined use of steel with timber counteracts the creeping behaviour of the last one.

Much more detailed information can be found in the chapter 6, but a introduction and summary is necessary at this point for the implications that this fact have on the design of cross-sections.

As time passes timber will experience the effects of its natural visco-elastic behaviour. This is reflected in an increasing deformation during time, but the steel pieces inside would oppose to these movements. The result is that the steel pieces , as time passes, take gradually fractions of the total load over the beam that where originally supported by the timber parts. The global performance shows a smaller creep deflection than a pure timber beam but, of course, bigger than a pure steel beam which doesn't go through these fluency effects.

For a case under constant load, without unloading and reloading, and for three different beams, steel, hybrid and timber, under the same load and with same instantaneous deflection, the comparative behaviour during time can be as shown in *Figure 131*.

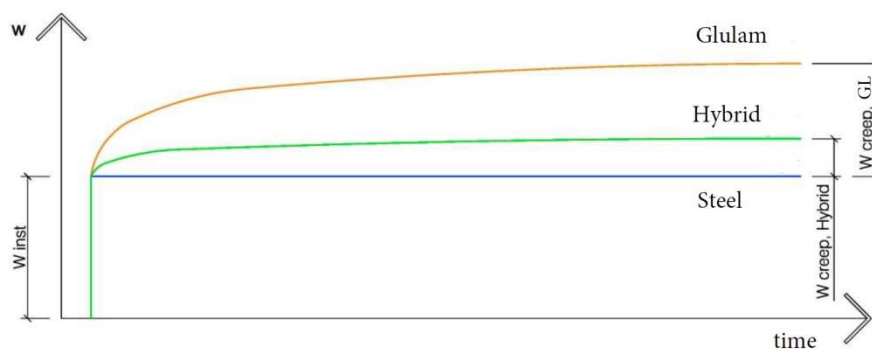


Figure 131: Comparative creeping deflection diagrams of steel, timber and hybrid beams.

The long-term loading final situation, where the steel part carries more load than at the beginning, should be taken into account for the design and calculations of timber-steel hybrid beams.

For the case of timber beams design codes like Eurocode 5 (6) take into account all the complex influence of these phenomena defining different “*Load duration classes*”, “*Service classes*” and the parameters k_{def} and k_{mod}

Eurocode 5 (6) proposes a method which deals with the global performance of “*structures*” composed of materials with different properties depending on time. These following analysis concepts can be applied to the hybrid elements under study.

Eurocode 5 (6) prescribes in its point “2.2.2 *Ultimate limit states*”:

“(1) *The analysis of structures shall be carried out using the following values for stiffness properties:*

(...) for a first order linear elastic analysis of a structure, whose distribution of internal forces is affected by the stiffness distribution within the structure (eg. composite members containing materials having different time-dependent properties), final mean values adjusted to the load component causing the largest stress in relation to strength shall be used; (...)”

And in its point “2.2.3 *Serviceability limit states*”:

“(4) If the structure consists of members or components having different creep behaviour, the final deformation should be calculated using final mean values of the appropriate moduli of elasticity, shear moduli and slip moduli, according to 2.3.2.2(1)”

And in the point “2.3.2.2 Load duration and moisture content in deformations” the following procedures are stated:

“(1) For serviceability limit states, if the structure is formed by pieces or components with different properties depending on time, the final mean value of the modulus of elasticity, $E_{mean,fin}$, the shear modulus $G_{mean,fin}$, and the slip modulus, $K_{ser,fin}$, which are used to calculate the final deformation should be taken from the following expresions:

$$E_{mean,fin} = \frac{E_{mean}}{(1 + k_{def})}$$

$$G_{mean,fin} = \frac{G_{mean}}{(1 + k_{def})}$$

$$K_{ser,fin} = \frac{K_{ser}}{(1 + k_{def})}$$

(2) For ultimate limit states, where the distribution of member forces and moments is affected by the stiffness distribution in the structure, the final mean value of the modulus of elasticity, $E_{mean,fin}$, the shear modulus $G_{mean,fin}$, and the slip modulus, $K_{ser,fin}$, should be calculated following the expressions:

$$E_{mean,fin} = \frac{E_{mean}}{(1 + \Psi_2 \cdot k_{def})}$$

$$G_{mean,fin} = \frac{G_{mean}}{(1 + \Psi_2 \cdot k_{def})}$$

$$K_{ser,fin} = \frac{K_{ser}}{(1 + \Psi_2 \cdot k_{def})}$$

Where:

E_{mean} is the mean value of modulus of elasticity

G_{mean} is the mean value of shear modulus

K_{ser} is the slip modulus

k_{def} is a factor for the evaluation of creep deformation taking into account the relevant service class

Ψ_2 is the factor for quasi-permanent value of the action causing the largest stress in relation to the strength (if this is a permanent action, Ψ_2 should be replaced by 1) ”

Using this approach the needed structural depth ratios defined until now (see 4.4.4) can be verified or modified if necessary for the conditions of ultimate limit state taking into account the long-term performance.

The consequent calculation of elements in the serviceability limit state will be also carried out with the values stated in the first paragraph of this point of the Eurocode 5 (6).

For using this calculation approach it is necessary to define some boundary conditions of the building in order to find the proper values for the factors Ψ_2 , k_{def} and k_{mod}

The security factors according to Eurocode 3 (7) and Eurocode 5 (6) will be:

For steel: $\gamma_{\text{steel}} = 1$

For wood: $\gamma_{\text{glulam}} = 1,25$ for glulam

$\gamma_{\text{timber}} = 1,30$ for solid timber

k_{mod} : For adopting a value for k_{mod} it is necessary to define the Service class and the load-duration class

Service class: As already stated, the main field of application for wood-steel hybrid elements will be multi-story buildings, therefore they will perform mainly in Service class 1.

Load duration: For multi-storey buildings usually the worst load combination is Dead Load (Permanent action) added with Live Load (Medium Term action), therefore a Medium term action of load combination is chosen.

$K_{\text{mod}} = 0,8$ For both solid timber and glulam, and in service class 1 (6).

K_{def} : For both solid timber and glulam, and in service class 1 (6).

$K_{\text{def}} = 0,6$

For determining Ψ_2 it is necessary to know which action causes the largest stress in relation to the strength of wood. This depends on the ratio between dead load and live load. For addressing this problem two exemplary case study are defined, the first one reproducing typical loads for residential and office buildings, Case Study A (category of uses A and B1) and the second reproducing typical loads for public buildings where people may congregate or shopping areas, Case Study B (category of uses C and D) following Eurocode 0 (223) and Eurocode 1 (224). Applying also the partial security factors for loads $\gamma_G = 1,35$ and $\gamma_Q = 1,50$

Case Study A	Dead load structure	2,5 kN/m ²		
	Superimposed dead load	1,6 kN/m ²		
	Total dead load	4,1 kN/m ²	Total design dead load	5,5 kN/m ²
	Live load	2,0 kN/m ²		
	Partitions	0,8 kN/m ²		
	Total live load	2,8 kN/m ²	Total design live load	4,2 kN/m ²
	Total load	6,9 kN/m²	Total design load	9,7 kN/m²
Case Study B	Dead load structure	2,5 kN/m ²		
	Superimposed dead load	1,6 kN/m ²		
	Total dead load	4,1 kN/m ²	Total design dead load	5,5 kN/m ²
	Live load	5,0 kN/m ²		
	Partitions	0,8 kN/m ²		
	Total live load	5,8 kN/m ²	Total design live load	8,7 kN/m ²
	Total load	9,9 kN/m²	Total design load	14,2 kN/m²

Paying attention to the proportion of design load of each case study:

Case Study A	Total design load	9,7 kN/m ²	
	Design Dead load	5,5 kN/m ²	(≈ 57%)
	Design Live load	4,2 kN/m ²	(≈ 43%)
Case Study B	Total design load	14,2 kN/m ²	
	Design Dead load	5,5 kN/m ²	(≈ 39%)
	Design Live load	8,7 kN/m ²	(≈ 61%)

Therefore for the Case Study A the main action is the dead load, meanwhile in Case Study B is the live load and the correspondent values of Ψ_2 are:

Case Study A	→	Main action: Dead load	→	$\Psi_2 = 1$
Case Study B	→	Main action: Live load (Category C and D)	→	$\Psi_2 = 0,6$

It is important to notice that this value of Ψ_2 is determined this way only in order to calculate $E_{\text{mean, fin}}$, $G_{\text{mean, fin}}$ and $K_{\text{ser, fin}}$, and is the one appropriate, inside each category of use, to the “*action causing the largest stress in relation to the strength*” inside each category of use.

This does not mean that in other situations, like for example some load combinations for deflection calculation, Ψ_2 has to adopt the appropriate value for the action that they modifies.

The concept underlying this calculation process is that, in order to find the values of the final situation drafted in *Figure 131*, where the steel part of the hybrid beam already took during time some load originally withstood by timber, the hybrid beam is originally calculated using a “reduced” $E_{\text{mean, fin}}$ for the timber part.

This way the wood part is considered originally less stiff and therefore capable of bearing less amount of load, that is taken by steel. This effect will be bigger or smaller depending on the proportion of long-term to short-term loads.

On one hand a big proportion of dead load will mean that this effect is important, and the wood should be calculated with a lower $E_{\text{mean, fin}}$ ($\Psi_2 = 1$; as in the Case Study A). On the other hand a bigger proportion of live load will mean that this effect will be less relevant, and the wood could be calculated with a not so reduced $E_{\text{mean, fin}}$ ($\Psi_2 = 0,6$; as in the Case Study B).

The expressions for calculating the serviceability limit state follow the same idea, reducing the Young Modulus of timber, and therefore taking into account that the steel will take more load, i.e. it will have a higher deflection. With a simple one-step calculation the final result of adding the instantaneous and the hybrid-creep deflections is obtained.

This calculation approach and its validity will be checked thanks to the analysis of the real performance of hybrid beams under long term testing (see Chapter 6)

Following this method it is easy to calculate, for each particular case, the variation of the ratio of bending stiffness between steel and timber from the initial to the final situation.

As an example for a combination of a beam of glulam GL28c and steel S355 which initially have the same bending stiffness for both materials (50%-50%), and for the Case Study A, the Young Modulus values and bending stiffness variation between components to be considered would be:

	<u>Time = 0</u>	<u>Time = ∞</u>
E_{steel} (N/mm ²)	210.000	210.000
E_{timber} (N/mm ²)	12.500	7.813
$(E \cdot I)_{\text{steel}}$	50%	62,5 %
$(E \cdot I)_{\text{timber}}$	50%	37,5 %

And for the Case Study B

	<u>Time = 0</u>	<u>Time = ∞</u>
E_{steel} (N/mm ²)	210.000	210.000
E_{timber} (N/mm ²)	12.500	9.191
$(E \cdot I)_{\text{steel}}$	50%	58%
$(E \cdot I)_{\text{timber}}$	50%	42%

It is important to notice, that the $E_{\text{mean, fin}}$ for the timber component it is a fictitious value for calculating the effect of load transmission from timber to steel due to creeping, because the real stiffness of the timber pieces does not change as time passes.

Taking all of this into account two calculation approaches are possible. The first one, elastic, is based on keeping the steel components inside the elastic range in the final situation.

For achieving this type of performance the depth ratios already calculated (see 4.4.4) should be adapted reducing the strain allowable for the steel part in the initial situation. It is easy to calculate that this reduction in strain, and therefore stress, should be, for cross-sections with an initial 50%-50% stiffness balance $62,5\% / 50\% = 1,25$ for the Case Study A and $58\% / 50\% = 1,16$ for the Case Study B.

In the *Figure 132* a study case is detailed for a timber steel hybrid beam of GL28c and steel S275, with an structural depth ratio of 1,37 corresponding to a Case Study A. The beam has an initial 50-50 bending stiffness balance between timber and steel. The upper part of the figure shows what would happen in the initial state where steel would not reach its elastic limit. But a calculation of the final state would reach the desired objective.

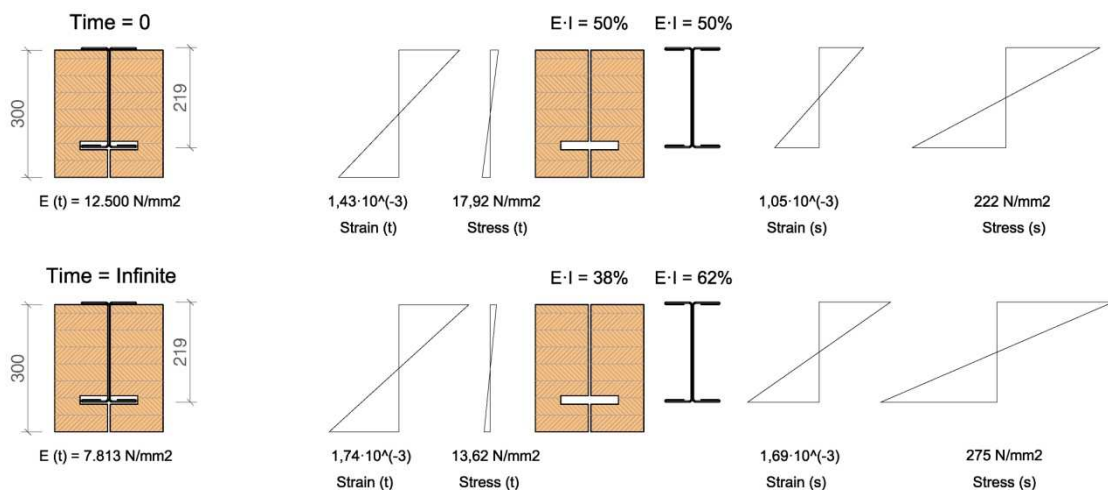


Figure 132: Initial and final strain and stress diagrams for a timber steel hybrid beam of glulam GL28c and steel S275. Case Study A; Structural depth ratio 1,37; Initial bending stiffness balance 50%-50%

The depth ratios proposed until now (see 4.4.4) can be adapted for taking into account the initial and final states. Designing a cross-section making use of these depth ratios would mean that the steel component is at the beginning performing under its elastic limit when timber reaches its maximum stress. But in a final state this limit is achieved.

The new depth ratios for the Cases Study A and B are gathered up in the *Table 11* and *Table 12* for the case of combinations with combined glulam, in *Table 13* for solid softwoods and *Table 14* for solid hardwoods.

It is important to notice that these tables and depth ratios are only valid for hybrid pieces with an initial stiffness balance between steel and timber of 50%-50%. If this is not the case the factor for limiting the steel stresses in the initial state should be calculated and modified. In the following tables the allowable steel strain in the final situation is divided by $62,5\% / 50\% = 1,25$ for the Case Study A and $58\% / 50\% = 1,16$ for the Case Study B. This way it can be guaranteed that the final steel stress would reach the elastic limit.

It should also be pointed out that all the reasoning and tables provided were produced strictly according to the current Eurocode 5 (6) prescriptions, especially regarding the decision of which value for the coefficient ψ_2 should be taken into account.

As already transcribed, ψ_2 is “the factor for quasi-permanent value of the action causing the largest stress in relation to the strength (if this is a permanent action, ψ_2 should be replaced by 1) ” (6), definition that accepts that for a combination of actions the value of ψ_2 should be the correspondent to one of the individual actions taking part in the combination.

It is clear that if only permanent actions occur ψ_2 should take a value of 1, and if only variable actions are present, for example only live load for the Categories of use C and D, this value should be 0,6. But in the case of a combination of both actions, permanent load and live load, the fact that the value of ψ_2 should be 1 or 0,6 depending of which action causes the largest stress in relation to the strength, as prescribed by Eurocode 5 (6) , is disputed.

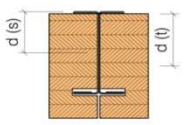
Some authors propose that in the case of a combination of actions the value of ψ_2 should be calculated proportionally to the value of load existent in the quasi-permanent combination of actions. That means, for example, that for a case of Categories of use C and D, with values of permanent load of 5 kN/m² and live load of 4 kN/m², the value of ψ_2 to take into account would be:

$$(1 \cdot 5 + 0,6 \cdot 4) / (5+4) = 0,822$$

This procedure results in a proportionally distributed value for ψ_2 .

In any case, and whatever final criterion for the determination of the ψ_2 value is adopted, the current Eurocode one or the last explained procedure, the design method conserves its validity. Only the specific calculation of the structural depth ratio proposed should be adapted with the appropriate values to the particular case and criterion chosen.

CASE STUDY A	S235	S275	S355	GL24c	GL28c	GL30c	GL32c
E ; E _{0,m} (N/mm ²)	210000	210000	210000	11000	12500	13000	13500
E mean, fin (N/mm ²)				6875	7813	8125	8438
f _y ; f _{m,k} (N/mm ²)	235	275	355	24	28	30	32
f _{y,d} ; f _{m,d} (N/mm ²)	235	275	355	15,36	17,92	19,2	20,48
ε max (final situation)	0,00112	0,00131	0,00169	0,00223	0,00229	0,00236	0,00243
ε max (initial situation)	0,00090	0,00105	0,00135	0,00140	0,00143	0,00148	0,00152
Assumptions							
γ _{steel}	1						
γ _{glulam}	1,25						
k _{mod}	0,8						
Ψ ₂ (only for E mean)	1						
k _{def}	0,6						

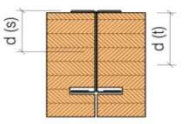


D.R.	GL24c	GL28c	GL30c	GL32c
S235	1,56	1,60	1,65	1,69
S275	1,33	1,37	1,41	1,45
S355	1,03	1,06	1,09	1,12

D.R. = d(t) / d(s)

Table 11: Case Study A. Depth ratios calculation for combined glulam; $\gamma_{steel}=1$; $\gamma_{glulam}=1,25$; $k_{mod}=0,8$; $k_{def}=0,6$; $\psi_2=1$

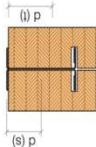
CASE STUDY B	S235	S275	S355	GL24c	GL28c	GL30c	GL32c
E ; E _{0,m} (N/mm ²)	210000	210000	210000	11000	12500	13000	13500
E mean, fin (N/mm ²)				8088	9191	9559	9926
f _y ; f _{m,k} (N/mm ²)	235	275	355	24	28	30	32
f _{y,d} ; f _{m,d} (N/mm ²)	235	275	355	15,36	17,92	19,2	20,48
ε max (final situation)	0,00112	0,00131	0,00169	0,00190	0,00195	0,00201	0,00206
ε max (initial situation)	0,00096	0,00113	0,00146	0,00140	0,00143	0,00148	0,00152
Assumptions							
γ _{steel}	1						
γ _{glulam}	1,25						
k _{mod}	0,8						
Ψ ₂ (only for E mean)	0,6						
k _{def}	0,6						



D.R.	GL24c	GL28c	GL30c	GL32c
S235	1,45	1,49	1,53	1,57
S275	1,24	1,27	1,31	1,34
S355	0,96	0,98	1,01	1,04

D.R. = d(t) / d(s)

Table 12: Case Study B. Depth ratios calculation for combined glulam; $\gamma_{steel}=1$; $\gamma_{glulam}=1,25$; $k_{mod}=0,8$; $k_{def}=0,6$; $\psi_2=0,6$

CASE STUDY A		S235	S275	S355	C14	C16	C18	C20	C22	C24	C27	C30	C35	C40	C45	C50
E : E _{0,m} (N/mm ²)		210000	210000	210000	7000	8000	9000	9500	10000	11000	11500	12000	13000	14000	15000	16000
E mean, fn (N/mm ²)					4375	5000	5625	5938	6250	6875	7188	7500	8125	8750	9375	10000
f _y : f _{m,k} (N/mm ²)		235	275	355	14	16	18	20	22	24	27	30	35	40	45	50
f _{y,d} : f _{m,d} (N/mm ²)		235	275	355	8,62	9,85	11,08	12,31	13,54	14,77	16,62	18,46	21,54	24,62	27,69	30,77
ε max (final situation)		0,00112	0,00131	0,00169	0,00197	0,00197	0,00197	0,00207	0,00217	0,00215	0,00231	0,00246	0,00265	0,00281	0,00295	0,00308
ε max (initial situation)		0,00090	0,00105	0,00135	0,00123	0,00123	0,00123	0,00130	0,00135	0,00134	0,00144	0,00154	0,00166	0,00176	0,00185	0,00192
Assumptions		 D.R. = d(t) / d(s)														
γ steel		1	1,37	1,37	1,37	1,37	1,37	1,45	1,51	1,50	1,61	1,72	1,85	1,96	2,06	2,15
γ timber		1,3	1,17	1,17	1,17	1,17	1,17	1,24	1,29	1,28	1,38	1,47	1,58	1,68	1,76	1,84
K mod		0,8	0,91	0,91	0,91	0,91	0,91	0,96	1,00	0,99	1,07	1,14	1,23	1,30	1,37	1,42
ψ ₂ (only for E mean)		1														
K def		0,6														

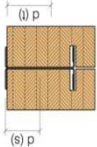
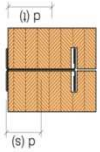
CASE STUDY B		S235	S275	S355	C14	C16	C18	C20	C22	C24	C27	C30	C35	C40	C45	C50
E : E _{0,m} (N/mm ²)		210000	210000	210000	7000	8000	9000	9500	10000	11000	11500	12000	13000	14000	15000	16000
E mean, fn (N/mm ²)					5147	5882	6618	6985	7353	8088	8456	8824	9559	10294	11029	11765
f _y : f _{m,k} (N/mm ²)		235	275	355	14	16	18	20	22	24	27	30	35	40	45	50
f _{y,d} : f _{m,d} (N/mm ²)		235	275	355	8,62	9,85	11,08	12,31	13,54	14,77	16,62	18,46	21,54	24,62	27,69	30,77
ε max (final situation)		0,00112	0,00131	0,00169	0,00167	0,00167	0,00167	0,00176	0,00184	0,00183	0,00196	0,00209	0,00225	0,00239	0,00251	0,00262
ε max (initial situation)		0,00096	0,00113	0,00146	0,00123	0,00123	0,00123	0,00130	0,00135	0,00134	0,00144	0,00154	0,00166	0,00176	0,00185	0,00192
Assumptions		 D.R. = d(t) / d(s)														
γ steel		1	1,28	1,28	1,28	1,28	1,28	1,34	1,40	1,39	1,50	1,59	1,72	1,82	1,91	1,99
γ timber		1,3	1,09	1,09	1,09	1,09	1,09	1,15	1,20	1,19	1,28	1,36	1,47	1,56	1,64	1,70
K mod		0,8	0,84	0,84	0,84	0,84	0,84	0,89	0,93	0,92	0,99	1,06	1,14	1,21	1,27	1,32
ψ ₂ (only for E mean)		1														
K def		0,6														

Table 13: Case Study A and Case Study B. Depth ratios calculation for sawn timber (softwood)

CASE STUDY A				D18	D24	D30	D35	D40	D50	D60	D70
S235	S275	S355									
E : E _{0m} (N/mm ²)	210000	210000		9500	10000	11000	12000	13000	14000	17000	20000
E _{mean} , f _m (N/mm ²)				5937,5	6250	6875	7500	8125	8750	10625	12500
f _y : f _{m,k} (N/mm ²)	235	275	355	18	24	30	35	40	50	60	70
f _{y,d} : f _{m,d} (N/mm ²)	235	275	355	11,08	14,77	18,46	21,54	24,62	30,77	36,92	43,08
e _{max} (final situation)	0,00112	0,00131	0,00169	0,00187	0,00236	0,00269	0,00287	0,00303	0,00352	0,00348	0,00345
e _{max} (initial situation)	0,00090	0,00105	0,00135	0,00117	0,00148	0,00168	0,00179	0,00189	0,00220	0,00217	0,00215
Assumptions											
γ _{steel}	1			1,30	1,65	1,87	2,00	2,12	2,45	2,43	2,41
γ _{timber}	1,3			1,11	1,41	1,60	1,71	1,81	2,10	2,07	2,06
K _{mod}	0,8			0,86	1,09	1,24	1,33	1,40	1,63	1,61	1,59
ψ ₂ (only for E _{mean})	1										
K _{def}	0,6										

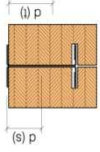
CASE STUDY B				D18	D24	D30	D35	D40	D50	D60	D70
S235	S275	S355									
E : E _{0m} (N/mm ²)	210000	210000		9500	10000	11000	12000	13000	14000	17000	20000
E _{mean} , f _m (N/mm ²)				6985	7353	8088	8824	9559	10294	12500	14706
f _y : f _{m,k} (N/mm ²)	235	275	355	18	24	30	35	40	50	60	70
f _{y,d} : f _{m,d} (N/mm ²)	235	275	355	11,08	14,77	18,46	21,54	24,62	30,77	36,92	43,08
e _{max} (final situation)	0,00112	0,00131	0,00169	0,00159	0,00201	0,00228	0,00244	0,00258	0,00299	0,00295	0,00293
e _{max} (initial situation)	0,00096	0,00113	0,00146	0,00117	0,00148	0,00168	0,00179	0,00189	0,00220	0,00217	0,00215
Assumptions											
γ _{steel}	1			1,21	1,53	1,74	1,86	1,96	2,28	2,25	2,23
γ _{timber}	1,3			1,03	1,31	1,49	1,59	1,68	1,95	1,92	1,91
K _{mod}	0,8			0,80	1,01	1,15	1,23	1,30	1,51	1,49	1,48
ψ ₂ (only for E _{mean})	0,6										
K _{def}	0,6										

Table 14: Case Study A and Case Study B. Depth ratios calculation for sawn timber (hardwood)

An alternative calculation method proposed is based on allowing a certain degree of plasticization in the steel components. In this case the cross section design would remain as explained in the point 4.4.4 (no modification of the depth ratios) and it would be carried out for the initial state. That is, the steel components would already reach their elastic limit in the initial state, and the additional loads that they would gradually take have to be withstood thanks to the steel plastic reserves.

In the *Figure 133* an example is detailed for a timber steel hybrid beam of GL28c and steel S235, with an structural depth ratio of 1,28. The beam has an initial 50%-50% bending stiffness balance between timber and steel. The upper part of the figure shows that the steel reaches already its plastic limit in the initial state. A calculation of the final state would lead to certain plasticization of the steel components.

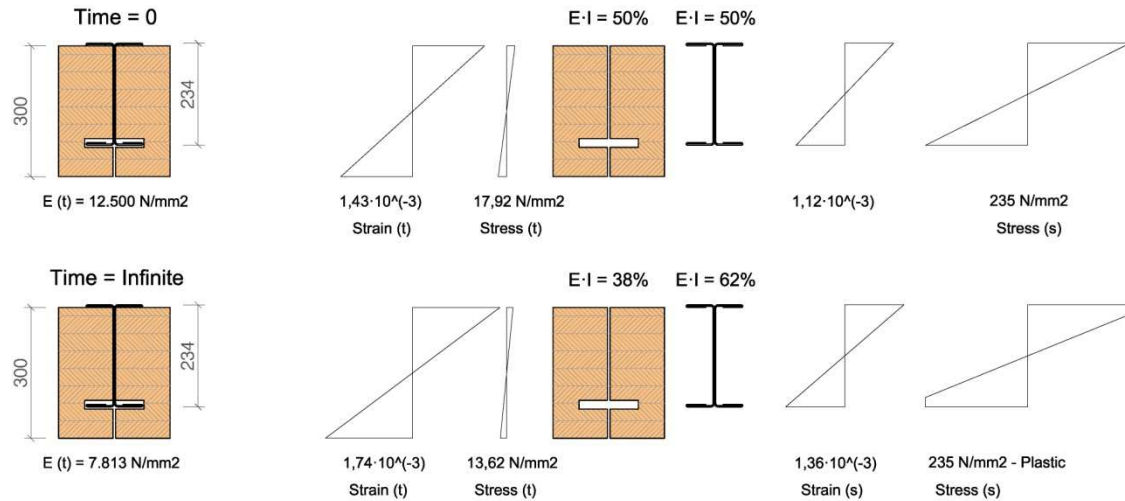


Figure 133: Initial and final strain and stress diagrams for a timber steel hybrid beam of glulam GL28c and steel S235 allowing partial plasticization. Structural depth ratio 1,28. Initial bending stiffness balance 50%-50%

Obviously the first proposed calculation method (elastic) is more conservative than the second one (plastic). The decision of using one of the other depends on the qualities of the steel cross-section and if its degree of plasticization would be allowed or not. Eurocode 3 (7), (220) would limit the application of this method to cross-sections type Class 1 and Class 2. Therefore the elastic design method is proposed as a comprehensive one, meanwhile the use of the plastic one should be considered depending on the steel-cross section designed. Although, as it will be detailed in the chapter 5, the beams tested were designed using the elastic method, the test results have shown that the steel-cross sections used, composed of folded steel plates with a thickness of 3 mm and 4 mm, could reach plasticization without any local buckling problems. The final objective of this design step is the verification, or adaptation if necessary, of all the geometrical decisions taken until now for addressing both the initial and final calculation situations.

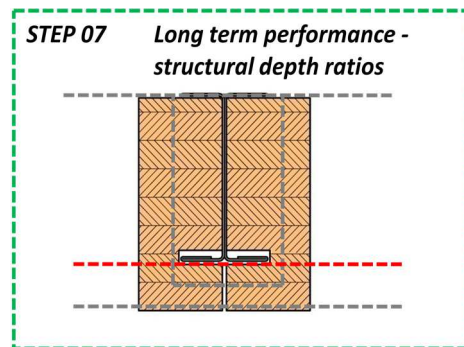


Figure 134: Cross-section design. Step 07 – Long term performance. Structural depth ratios

4.5 SUMMARY: CROSS-SECTION DESIGN IN SEVEN STEPS

A graphic for making visually understandable all the design steps proposed until now is shown in *Figure 135*.

The design process follows the order of the seven steps detailed. This way the definition of the cross section dimensions and materials chosen can be taken following clear criteria. The final goal is the design of an economical and structural well-performing timber steel hybrid beam.

Although it is proposed as a continuous path for designing a hybrid cross-section, the many factors and design conditions to take into account make in some cases inevitable that some design step could cause some type of adjustment of the previous ones. A clear example of this is the discussion of the structural depth ratios, summarized in the graphic as a combined Step 3 / Step 7. Another would be that not demanding fire protection situations (Step 2) would lead to too thin lateral timber coverings that could make the shear capacity calculation (Step 6) a limiting factor.

This design method proved to be useful and successful for the design of the hybrid beams used for two different testing series (see Chapter 5).

In any case the final cross-section adopted should be checked and verified for all the design conditions detailed and taken into account during the seven design steps.

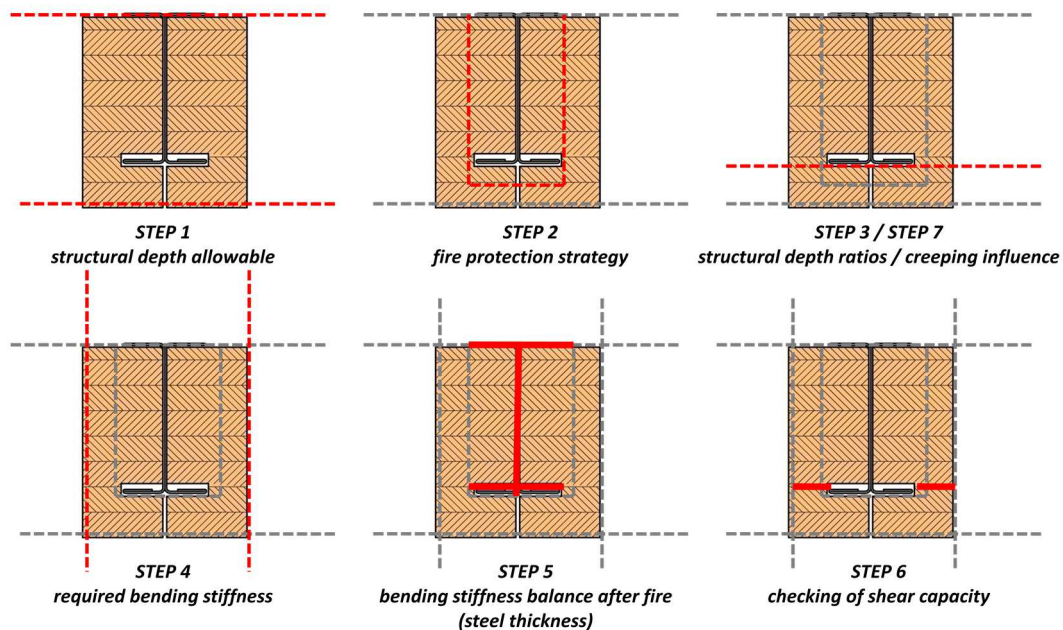


Figure 135: Summary – cross-section design in seven steps

4.6 CALCULATION OF SINGLE SPAN BEAMS

4.6.1 Simplified methods for single span beams

Two different calculation models were used. The first one used exclusively classic strength of materials equations, implemented into EXCEL sheets, and representing two beams, timber and steel, which share their load and deflection.

This calculation procedure does not take into account the influence of the shear stiffness, but proved to be useful and accurate enough for the pre-dimensioning, dimensioning and fast assessment of the capacity and performance of the hybrid beams.

The calculation model an equations used and programmed are detailed in the point 4.4.1

4.6.2 Matrix based calculation model

The second and more precise method is carried out using a matrix-based model of connected bars as shown in *Figure 136*. Each material is represented by a different bar and they are connected for sharing the load and having the same deformation. This connection bars are pinned connected to the main beams, they are infinite stiff and do not have weight.

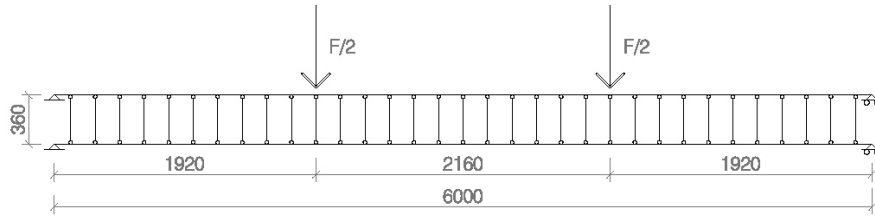


Figure 136: Calculation model and positioning of loads for four point bending test with 6 meters span

This calculation model can be implemented in computer programs that take into account both the influence of moment and shear deformation.

Following Blanco et al (225), for straight beam with a constant cross section and length l , taking into account the deformations caused by bending moments, tension/compression and shear, see *Figure 137*

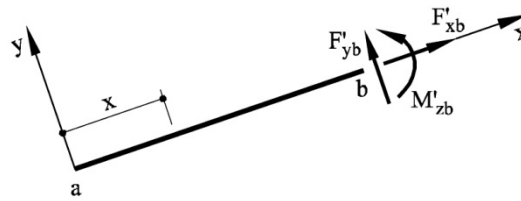


Figure 137: Straight bar considering shear flexibility (225)

the matrix expressing the relation between displacements and rotation of the point b (u'_b ; v'_b ; φ'_b) and forces and moments applied at the same point (F'_{xb} ; F'_{yb} ; M'_{zb}), considering a as a fixed point, would be:

$$\mathbf{d}'_b = \begin{bmatrix} u'_b \\ v'_b \\ \varphi'_b \end{bmatrix} = \begin{bmatrix} \frac{l}{EA} & 0 & 0 \\ 0 & \frac{l^3}{3EI} + \frac{l}{GA} & \frac{l^2}{2EI} \\ 0 & \frac{l^2}{2EI} & \frac{l}{EI} \end{bmatrix} \cdot \begin{bmatrix} F'_{xb} \\ F'_{yb} \\ M'_{zb} \end{bmatrix}$$

where G is the shear modulus and \tilde{A} the reduced shear area. The matrix wrote in compact form would be:

$$\mathbf{d}'_b = \mathbf{F}'_{bb} \cdot \mathbf{f}'_b$$

where \mathbf{F}'_{bb} is the flexibility matrix of the bar using the local reference system. Its inverse would be the rigidity matrix \mathbf{K}'_{bb} .

This calculation model is easy to implement in any standard matrix-based calculation program which takes into account the shear deformation of the bars. The beams assessed for the two bending test series (see Chapter 5) and other examples analysed were calculated with two different programs. The first one is *Metal3D* from the company *Cype* and the second one *RStab* from the company *Dlubal*. As expected both calculation programs yielded the same results.

The difference of results between the matrix-calculation model and the simplified method implemented in EXCEL, without taking into account the influence of the shear flexibility, is very small for simply supported single span beams. This will be detailed with more precision in the point 4.8.1

4.6.3 Ultimate limit state verifications

For a structural elastic analysis, after using one of the two calculation methods proposed, the verifications to be made do not differ from any other standard timber or steel structure.

It should be pointed out that these verifications should be carried out for both the initial state and the final state taking into account long-term behaviour effects as detailed in 4.4.8, and the normal and fire situations as detailed in 4.4.3

For the timber components the prescriptions of Eurocode 5 (6), (18) are applicable.

For the steel components the prescriptions of Eurocode 3 (7), (16), (220) are applicable.

Knowledge gained regarding this issue thanks to the series of short term tests carried out will be discussed in the point 5.5.

4.6.4 Serviceability limit state verifications

For a structural elastic analysis, after using one of the two calculation methods proposed, the verifications to be made do not differ from any other standard timber or steel structure.

It should be pointed out that these verifications should be carried out for both the initial state and the final state taking into account long-term behaviour effects as detailed in 4.4.8.

For the timber components the prescriptions of Eurocode 5 (6), (18) are applicable.

For the steel components the prescriptions of Eurocode 3 (7), (16), (220) are applicable.

Knowledge gained regarding this issue thanks to the series of short and long term tests carried out will be discussed in the points 5.5 and 6.8.

4.7 SINGLE SPAN BEAMS PERFORMANCE

4.7.1 Conclusions: structural performance, economical and ecological considerations

A series of case studies are analyzed in this point in order to evaluate the hybrid single span beams performance in comparison with other structural options, namely steel and timber.

The beams designed for the second test series, beams Type G, Type H, Type I and Type J (see 5.4.1) are used for this comparison. Their cross-sections were designed following the design criteria specified in 4.4 for the particular conditions detailed in 5.4.1. All the details about each cross-section can be found in the respective chapter of the point 5.4.

Obviously these are not the only cross-sections possible for hybrid beams. Each particular design case will lead to a different cross-section. But the idea of this chapter is to illustrate the particularities of the hybrid performance in comparison with the only-steel and only-timber options. In addition these cross-sections were validated during the second series of the short term tests, see 5.4, so the certainty about their structural behaviour exists and can be checked in the test results.

The bases of the comparisons are very simple. Each cross section is, for a determined dimensioning situation (span, spacing, loads, category of use and allowable deformation) compared to two equally performing pure steel and pure glulam beams. The materials used for these comparison beams are the same as the ones used for the hybrid beams, S355 for the steel beams and glulam GL28c for the timber ones.

For all the beams the same allowable structural depth is defined as a condition for reproducing a realistic comparison for the case of multi-storey buildings.

Due to the variability of steel prices and stability of the timber ones, as argued in 2.2.3 and detailed in 5.5, two situations are defined for the price comparisons. Both of them take into account a price of 450 €/m³ for the glulam components, as it was usual during the period of testing of beams. On the other hand a price of 2 €/kg for the steel ones is considered for the first situation, meanwhile a price of 1,5 €/kg is fixed for the second one.

The first price, 2 €/kg, reflects the mean value of the steel prices for the cross-sections ordered in November 2013, see *Table 48*, and is considered as a benchmark of steel prices for ordering small quantities of material. The second price, 1,5 €/kg, is proposed as a hypothetical case when the quantity of materials ordered is bigger, needed for building a multi-storey structure.

The study cases correspond to the design conditions stated in *Table 15*. Their results can be seen from *Table 16* to *Table 23*. A short comment is provided after the results of each type of hybrid beam.

Study case	Hybrid Beam	Span (m)	Structural Depth	Category of use
1	Type G	6	L/17	A, B1
2	Type G	6	L/17	C, D
3	Type H	6	L/20	A, B1
4	Type H	6	L/20	C, D
5	Type I	8	L/17	A, B1
6	Type I	8	L/17	C, D
7	Type J	8	L/20	A, B1
8	Type J	8	L/20	C, D

Table 15: Study cases for the evaluation of the single span hybrid beams performance

Calculation data				Prices	
Span (m)	6	w_{inst}	L/300	GL28c (€/m³)	GL28c (€/m³)
Spacing (m)	3,15	w_{fin}	L/250	450,00	450,00
Dead Load (kN/m²)	4,1	k_{mod}	0,8	+	+
Live Load (kN/m²)	2,8	k_{def}	0,6	Steel S355 (€/kg)	Steel S355 (€/kg)
		Ψ_2	0,3	2,00	1,50
Beam Type		Utilization grade		Price (€/m)	Price (€/m)
		SLS	ULS		
Hybrid Type G 190x360	Glulam		96%	30,78	30,78
	Steel		75%	54,96	41,22
	Total	100%		85,74	72,00
IPE 330	Steel	74%	58%	98,20	73,65
Glulam GL28c 400 x 360	Glulam	94%	89%	64,80	64,80

Table 16: Comparison between hybrid, steel and glulam performances. Six metres span, total structural depth L/17; Category of use A and B1

Calculation data				Prices	
Span (m)	6	w_{inst}	L/300	GL28c (€/m³)	GL28c (€/m³)
Spacing (m)	2,2	w_{fin}	L/250	450,00	450,00
Dead Load (kN/m²)	4,1	k_{mod}	0,8	+	+
Live Load (kN/m²)	5,8	k_{def}	0,6	Steel S355 (€/kg)	Steel S355 (€/kg)
		Ψ_2	0,6	2,00	1,50
Beam Type		Utilization grade		Price (€/m)	Price (€/m)
		SLS	ULS		
Hybrid Type G 190x360	Glulam		98%	30,78	30,78
	Steel		76%	54,96	41,22
	Total	100%		85,74	72,00
IPE 330	Steel	74%	59%	98,20	73,65
Glulam GL28c 400 x 360	Glulam	97%	91%	64,80	64,80

Table 17: Comparison between hybrid, steel and glulam performances. Six metres span, total structural depth L/17; Category of use C and D

From the material costs point of view the hybrid option is always more economic than the only-steel alternative. In addition, and for the steel case, the cost of fire protection measures in order to achieve the sixty minutes fire resistance offered by the hybrid option should still be added to the global price.

The only-timber option is in any case the cheapest option, although not offering the robustness of behaviour (understood as the capacity of withstanding loads after a first rupture as detailed in 5.5) of the hybrid alternative. The hybrid option is around 10% more expensive than only glulam for the second price-benchmark comparison.

Calculation data				Prices	
Span (m)	6	w_{inst}	L/300	GL28c (€/m³)	GL28c (€/m³)
Spacing (m)	2,40	w_{fin}	L/250	450,00	450,00
Dead Load (kN/m²)	4,1	k_{mod}	0,8	+	+
Live Load (kN/m²)	2,8	k_{def}	0,6	Steel S355 (€/kg)	Steel S355 (€/kg)
		Ψ_2	0,3	2,00	1,50
Beam Type		Utilization grade		Price (€/m)	Price (€/m)
		SLS	ULS		
Hybrid Type H 230x300	Glulam		81%	31,05	31,05
	Steel		61%	57,46	43,10
	Total	100%		88,51	74,15
IPE 300	Steel	80%	56%	84,40	63,30
Glulam GL28c 500 x 300	Glulam	99%	78%	67,50	67,50

Table 18: Comparison between hybrid, steel and glulam performances. Six metres span, total structural depth L/20; Category of use A and B1

Calculation data				Prices	
Span (m)	6	w_{inst}	L/300	GL28c (€/m³)	GL28c (€/m³)
Spacing (m)	1,65	w_{fin}	L/250	450,00	450,00
Dead Load (kN/m²)	4,1	k_{mod}	0,8	+	+
Live Load (kN/m²)	5,8	k_{def}	0,6	Steel S355 (€/kg)	Steel S355 (€/kg)
		Ψ_2	0,6	2,00	1,50
Beam Type		Utilization grade		Price (€/m)	Price (€/m)
		SLS	ULS		
Hybrid Type H 230x300	Glulam		81%	31,05	31,05
	Steel		61%	57,46	43,10
	Total	100%		88,51	74,15
IPE 300	Steel	79%	56%	84,40	63,30
Glulam GL28c 500 x 300	Glulam	100%	79%	67,50	67,50

Table 19: Comparison between hybrid, steel and glulam performances. Six metres span, total structural depth L/20; Category of use C and D

In this case and from the material costs point of view the hybrid option is more expensive than the only-steel alternative. Although in the first price-benchmark comparison the difference is very small, less than 5%. In addition, and for the steel case, the cost of fire protection measures in order to achieve the sixty minutes fire resistance offered by the hybrid option should still be added to the global price.

The only-timber option is in any case the cheapest option, although not offering the robustness of behaviour (understood as the capacity of withstanding loads after a first rupture as detailed in 5.5) of the hybrid alternative. The hybrid option is around 10% more expensive for the second price-benchmark comparison.

Calculation data				Prices	
Span (m)	8	w_{inst}	L/300	GL28c (€/m³)	GL28c (€/m³)
Spacing (m)	4,00	w_{fin}	L/250	450,00	450,00
Dead Load (kN/m²)	4,1	k_{mod}	0,8	+	+
Live Load (kN/m²)	2,8	k_{def}	0,6	Steel S355 (€/kg)	Steel S355 (€/kg)
		Ψ_2	0,3	2,00	1,50
Beam Type		Utilization grade		Price (€/m)	Price (€/m)
		SLS	ULS		
Hybrid Type I 240x480	Glulam		95%	51,84	51,84
	Steel		76%	82,46	61,85
	Total	100%		134,30	113,69
IPE 450	Steel	78%	62%	155,20	116,40
Glulam GL28c 500 x 480	Glulam	96%	91%	108,00	108,00

Table 20: Comparison between hybrid, steel and glulam performances. Eight metres span, total structural depth L/17; Category of use A and B1

Calculation data				Prices	
Span (m)	8	w_{inst}	L/300	GL28c (€/m³)	GL28c (€/m³)
Spacing (m)	2,80	w_{fin}	L/250	450,00	450,00
Dead Load (kN/m²)	4,1	k_{mod}	0,8	+	+
Live Load (kN/m²)	5,8	k_{def}	0,6	Steel S355 (€/kg)	Steel S355 (€/kg)
		Ψ_2	0,6	2,00	1,50
Beam Type		Utilization grade		Price (€/m)	Price (€/m)
		SLS	ULS		
Hybrid Type I 240x480	Glulam		98%	51,84	51,84
	Steel		78%	82,46	61,85
	Total	100%		134,30	113,69
IPE 450	Steel	78%	63%	155,20	116,40
Glulam GL28c 500 x 480	Glulam	98%	93%	108,00	108,00

Table 21: Comparison between hybrid, steel and glulam performances. Eight metres span, total structural depth L/17; Category of use C and D

From the material costs point of view the hybrid option is always more economic than the only-steel alternative. In addition, and for the steel case, the cost of fire protection measures in order to achieve the sixty minutes fire resistance offered by the hybrid option should still be added to the global price.

The only-timber option is in any case the cheapest option, although not offering the robustness of behaviour (understood as the capacity of withstanding loads after a first rupture as detailed in 5.5) of the hybrid alternative. The hybrid option is only around 5% more expensive than the only-glulam option for the second price-benchmark comparison.

Calculation data				Prices	
Span (m)	8	w_{inst}	L/300	GL28c (€/m³)	GL28c (€/m³)
Spacing (m)	3,25	w_{fin}	L/250	450,00	450,00
Dead Load (kN/m²)	4,1	k_{mod}	0,8	+	+
Live Load (kN/m²)	2,8	k_{def}	0,6	Steel S355 (€/kg)	Steel S355 (€/kg)
		Ψ_2	0,3	2,00	1,50
Beam Type		Utilization grade		Price (€/m)	Price (€/m)
		SLS	ULS		
Hybrid Type J 310x400	Glulam		80%	55,80	55,80
	Steel		64%	90,00	67,50
	Total	100%		145,80	123,30
IPE 400	Steel	92%	65%	132,60	99,45
Glulam GL28c 700 x 400	Glulam	96%	76%	126,00	126,00

Table 22: Comparison between hybrid, steel and glulam performances. Eight metres span, total structural depth L/20; Category of use A and B1

Calculation data				Prices	
Span (m)	8	w_{inst}	L/300	GL28c (€/m³)	GL28c (€/m³)
Spacing (m)	2,25	w_{fin}	L/250	450,00	450,00
Dead Load (kN/m²)	4,1	k_{mod}	0,8	+	+
Live Load (kN/m²)	5,8	k_{def}	0,6	Steel S355 (€/kg)	Steel S355 (€/kg)
		Ψ_2	0,6	2,00	1,50
Beam Type		Utilization grade		Price (€/m)	Price (€/m)
		SLS	ULS		
Hybrid Type J 310x400	Glulam		81%	55,80	55,80
	Steel		64%	90,00	67,50
	Total	100%		145,80	123,30
IPE 400	Steel	92%	66%	132,60	99,45
Glulam GL28c 700 x 400	Glulam	97%	77%	126,00	126,00

Table 23: Comparison between hybrid, steel and glulam performances. Eight metres span, total structural depth L/20; Category of use C and D

In this case and from the material costs point of view the hybrid option is more expensive than the only-steel alternative. Although in the first price-benchmark comparison the difference is small, less than 10%. In addition, and for the steel case, the cost of fire protection measures in order to achieve the sixty minutes fire resistance offered by the hybrid option should still be added to the global price.

In the second price-benchmark comparison it can be seen that the only-glulam option would be the more expensive one and not offering the robustness of behaviour (understood as the capacity of withstanding loads after a first rupture as detailed in 5.5) of the hybrid alternative.

As a summary of the study cases detailed, and from the material costs point of view, it can be stated that than the hybrid option is cheaper than an only-steel alternative when the structural depth ratio is $L/17$. To the costs of the steel option the appropriate fire protection measures should be still added to the total price.

In the case of a structural depth of $L/20$ the only-steel alternative is cheaper (not taking into account the fire protection issues) although the difference in the cases studied is small (less than 10%) or very small (less than 5%) for the first price-benchmark comparison, taking into account a steel price of 2 €/kg, and depending on the study case.

The only timber-option is, compared to the hybrid one, cheaper for six metres span beams, although not offering the robustness of behaviour (understood as the capacity of withstanding loads after a first rupture as detailed in 5.5) of the hybrid alternative.

For the case of the eight metres span beams the difference in price is small or very small (depending on the price-benchmark comparison) or the hybrid alternative is even cheaper than a pure-glulam alternative.

A preliminary evaluation of the kg of CO₂-equivalent generated by each solution can be done.

Taking into account the CO₂ storing effect during the production of glulam, a value of -1,235 kg CO₂-equivalent per kilogram of glulam is adopted for the comparison. For the steel components a factor of +1,188 kg CO₂-equivalent per kilogram of steel is adopted (226).

The results of the comparison among equally performing hybrid, only steel and only glulam options are gathered in *Table 24*.

Equally performing beams	Glulam (kg/m)	Steel (kg/m)	kg CO ₂ eq.
Hybrid G 190x360	30,54	27,48	-5,07
IPE 330		49,10	+58,33
Glulam GL28c 400x360	64,80		-80,03
Hybrid H 230x300	30,54	28,73	-3,59
IPE 300		42,20	+50,13
Glulam GL28c 500x300	67,50		-83,36
Hybrid I 240x480	51,70	41,23	-14,87
IPE 450		77,60	+92,19
Glulam GL28c 500x480	108,00		-133,38
Hybrid J 310x400	55,11	45,00	-14,60
IPE 400		66,30	+78,76
Glulam GL28c 700x400	126,00		-155,61

Table 24: Comparison of kg CO₂ eq. for equally performing hybrid, steel and glulam beams taking into account a factors of -1,235 kgCO₂eq / kg for glulam and +1,188 kg CO₂ eq / kg for steel

Apart from the obvious fact that the only-timber solution is the one which more CO₂-equivalent can store during their useful life, and that the only-steel is the one which more quantity causes, it is interesting to note that hybrid options are under the carbon-neutral limit, being capable of storing some quantities of CO₂-equivalent during their useful life.

This happens because the mass of timber used per meter of beam is slightly higher than the mass of steel, combined with the fact that the capacity of standard glulam to store CO₂-equivalent per kg of mass is slightly higher than the CO₂-equivalent caused by a kg of steel.

At the end of this chapter it should be pointed out again that the study cases calculated and detailed here were show with the intention of illustrating the capabilities, potential and also limits of the hybrid solutions in comparison with only-steel and only-timber alternatives. But the necessarily limited number of examples shown restricts the conclusions and results of the analysis to similar cases to the ones studied.

For each particular structural problem a hybrid alternative can be designed following the design criteria exposed in 4.4 and compared to other alternatives following the procedures used in this chapter.

Although limited, the comparisons carried out give an overview of the most common conditions found in the design of multi-storey buildings and the single-span performance of timber-steel hybrid beams for this purpose.

4.8 STATICALLY UNDETERMINED SYSTEMS PERFORMANCE

4.8.1 Performance of single span beams. Influence of shear flexibility

The cross-section design process proposed until now does not take into account the effects of the shear flexibility for the calculation of the recommended structural depth ratios. This is not relevant for the case of single span beams, as will be detailed in the following paragraphs.

Following Argüelles et al (227):

“in timber the influence of the deformation due to the shear flexibility compared to the one due to the pure bending is bigger than in other materials and in cases cannot be ignored. This is due to the reduced value of the shear modulus G in relation to the value of the Young modulus E . For timber the ratio $E/G = 16$ is adopted. This ratio is for steel 2,6 and for concrete around 2,5.

(...) the influence of the shear flexibility depends on the ratio E/G , value almost constant ($E/G = 16$), the slenderness of the beam (ratio L/h ; span / depth) and the type of load and supporting conditions.

For example, for a simply supported beam under an uniformly distributed load, the deformation due to the shear flexibility is a 15% of the deformation due to pure bending, when $L/h=10$. This percentage is of only 5,3% when $L/h=17$, which is an usual value for timber beams. This proofs that the effect of the shear flexibility is, in general, negligible.

For the case of single span beams with a rectangular cross-section, the total deformation due to pure bending and shear can be obtained multiplying the deformation due to pure bending by an amplification factor, $k_{f,v}$, defined by the equation:

$$k_{f,v} = 1 + c \cdot (E_{0,mean}/G_{0,mean}) \cdot (h/L)^2$$

where c is a coefficient which depends on the configuration of the applied loads:

$$\begin{aligned} c &= 0,960 && \text{for uniformly distributed loads} \\ c &= 1,200 && \text{for a point load at the middle of the span"} \end{aligned}$$

It can be easily calculated the influence of the shear flexibility for simply supported single span beams. Taking $E/G = 16$, and beams with a structural depth $L/17$ to $L/20$:

For beams with a structural depth $L/17$:

$$k_{f,v} = 1 + 0,96 \cdot (16) \cdot (1/17)^2 = 1,053 \quad \text{For uniformly distributed load} \quad \rightarrow \quad 5,3\%$$

$$k_{f,v} = 1 + 1,20 \cdot (16) \cdot (1/17)^2 = 1,066 \quad \text{For a point load} \quad \rightarrow \quad 6,6\%$$

For beams with a structural depth $L/20$:

$$k_{f,v} = 1 + 0,96 \cdot (16) \cdot (1/20)^2 = 1,038 \quad \text{For uniformly distributed load} \quad \rightarrow \quad 3,8\%$$

$$k_{f,v} = 1 + 1,20 \cdot (16) \cdot (1/20)^2 = 1,048 \quad \text{For a point load} \quad \rightarrow \quad 4,8\%$$

These calculations show that the influence of the shear deformation is very small in the case of simply supported span beams with usual structural depths. The most unfavourable case (point load) represents only the 6,6% of the pure bending deformation.

This indirectly means that the rigidity relations between the steel and timber components inside a hybrid beam is precise enough without taking into account the higher shear flexibility of timber. For a designed timber-steel hybrid cross section with an stiffness balance of 50%-50% between materials (without taking

into account the shear deformation), the overall real stiffness balance (taking into account the shear deformation) would be around 53% for steel and 47% for timber in the most unfavourable case. The usual range of variation for uniformly distributed loads would be smaller than 3% (for $L/17$ structural depths), and less than 2% (for $L/20$ structural depths).

Therefore the design recommendations and ratios of structural depth proposed offer enough precision and preserve their full validity for the case of simply supported single span beams with usual structural depths, whatever the load case it is.

4.8.2 The performance of statically indeterminate systems. Influence of shear flexibility

The design and use of statically indeterminate (or hyperstatic) systems are interesting from a structural design point of view because they offer the possibility of balancing the demands of the Ultimate Limit State and Serviceability Limit State situations.

The comparison between a simply supported single span beam and the same beam spanning over two fields with exactly the same loads is a good example. Meanwhile the bending moment (ULS) to be withstood has the same value for both systems, although in the middle point of the field for the single span beam and over the support for the two fields beam, the deformation (SLS) is for the second around one half of the first one. For a single span beams the limiting of deformations is clearly the most restrictive parameter. Deformations are usually also the limit design condition for continuous beams, but the difference between both cases (ULS and SLS) is much closer that for the single span beams. This leads to an overall better optimization of the consumption of materials needed.

In the case of statically indeterminate (or hyperstatic) systems the influence of the shear flexibility is more relevant than in the statically determined (or isostatic) and it should be taken into account.

This is due to the distribution of bending moments and shear forces caused by the hyperstatic behaviour. For a single supported span beam the maximum values of bending moments are located in the middle point of the span, meanwhile the maximum shear forces occur over the external supports. But for two fields continuous beams, for example, the maximum value of bending moments occurs over the inner support, at the same point where the biggest shear forces appear. Moreover, the absolute values of shear forces are bigger than in the case of the simply supported beam.

As it is well-known the balance of bending moments and shear forces depends on the rigidity of the structural members of the system and should be calculated for each individual case.

The analysis of two simple examples gives light to the importance of this issue.

The deflection of straight beams that are elastically stressed and have a constant cross-section throughout their length is given by (20):

$$w_{\text{inst}} = k_b \cdot \frac{W \cdot l^3}{E \cdot I} + k_s \cdot \frac{W \cdot l}{G \cdot A'}$$

Where W is total beam load acting perpendicular to beam neutral axis, l the beam span, and k_b and k_s constants dependent upon beam loading, support conditions, and location of point whose deflection is to be calculated. A' is the modified beam area, that for beams of rectangular cross section has a value of $A' = \frac{5}{6} b \cdot h$ and for beams with a I cross-section $A' = 0,90 \cdot A_{\text{web}}$.

For a simply supported beam (isostatic) and a uniformly distributed load, as shown in figure *Figure 138* :



Figure 138: Simply supported single span beam with uniformly distributed load

$$k_b = \frac{5}{384} \quad \text{and} \quad k_s = \frac{1}{8}$$

$$w_{\text{inst}} = \frac{5}{384} \cdot \frac{q \cdot l^4}{E \cdot I} + \frac{1}{8} \cdot \frac{q \cdot l^2}{G \cdot A'}$$

But for the same uniformly loaded beam but with clamped supports (hyperstatic), as shown in *Figure 139*:



Figure 139: Single span beam with clamped support ends and uniformly distributed load

$$k_b = \frac{1}{384} \quad \text{and} \quad k_s = \frac{1}{8}$$

$$w_{\text{inst}} = \frac{1}{384} \cdot \frac{q \cdot l^4}{E \cdot I} + \frac{1}{8} \cdot \frac{q \cdot l^2}{G \cdot A'}$$

Therefore it can be calculated that, if the span, materials and cross-section parameters are common for the two beams, the influence of the shear deformation (as calculated in the previous point 4.8.1) for the simply supported beam case is:

For beams with a structural depth $L/20$:

$$k_{f,v} = 1 + 0,96 \cdot (16) \cdot (1/20)^2 = 1,038 \quad \text{For uniformly distributed load} \quad \rightarrow \quad 3,8\%$$

$$\frac{1}{8} \cdot \frac{q \cdot l^2}{G \cdot A'} = (3,8\%) \frac{5}{384} \cdot \frac{q \cdot l^4}{E \cdot I}$$

For the case of the same beam with fixed end points the influence of the shear deformation would be five times bigger:

$$\frac{1}{8} \cdot \frac{q \cdot l^2}{G \cdot A'} = (19\%) \frac{1}{384} \cdot \frac{q \cdot l^4}{E \cdot I}$$

due that the k_b factor is five times smaller.

The difference between the two beams is only the support conditions and makes the structural system change from an isostatic to a hyperstatic one.

This reasoning and calculation applies only to the timber component of the hybrid beam, for the steel one the influence of the shear deformation is in any case negligible. This means that the total influence of the timber shear deformation in the whole hybrid beam is smaller than 19%, but around the half of this value.

In other words, for a designed timber-steel hybrid cross section with an stiffness balance of 50%-50% between materials (without taking into account the shear deformation), the overall real stiffness balance

(taking into account the shear deformation) would be around 59% for steel and 41% for timber in this particular case.

In any case these ranges of values are not negligible anymore and have to be taken into account for the design and verification of timber-steel hybrid elements forming part of statically indeterminate structural systems. For these cases calculation models with the implementation of the effects of the shear flexibility, as the one explained in the point 4.6.2, are necessary for achieving an enough precision.

4.8.3 Statically indeterminate systems performance

As already explained, statically indeterminate hybrid systems have to be calculated taking into account the contribution of the shear flexibility. The cross-section design criteria (see chapter 4.4) are still useful, but the final validity of the cross-section adopted should be verified for each particular case. The influence of the shear flexibility in hyperstatic systems makes that the stiffness balance between the steel and timber components can suffer relevant variations that will affect the distribution of structural moments and shear forces between them.

Although this implies that a “particular-case” analysis is necessary (as usual for any statically indeterminate structural system of any structural material) useful pre-dimensioning rules can be proposed for adapting the general cross-section design procedure (see chapter 4.4) to the case of hyperstatic systems.

In order to analyse the behaviour of hyperstatic systems a series of case studies were calculated. The cross-section of two different timber-steel hybrid beams, Type G and Type H (see chapter 5.4), were used and calculated inside different simple hyperstatic structural systems.

These beams were chosen because their structural behaviour was known due to the structural tests carried out, their initial stiffness balance between steel and timber components is approximately 50%-50% and their structural depth is $L/17$ (Type G) and $L/20$ (Type H), as can be seen in the chapter 5.4. That is, both beams are representative examples for the timber-steel hybrid structural field of application.

Both beams were modelled in matrix-based calculation programs that take into account the influence of the shear flexibility and they were calculated forming part of different simple hyperstatic systems for analysing their behaviour. In all the models, as in the general case (see 4.6.2), the upper bar represents the steel component of the hybrid beam and the bottom bar the timber one. The models analysed represented two span continuous beams and beams forming part of a structural frame.

The supporting conditions of the two span continuous beams were different in three cases. Namely pinned outer supports for both steel and timber (see *Figure 140*), fixed outer supports for both steel and timber (see *Figure 141*)

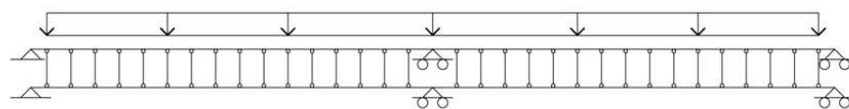


Figure 140: Calculation model for a timber-steel hybrid continuous beam with pinned outer supports

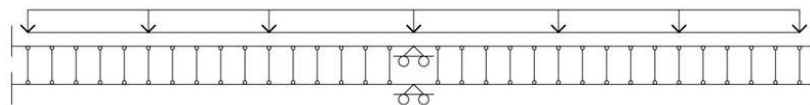


Figure 141: Calculation model for a timber-steel hybrid continuous beam with fixed outer supports

and a mixed case where the steel is fixed at the outer supports meanwhile timber remains pinned as shown in *Figure 142*. This case is interesting because one of the ideas behind the timber-steel hybrid structural elements is the use of both materials making the most of their respective characteristics. And the possibility of achieving with steel rigid or semi-rigid joints is a quite standard solution that could be useful to be use for optimizing the structural performance of the designed systems. On the other hand, building rigid joints with timber is nowadays possible but still not so a common solution as for the steel case.

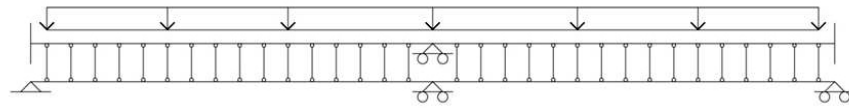


Figure 142: Calculation model for a timber-steel hybrid continuous beam with fixed (steel) and pinned (timber) outer supports

The last case studied (calculation model of *Figure 143*) represents the beams forming part of a structural frame. The supports were modelled as IPE400, being the connecting bars representing a semi-rigid joint two UPE300 profile. The concept behind this semi-rigid joint and its analysis was developed later as a continuation of the work initiated as a part of this doctoral thesis, being the author a member of the researching team.

For the problem discussed now it is enough to mention that the two joint-bars (UPE300 profiles) are connected with two ideal and infinite stiff bars to the hybrid beams. Two vertical forces can therefore be transmitted between beams and joint-bars, and from the joint-bars to the supports, representing the performance of a rigid connection. The supports are in this first model only represented between the points where the bending moments are zero for the supports inside a multi-storey frame. More detailed information can be found in Tavoussi et al (228).

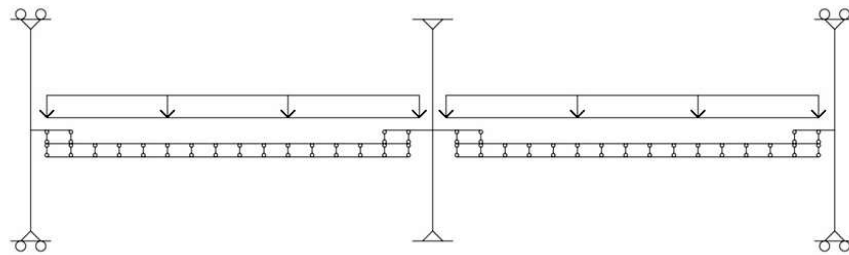


Figure 143: Calculation model for a timber-steel hybrid beams inside a structural frame

In all the cases the beams had a span of six metres. All the systems were loaded until reaching their correspondent maximum structural capacity.

The calculations showed that, as expected, the balance of bending stiffness 50%-50% does not mean in these cases that the bending moments will be distributed between both materials in the same proportion, as is the case in simply supported single span beams. In all these situations the influence of the shear flexibility (being the steel component stiffer) and hyperstatic structural performance makes the steel take a higher proportion of the applied loads.

Especially interesting are the cases where the maximum bending moments for the steel and timber are not located at the same point. This happens logically for the continuous beams if the steel is externally clamped and timber remains pinned, but also for the beams forming part of structural frames.

The diagrams of bending moments with the indication of the position maximum values for the bending moment in steel (M_s) and timber (M_t) for timber-steel hybrid beams Type G can be seen in *Figure 144*, *Figure 145*, *Figure 146* and *Figure 147* for the different structural systems studied.

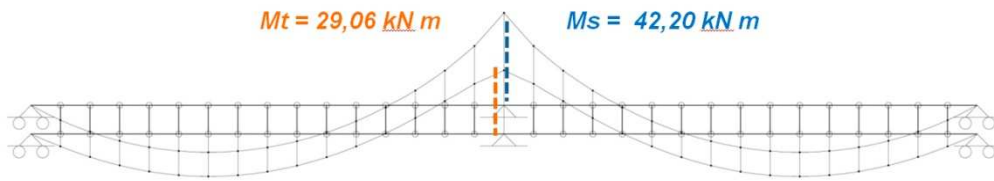


Figure 144: Maximum bending moments – Hybrid Type G, continuous beam with pinned outer supports. $M_s/M_t=1,452$

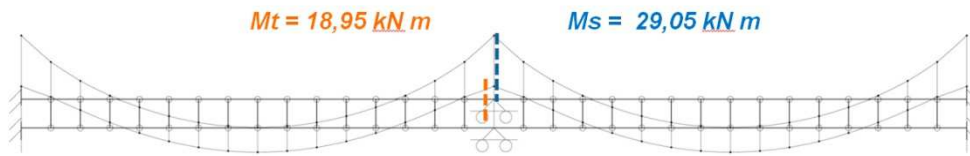


Figure 145: Maximum bending moments – Hybrid Type G, continuous beam with fixed outer supports. $M_s/M_t=1,533$

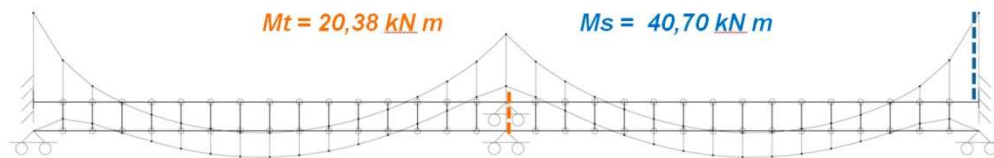


Figure 146: Maximum bending moments – Hybrid Type G, continuous beam with fixed (steel) and pinned (timber) outer supports. $M_s/M_t=1,421$

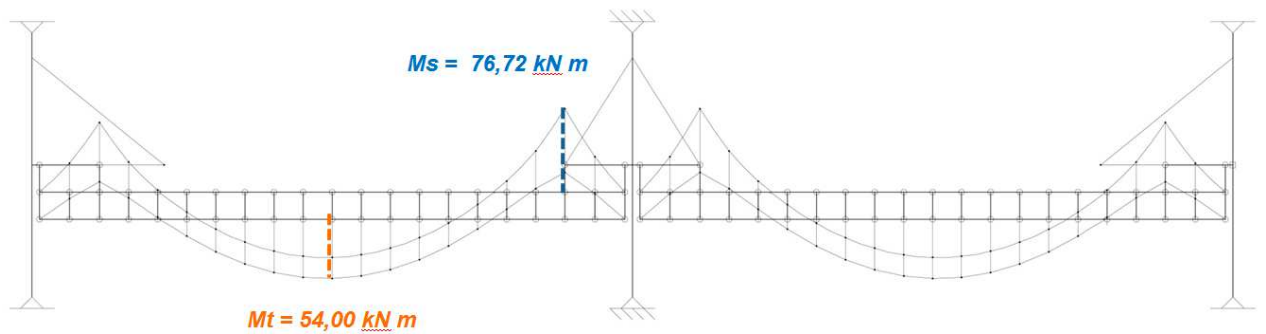


Figure 147: Maximum bending moments – Hybrid Type G, beams inside a structural frame. $M_s/M_t=1,533$

It is interesting to notice that the ratio between the maximum values of bending steel and timber moments remains close to a value of 1,5.

The calculations using the hybrid beam Type H yield the same kind of results, summarized in the Table 25.

Structural system	Hybrid beam	M _s /M _t
Continuous beam	Type G	1,452
Steel pinned		
Timber pinned	Type H	1,486
Continuous beam	Type G	1,533
Steel fixed		
Timber fixed	Type H	1,555
Continuous beam	Type G	1,421
Steel fixed		
Timber pinned	Type H	1,510
Beams inside a frame	Type G	1,533
	Type H	1,498

Table 25: Ratio of maximum bending moments between and steel and timber M_s/M_t

As can be seen this M_s/M_t factor is for the beams and structural systems calculated always close to 1,5, being the mean value of all the cases 1,4985, the lower one 1,421 and the highest one 1,533.

This factor can be used for, in a simplified way, evaluate which would be a more reasonable bending stiffness balance between the timber and steel components for beams to be used inside hyperstatic systems.

Using classic strength of material equations, and assuming that M_s/M_t = 1,5:

$$M_s = 1,5 \cdot M_t$$

$$\begin{aligned} \sigma &= E \cdot \varepsilon \\ \varepsilon_t &= \frac{M_t \cdot y_t}{E_t \cdot I_t} \\ \varepsilon_s &= \frac{(1,5 \cdot M_t) \cdot y_s}{E_s \cdot I_s} \\ \varepsilon_{limit,t} &= (const.) \cdot \varepsilon_{limit,s} \\ \sigma &= \frac{M \cdot y}{I} \\ \varepsilon &= \frac{M \cdot y}{E \cdot I} \end{aligned} \quad \begin{aligned} &\rightarrow \\ &\rightarrow \\ &\rightarrow \end{aligned} \quad \begin{aligned} \frac{M_t \cdot y_t}{E_t \cdot I_t} &= (const.) \cdot \frac{(1,5 \cdot M_t) \cdot y_s}{E_s \cdot I_s} \\ \frac{E_s \cdot I_s}{E_t \cdot I_t} &= (const.) \cdot \frac{1,5 \cdot y_s}{y_t} \end{aligned}$$

If we know or define y_s and y_t because of a determined combination of materials and fire protection strategy (see chapter 4.4) , and also know the value of maximum strain allowable for our particular case (see chapter 4.4), then the constant relating strains can be found and a new stiffness balance between the timber and steel components determined.

For the hybrid beam Type G (y_t/y_s=180/157,5=1,143) and Type H (y_t/y_s=150/127,5= 1,176) of this example, composed of steel S355 and glulam GL28c, the equations would be solved as follows:

For Type G:

$$\begin{aligned} \frac{\varepsilon_t}{\varepsilon_s} &= \frac{1,43 \cdot 10^{-3}}{1,69 \cdot 10^{-3}} = 0,846 \\ \frac{E_s \cdot I_s}{E_t \cdot I_t} &= (0,846) \cdot \frac{1,5 \cdot y_s}{y_t} = (0,846) \cdot \frac{1,5}{1,143} = 1,11 \\ \frac{E_s \cdot I_s}{E_t \cdot I_t} &= 1,11 \end{aligned}$$

For Type H:

$$\frac{\varepsilon_t}{\varepsilon_s} = \frac{1,43 \cdot 10^{-3}}{1,69 \cdot 10^{-3}} = 0,846$$

$$\frac{E_s \cdot I_s}{E_t \cdot I_t} = (0,846) \cdot \frac{1,5 \cdot y_s}{y_t} = (0,846) \cdot \frac{1,5}{1,176} = 1,08$$

$$\frac{E_s \cdot I_s}{E_t \cdot I_t} = 1,08$$

This means that the initial stiffness balance needed would not be 50%-50%, but the steel bending stiffness should be around 10% bigger compared to the timber one.

This means for Type G a bending stiffness balance of 53% for steel and 47% for timber:

$$E_s \cdot I_s = 1,11 \cdot E_t \cdot I_t$$

$$(E_s \cdot I_s) + (E_t \cdot I_t) = 100\%$$

$$1,11 \cdot (E_t \cdot I_t) + (E_t \cdot I_t) = 100\%$$

$$(E_t \cdot I_t) = 47\%$$

For Type H the difference would be even smaller, 52% for steel and 48% for timber:

$$E_s \cdot I_s = 1,08 \cdot E_t \cdot I_t$$

$$(E_s \cdot I_s) + (E_t \cdot I_t) = 100\%$$

$$1,08 \cdot (E_t \cdot I_t) + (E_t \cdot I_t) = 100\%$$

$$(E_t \cdot I_t) = 48\%$$

This precision is difficult to achieve when designing real cross-sections, but it is important to foresee that the bending stiffness of the steel components should be slightly bigger than the timber ones for hyperstatic structural systems.

If long term effects are taken into account the allowable strain ratio should be calculated as explained in 4.4.8, that is for steel S355 and glulam GL28c:

$$\frac{\varepsilon_t}{\varepsilon_s} = \frac{1,43 \cdot 10^{-3}}{1,35 \cdot 10^{-3}} = 1,059$$

And the new balance of bending stiffness for beams Type G would be 60% for steel and 40% for timber:

$$\frac{E_s \cdot I_s}{E_t \cdot I_t} = (1,059) \cdot \frac{1,5 \cdot y_s}{y_t} = (1,059) \cdot \frac{1,5}{1,143} = 1,39$$

$$E_s \cdot I_s = 1,39 \cdot E_t \cdot I_t$$

$$(E_s \cdot I_s) + (E_t \cdot I_t) = 100\%$$

$$1,39 \cdot (E_t \cdot I_t) + (E_t \cdot I_t) = 100\%$$

$$(E_t \cdot I_t) = 40\%$$

For beams Type H would be 57% for steel and 43% for timber:

$$\frac{E_s \cdot I_s}{E_t \cdot I_t} = (1,059) \cdot \frac{1,5 \cdot y_s}{y_t} = (1,059) \cdot \frac{1,5}{1,176} = 1,35$$

$$E_s \cdot I_s = 1,35 \cdot E_t \cdot I_t$$

$$(E_s \cdot I_s) + (E_t \cdot I_t) = 100\%$$

$$1,35 \cdot (E_t \cdot I_t) + (E_t \cdot I_t) = 100\%$$

$$(E_t \cdot I_t) = 43\%$$

4.8.4 Conclusions

It should be pointed out again that the method proposed for calculating the desirable ratio of bending stiffness balance for beams forming part of hyperstatic structures is a simplified one. A final individual analysis of each particular case is needed.

It is also not a linear design process, and some iteration may be needed until finding a cross-section with a good bending stiffness balance for each particular case.

In any case the pre-dimensioning rule that the steel elements should provide around 60% of the total bending stiffness and the timber ones 40% is a good starting approximation for the most common cases. That is, cases similar as the ones used for the reasoning in the previous point 4.8.3.

As a conclusion it is useful to summarize the main concepts and implications for the design of timber-steel hybrid beams in isostatic or hyperstatic situations.

For the isostatic cases the cross-design process proposed in 4.4 is consistent, due that the effects of the shear flexibility do not play a relevant role, as it was demonstrated in 4.8.1. Simplified calculation procedures neglecting the effects of shear flexibility can be used. The desirable bending stiffness balance is around 50%-50% for most usual cases, being usually the determining parameter the fact that the beam cross-section in a fire situation has to be withstood the pertinent loads as explained in 4.4.6.

For the hyperstatic cases shear flexibility plays a relevant role. The calculation models have to take it into account. The cross-section design process has to be adapted for increasing the bending stiffness of the steel component as explained in the previous point 4.8.3. This adaptation to the general cross-section design process is a simplified method and some iteration may be needed, but for most usual cases the “rule of thumb” that the steel components should provide around 60% of the bending stiffness is a good pre-dimensioning starting point.

In any case, for isostatic or hyperstatic systems, a final accurate and precise calculation verifying all the until now described design situations is needed. The cross-section design process is a general method for establishing a good-as-possible performing timber-steel cross-section taking into account all the relevant verifications, but these should be of course checked carefully at the end for each particular case.

5. SHORT-TERM LOADING TESTS

5.1 LOAD DEFINITION AND PRE-DIMENSIONING

As a first step the actions on the structure for the dimensioning and cross-section design of the structural elements are defined. Their use for multi-storey was stated as the first objective and therefore the load values were defined for one case of Housing (Category A) and Office (Category B1 – in existing buildings) buildings, and another case for areas where people may congregate (Category C) and Shopping areas (Category D).

All of this was done following EN 1990 (223) and EN 1991 (224). The list of the adopted loads is stated in the Table 26.

Load Type	Cat. A, B1	Cat. C, D	Units
Self-weight	2,5	2,5	kN/m ²
SI dead load	1,6	1,6	kN/m ²
Live load	2,0	5,0	kN/m ²
Partitions	0,8	0,8	kN/m ²
Total d.l.	4,1	4,1	kN/m ²
Total l.l.	2,8	5,8	kN/m ²
Design d.l. ($\gamma_G=1,35$)	5,5	5,5	kN/m ²
Design l.l. ($\gamma_Q=1,50$)	4,2	8,7	kN/m ²
Total design load	9,7	14,2	kN/m ²

Table 26: Loads for dimensioning of structural elements

The adopted surface loads were transformed in lineal loads considering a different spacing depending on the type of beam and category of use.

For the types of beams tested during the second testing series, see 5.4.1, the spacing was for Housing and Office buildings: 3,15 m (Type G); 2,4 m (Type H); 4 m (Type I) and 3,25 m (Type J). For the Category C and D the spacing was 2,2 m (Type G); 1,65 m (Type H); 2,8 m (Type I) and 2,25 m (Type J).

With the resulting bending moment and shear values for single span beams of 6 and 8 metres, the hybrid beams can be calculated and pre-dimensioned.

Two limiting values of $L/17$ and $L/20$ for the beams structural depths were defined, being L the span of the beam, in order to adapt to a realistic allowable space for structural elements in the frame of a multi-storey building.

In the first testing series the highest value ($L/17$) was used for 6 metres span beams. In the second test series both values ($L/17$ and $L/20$) were applied for both 6 and 8 metres span hybrid beams.

The structural performance concept behind a hybrid beam is a pure additive strategy of two independent beams without horizontal shear connection between them. The design of the cross-section allows that both cross-section components, timber and steel, reach at the same moment their respective limit stress values as explained in 4.4.4 .

The effects of the shear flexibility were not considered for the cross-section design of the testing beams for the reasons detailed in 4.8.1 . This way it can be stated that the hybrid cross-section remains flat

before and after the bending deformation, and for beams with a common position of the centre of gravity a certain optimum ratio between the structural depth of both materials can be found, as it was detailed in 4.4.4 .

The calculations models (see 4.6.2) used for the final comparisons between the structural performance of theoretical beams and the real tested ones took always into account the effects of the shear flexibility.

5.2 CALCULATION OF SINGLE SPAN BEAMS

5.2.1 Calculation of deflection, moment of inertia for steel and elastic modulus of timber

In a first step only the elastic range is considered for the calculation of a hybrid beam. The cross-sections designed were considered theoretically as fully performing, both timber and steel components. The full bending stiffness from the elements was calculated and possible local losses of stiffness were not considered to find the maximum possible value for this parameter.

One goal of the tests was the minimization of the difference between this theoretically maximum possible bending stiffness and the real one that was measured in tests. For assessing this difference, the slopes of the calculated load-displacement diagram and the real obtained from the tests was compared. Real load-deformation lines not fitting the theory ones and with smaller slope values would represent losses of bending stiffness. The real value of the Young Modulus for the timber components was always obtained from tests in advance and then updated in the calculations models before the theory-test results comparison.

Local losses of stiffness can be occasioned by defect load application, tolerances in contact points or by the variability of the material properties, especially in the case of timber. Also, although to a smaller degree, a certain lack of precision during the cold-forming process for the folded steel elements could lead to variations between the maximum stiffness to be expected and the real one.

From a structural performance point of view the hybrid beams is considered as two vertically coupled individual beams, without horizontal shear connections, as shown in *Figure 148*.

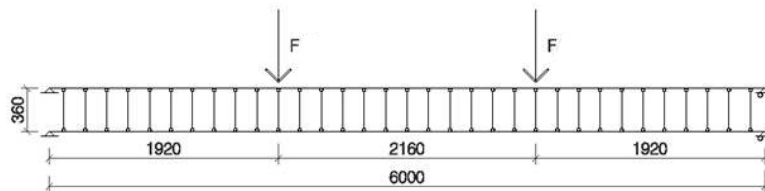


Figure 148: Calculation model and positioning of loads for four point bending test with 6 meters span

This structural behaviour was modelled using the matrix-based programs Metal 3D, from the company Cype Ingenieros, and the program RSTAB from the company Dlubal, and was also programmed in Microsoft Excel making use of static equations. Both methods, which basically follow the same conceptual procedures, provided the same kind of results and were used to detect possible mistakes and to check the validity of each other. The calculation methods were detailed in the point 4.6.

It is common not to take into account the contribution of the shear flexibility for the case of slender bars under bending. But in some cases, like not slender bars and especially with materials like timber, the influence of the shear flexibility on the overall structural performance can start to be relevant. This influence is in any case reduced for single span beams inside a range of slenderness from $L/17$ to $L/20$ like the ones studied, as it was demonstrated in 4.8.1 .

The shear stiffness of the timber components of the real tested beams was not experimentally measured. A given shear stiffness ($G \cdot A'$) using the shear modulus mean value following EN 14080 (14) was always implemented in the calculation models. The possible difference between the shear stiffness assumed in the models and the real one could contribute in any case to really small differences between the ideal and the real beam performance, as explained in 4.8.1. Therefore the experimental measurement of the timber shear modulus was not considered as necessary.

5.2.2 Effective width of flanges

It was checked that the length of flanges for the steel components of the hybrid beams, even considering their total length as a non-folded flange, would fulfil the criteria established by Eurocode 3(229) for the effective width for elastic shear lag of flanges. They were therefore considered as fully performing in their contribution to the total bending stiffness of the steel cross-section.



Figure 149: Dimensions of flanges of hybrid beams Type D (left-first testing series) and Type J (right-second testing series)

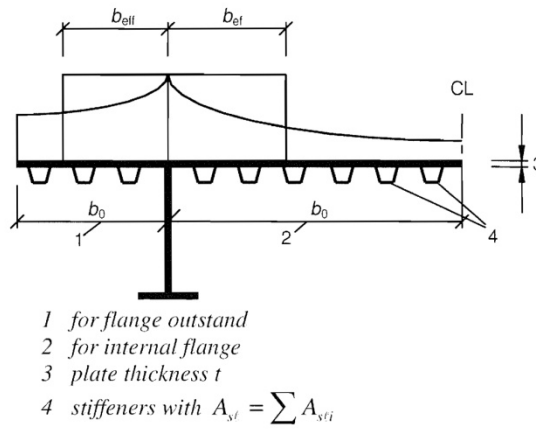


Figure 150: Definition of effective width parameters following EC3 (229)

5.3 FIRST TESTING SERIES

The first testing series of timber-steel hybrid beams was designed to check their structural performance and other relevant issues. It was carried out during May 2013.

In this series all the specimens were double-symmetric, sharing the timber and the steel components the position of their centres of gravity. That is the cross section followed the principles exposed in 4.3.3.

The main objectives of the first testing series were:

- Evaluation of the timber-steel hybrid beams overall structural performance.
- Validation and calibration of the models used for the calculation of the beams.
- Checking of the easiness and reliability of the assembling and disassembling procedures.
- Making a first material price comparison of the different options tested.

In order to study their structural performance, single span hybrid beams were tested under a four-point bending test procedure following EN 408 (230).

The two timber components of each hybrid beams were ordered and cut from a bigger timber piece with a cross-section of 220x360 mm. From each timber block two timber components 80x360 were obtained for the hybrid beam. The remaining piece with a cross dimension of 60x360 mm (beams Type A) was tested until rupture for obtaining the Young Modulus and rupture values of timber.

The determination of the Young modulus for the timber pieces was carried out following EN 408 (230) and corresponded to the global E-modulus value, as recommended in EN 384 (231). For controlling purposes the local values of the E-modulus were also measured and evaluated following the same norm. These values differed minimally from the global ones and were not taken into account anymore. More information about the relationships between local and global modulus of elasticity can be found in Ravensshorts and van de Kuilen (232).

5.3.1 Specimens

A total number of ten hybrid timber-steel beams were assembled and tested.

The combination of materials glulam GL28c and steel S355 (and CLT and steel S355) was chosen for combining the highest capacity materials available at a reasonable market price and with a guaranteed supply. The global research aim was the verification of the hybrid strategy validity, regardless of the materials used. If the calculation models could reproduce correctly the hybrid performance of the beams tested they could also be used with any other combination of materials.

The ratio of structural depth adopted for all the specimens was 1,31, calculated for the combination of materials GL28c and steel S355, in the case of $k_{mod}=1$, $\gamma_{steel}=1$ and $\gamma_{timber}=1$. This value differs minimally from the 1,33 stated in the *Table 7*. The reason is that the design of tests and beams was started considering a mean value for the young modulus of GL28c of $E_{0,mean}= 12.600 \text{ N/mm}^2$. Later a new EN 14080 (14) stated in the year 2013 a new value for $E_{0,mean}= 12.500 \text{ N/mm}^2$. This last value was the one used for the update of the theory exposed in the chapter 4.4. In any case the difference is not relevant for the testing results because, as already explained, the tested real value of the Young Modulus of timber was the one used for the evaluation of tests and hybrid beams performance.

This design situation ($k_{mod}=1$, $\gamma_{steel}=1$ and $\gamma_{timber}=1$) was the one chosen for the first testing series due that the properties of timber (Young Modulus, Rupture) were going to be tested, so there was no uncertainty about their value. The tests were going to be carried out in less than five minutes, so no long term effects were expected. In any case in the second testing series these factors ($k_{mod}=0,8$, $\gamma_{steel}=1$ and $\gamma_{timber}=1,25$) were going to be taken into account for the cross-section design for verifying also this other option.

The performance in a fire situation was not an objective of this first test series, therefore the minimum thickness of wood protecting the steel pieces was not taken into account as a relevant parameter for the beams design.

Three different glulam-steel hybrid-beam types were designed and tested for different purposes, but all of them presenting a theoretically equivalent bending stiffness.

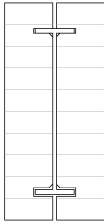
These types are detailed in the *Table 27* and were:

- Four glulam-cold formed steel specimens (D1, D2, D3, D4), being the assessment of their performance the main objective of the testing series.
- Two hybrid glulam-welded steel specimens (B1, B2), made from welded plates but with a “free” steel arrangement, and narrower flanges.
- Two comparison glulam-welded steel specimens (C1, C2), with an equivalent arrangement of steel in web and flanges to the D type, but manufactured from welded steel plates.
- In addition two hybrid CLT-folded steel specimens (E1, E2) were tested for checking the performance of the combination of CLT with glulam.

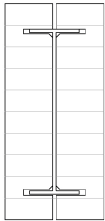
The cross-section Type A were eight pure-glulam 60x360 mm specimens used for determining the Young Modulus of the timber used. A Type A beam was tested in correspondence to each hybrid beam. In the case of the CLT specimens an only-CLT beam (Type CLT) was tested for finding the bending stiffness of the real CLT plates under bending.

All the timber specimens were spruce. The CLT specimens were manufactured from C24 spruce boards.


Cross-section	Specimens	Timber	Steel (S355)
A	8	GL28c	-
B	2	GL28c	welded
C	2	GL28c	welded
D	4	GL28c	cold formed
E	2	CLT	cold formed
CLT	2	CLT	-



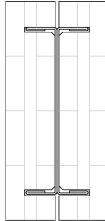
Type B



Type C



Type D



Type E

Table 27: *Specimens of the first testing series. The global cross-section dimensions are 160x360 mm for all the specimens.*

The main questions to be answered, regarding the Type D design option were:

- Global performance of the hybrid design and comparison with the calculation models.
- Performance of the folded steel arrangement in flanges regarding stiffness.
- Performance of both web and flanges regarding local buckling.



Figure 151: Type D hybrid beam during assembling

With the objective of answering these questions for the beams type D the comparison welded type C was designed.

This last one is mechanically equivalent and with an almost identical steel arrangement, but made from welded plates. It was used for comparison purposes and for devising if the global performance, performance of the folded flanges, or possible buckling of web in the type D beams could suffer problems in comparison to a welded beam and with the theoretical values obtained from calculations.

The welded type B hybrid beams, with an optimized steel design and also an equivalent mechanical performance, shows a different steel arrangement with shorter and thicker flanges. Their performance values were compared with both type C and type D in order to assess any loss of capacity or unexpected problem with the goal designs.

Type E, made from CLT, was an independent option.

For each type of hybrid beam, with the exception of Type B, two different types of wood pieces were ordered. The only difference was the available gap of the assembling grooves for receiving the steel flanges, being bigger in one of the two options. On the other hand the Type B wooden pieces were ordered without any tolerance for the upper groove, being the gap exactly of the same thickness as the steel flange to be put inside.

This was made only with the aim of checking the precision of the timber cutting machines, the easiness of assembling and disassembling procedures in relation with the available gaps and if these differently defined tolerances would have some effect on the overall structural performance.

5.3.2 Production, delivery and assembly

All the hybrid beams for B, C, and D types were obtained from the cutting of single pieces of GL28c glulam with dimensions of 220x360 mm. The original block was cut in three pieces, two pieces with dimensions of 80x360 mm with cut grooves for the hybrid beams and a remaining single glulam piece of 60x360 mm for the beams Type A. The beams using CLT, Type E and CLT beams, were cut from a single CLT plate with dimensions of 2.200x6.000 mm.

The grooves were mechanized in the wood factory with the aid of CNC cutting machines. The dimensional precision of both pieces and grooves was excellent.



Figure 152: Delivery of timber components. First testing series



Figure 153: Delivery of steel components, cold formed steel profiles (left) and welded elements (right)



Figure 154: Glulam and steel components for beams before assembling. Beams Type A in the middle of the timber components for the correspondent hybrid beam

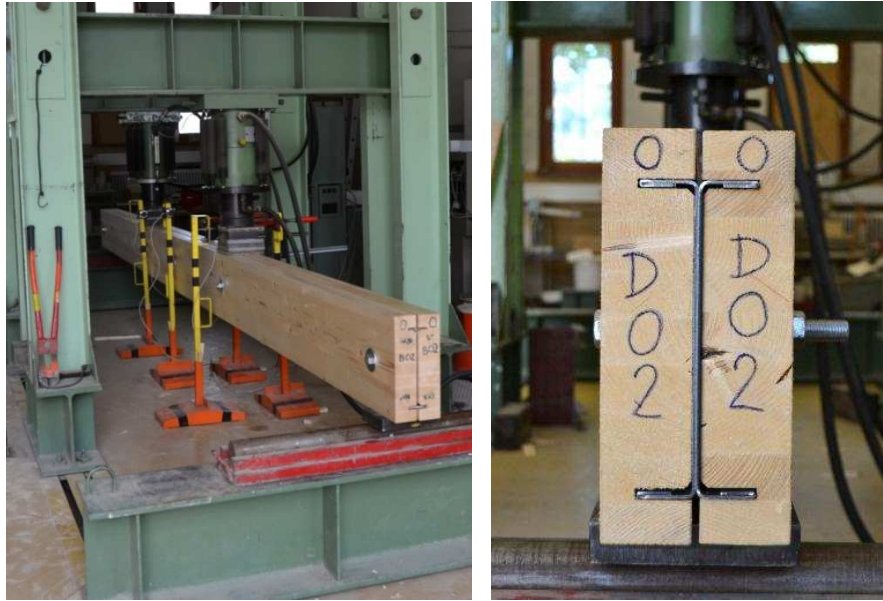


Figure 155: Image of specimens Type C (left: welded steel) and Type D (right: cold-formed steel) from the first testing series

5.3.3 Test set-up, testing procedures and measuring techniques

Due to the known high variability of timber properties, the single glulam pieces (beams Type A) were tested first in order to obtain the rupture and Young modulus values. These values were used later to assess the real performance of the correspondent hybrid beam, due to that they are obtained from the same piece of glulam.

The steel components do not present this variability in performance, so their Young modulus, shear modulus and elastic limit are precisely known. With this procedure the real values for the properties of both materials were known for the final hybrid beams.

This procedure proved to be useful although it was responsible of some incidents.

The original glulam blocks, with dimensions of 220x360 mm, fulfilled on their own the requirements regarding position and size of knots to be graded as glulam GL28c. But in one case (beam B02), and after the cutting of the original piece in the three components described, one of the derived components for the hybrid beam presented a knot occupying almost the whole width of the piece in the tension area, as is shown in *Figure 156*.

Obviously this component did not fulfil the GL28c classification requirements anymore. This beam broke in this area under really low load values. Therefore it is important to notice that the individual components of the hybrid beams are the ones which have to fulfil the requirements of the glulam grade considered in the design.



Figure 156: Rupture due to a big knot in the specimen B02

All the beams were tested following a four point bending arrangement for 6 metres span as shown in the Figure 157.

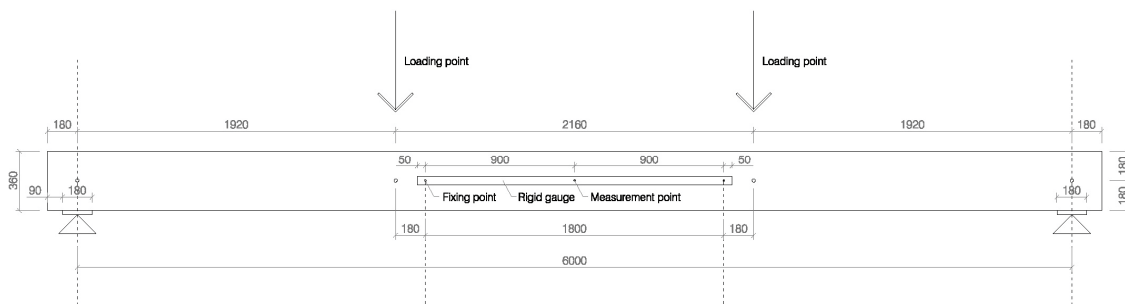


Figure 157: Four point bending test arrangement

Glulam beams Type A were tested for obtaining the values of the global Young Modulus before rupture, and later bending strength until rupture of the piece following the procedures stated in EN 408 (230).

Hybrid beams Types B, C and D were also tested following an analogous procedure. They were tested first until a representative value of load and deformation, around 55 mm deflection, for calculating their bending stiffness, and later until rupture.

In the second part of the tests, until rupture, the measuring devices placed at first inside the shear free area could not be used anymore because of security reasons. Therefore the deformation values are in the detailed graphics until around 55 mm deformation the one correspondent to the middle point of the beam, meanwhile the full graphics until rupture reproduce the load-deformation curve of the loading cell. The criteria from EN 408 (230) were followed for the testing.

After each test the humidity content of wood was measured by the electrical resistance method following EN 13183-2 (233), and its density calculated following EN 384 (231). In all the cases the tested beams were in a dry condition, with humidity contents inferior to 12%. The density was also very regular with values close to $\rho_{g,mean} = 420 \text{ kg/m}^3$, the mean value for the density of GL28c stated in EN 14080 (14).

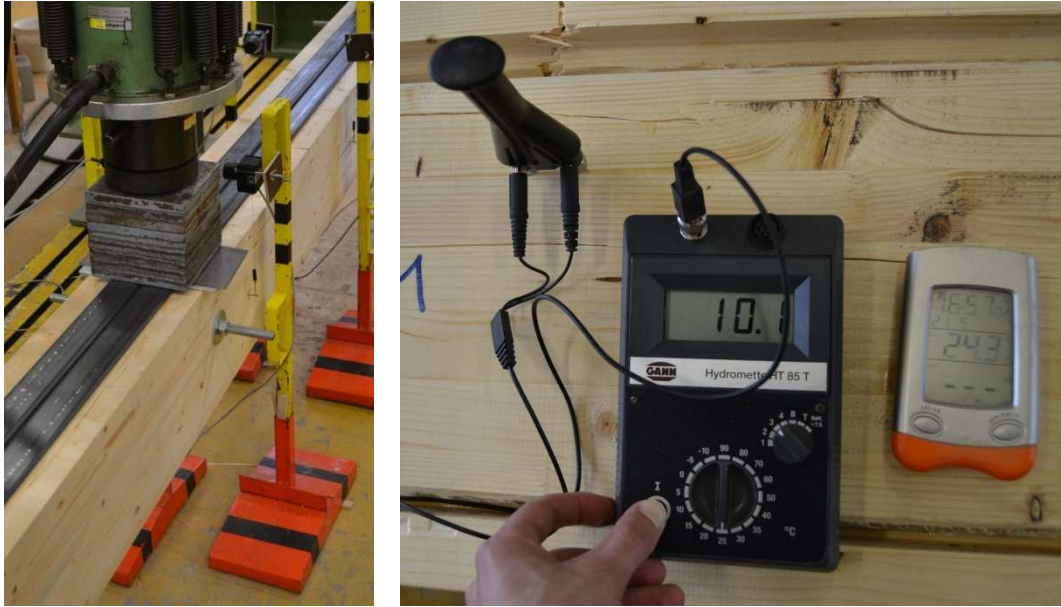


Figure 158: Installations of measuring devices and measuring of temperature and timber humidity content

All the beams were tested and, after breaking, disassembled and opened for checking both the flanges and the web performance regarding buckling. In addition two cameras were filming the tests to supervise if some trace of buckling could appear and in which moment.

The testing machine was a Walter+Bai AG with two load heads capable of a maximum load of 500 kN. The data acquisition system used was ALMEMO 5690-2, recording the data from five string measurement recorders placed over the neutral axis of the beam.

In addition the testing machine recorded the advance values of its loading heads. The data acquisition system recorded also the temperature and relative humidity of the air. All the tests were carried out fulfilling the conditions of a Service Class 1 following Eurocode 5 (6), that is characterised by a moisture content in the materials corresponding to a temperature of 20% and the relative humidity of the surrounding air only exceeding 65% for a few weeks per year.

5.3.4 Testing series A – Assessment of the global modulus of elasticity of glulam beams

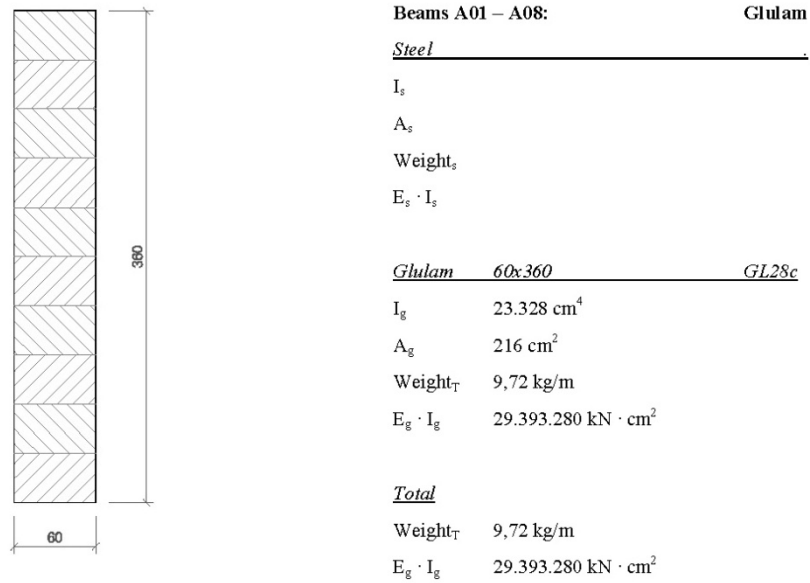


Figure 159: Characteristics of specimens Type A

The cross-section parameters of beams Type A can be seen in Figure 159.

Glulam beams type A were tested for obtaining the values of the global Young Modulus before rupture, and bending strength until rupture of the piece following the procedures stated in EN 408 (230).

Following EN 14080 (14) the Young Modulus middle value of GL28c is of 1.250 kN/cm². The real tested value of each specimen is stated in Table 28. Inside the brackets the reference of the hybrid beam which have the same glulam piece as source is indicated.

Cross-section (Hybrid beam)	E-Modulus (kN/cm ²)	Comparison with EN 14080	f_m (N/mm ²)
A01 (B01)	1208	96,7%	49,3
A02 (B02)	1282	102,5%	38,9
A03 (C01)	1384	110,7%	51,4
A04 (C02)	1255	100,4%	48,2
A05 (D01)	1282	102,6%	40,9
A06 (D02)	1137	90,9%	46,1
A07 (D03)	1260	100,8%	44,3
A08 (D04)	1257	100,6%	37,0

Table 28: Determined global E-Modulus of cross-sections A

It can be seen that the E-modulus values were always very close to the mean value stated in EN 14080 (14), being the difference less than 11%. The tension strength f_m was for all specimens clearly higher than the characteristic value of 28 N/mm² for GL28c.

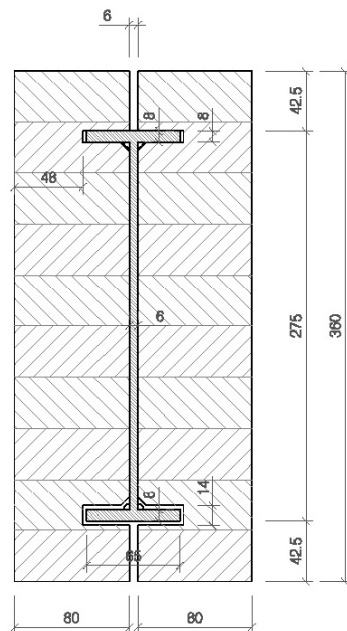
These values were used later for assessing the real performance of the correspondent hybrid beam, updating the calculation models with the real E-modulus values before the comparison with the hybrid beam test.

5.3.5 Testing series B – Cross-sections and results

The two specimens Type B were composed by welded S355 steel profiles and glulam GL28c. Their cross-section properties can be seen in *Figure 161*.



Figure 160: Specimens B02 (left) and assembling of hybrid beams Type B



Beams B01 – B02:		Hybrid welded
<u>Steel</u>	<u>Welded profile</u>	<u>S355</u>
I_s	2.722,77 cm ⁴	
A_s	25,94 cm ²	
Weight _s	20,36 kg/m	44%
$E_s \cdot I_s$	57.178.170 kN · cm ²	42%
<u>Glulam</u>	<u>2x(80x360)</u>	<u>GL28c</u>
I_g	62.208 cm ⁴	
A_g	576 cm ²	
Weight _T	25,92 kg/m	56%
$E_g \cdot I_g$	78.382.080 kN · cm ²	58%
<u>Total</u>		
Weight _T	46,28 kg/m	
$E_g \cdot I_g$	135.560.250 kN · cm ²	

Figure 161: Characteristics specimens Type B

Welded steel elements type B resulted not geometrically regular. The welding caused certain warping and longitudinal curve in the pieces due to thermal deformations, making them much more difficult to assemble than cold-formed specimens. They were also much more difficult to carry and put in place due

to their double self-weight compared with the folded elements. A minimum of four men were needed to handle and operate them.

The comparison between the hybrid performance regarding the total stiffness expected, updating the calculation models with the real Young Modulus obtained from the specimens A01 and A02, and the tested one can be compared in *Figure 162* until a deformation of 50 mm. Maximum loads and rupture values are shown in *Table 29*.

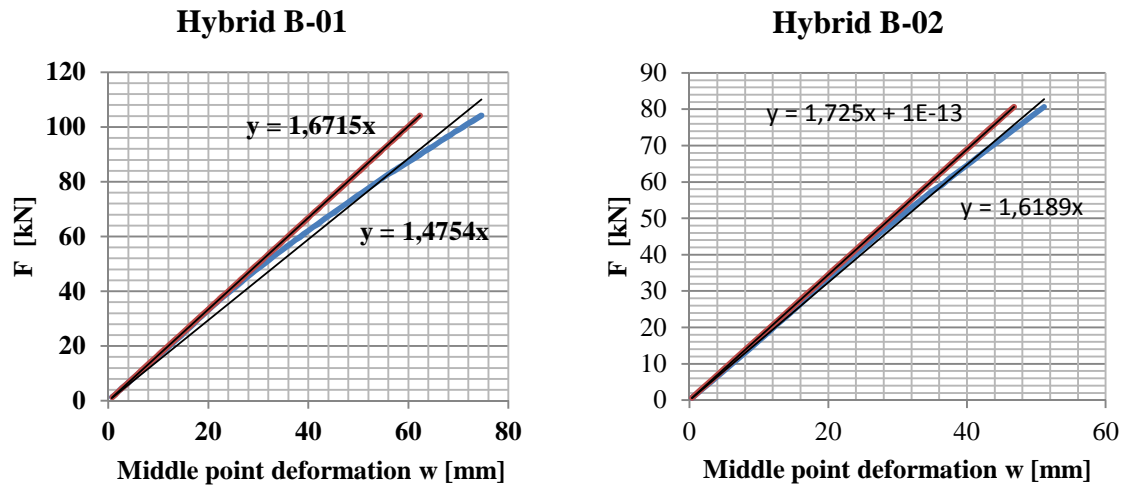


Figure 162: Results. Stiffness in elastic range for the specimens B01 and B02. Red: calculation - Blue: test

Beam	Stiffness comparison (Test/Theory)	First Rupture (kN)	Maximum Load (kN)
B01	88,3%	122,3	122,3
B02	93,8%	90,4	106,9

Table 29: Results tests B01 – B02

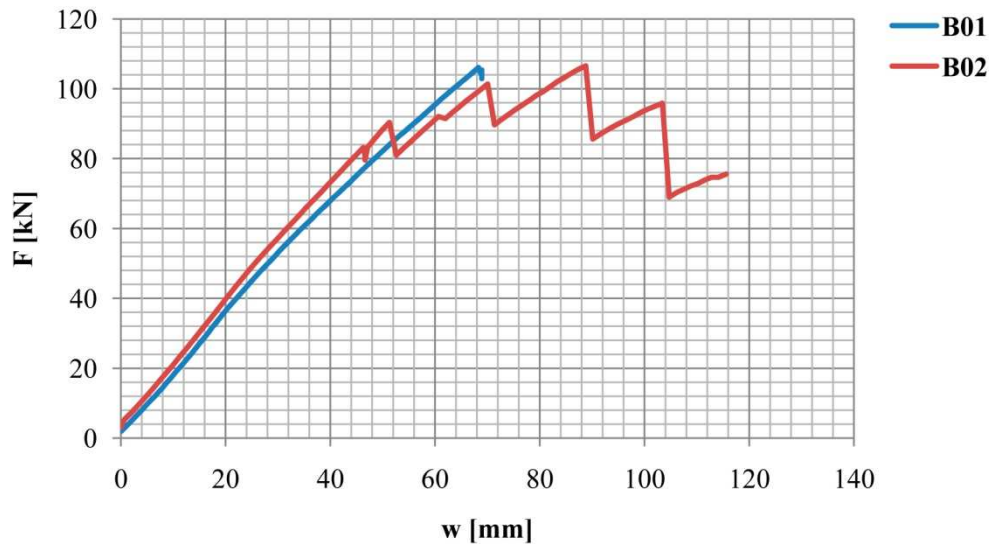


Figure 163: Load deformation graphics tests B01-B02

The total load-deformation diagram can be seen in *Figure 163*, referred to the displacements of the loading head of the testing machine.

In the case of the specimen B01 it should be pointed out that a problem with the data system caused an interruption of the digital recording of data after 105 kN of load. That is why the B01 graphic in the *Figure 163* is not complete. But in any case the testing machine recorded automatically the last part of the test, and the rupture loads provided in the *Table 29* are the correct ones.

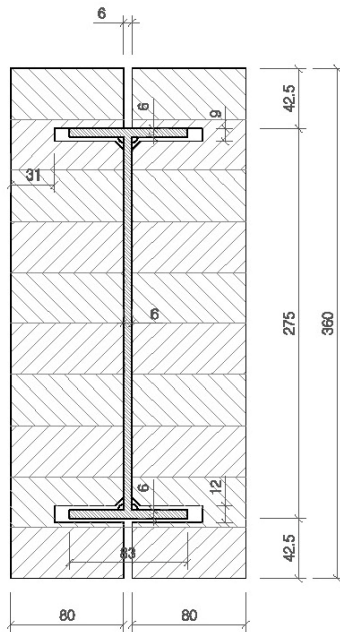
5.3.6 Testing series C – Cross-sections and results

The two specimens Type C were composed by welded S355 steel profiles and glulam GL28c. Their cross-section properties can be seen in *Figure 165* and *Figure 166*. The only difference between both specimens is the bigger tolerance of the grooves for the steel flanges in the specimen C02.

The steel cross-section arrangement reproduces as exactly as possible the dimensions of the steel parts of specimens Type D. The objective was the comparison of performance between folded steel elements (Type D) and an equivalent welded cross-section (Type C).



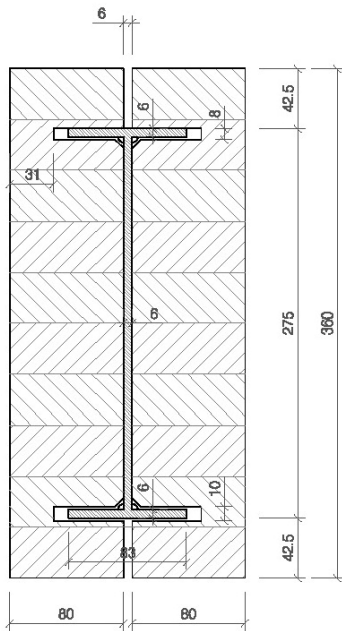
Figure 164: Specimen C02 after testing (left) and disassembled (right)



Beam C01: Hybrid welded comparison (big tolerance)

<i>Steel</i>	<i>Welded profile</i>	<i>S355</i>
I_s	2.711,66 cm ⁴	
A_s	25,74 cm ²	
Weight _s	20,21 kg/m	44%
$E_s \cdot I_s$	56.944.860 kN · cm ²	42%
<i>Glulam</i>	<i>2x(80x360)</i>	<i>GL28c</i>
I_g	62.208 cm ⁴	
A_g	576 cm ²	
Weight _T	25,92 kg/m	56%
$E_g \cdot I_g$	78.382.080 kN · cm ²	58%
<i>Total</i>		
Weight _T	46,13 kg/m	
$E_g \cdot I_g$	135.326.940 kN · cm ²	

Figure 165: Characteristics specimen C01



Beam C02: Hybrid welded comparison (small tolerance)

<i>Steel</i>	<i>Welded profile</i>	<i>S355</i>
I_s	2.711,66 cm ⁴	
A_s	25,74 cm ²	
Weight _s	20,21 kg/m	44%
$E_s \cdot I_s$	56.944.860 kN · cm ²	42%
<i>Glulam</i>	<i>2x(80x360)</i>	<i>GL28c</i>
I_g	62.208 cm ⁴	
A_g	576 cm ²	
Weight _T	25,92 kg/m	56%
$E_g \cdot I_g$	78.382.080 kN · cm ²	58%
<i>Total</i>		
Weight _T	46,13 kg/m	
$E_g \cdot I_g$	135.326.940 kN · cm ²	

Figure 166: Characteristics specimens C02

Comparison welded steel elements type C resulted not geometrically regular. The welding caused certain warping and longitudinal curve in the pieces due to thermal deformations making them much more difficult to assemble. They were also much more difficult to carry and put in place due to their double self-weight compared with the folded elements. A minimum of four men were needed to handle and operate them.

The comparison between the hybrid performances regarding the total stiffness expected, updating the calculation models with the real Young Modulus obtained from the specimens A03 and A04, can be seen in *Figure 167* until a deformation of 50 mm. Maximum loads and rupture values are shown in *Table 30*.

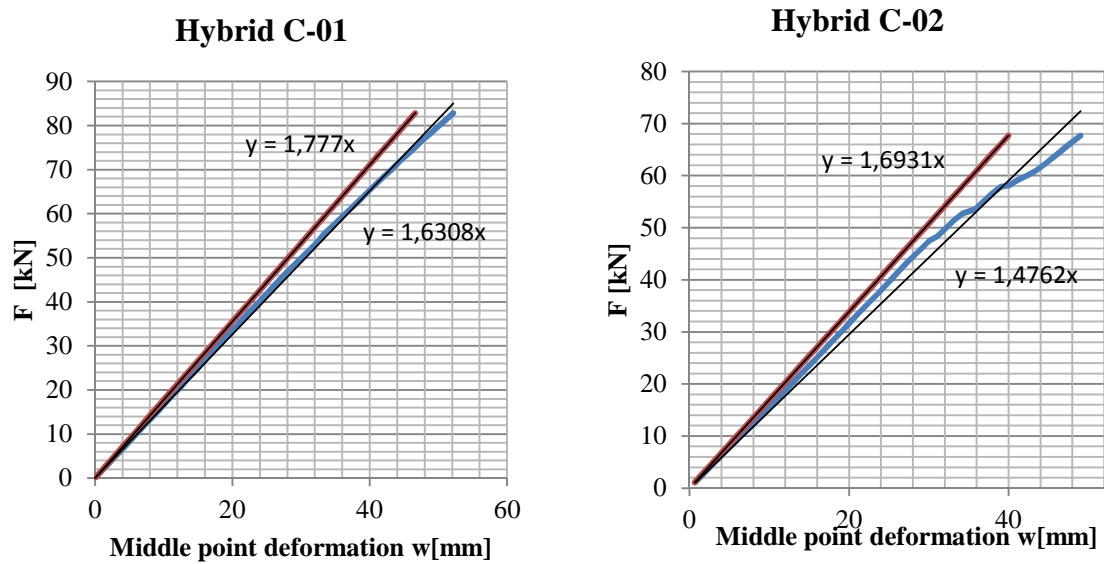


Figure 167: Results. Stiffness in elastic range for the specimens C01 and C02. Red: calculation - Blue: test

Beam	Stiffness comparison (Test/Theory)	First Rupture (kN)	Maximum Load (kN)
C01	91,8%	128,6	128,6
C02	87,2%	117,4	117,4

Table 30: Results and tests C01 – C02

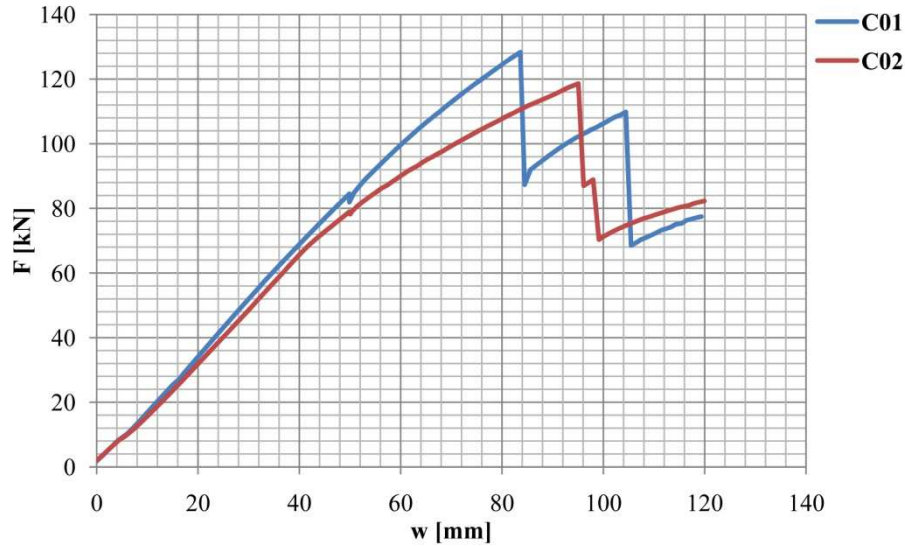


Figure 168: Load deformation graphics tests C01-C02

The total load-deformation diagram can be seen in *Figure 168*, referred to the displacements of the loading head of the testing machine.

5.3.7 Testing series D – Cross-sections and results

The performance of the four timber-steel specimens Type D was the main research objective of this first testing series. They were composed of two cold-formed steel profiles with a U cross-section and glulam GL28c. Their cross-section properties can be seen in *Figure 170* and *Figure 171*. The only difference between specimens D01-D03 and the specimens D02-D04 is the bigger tolerance of the grooves for the first group.

The folded steel components for type D proved to be dimensionally reliable, their straightness being almost perfect. They could also be easily carried and assembled by only two men.

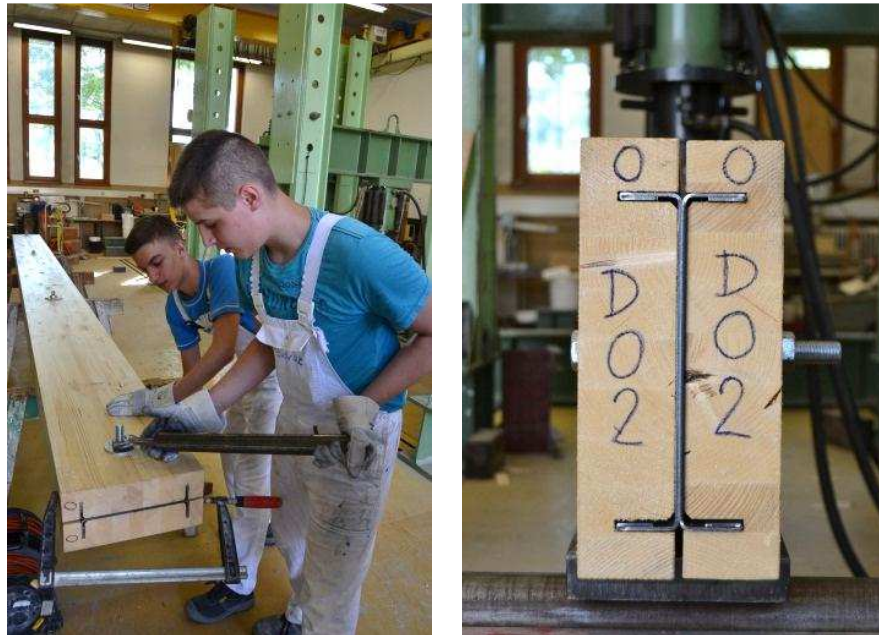
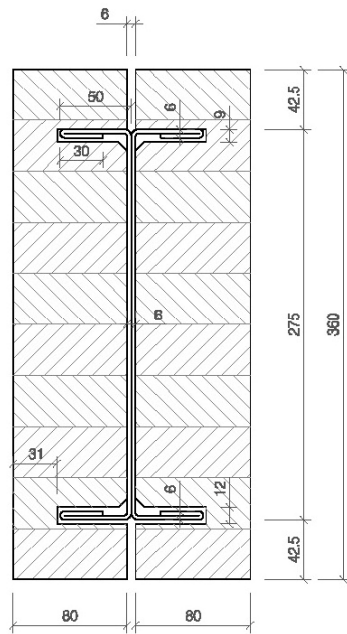
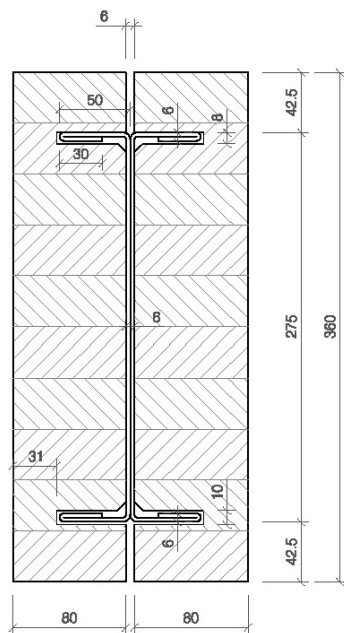


Figure 169: Assembling of specimen D02 (left) and finished cross section (right)



Beams D01 / D03: Hybrid folded		(big tolerance)
<i>Steel</i>	<i>Cold formed profiles</i>	<i>S355</i>
I _s	2.719,41 cm ⁴	
A _s	25,74 cm ²	
Weight _s	20,21 kg/m	44%
E _s · I _s	57.107.610 kN · cm ²	42%
<i>Glulam</i>	<i>2x(80x360)</i>	<i>GL28c</i>
I _g	62.208 cm ⁴	
A _g	576 cm ²	
Weight _T	25,92 kg/m	56%
E _g · I _g	78.382.080 kN · cm ²	58%
<i>Total</i>		
Weight _T	46,13 kg/m	
E _g · I _g	135.489.690 kN · cm ²	

Figure 170: Characteristics specimens D01 and D03



Beams D02 / D04: Hybrid folded		(small tolerance)
<i>Steel</i>	<i>Cold formed profiles</i>	<i>S355</i>
I_s	2.719,41 cm ⁴	
A_s	25,74 cm ²	
Weight _s	20,21 kg/m	44%
$E_s \cdot I_s$	57.107.610 kN · cm ²	42%
<i>Ghulam</i>	<i>2x(80x360)</i>	<i>GL28c</i>
I_g	62.208 cm ⁴	
A_g	576 cm ²	
Weight _T	25,92 kg/m	56%
$E_g \cdot I_g$	78.382.080 kN · cm ²	58%
<i>Total</i>		
Weight _T	46,13 kg/m	
$E_g \cdot I_g$	135.489.690 kN · cm ²	

Figure 171: Characteristics specimens D02 and D04

The comparison between the hybrid performance regarding the total stiffness expected, updating the calculation models with the real Young Modulus obtained from the specimens A05, A06, A07 and A08 can be seen in *Figure 172* until a deformation of 60 mm. Maximum loads and rupture values are shown in *Table 31*.

The total load-deformation diagram until rupture can be seen in *Figure 173*, referred to the displacements of the loading head of the testing machine.

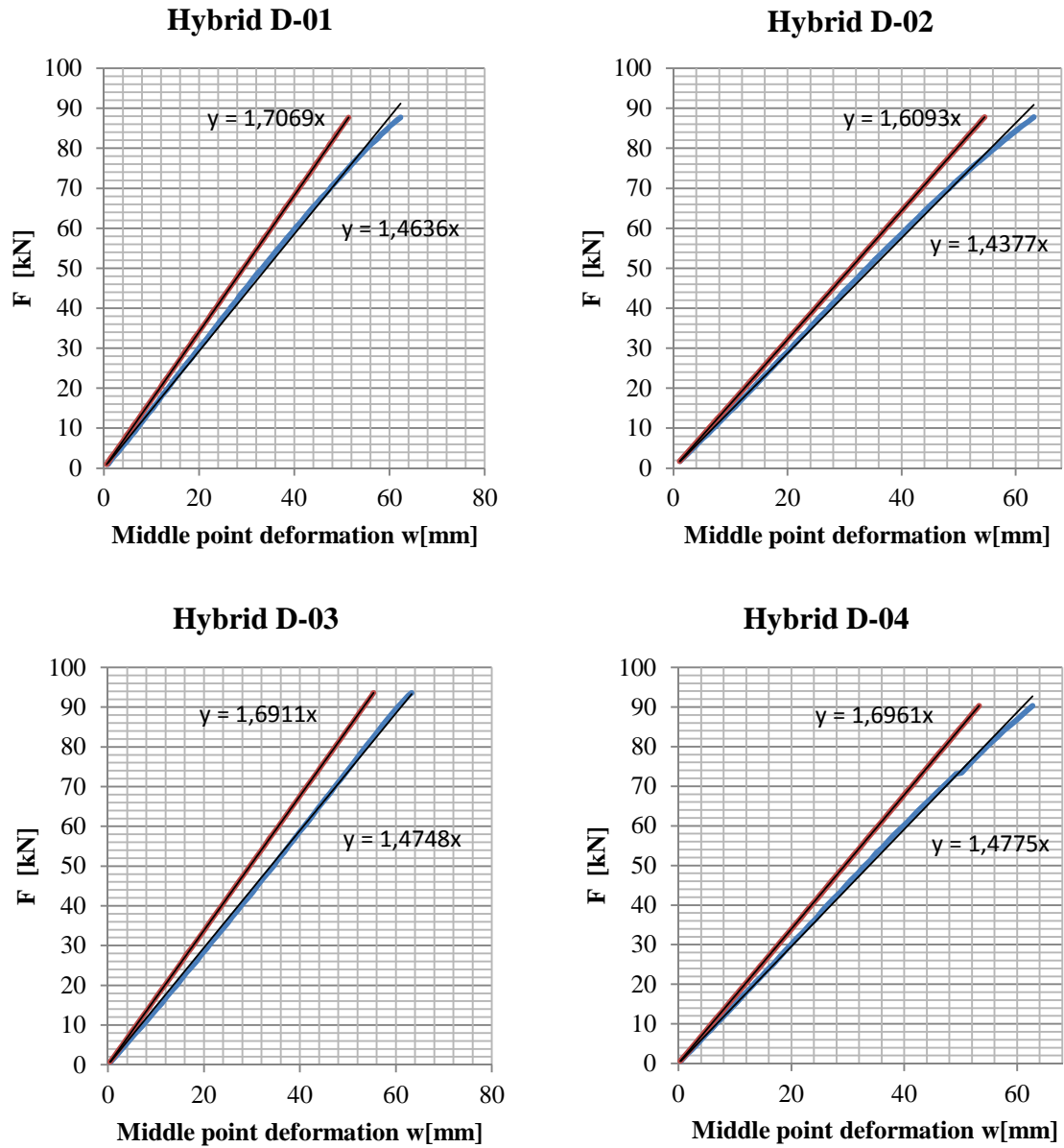


Figure 172: Results. Stiffness in elastic range for the specimens D01 to D04. Red: calculation - Blue: test

Beam	Stiffness comparison (Test/Theory)	First Rupture (kN)	Maximum Load (kN)
D01	85,8%	122,4	122,4
D02	89,4%	107,8	107,8
D03	87,2%	112,4	119,4
D04	87,1%	106,1	108,1

Table 31: Results tests D01 – D04

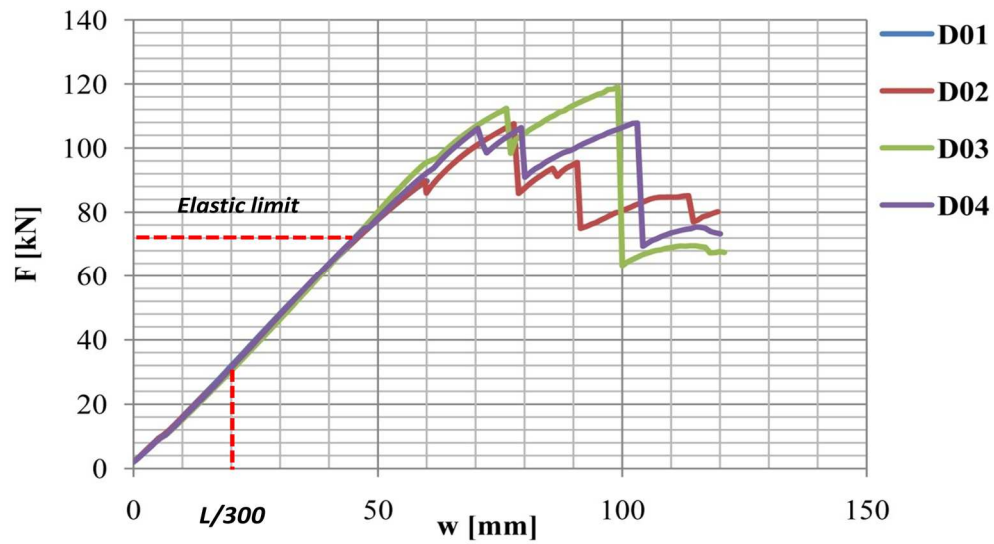


Figure 173: Load deformation graphics tests D01-D04

In the case of the specimen D01 it should be pointed out that a problem with the data system caused an interruption of the digital recording of data after 65 kN of load. That is why the D01 graphic in the *Figure 173* is almost not visible and not complete. But in any case the testing machine recorded automatically the last part of the test, and the rupture loads provided in the *Table 31* are the correct ones.



Figure 174: Hybrid beam D01 after rupture

5.3.8 Testing series E– Cross-sections and results

The two timber-steel specimens Type E were studied as an alternative to the use of glulam. They were composed of two cold-formed steel profiles with a U cross-section and cross laminated timber lateral elements. The folded steel elements were similar to the used for specimens Type D.

Their cross-section properties can be seen in *Figure 178* and *Figure 179*. The only difference between specimen F01 and the specimen F02 is the bigger tolerance of the grooves for the first one. The properties of the CLT were tested under bending using the beam Type CLT01, which properties can be seen in *Figure 177*. For the calculation of the bending stiffness values stated in the table only the layers in grain direction were considered. The mean value of E-Modulus for the C24 boards, $E_{0,mean} = 11.000 \text{ N/mm}^2$, was adopted following EN 338 (13).

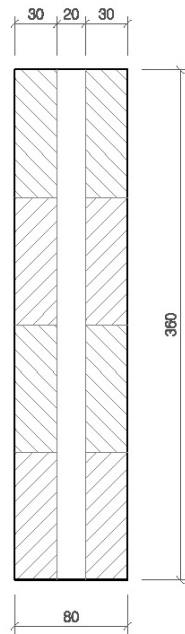
The folded steel components for type D proved to be dimensionally reliable, their straightness being almost perfect. They could also be easily carried and assembled by only two men.



Figure 175: Assembling of specimen CLT- Hybrid F02

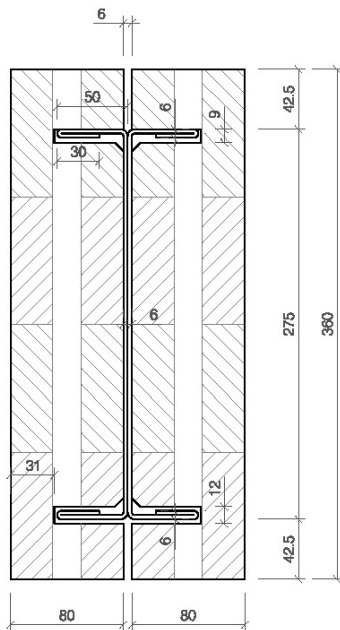


Figure 176: Testing of CLT- Hybrid F01



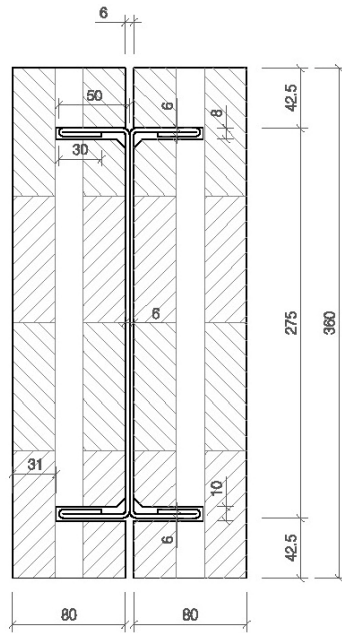
Beam CLT01:		CLT
<u>Steel</u>		
I_s		
A_s		
$Weight_s$		
$E_s \cdot I_s$		
<u>CLT</u>		<u>80x360</u>
I_g	23.328 cm ⁴	<u>C24</u>
A_g	288 cm ²	
$Weight_T$	12,96 kg/m	
$E_g \cdot I_g$	67.141.879 kN · cm ²	
<u>Total</u>		
$Weight_T$	12,96 kg/m	
$E_g \cdot I_g$	67.141.879 kN · cm ²	

Figure 177: Characteristics of specimen CLT01



Beam F01: CLT option		(big tolerance)
<u>Steel</u>		<u>Cold formed profiles</u>
I_s	2.719,41 cm ⁴	<u>S355</u>
A_s	25,74 cm ²	
$Weight_s$	20,21 kg/m	44%
$E_s \cdot I_s$	57.107.610 kN · cm ²	62%
<u>CLT</u>		<u>2 x (80x360)</u>
I_g	32.116 cm ⁴	<u>C24</u>
A_g	576 cm ²	
$Weight_g$	25,92 kg/m	56%
$E_g \cdot I_g$	35.327.600 kN · cm ²	38%
<u>Total</u>		
$Weight_T$	46,13 kg/m	
$E_T \cdot I_T$	92.435.210 kN · cm ²	

Figure 178: Characteristics of specimen E01



Beam F02: CLT option (small tolerance)

Steel Cold formed profiles S355

I_s	2.719,41 cm ⁴	
A_s	25,74 cm ²	
Weight _s	20,21 kg/m	44%
$E_s \cdot I_s$	57.107.610 kN · cm ²	62%

CLT 2 x (80x360) C24

I_g	32.116 cm ⁴	
A_g	576 cm ²	
Weight _g	25,92 kg/m	56%
$E_g \cdot I_g$	35.327.600 kN · cm ²	38%

Total

Weight _T	46,13 kg/m	
$E_T \cdot I_T$	92.435.210 kN · cm ²	

Figure 179: Characteristics of specimen E02

The comparison between the hybrid performance regarding the total stiffness expected, updating the calculation models with the real Young Modulus obtained from the specimens CLT01 and CLT02 can be seen in Figure 180 until a deformation of 50 mm. Maximum loads and rupture values are shown in Table 32.

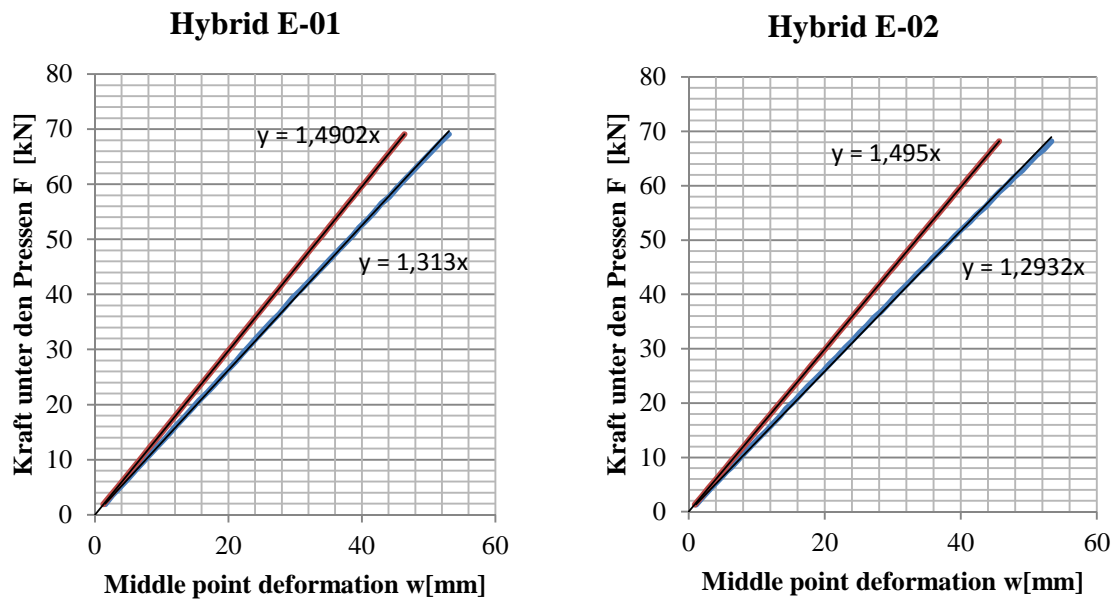


Figure 180: Results. Stiffness in elastic range for the specimens E01 to E02. Red: calculation - Blue: test

Beam	Stiffness comparison (Test/Theory)	First Rupture (kN)	Maximum Load (kN)
E01	88,1%	98,5	98,5
E02	86,5%	95,4	95,4

Table 32: Results Tests E01-E02

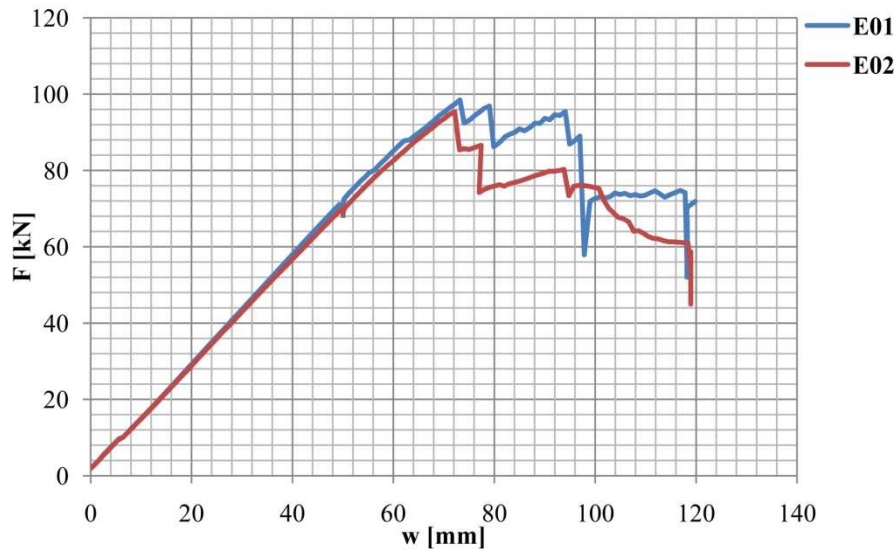


Figure 181: Load deformation graphics tests E01-E04

The total load-deformation diagram until rupture can be seen in *Figure 181*, referred to the displacements of the loading head of the testing machine.

5.3.9 Interpretation and conclusions

There were no buckling problems neither in web nor in steel flanges for the hybrid beams Type B and C.

The local buckling happened only in the flanges in beams Type D, and never in the web, under very high loads and always after the rupture of the timber pieces, when theoretically the steel parts were already inside the plastic range. This could be directly observed during the test (the upper timber covering suffered deformations during the steel buckling) and it was recorded with cameras.

The buckling of flanges caused also the opening of a gap between the assembled hybrid beam components and it was verified after the disassembling of the beams.

The analysis of results shows that the hybrid beams with cold-formed steel profiles are only in average 3% less stiff than the welded options. It is important to note that the real thickness of the welding seams were at first not taken into account for the calculation of the bending stiffness of the welded pieces, and therefore the real difference between the two options is almost inexistent.

Due to their good performance it was decided to use only cold-formed steel profiles for the second testing series.

The real value of the bending stiffness of all the glulam-hybrid beams is in average 89% of the expected stiffness. These results show that there was still potential for improvements, especially at the points of application of load and support areas.

It turned out that the procedures followed during the testing were not appropriate enough for dealing with this particular question, particularly because of two decisions:

The steel components were not tested alone on their own, so their exact performance remained unknown. Their performance was assessed only to some extent comparing them between theoretically stiff-equivalent welded steel profiles.

The fact that there was a difference in performance from the predicted values in all the cases (but with more losses of expected stiffness in the folded beams than in the welded ones) posed several questions, mainly if the loss of stiffness was due to the folded technology, the hybrid design or other reasons. Probably the most realistic answer to this question is that the real bending stiffness of the steel welded elements was at the beginning, and in the calculation models, underrated. The geometry of the continuous welding seams was not taken into account for the assessment of the moment of inertia of the cross section. After the tests the calculation models were checked again and this part of the geometry added to the cross section. The results showed that in this case, that is, taken into account the real thickness of the welding seams, there is no relevant difference between the performances of hybrid beams using welded or cold-formed profiles.

The glulam components were also not tested on their own. The procedure of cutting a sample piece, and the two glulam pieces for the hybrid from a common glulam block was used. The samples, beams Type A, were tested until rupture for finding the values of E modulus and rupture. But, strictly speaking, the performance of the sample does not have to be exactly the same as the pieces forming the hybrid beam, so in any case some degree of inaccuracy remained in the procedure assessing the stiffness of the glulam components of the hybrid beams.

Anyway, the objectives of the first testing series were far more general: constructive and assembling issues, general performance of beams, cost-performance assessment, checking of possible general or local buckling problems. They provided successful answers to a big number of originally open questions and served to identify these, from now on, important issues.

The comparison of the maximum loads achieved for the series B, C and D showed similar results for all of them.

The rupture mode was defined by consecutive tension ruptures in the individual layers of the glulam components as shown in *Figure 182*.

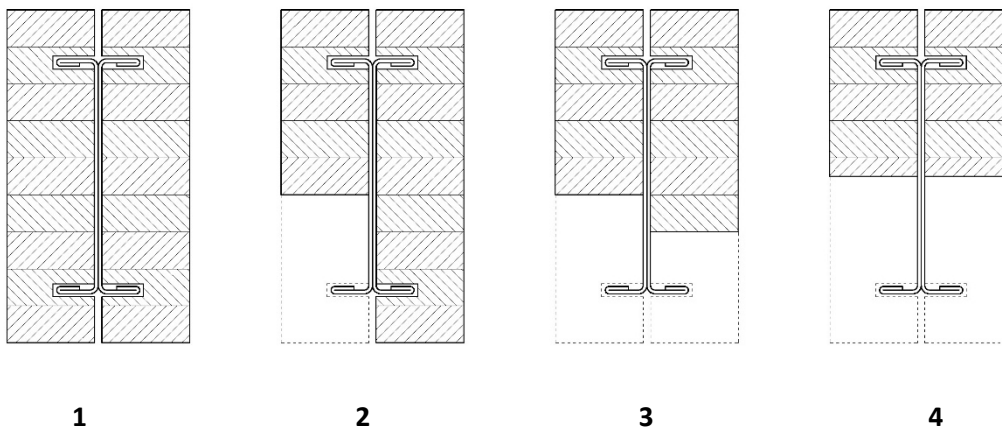
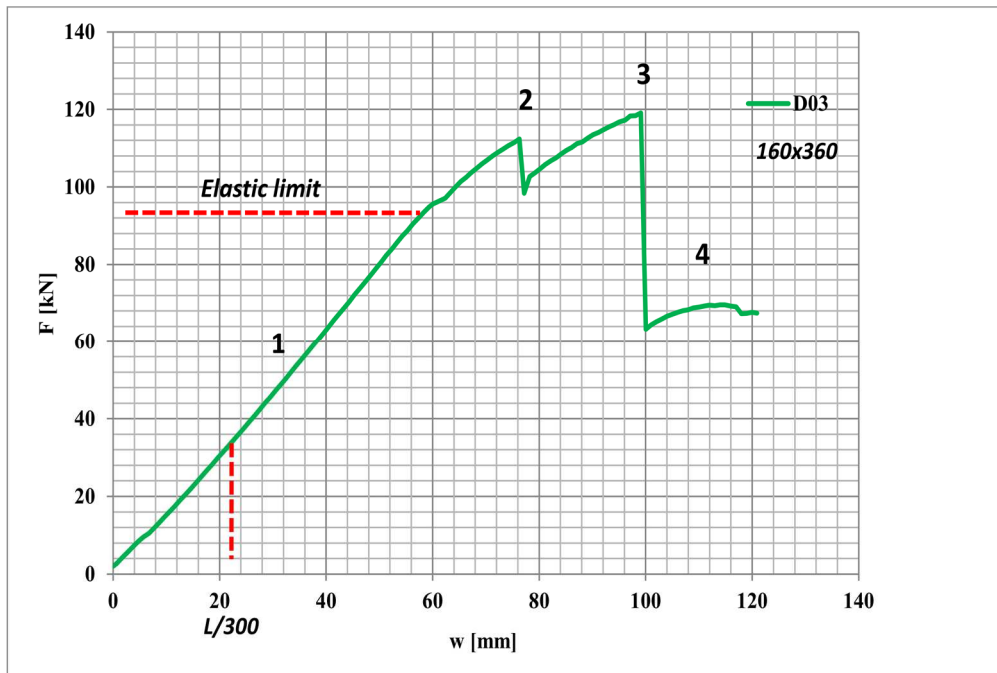


Figure 182: Rupture sequence of a hybrid beam

After several ruptures a certain carrying capacity for the timber part is still remaining. It is interesting to note that in all the tested cases the upper remaining timber pieces helped to avoid both the local buckling of the steel web and the possible lateral buckling of the whole beam. With increasing load the system reached a point that led to the plasticization of steel and local buckling of upper steel flanges.



Figure 183: Image of specimen D01 after testing and opening of the section



Figure 184: Image of specimen D01 after showing local buckling beginning at the upper steel flange and extending to web

The failure mode of specimens Type F, built with CLT plates, was determined by initial tension ruptures like in the general case, but followed by a compression failure of the upper part of the CLT beams, due to the weakness of the cross layer suffering perpendicular to grain compression. Lateral rupture or buckling of the outer timber boards was a related phenomenon. An image of this failure mode can be seen in Figure 185.



Figure 185: Failure of compression area in specimen Type F

5.4 SECOND TESTING SERIES

The second testing series started in December 2013. Sixteen hybrid beams in total, with a span of 6 and 8 metres, were planned, calculated, produced and tested. Only cold-formed steel profiles were used with a steel plate thickness of 4 mm.

An important difference in comparison to the first testing series is the geometrical arrangement of the cross section. In this case the upper steel flanges lay over the top edge of the timber components, using the asymmetrical hybrid beam arrangement explained in 4.3.4. This would allow an easy connection between beam and floor structure or between beam and other elements like supports. Moreover, the joint with the floor structure would help to improve the local buckling performance of flanges and provide fire protection to the upper steel parts.

Thanks to this new disposition the tolerances needed between timber and steel in the grooves are smaller than in the first testing series. The timber-steel hybrid cross-section performs as two independent components without horizontal shear connection. Therefore the new disposition does not cause any difference from a statically performance point of view.

5.4.1 Specimens

The second testing series is composed of four different cross-sections with 16 hybrid beams in total.

Cross-section	Specimens	Span (m)	Structural Depth	Structural depth ratio	Materials
G	6	6	L/17	1,14	GL28c/S355
H	6	6	L/20	1,18	GL28c/S355
I	2	8	L/17	1,11	GL28c/S355
J	2	8	L/20	1,13	GL28c/S355

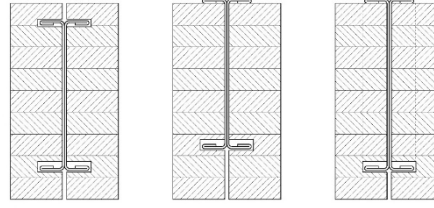
Table 33: *Specimens of the second testing series*

5.4.2 Design and dimensioning

Hybrid beams with spans of 6 (Type G and Type H) and 8 (Type I and Type J) metres, and with a structural depth-span ration of L/20 (Type H and Type J) and L/17 (Type G and Type I) were designed and dimensioned.

In this case the structural depth ratio of all the specimens is close to the ideal value of 1,06 (see *Table 11*) for the combination of steel S355 and glulam GL28c. This is the situation calculated for a Case Study A taking into account long term effects, as it was explained in 4.4.8. The partial security factors for the properties of the materials and modification factor k_{mod} are included in the calculation. For this last parameter the value corresponding to Service class 1 and a medium-term Load-duration class was adopted.

The difference between the designing parameters taken into account in the first testing series and the second one can be seen in *Table 34*. In the first testing series a cross-section was designed for making steel reach their elastic limit at the same time that timber reaches its characteristic strength for the case $k_{mod}=1$ and $\gamma_M=1$. The transition cross-section is an equivalent section, only moving the steel profile to the upper part of the cross-section. The structural performance does not change. The cross-section for the profiles of testing series two take into account the factors $k_{mod}=0,8$ and $\gamma_M=1,25$, and increase the structural depth of steel for making it not to reach its elastic limit in the initial state and have still reserves for facing long-term performance effects.



	Series 1	Transition	Series 2
k_{mod}	1,0	1,0	0,8
γ_M	1,0	1,0	1,25
Elastic use T=0 (S355)	100%	100%	75%
Elastic use T=0(GL28c)	100%	100%	100%

Table 34: Development of the cross-section geometry

The fact that the structural depth ratio adopted is not exactly the ideal value was due to the fire protection requirements influencing the cross section design. In this case a timber covering of 50 mm for the inner steel elements was chosen for providing enough protection for 60 minutes fire. This constant thickness for the timber cover was adopted for all the specimens, causing therefore small changes in the structural depth ratio for each specimen type, as is reflected in *Table 33*. In any case this small variation would not make any difference for the instant hybrid performance which was going to be checked in the second series of short-term tests. The open gap in the bottom part of the beams should be closed for real applications because of fire protection issues, as was already explained in 4.2.7.

5.4.3 Production, delivery and assembly

In this testing series the timber and steel components were delivered in two groups.

The first delivery comprised the elements for the specimens G01, G02, G03, H01, H02, H03, I01 and J01. The second delivery was composed by the materials for the specimens G04, G05, G06, H04, H05, H06, I02 and J02.

Only folded steel elements with a plate thickness of 4 mm were used. The materials used were steel S355 and spruce glulam GL28c as in the first testing series. The geometrical regularity of all specimens was very good, and the assembly was carried out easily as expected after the experienced gained during the first testing series. The timber components of the second delivery were adapted on-site for allowing different support conditions, as can be seen in *Figure 187* and will be detailed in 5.4.5.



Figure 186: Timber components for beams type G (left) and 8 m and 6 m long steel components (right)



Figure 187: Preparation of the supporting details of specimen H04

5.4.4 Test set-up, testing procedures and measuring techniques

The four point bending tests followed the same procedures as stated for the first testing series.

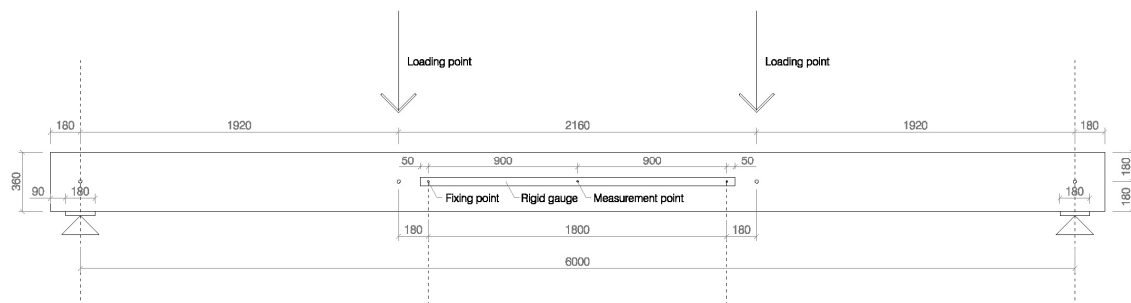


Figure 188: Four point bending test arrangement

A special procedure was adopted in order to obtain data for answering the open questions stated in 5.3.9 . Before the testing of each hybrid beam, an individual four point bending test of its different material components was carried out.

The two steel components forming part of a hybrid beam, paired and bolted together, were tested in bending, at a constant speed of 0,2 mm/s and until a maximum deformation of 20 mm under the loading head of the press. This way the load-deformation behaviour of the folded steel part of the hybrid beam could be assessed on its own. Considering a Young Modulus of $E = 210.000 \text{ N/mm}^2$ for the steel, and with the recording data, the real bending stiffness (or effective Inertia) of the steel folded beam could be found.

Auxiliary wooden pieces were laterally paired and bolted under the loading heads and over the support points in order to avoid possible local buckling or damages in the web or flanges of the steel cross-sections. Other smaller auxiliary wooden blocks were bolted for fixing the measuring devices in the points needed.

The glulam pieces were also tested following the same procedure although in this case the real value of its Young Modulus was the incognita of the test. An image of the disposition for testing the steel and glulam pieces on their own can be seen in *Figure 189*.



Figure 189: Four point bending test of steel and glulam components of hybrid beam Type H on their own

These values were used later for assessing the real performance of each hybrid beam. The calculation models for hybrid beams were updated with the real E-modulus of each timber component and real inertia of steel cross-section before the comparison between hybrid theory and test.

After these two previous tests, the hybrid beam itself was assembled and tested at the same constant speed of 0,2 mm/s like their components.

The test of hybrid beams was carried out in two steps, the first one until a deformation of 50 mm under the loading heads and, after a pause for taking back the measuring devices, a second step until rupture of both glulam components and global failure of hybrid beams. An image of the disposition for testing the hybrid beams can be seen in *Figure 190*.



Figure 190: Four point bending test of hybrid Type H

5.4.5 Load implementation and support conditions

The results of the first testing series pointed out to the possibility of improvements, especially in relation to the load transmission at the supports.

In this second series three different configurations for the supports were tested. The configuration “Timber (T)” is the same as in the first series. In this case the hybrid beams rests only over their timber components, having the steel cross-section no direct contact with the support.

The support configurations “Timber+Steel (T+S)” and “Steel (S)” were new and defined the materials in direct contact with the base plates to allow the load transmission from beam to the supports, as shown in *Figure 191* and *Figure 192*. The idea behind this was to check if the support configuration was responsible, and in which measure, of the differences between the expected and real stiffness of the hybrid beams found during the first testing series.

The list of specimens with their particular support conditions can be seen in *Table 35*.

G – 6 [m]		H – 6 [m]		I – 8 [m]		J – 8 [m]	
G01	Timber	H01	Timber	I01	Timber-Steel	J01	Timber-Steel
G02	Timber	H02	Timber	I02	Steel	J02	Steel
G03	Timber	H03	Timber				
G04	Timber-Steel	H04	Timber-Steel				
G05	Steel	H05	Steel				
G06	Steel	H06	Steel				

Table 35: List of specimens with indication of length of span and support conditions



Figure 191: Image of specimens type G from the second testing series, with support conditions “Timber(T)” (left) and “Timber+Steel (T+S)” (right)



Figure 192: Frontal (left) and lateral (right) images of specimen G05 from the second series, with support conditions “Steel (S)”

In the case of the support condition “Steel”, where only the steel profiles take contact with the supporting plates, the gap created between the steel flanges and the upper timber surface was filled up with steel plates until the loading head for getting a good load transmission for steel and timber, as can be seen in *Figure 193*. This was because due the timber components rested directly on the inferior flanges of the steel elements, causing a tolerance gap between steel and timber on the upper part of the beam.

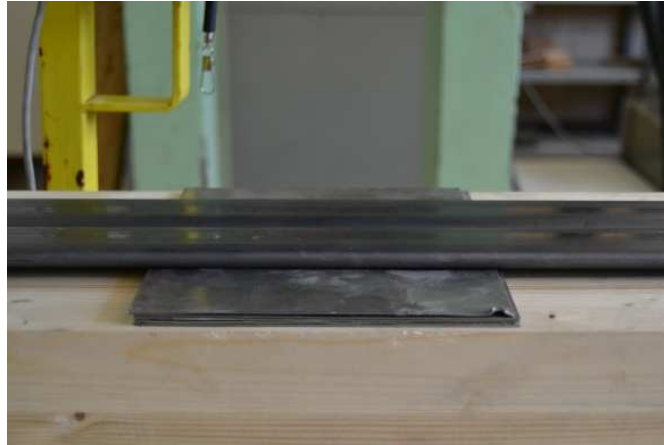


Figure 193: Filling with steel plates under the loading heads between the steel flange and timber in the case of the supporting condition “steel”

5.4.6 Testing series G – Cross-sections and results

The six timber-steel specimens Type G were composed of two cold-formed steel profiles with a U S355 steel cross-section and glulam GL28c. Their cross-section properties can be seen in *Figure 195*.

The span was 6 metres, the total structural depth $L/17$ and the ratio of structural depth between timber and steel 1,14.

The comparison between the expected performance regarding total stiffness and the real one can be seen in *Figure 196* until a deformation of 40 mm. Maximum loads and rupture values are shown in *Table 37* and *Table 38*.

The total load-deformation diagram until rupture can be seen in *Figure 197* and *Figure 198*, referred to the displacements of the loading head of the testing machine.

It should be pointed out again that the timber components were ordered in two different moments. The real quality of the second order (beams G04-G6) was of much lower quality than the first one. The tested E-modulus was in these cases clearly lower than the previous ones, as can be seen in *Table 36*. In addition, the relevant higher number of big knots in the pieces explains the lower timber rupture values obtained from these specimens. On the other hand the folded steel elements did not show any relevant reduction on their predicted stiffness.



Figure 194: Example of faulty finger-joint in the specimen G05

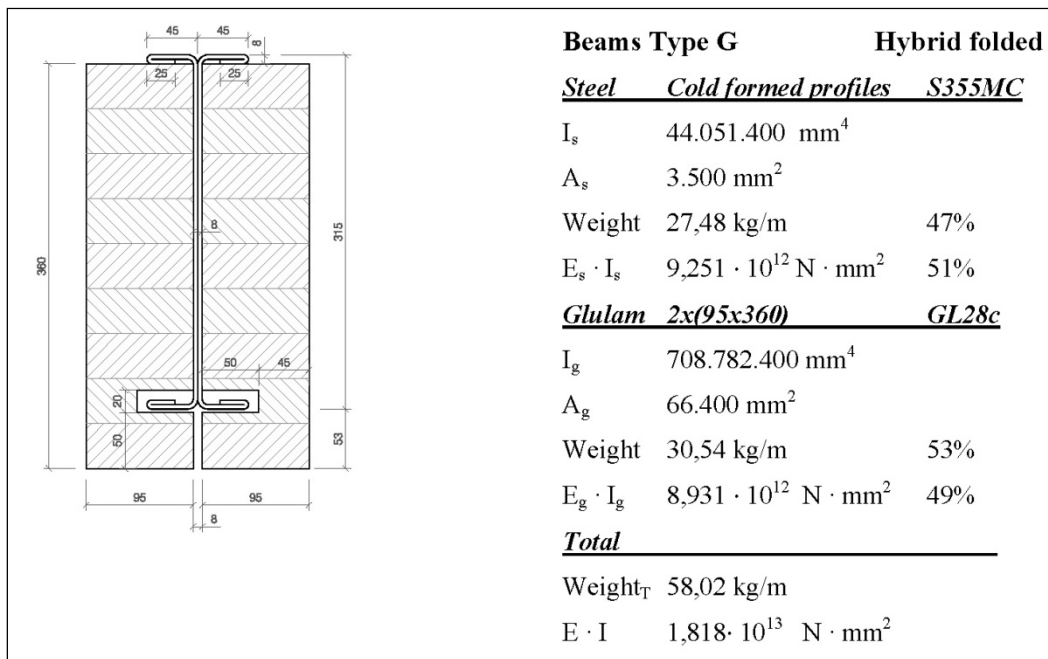


Figure 195: Cross-section parameters of hybrid beams Type G

Components of hybrid beam	Tested timber E-modulus (kN/cm ²)	Comparison to GL28c mean value ($E_{0,mean}$) according to EN 14080	Tested moment of Inertia $I_{y,s}$ for the steel components in comparison to the predicted value
G01	1.223	97,8 %	100,6 %
G02	1.253	100,2 %	99,4 %
G03	1.234	98,7 %	99,0 %
G04	1.105	88,4 %	97,9 %
G05	1.090	87,2 %	97,9 %
G06	1.070	85,6 %	98,6 %

Table 36: Tested E-modulus of timber components and tested moment of inertia of steel elements for hybrid beams Type G

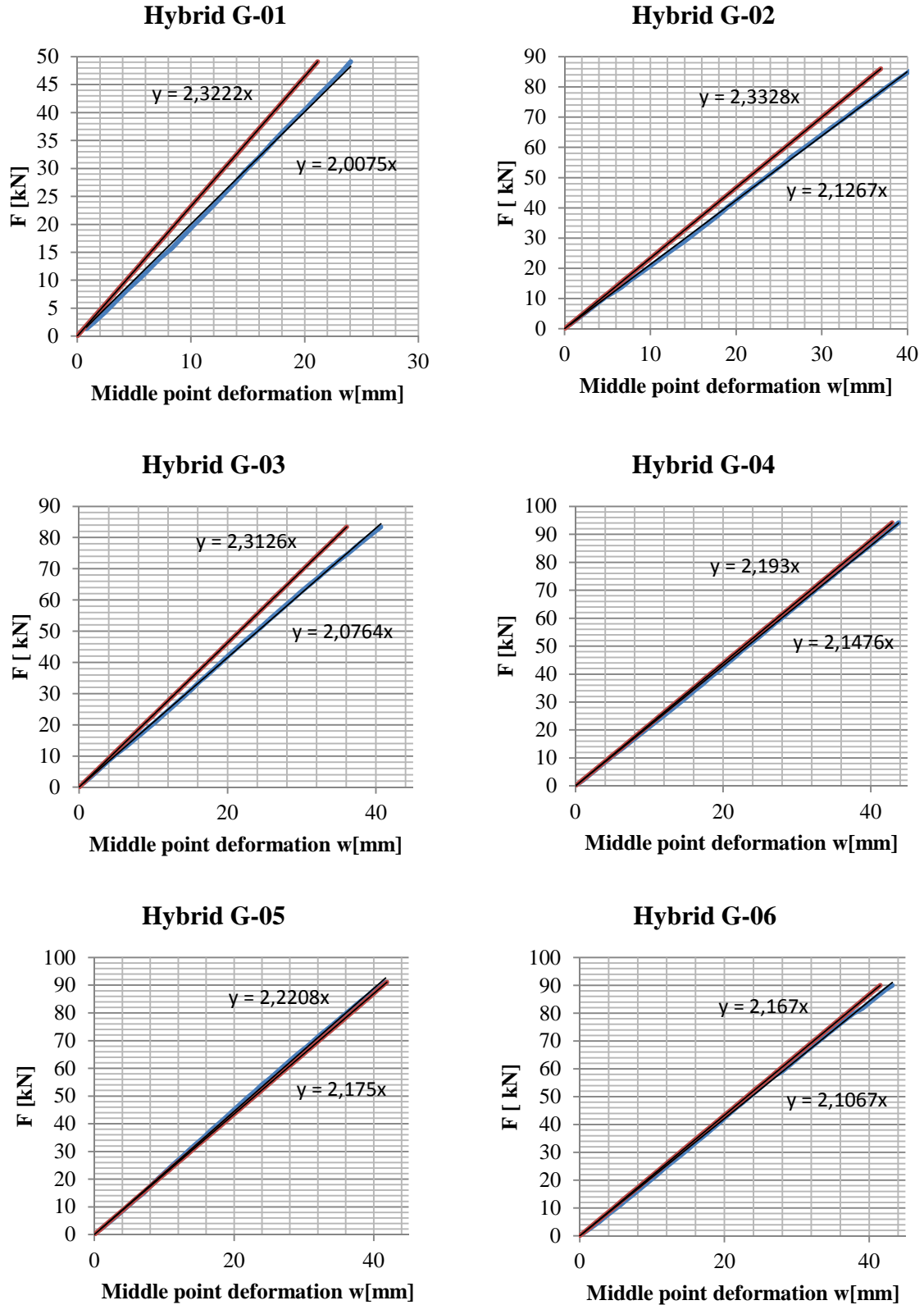


Figure 196: Results. Stiffness in elastic range for the specimens G01 to G06. Red: calculation - Blue: test

Beam (support conditions)	Stiffness comparison (Test/Theory)	First Rupture (kN)	Maximum Load (kN)
G01 (T)	86,4%	118,3	135,2
G02 (T)	91,2%	128,6	150,6
G03 (T)	89,8%	164,7	164,7

Table 37: Results tests G01 – G03

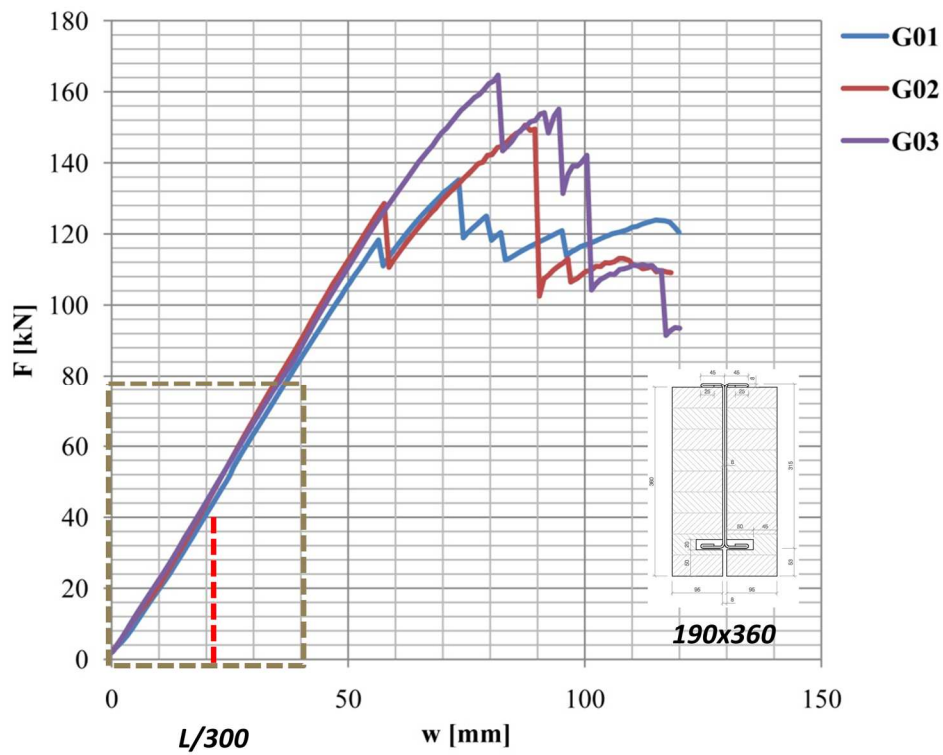


Figure 197: Load deformation graphics tests G01-G03

Beam (support conditions)	Stiffness comparison (Test/Theory)	First Rupture (kN)	Maximum Load (kN)
G04 (T+S)	97,9%	118,1	118,1
G05 (S)	97,9%	147,9	147,9
G06 (S)	97,2%	127,3	127,3

Table 38: Results tests G04 – G06

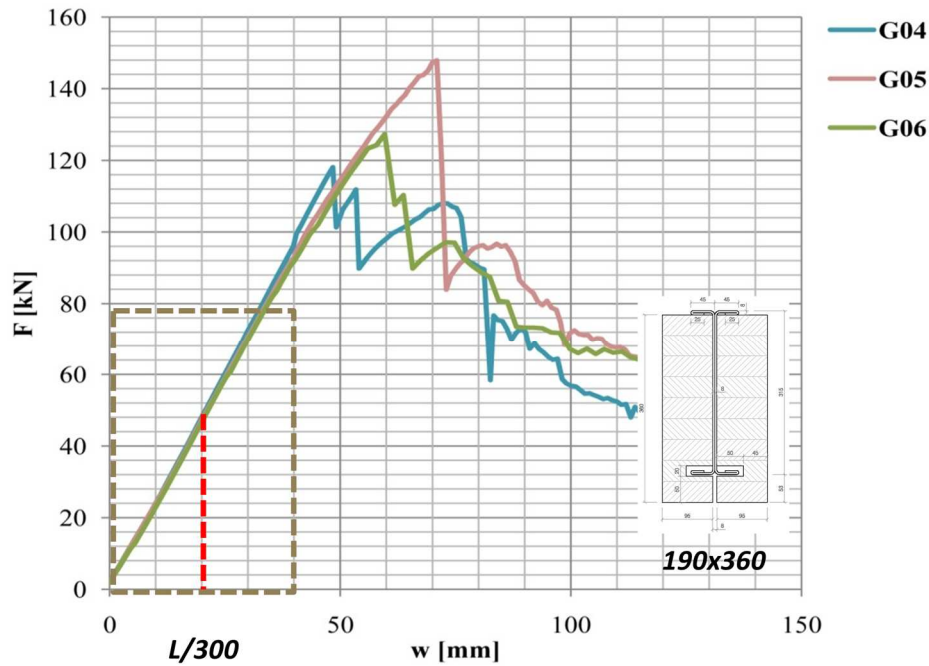


Figure 198: Load deformation graphics tests G04-G06

5.4.7 Testing series H – Cross-sections and results

The six timber-steel specimens Type H were composed of two cold-formed steel profiles with a U cross-section of steel S355 and glulam GL28c. The cross-section properties can be seen in *Figure 199*.

The span was of six metres, the total structural depth $L/20$ and the ratio of structural depth between timber and steel of 1,18.

The comparison between the expected performance regarding total stiffness and the real one can be seen in *Figure 200* until a deformation of 40 mm. Maximum loads and rupture values are shown in *Table 40* and *Table 41*.

The total load-deformation diagram until rupture can be seen in *Figure 201* and *Figure 202*, referred to the displacements of the loading head of the testing machine.

It should be pointed out that the timber components were ordered in two different moments. The real quality of the second order (beams H04-06) was of much lower quality than the first one. The tested E-modulus was in these cases clearly lower than the previous ones and, as can be seen in *Table 39*. In addition, the relevant higher number of big knots in the pieces explains the lower timber rupture values

obtained from these specimens. On the other hand the folded steel elements did not show any relevant reduction on their predicted stiffness.

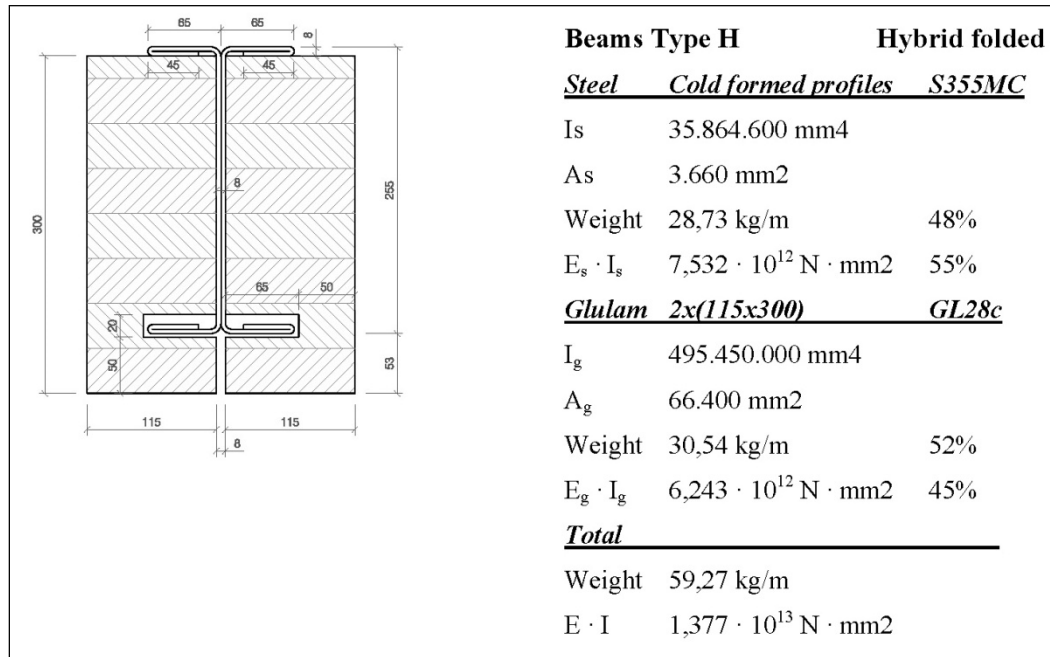


Figure 199: Cross-section parameters of hybrid beams Type H

Components of hybrid beam	Tested timber E-modulus (kN/cm ²)	Comparison to GL28c mean value ($E_{0,mean}$) according to EN 14080	Tested moment of Inertia $I_{y,s}$ for the steel components in comparison to the predicted value
H01	1.260	100,8 %	97,6 %
H02	1.253	100,2 %	98,6 %
H03	1.225	98,0 %	98,0 %
H04	1.065	85,2 %	97,8 %
H05	954	76,3 %	98,4 %
H06	1.085	86,8 %	98,8 %

Table 39: Tested E-modulus of timber components and tested moment of inertia of steel elements for hybrid beams Type H

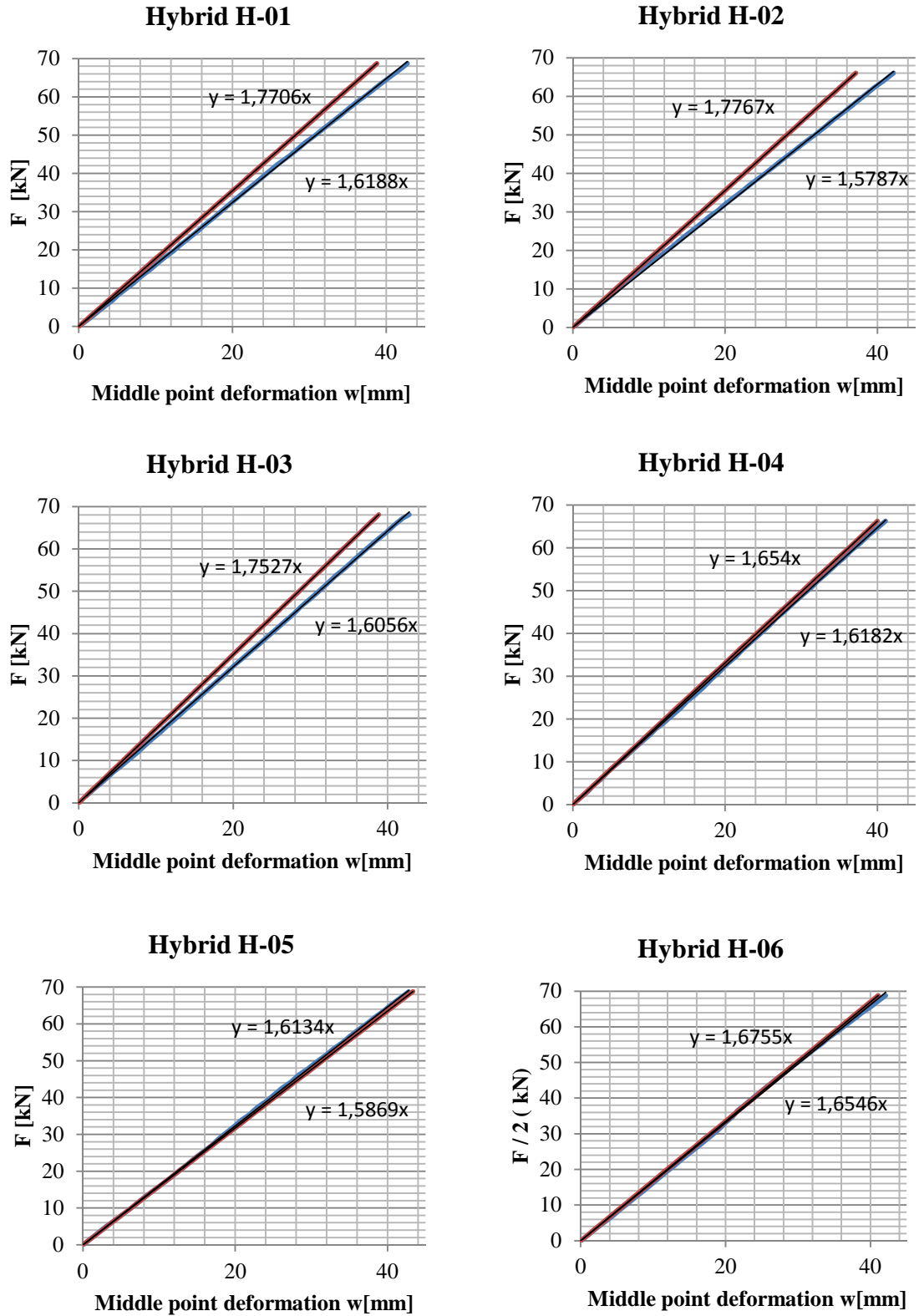


Figure 200: Results. Stiffness in elastic range for the specimens H01 to H06. Red: calculation - Blue: test

Beam (support conditions)	Stiffness comparison (Test/Theory)	First Rupture (kN)	Maximum Load (kN)
H01 (T)	91,4%	131,5	131,5
H02 (T)	88,9%	125,5	125,5
H03 (T)	91,6%	134,7	134,7

Table 40: Results tests H01 – H03

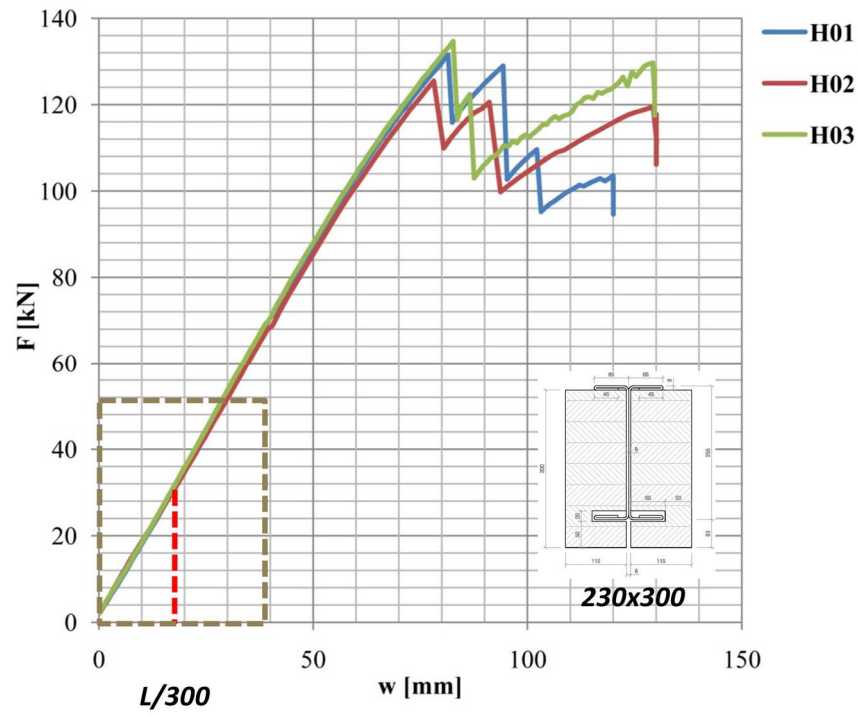


Figure 201: Load deformation graphics tests H01-H03

Beam (support conditions)	Stiffness comparison (Test/Theory)	First Rupture (kN)	Maximum Load (kN)
H04 (T+S)	97,8%	100,0	107,2
H05 (S)	98,4%	100,5	102,4
H06 (S)	98,8%	103,9	103,9

Table 41: *Results tests H04 – H05*

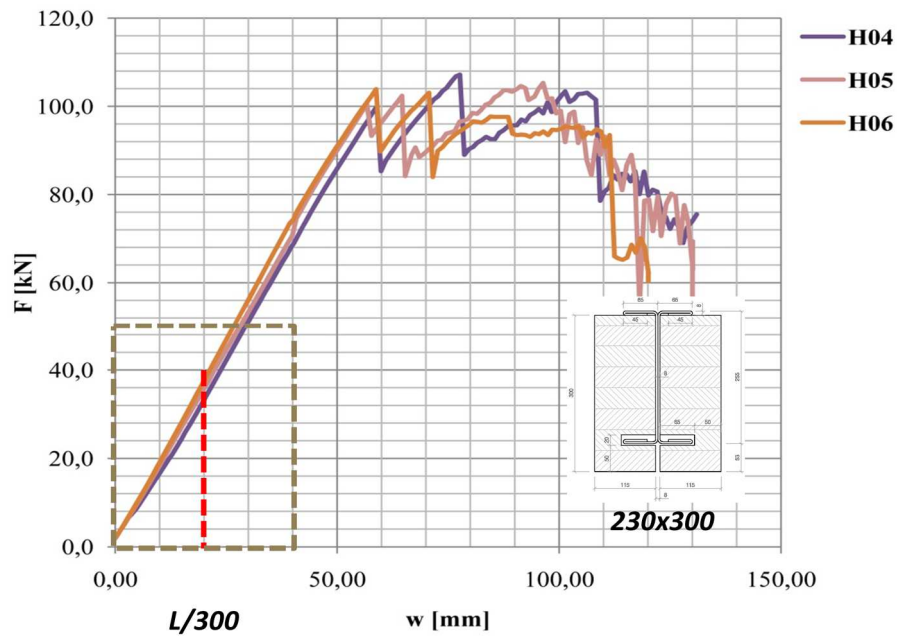


Figure 202: Load deformation graphics tests H04-H06

5.4.8 Testing series I – Cross-sections and results

The two timber-steel specimens Type I were composed of two cold-formed steel profiles with an U cross-section of S355 steel and glulam GL28c. Their cross-section properties can be seen in *Figure 204*.

The span was of eight metres, the total hybrid structural depth $L/17$ and the ratio of structural depth between timber and steel of 1,11.

The comparison between the expected performance regarding total stiffness and the real one can be seen in *Figure 205* until a deformation of 40 mm. Maximum loads and rupture values are shown in *Table 43*.

The total load-deformation diagram until rupture can be seen in *Figure 206*, referred to the displacements of the loading head of the testing machine.

It should be pointed out that the timber components were ordered in two different moments. The real quality of the second order (beams I02) was of much lower quality than the first one. The tested E-modulus was in this case clearly lower than the previous one, as can be seen in *Table 42*. On the other hand the folded steel elements did not show any relevant reduction on their predicted stiffness.

The first rupture of the specimen I01, which occurred with a quite load value, was a shear failure. The cause was a mistake in the adaptation of the support detail, which weakened the beam as can be seen in *Figure 207*.



Figure 203: Assembling of 8 metres long specimen I02 (left) and ready for testing (right)

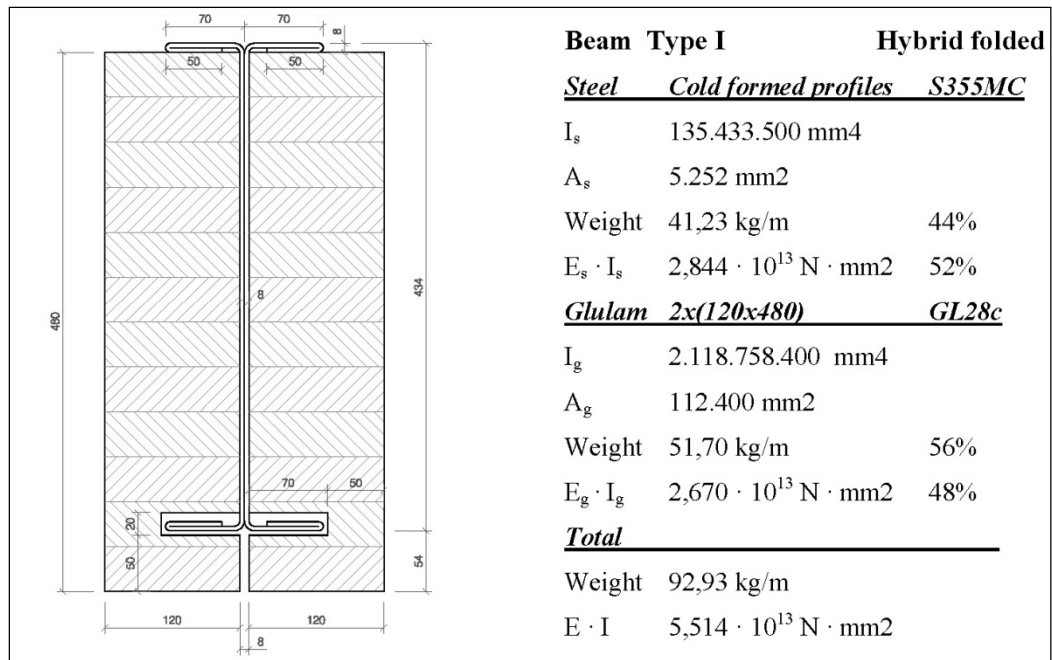


Figure 204: Cross-section parameters of hybrid beams Type I

Components of hybrid beam	Tested timber E-modulus (kN/cm ²)	Comparison to GL28c mean value ($E_{0,mean}$) according to EN 14080	Tested moment of Inertia $I_{y,s}$ for the steel components in comparison to the predicted value
I01	1.318	105,4 %	99,9 %
I02	930	74,4 %	97,8 %

Table 42: Tested E-modulus of timber components and tested moment of inertia of steel elements for hybrid beams Type I

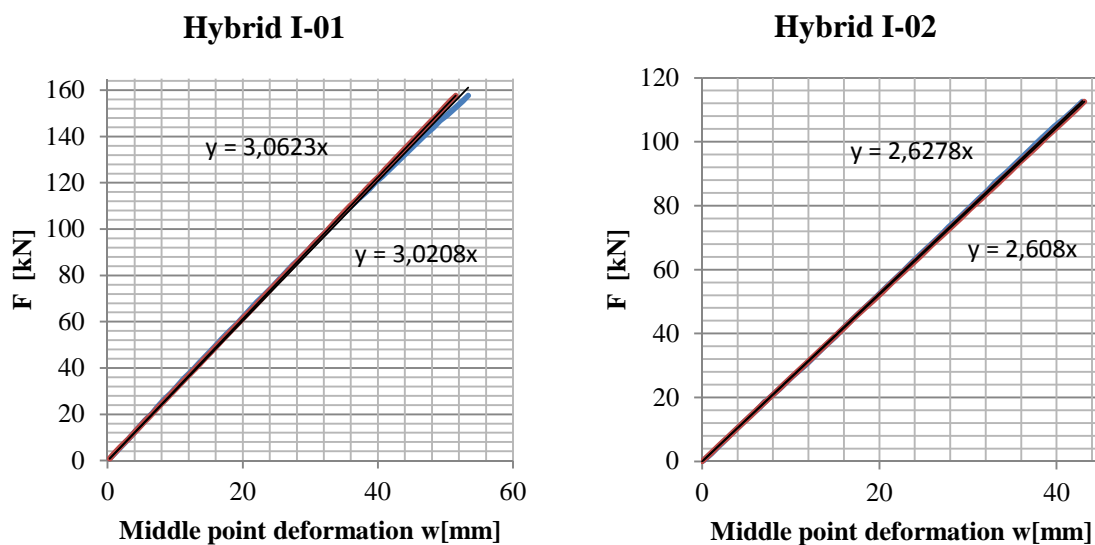


Figure 205: Results. Stiffness in elastic range for the specimens I01 to I02. Red: calculation - Blue: test

Beam (support conditions)	Stiffness comparison (Test/Theory)	First Rupture (kN)	Maximum Load (kN)
I01 (T+S)	98,6%	168,2	201,0
I02 (S)	99,2%	184,6	184,6

Table 43: Results tests I01 – I02

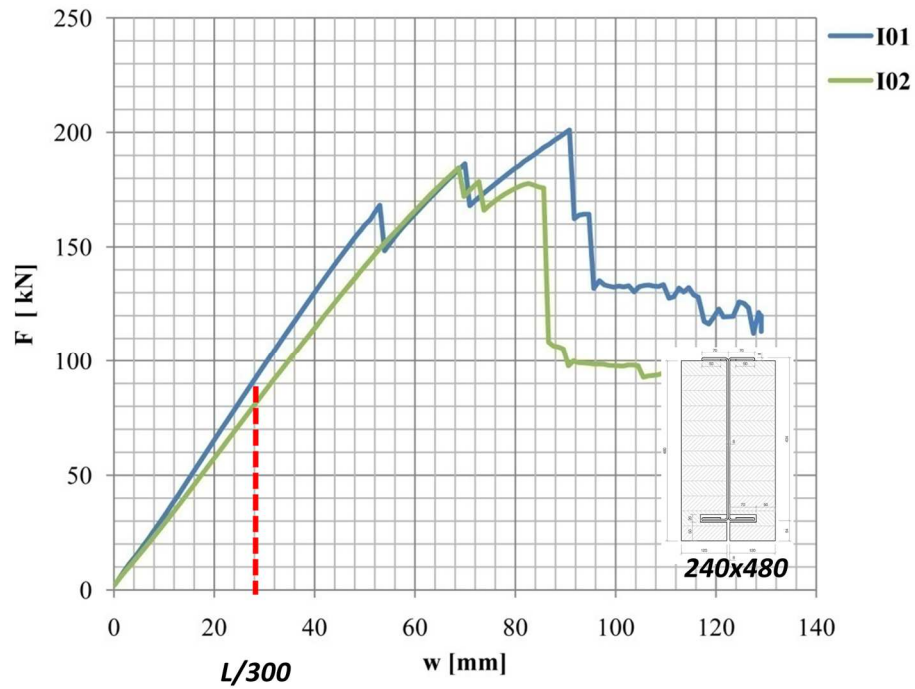


Figure 206: Load deformation graphics tests I01-I02



Figure 207: Support of specimen I01 (left) and shear rupture of the same specimen (right)

5.4.9 Testing series J– Cross-sections and results

The two timber-steel specimens Type J were composed of two cold-formed steel profiles with a U cross-section of S355 steel and glulam GL28c. Their cross-section properties can be seen in *Figure 209*.

The span was of eight metres, the hybrid structural depth $L/20$ and the ratio of structural depth between timber and steel components 1,13.

The comparison between the expected performance regarding total stiffness and the real one can be seen in *Figure 210* until a deformation of 40 mm. Maximum loads and rupture values are shown in *Table 40* and *Table 45*.

The total load-deformation diagram until rupture can be seen in *Figure 211*, referred to the displacements of the loading head of the testing machine.

It should be pointed out that the timber components were ordered in two different moments. The real quality of the second order (beams J02) was of much lower quality than the first one. The tested E-modulus was in this case clearly lower than the previous one, as can be seen in *Table 44*. In addition, the relevant higher number of big knots in the pieces explains the lower timber rupture values obtained from these specimens. On the other hand the folded steel elements did not show any relevant reduction on their predicted stiffness.



Figure 208: Assembling of specimen J02

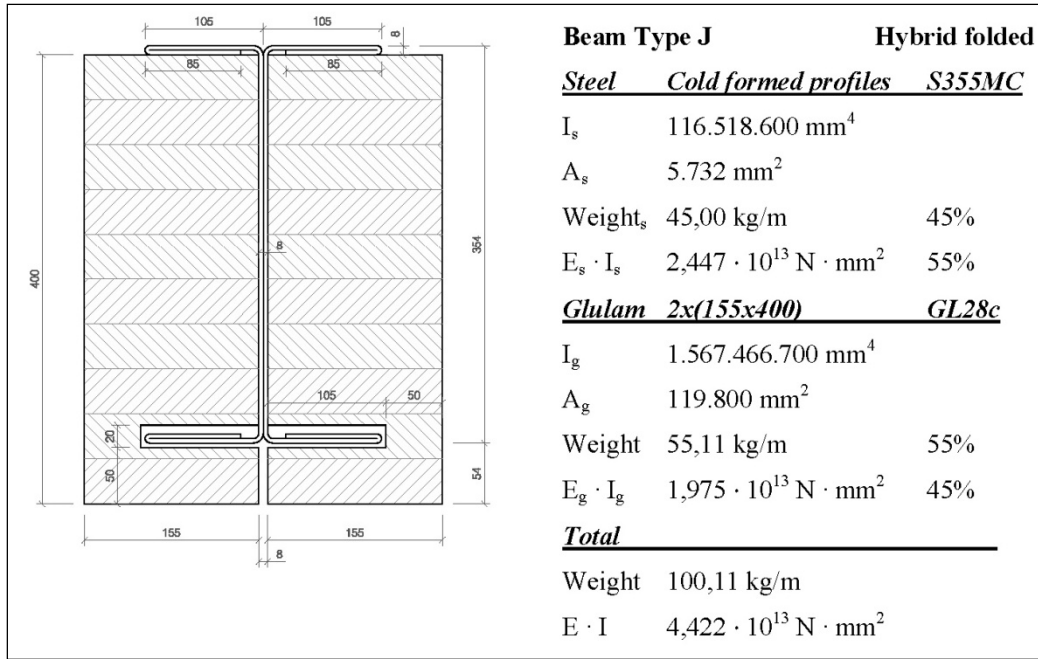


Figure 209: Cross-section parameters of hybrid beams Type J

Components of hybrid beam	Tested timber E-modulus (kN/cm ²)	Comparison to GL28c mean value ($E_{0,mean}$) according to EN 14080	Tested moment of Inertia $I_{y,s}$ for the steel components in comparison to the predicted value
J01	1.149	91,9 %	95,6 %
J02	1.083	86,6 %	99,4 %

Table 44: Tested E-modulus of timber components and tested moment of inertia of steel elements for hybrid beams Type J

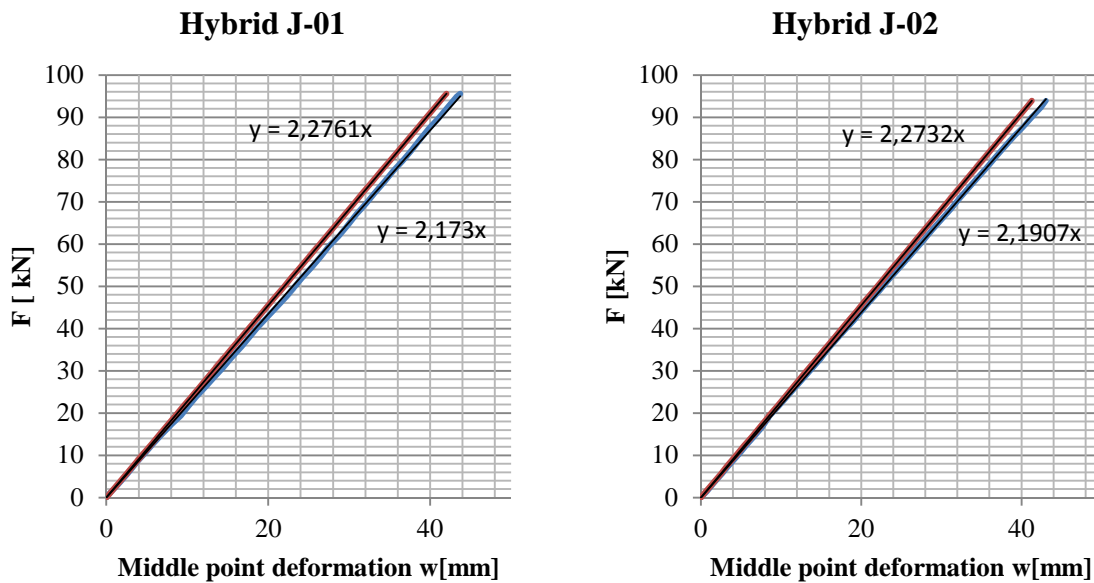


Figure 210: Results. Stiffness in elastic range for the specimens J01 to J02. Red: calculation - Blue: test

Beam (support conditions)	Stiffness comparison (Test/Theory)	First Rupture (kN)	Maximum Load (kN)
I01 (T+S)	95,5%	211,8	211,8
I02 (S)	96,4%	147,1	167,9

Table 45: Results tests J01 – J02

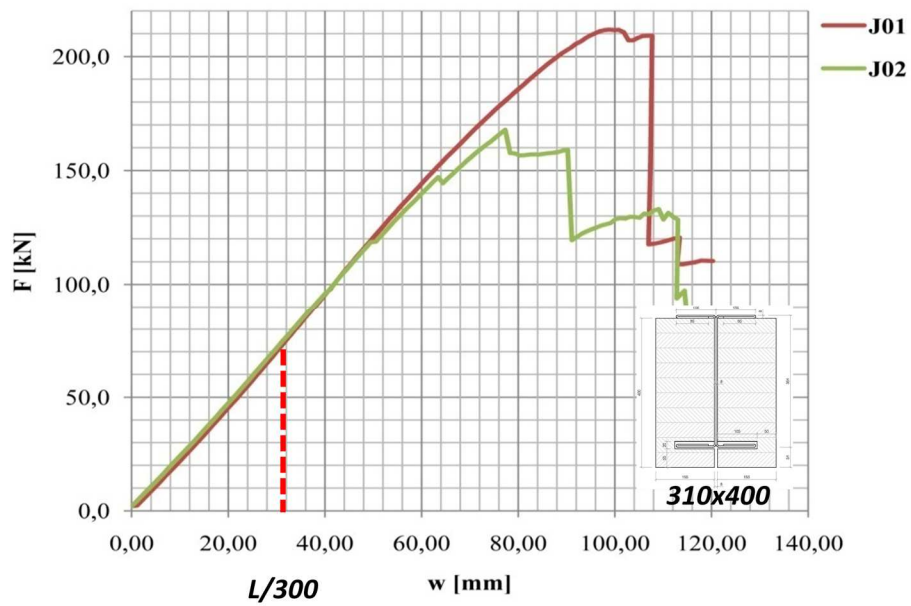


Figure 211: Load deformation graphics tests J01-J02



Figure 212: predicted timber ruptures of specimen J02 due to faulty finger-joints

5.4.10 Interpretation and conclusions

The basic rupture patterns and failure modes were similar to the ones observed during the first testing series, and can exemplarily be seen in *Figure 213*.

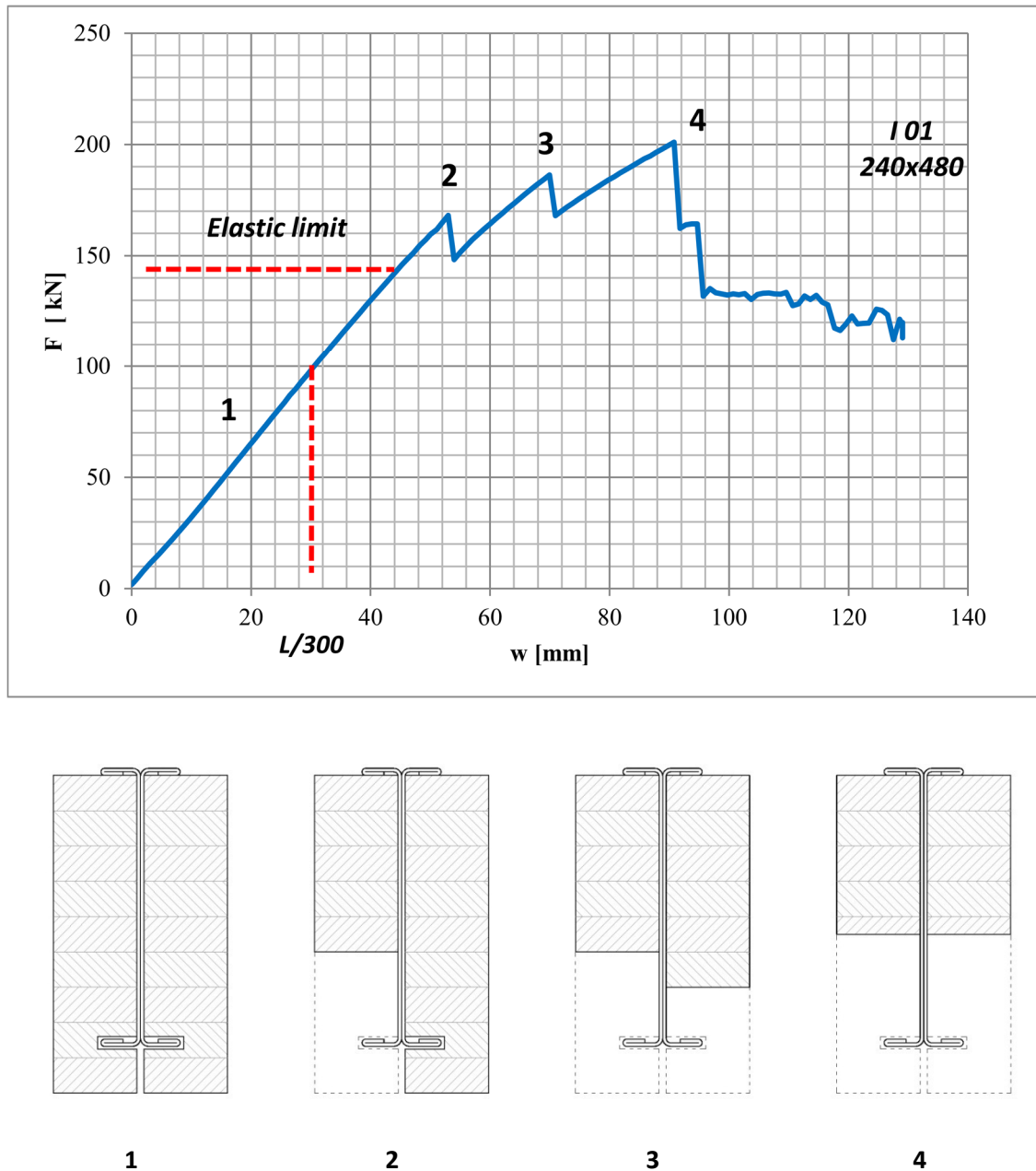


Figure 213: Rupture pattern of asymmetric timber-steel hybrid beams

In this case the local buckling of the upper steel flange could be observed directly thanks to its visible position. This happened always already inside the plastic range of the steel components, and after several timber ruptures occasioning a relevant weakening of the section.

The assumption that the steel cross-section in hybrid beams can be counted as full performing was confirmed by the tests. The covering of the upper steel flange in practical cases with deck materials would contribute in practice to even improve further its performance against local buckling.

It is important to notice the relevance of the support conditions for the optimum performance of the hybrid beams.

The solutions “Timber / Steel” and “Steel” are from both constructive and structural points of view the best options. The values of the calculated stiffness and the one measured in the tests is almost the same, as can be seen in *Table 38*, *Table 41*, *Table 43* and *Table 45*. That means that no loss of stiffness happened.

In the case of the support condition “Timber” the range of loss of stiffness detected was of the same order of magnitude as in the first testing series, being the mean value of the real stiffness the 90% from the calculated one in the second series, meanwhile it was of 89 % in the first testing series. This confirmed the hypothesis that the support conditions were the cause of the loss of stiffness in hybrid beams detected in the first testing series.

This fact could be explained making use of calculation models.

In the proposed matrix-based calculation model (see 4.6.2) both materials, steel and timber, have pinned resting points and are able to transmit vertical loads to the supports. This reproduces the physical reality of the support conditions “Steel”, because in this case the timber pieces rest directly over the steel flanges, and “Timber / Steel” where both materials have a direct contact with the supporting plates. But this is not true in the case of the support condition “Timber”. In this last case the steel components are not able to transmit directly vertical loads to the supports and at the end all the vertical loads are transmitted through timber to the supports. This reduces the effectiveness of the hybrid beam to approximately a 90% of the expected stiffness.

Calculations models where the direct support of the steel components is removed, and the common deformation of steel and timber members guaranteed until a distance to the supports of 1,5 times the total structural depth, confirmed this hypothesis, yielding very similar results to the tested ones.

The elastic deformation of timber perpendicular to the grain plays also a role in these cases. At the very end of the beams all the vertical loads are transmitted through timber, fact which causes an increase in its elastic deformation perpendicular to grain. Calculation models taking into account this parameter confirmed this fact, although made it responsible of only from 2 to 3% of the total loss of stiffness.

In any case, the combination of these two effects explained the loss of stiffness detected during the tests, and pointed to the importance of a correct constructive design and execution of the support points for optimizing the structural performance of timber-steel hybrid beams.



Figure 214: Image of specimen type I showing local buckling of steel flanges after rupture of timber components



Figure 215: Successive timber ruptures in specimen I02

5.5 GLOBAL CONCLUSIONS – SHORT TERM LOADING TESTS

The hybrid beams performed as expected, validating the design (see 4.4) and calculation procedures (see 4.6) proposed.

It is important to take into account the support conditions for both the steel and timber components of a hybrid beam in order to optimize its structural performance regarding stiffness, as commented in 5.4.10. The support condition timber-steel is because of constructive simplicity and optimum structural performance the recommended one.

Both cross-section design proposals, the symmetrical and asymmetrical arrangements (see 4.3) , can be used although the second one is a better alternative.

From a structural point of view the vertical load transmission is better from the steel to timber. In the symmetrical arrangement, vertical load transmission from timber to steel, some kind of gap between the two components is inevitable. From a constructive point of view the tolerances needed for assembling are more reduced and the possibility of connection of the visible upper steel flange to other elements (supports, floors) should in practical cases also taken into account.

On the other hand, the use of the symmetrical arrangement can be justified in the particular cases where fire protection to the upper steel flange is needed.

The failure mechanism was, with the exception of the specimen I01 and for the reasons already explained in 5.4.8, always constant. A sequence of tension ruptures in timber followed by local buckling of the upper steel flange.

Although the total number of specimens tested, twenty-four, is reduced a statistical analysis of the results shows interesting trends.

In nine of the twenty-four hybrid glulam-steel beams the first rupture was smaller than the maximum load that the beam could withstand during the test, as can be seen in *Table 46* .

The ratio of maximum load to the first rupture load reached values until 1,20. This fact was particularly interesting in the cases where, due to any quality defect or manufacturing mistake, a premature failure of

a timber component occurs, like it was the case in the specimens B02 (big knot in the tension zone) or I01 (beam weakened for shear)

Specimen	First rupture (kN)	Maximum load (kN)	Maximum load / First rupture	Deformation first rupture (mm)	Maximum deformation (mm)	Max. def. / Def. first rupt.	Buckling load (kN)	Buckling load / Maximum load
B01	122,3	122,3	1,00	68	120	1,76	84	0,69
B02	90,4	106,9	1,18	52	116	2,23	76	0,71
C01	128,6	128,6	1,00	84	120	1,43	77	0,60
C02	117,4	117,4	1,00	96	120	1,25	83	0,71
D01	122,4	122,4	1,00	97	115	1,19	68	0,56
D02	107,8	107,8	1,00	78	110	1,41	85	0,79
D03	112,4	119,4	1,06	76	115	1,51	69	0,58
D04	106,1	108,1	1,02	71	115	1,62	75	0,69
G01	118,3	135,2	1,14	73	117	1,60	124	0,92
G02	128,6	150,6	1,17	90	107	1,19	115	0,76
G03	164,7	164,7	1,00	82	113	1,38	112	0,68
G04	118,1	118,1	1,00	49	73	1,49	107	0,91
G05	147,9	147,9	1,00	72	85	1,18	97	0,66
G06	127,3	127,3	1,00	61	75	1,23	97	0,76
H01	131,5	131,5	1,00	83	120	1,45	103	0,78
H02	125,5	125,5	1,00	79	107	1,35	109	0,87
H03	134,7	134,7	1,00	83	130	1,57	130	0,97
H04	100,0	107,2	1,07	60	105	1,75	103	0,96
H05	100,5	102,4	1,02	57	93	1,63	102	1,00
H06	103,9	103,9	1,00	58	110	1,90	95	0,91
I01	168,2	201,0	1,20	53	105	1,98	132	0,66
I02	184,6	184,6	1,00	69	120	1,74	97	0,53
J01	211,8	211,8	1,00	105	118	1,12	110	0,52
J02	147,1	167,9	1,14	77	110	1,43	134	0,80
Mean value						1,52		0,75
Characteristic value (0,05)						1,18		0,53

Table 46: Summary of test results and statistical evaluation

Another interesting fact is the ratio between the maximum deformation the beam achieved during the test until total collapse, defined this as the point when the upper steel flanges buckle locally, and the deformation at the first rupture. The values for the deformation in *Table 46* are the ones under the loading head of the tests.

The mean value of this ratio is 1,52, varying from values from 1,12 to 1,90, being the standard deviation 0,28. Defining the characteristic value as the 5 percentile (0,05) this would be 1,18.

This means that a hybrid beam would be able to withstand an additional 18% of deformation before total collapse, taking as a reference the first rupture deformation.

In the case of a pure glulam beam the first rupture point, in normal case because of tension, defines the collapse of the structure, due to its brittle failure. In the case of a hybrid beam an extra ductility of 18% is achieved as a characteristic value.

Comparing the loads the beams still can withstand when they reach the buckling point to the maximum load supported the factors vary from 0,52 to 1,00, being the mean value 0,75 and the standard deviation 0,14. Defining the characteristic value as the 5 percentile (0,05) this would be 0,53.

This means that a hybrid beam is capable of withstanding, after the first rupture, still more than half of the load that caused it before total collapse. The first rupture would be the collapsing point of a pure timber beam.

These two ratios and the characteristic values calculated are a measure of the security reserves that the hybrid beams offer, compared to pure glulam structures.

In the case of pure glulam beams the partial safety factor for the material stated in Eurocode 5 (6) has a value of $\gamma_M = 1,25$. This, combined with the modification factor k_{mod} , which for a determined material depends on the service and load duration class, modify the characteristic strength values as follows:

$$X_d = \frac{k_{mod} \cdot X_k}{\gamma_M}$$

This way the strength design value is reduced, with a global safety margin for the material of , for a value of $k_{mod} = 0,8$, with a global safety margin for the material of $1,25/0,8 = 1,56$.

But as already explained the failure mode in pure glulam beams is a brittle one. The discussion of if the security reserves existing in a timber-steel hybrid beam detailed in the previous paragraphs could be addressed here appears, because of a more complex failure mechanism involving two but not simultaneous timber brittle failures and final local buckling of steel components. The steel profiles used have a recommended material security factor of $\gamma_{M0} = 1,00$ according to Eurocode 3 (7).

In any case all the design procedures and verifications proposed until now are compatible with and follow the Eurocode 5 (6)(18) and Eurocode 3 (7) (16) criteria. The safety factor discussion is presented at this point as a future research line which needs to be studied with more detail in the future.

Regarding the material price of the hybrid beams components, the steel prices received were quite variable during the period of ordering the materials. The steel profiles were ordered at three different times, April 2013, November 2013 and April 2014.

The ordered profiles were manufactured using bending presses, see 4.3.2. Firms that used roll-forming procedures were consulted but refused to produce the profiles due to the reduced quantity of the order.

The steel prices for these three different orders are compiled in *Table 48*, *Table 48* and *Table 49*, for April 2013, November 2013 and April 2014 respectively. The prices include folding or welding, depending on the type of hybrid beam, as well as the mechanizations for the lateral assembling holes.

Hybrid beam	Welded profiles		Cold-formed profiles
	Type B	Type C	Type D / Type E
Number of specimens	2	2	4 / 2
Steel thickness (mm)	6/8	6	3
Price (€/kg)	5,40	5,30	2,66
Average price (€/kg)	5,35		2,66

Table 47: Steel prices for the specimens tested – April 2013

Hybrid beam	Cold-formed profiles			
	Type G	Type H	Type I	Type J
Number of specimens	3	3	1	1
Steel thickness (mm)	4	4	4	4
Price (€/kg)	2,38	2,27	1,91	1,76
Average price (€/kg)	2,08			

Table 48: Steel prices for the specimens tested – November 2013

Hybrid beam	Cold-formed profiles			
	Type G	Type H	Type I	Type J
Number of specimens	3	3	1	1
Steel thickness (mm)	4	4	4	4
Price (€/kg)	3,02	2,89	2,24	2,06
Average price (€/kg)	2,55			

Table 49: Steel prices for the specimens tested – April 2014

Although the number of specimens ordered was in any case very reduced some price trends can be detected.

The comparison between welded steel profiles and the cold formed ones is clear. At the same time of ordering welded profiles were twice as expensive as the cold-formed ones, as can be seen in *Table 47*. This fact, together with the thermal deformations due to welding, makes cold-formed profiles more suitable than the welded one in hybrid beams, as it was already commented in 5.3.

The prices for the cold-formed steel profiles varied from a minimum of 1,76 €/kg for Type J in November 2013 to a maximum of 3,02 €/kg to Type G in April 2014. The average price of cold-formed steel profiles varied, ordering exactly the same quantity and type of beams, a +22% from November 2013 to April 2014.

It is interesting to notice that hybrid beams Type I and Type J were always cheaper than the other specimens, even ordering less number of specimens and less kg of steel in total. This is probable due to the repercussion of the manufacturing process. Type I and Type J beams were eight metres long, meanwhile the other specimens only six. The specimens were manufactured using bending presses and this makes the repercussion of the bending procedure cheaper for the longer beams.

On the other hand the timber price was constant, being of 450 €/m³ for glulam GL28c during the whole period.

These two facts, stability of timber price and variability of the steel one, confirmed the trends commented on 2.2.3.

As a suggestion it would be interesting to take into account the current steel price at the moment of design before the structural definition of a hybrid beam. The quantity of steel needed, or balance of bending stiffness between steel and timber, could be modified until some point for using more or less steel depending on the prices available. Of course the final cross-section designed has to satisfy in any case all the design conditions detailed in 4.4

As general criteria it is recommended to keep the folding design of steel flanges as simple as possible in order to allow a simple production.

The use of thin plates is also recommended because they allow an easier folding and better geometrical accuracy than the thicker ones.

The use of other steel types, welded profiles or castellated beams, is also possible, if the problem regarding geometrical accuracy for the first ones are solved. In any case welded beams were more expensive than the cold-formed ones.

On the other hand, timber machining should be also kept simple as possible, due that every production step makes the final product more expensive.

The use of cross laminated timber as wood component could be of interest and economically feasible in the case of high pressure perpendicular to grain in the support areas. In cases like this its use could compensate their comparatively smaller bending stiffness with its better performance under transversal compression.

Due that the difference in price from steel grade S355 to S235 was really small (in Austria and during the testing periods it was less than a 10% difference), the quality S355 was chosen for reaching higher capacities.

The relatively high price of the steel profiles ordered was partially due to their low quantity, and the fact that they should be produced as prototypes. It is expected that for bigger quantities the price would be lower, or at least equal to the cheaper prices received, being comparable to the steel price for standard steel profiles.

High accuracy of production was requested for the two testing series for being able of studying with precision the structural performance of the beams. This high accuracy is for the prefabrication of elements and standard construction site conditions not necessary anymore and is considered as a factor which would contribute to make the price of components demanded even cheaper.



Figure 216: Hybrid beam H1 after test

6. LONG-TERM LOADING TESTS: CREEPING

6.1 INTRODUCTION

It is expected that the use of steel will help to counteract the creeping behaviour of timber. As time passes timber experiences the effects of its viscous-elastic behaviour. This is reflected in an increasing deformation during time, but the steel pieces from a hybrid beam would oppose to these movements. Therefore the creep deflection of a hybrid beam would be smaller than a pure timber beam, but bigger than a pure steel beam which does not creep at all. This phenomenon should be taken into account for the calculation of the final deflection of structural elements.

The comparative behaviour during time, for three different beams, steel, hybrid and timber, under the same load and with same instantaneous deflection, could be simplified as shown in *Figure 217*.

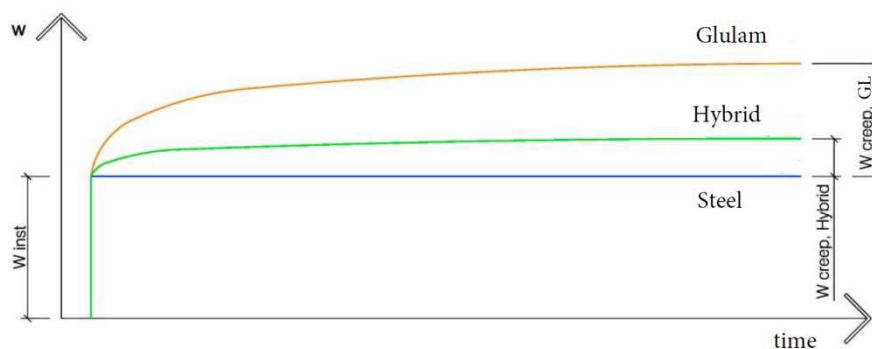


Figure 217: Comparative creeping deflection diagrams of steel, timber and hybrid beams.

Although the overall quantity of literature existent on the topic of creeping of timber-steel structural solutions is still nowadays quite reduced, some authors have both theoretically and experimentally studied these and close related phenomena.

R. Kliger (234) studied the creeping behaviour of stressed -skin panels composed of wood-based materials in the web and compression flange and steel sheet in the tension flange.

M. Kimura et al (141) studied experimentally the structural and long term behaviour of LVL-steel composite beams, composed of vertically arranged LVL members and an inner steel lattice. The steel lattices were successful in suppressing creep deflection during the 200 days-long test.

R. Kliger (235) studied the problem of deformation modification factors for calculating built-up structures. This study is useful not only for timber-based built-up structures, but also for other possible combinations of materials.

S. Nakajima et al (52) evaluated the creep performance of hybrid timber beams composed of glulam with upper and lower steel or carbon fiber plates. The steel plates were jointed with going through bolts. In these cases, and following the authors, the results were less promising, being the creep performance not affected by the steel or carbon fiber sheets.

S. Hansson and K. Karlsson (38) carried out creeping tests of combined cross sections of timber, timber and steel and timber and carbon fiber reinforced polymers. The reinforcements were successful for the reduction of both the initial deformation and the mechano-sorptive creep. The creeping tests were in this case quite short, with a total duration of 10 weeks.

Lu et al (66) studied the creeping behaviour of glulam reinforced with steel bars.

From a theoretical point of view, the TRADA Technology Timber frame housing manual (121) proposes a series of calculation procedures for steel flitch beams. These beams are composed by two timber components with an intermediate steel plate. The connection of elements is carried out with going-through bolts and the calculation procedures provide guidance for the calculation of deformations and stresses for both the initial and long term situations.

It is also stated in the literature that the most important factors affecting the creeping behaviour of timber and glulam beams are the stress level, timber quality and Young Modulus, humidity content and its variation during time (depending on climatic factors, as temperature and atmospheric humidity), duration of loads and sequences of loading (12) (20).

6.2 ASSESSMENT FOLLOWING EUROCODE 5

Eurocode 5 (6) in its point 2.3.2.2 *Load-duration and moisture influences on deformations* proposes a method which deals with the global performance of “structures” composed of materials with different properties depending on time. This method, although inside the timber Eurocode and therefore proposed for wood-based products, could be useful for the analysis of mixed components like the beams object of this study.

Following Eurocode 5 (6):

“The analysis of structures shall be carried out using the following values for stiffness properties:

(...) for a first order linear elastic analysis of a structure, whose distribution of internal forces is affected by the stiffness distribution within the structure (eg. composite members containing materials having different time-dependent properties), final mean values adjusted to the load component causing the largest stress in relation to strength shall be used; (...)”

In its point “2.2.3 Serviceability limit states” it is stated:

“(4) If the structure consists of members or components having different creep behaviour, the final deformation should be calculated using final mean values of the appropriate moduli of elasticity, shear moduli and slip moduli, according to 2.3.2.2(1)”

And in the point “2.3.2.2 Load duration and moisture content in deformations” the following procedures are stated:

“(1) In serviceability limit states, if the structure is formed by pieces or components with different properties depending on time, the final medium value of the modulus of elasticity, $E_{mean, fin}$, the shear modulus $G_{mean, fin}$, and the slip modulus, $K_{ser, fin}$, used for calculating the final deflection, should be taken from the equations:

$$E_{mean, fin} = \frac{E_{mean}}{(1 + k_{def})}$$

$$G_{mean, fin} = \frac{G_{mean}}{(1 + k_{def})}$$

$$K_{ser, fin} = \frac{K_{ser}}{(1 + k_{def})}$$

Also following Eurocode 5 (6), “ *in ultimate limit states, where the load and moment distribution will be affected by the rigidity of the structure, the final medium value of the modulus of elasticity, $E_{mean, fin}$, the shear modulus $G_{mean, fin}$, and the slip modulus, $K_{ser, fin}$, should be calculated following the equations:*

$$E_{mean, fin} = \frac{E_{mean}}{(1 + \psi_2 \cdot k_{def})}$$

$$E_{mean, fin} = \frac{E_{mean}}{(1 + \psi_2 \cdot k_{def})}$$

$$K_{ser, fin} = \frac{K_{ser}}{(1 + \psi_2 \cdot k_{def})}$$

being ψ_2 the factor for the quasi-permanent value of the action defined in EN 1990 (223) causing the largest stress in relation to the strength. If this action is a permanent action ψ_2 should be replaced by 1.”

These methods, conceptually quite similar to the proposed by TRADA (121), are taken as a reference and will used and examined through testing for assessing their use in the particular case of the timber-steel hybrid beams focus of this research.

6.3 OBJECTIVES OF THE TESTS

The main objective of the creeping tests is the checking and verification of the assumed creeping behaviour of timber-steel hybrid elements and the methods proposed for their analysis.

The design of the test looks for the control, or at least the knowledge, of all of the main parameters involved influencing creeping behaviour.

It is important to point out that creeping is an extremely complex phenomenon depending on a high number of factors, very difficult to control or to measure in their totality.

In any case, following the experiences of previous researchers, and accepting that the most important factors affecting the creeping behaviour of timber beams are the stress level, timber quality and Young Modulus, humidity content and its variation during time (depending on climatic factors, as temperature and atmospheric humidity), duration of loads and sequences of loading, a specific creeping test was designed.

The basic concept was to test during one year a hybrid beam under a constant load, and use as a comparison a glulam beam with an equivalent initial stress level, similar quality and an equal as possible Young Modulus as the glulam part of the hybrid beam, as shown in *Figure 218*.

The climatic conditions and their variation will be common for the two beams, due that they will share the same space. Temperature, air humidity and also timber humidity content will be recorded periodically.

If the loads to be applied over the two beams are designed to produce the same normal stress level in the timber parts the results of the two beams can be comparable and would give light to the questions posed.

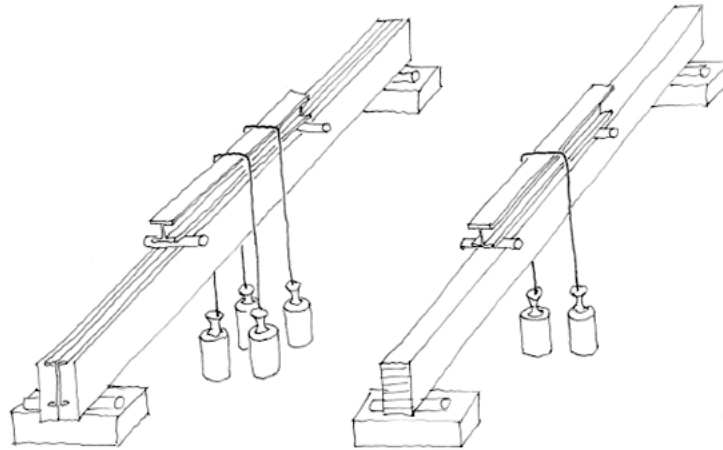


Figure 218: Conceptual design of the test for a hybrid beam (left) and a timber comparison beam (right).

This way, the assumption of difference in creeping behaviour due to the hybrid performance can be verified, and the hypothesis stated about performance and calculation procedures following Eurocode 5 (6) could be checked, validated, adjusted or corrected.

The test was carried out with two timber-steel hybrid specimens compared to two respective reference “only timber” beams during one year.

6.4 DESIGN CRITERIA OF SPECIMENS

One of the main problems of designing a creeping test is the difficulty of implement high loads over the beams during long periods of time. The space required for the real scale beams during the time needed is another important issue. Most researchers face this problem designing their experiments following one of these three possibilities:

- Test real dimension beams but at lower levels of normal stresses than the serviceability ones.
- Scale the problem of the beam: i.e. test smaller beams but reaching real serviceability normal stress values.
- Design a test that combines in some way both previous possibilities.

The implementation of high loads and space needed for testing during long time the same beams as in the short-term tests of timber-steel hybrid beams (see chapter 5) was not possible in the available testing laboratory. That is why a special design of four meters long timber-steel “flat” hybrid beam was used, as shown in *Table 50*. For this special type of beam the space was enough and the values of static load required possible to implement with concrete blocks. Their reduced dimensions made the use of double folded steel profiles as originally designed not possible. The steel profile was then substituted by a single folded beam but following several criteria in order to reproduce the most important features of the mechanical performance of full-scale hybrid beams:

- The transmission of vertical load should take place from the steel parts to the glulam ones. That is why a lied down steel U cross-section is placed upon a horizontal rectangular timber beam.
- The distribution of bending stiffness should be similar to the bending stiffness distribution of the full-scale hybrid beams. That means approximately 50% for glulam and 50% for steel.
- Due to the lying-down arrangement of the beams a GL28h grade for the timber pieces was chosen instead of the original GL28c of the full-scale hybrid beams. This way the quality of the material is the same for all the most stressed fibres in the upper and downer part of the section.

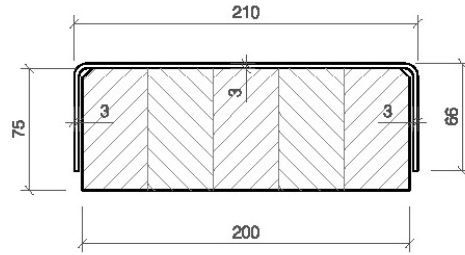
- The relation of structural depth between steel and timber was chosen in order to reach the same maximum normal stresses in both glulam, and steel and in the same proportion, as in the original hybrid beams.
- In order to constantly ensure a common bending deformation for the two parts, three vertically arranged thin bolts, as shown in *Figure 219*, hold the pieces together along the middle part of the beam, with end washers and nuts. The pre-drilled holes have enough tolerance to avoid any horizontal shear transmission through the bolts and the nuts are not tightened. This way the vertical contact between the two pieces is guaranteed in case of any vertical movement, ascending or descending, without horizontal shear transmission between the pieces thanks to the tolerance inside the holes. The fact of not tightening the nuts looks also for avoiding any favourable effect due to increased friction between materials.



Figure 219: Vertical connector through glulam and steel for the creeping hybrid beams.

The creeping beams were loaded following a four point bending test schema. As time passes the creeping effect starts to affect the glulam components, and the timber part tends to have an increased deformation. Then the connection rods will be able to support it and transmit little by little fractions of the load to the steel profile placed over.

For this purpose the three connectors are established along the central part of the beam, where the maximum value of bending moment occurs.



Steel -S355				
Is=	37,9	cm4		
As=	9,91	cm2		
Weights=	7,78	kp/m	51%	
Es · Is=	795 000	kN·cm2	47%	
As, shear,z=	3,22	cm2		
Glulam-GL28h				
Ig=	698,55	cm4		
Ag=	149,64	cm2		
Weightg=	7,33	kp/m	49%	
Eg·Ig	880 173	kN·cm2	53%	
Ag, shear,z	124,19	cm2		
Hybrid section				
Weighth	15,11	kp/m		
E·Ih	1 676 073	kN·cm2		

Table 50: Cross section properties of hybrid beams for the creeping test

6.5 CALCULATION OF THE DESIRED STRESS LEVEL

For determining the magnitude of load to be implemented over the testing specimens, the criterion of finding which would be the maximum allowable normal stress level in Serviceability Limit State was used.

First, it is necessary to calculate which would be the maximum stress allowable in an Ultimate Limit State situation, and then calculate back which would be the correspondent real stress value in Serviceability Limit State. In order to determine it, the values of k_{mod} and partial security factors for loads γ_F and for the material $\gamma_{M,g}$ are set for the case of a glulam beam under permanent load and Service Class 1 as stated in Table 51.

$\gamma_{M,g}$	γ_F	k_{mod}
1,25	1,35	0,6

Table 51: Partial and modification factors

Therefore the calculation for the chosen GL28h follows as:

$$\sigma_{m,d} \leq f_{m,d} = k_{mod} \cdot \left(\frac{f_{m,k}}{\gamma_{M,g}} \right)$$

$$\sigma_{m,d} \leq f_{m,d} = 0,6 \cdot \left(\frac{28}{1,25} \right) = 13,44 \text{ N/mm}^2$$

In the next step the effect of the load security factor is removed as it follows:

$$\sigma_m \leq \frac{0,6 \cdot \left(\frac{28}{1,25}\right)}{1,35} = 9,95 \text{ N/mm}^2 = 35,5\% f_{m,k}$$

This way is the desired stress level fixed. It is important to notice that this stress level can be quite high compared with the real for many structural applications of only-timber or even timber steel-hybrid beams governed by deflections or vibrations (SLS) and not by stress levels (ULS). In any case, it was adopted for the tests with the idea of reproducing a “worst-case” stress-level scenario. This way the results obtained can be considered to be on the safe side of the creeping problem.

6.6 TESTING PROCEDURES

In order to select four tests specimens with a similar-as-possible value of E-Modulus, twelve specimens of glulam beams K01-K012 were ordered and tested following a three point bending test procedure.

The load velocity was 0,15 mm/s and the maximum deformation limited to 20 mm for being sure that the timber fibres remained in an elastic state and the pieces were not damaged.



Figure 220: Timber specimens to be tested and classified regarding their Young Modulus values



Figure 221: Three point bending tests for selecting the timber specimens regarding their Young Modulus

The specimens K01, K03, K05 and K09 were rejected through a visual selection due to a higher number of knots in the middle part of the beams, compared with the other specimens. Specimens K06 and K12 were discarded due to geometrical irregularities like warping.



Figure 222: Comparison of the central and bottom face of the beams K01 (rejected due to presence of knots in the middle part and in the proximity to the connecting holes) and K02 (accepted)



Figure 223: Image where the warping of the specimen K06 can be observed

All the selected pieces showed a slightly higher Young Modulus than the mean value correspondent to GL28h, $E_{0,g,m}=12.600 \text{ N/mm}^2$ following EN 14080 (14), with improvements between 1% and 10%, as shown in *Table 52*.

From the six specimens K02, K04, K07, K08, K10 and K11, two pairs were selected.

These were specimens K02 + K10 and specimens K11 + K04 with an E-modulus difference of 1%. Specimens K02 and K11 were selected as components for the hybrid beams and K10 and K04 as comparison pure glulam beams.

The specimens K07 and K08, with the maximum and minimum values of Young Modulus, were selected for control rupture tests.

Specimen	E (kN/cm ²)	Comparison EN14080 (%)
K02	1325	105
K04	1322	105
K07	1270	101
K08	1386	110
K10	1339	106
K11	1314	104

Table 52: *E-modulus for the selection of glulam beams Type K*

Specimen	E (kN/cm ²)	Comparison EN14080 (%)
K10 (Glulam)	1339	106
K02 (Hybrid)	1325	105
K04 (Glulam)	1322	105
K11 (Hybrid)	1314	104

Table 53: *Pairs of beams formed for the comparison creeping test*

Knowing the stress value to be reached for the timber components, the loads to be applied for both hybrid beams can be found using common calculation methods.

The relevant parameter and values are summarized in *Table 54*.

Therefore the hybrid specimens were loaded with 5,40 kN and the glulam ones with 2,83 kN. These weights were prepared from concrete blocks and steel elements, weighted in the laboratory and installed over the beams with the help of a crane. The values of deflection were recorded under the middle point and under the two loading points of the beams during one year. Temperature and relative air humidity were also continuously recorded.

Hybrid beam			
Total Load	5,40	kN	
Glulam Bending Moment	185,03	kN·cm	
Timber Stress	9,95	N/mm ²	
% fm,k	35,5	%	
Steel Bending Moment	167,61	kN·cm	
Steel Stress (tension)	229	N/mm ²	
Steel Stress (compression)	62	N/mm ²	
Glulam comparison beam			
Total Load	2,83	kN	
Glulam Bending Moment	185,03	kN·cm	
Timber Stress	9,95	N/mm ²	
% fm,k	35,5	%	

Table 54: *Loads applied and tension values for the different beams and components*



Figure 224: Preparation of the test set-up for the long-term four point bending test

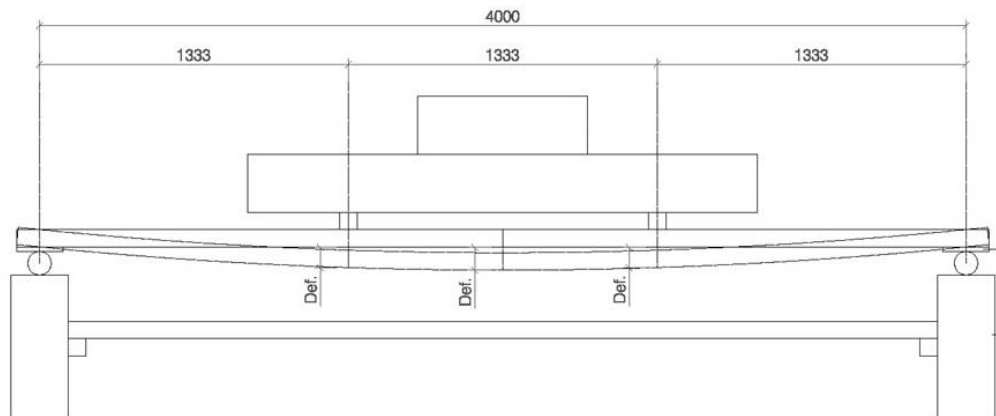


Figure 225: Test set-up for the long-term four point bending test

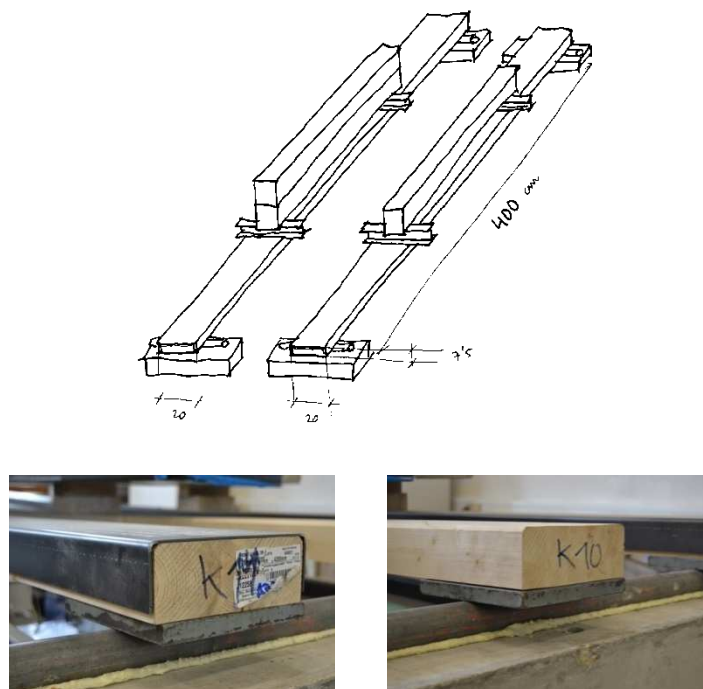


Figure 226: Test set-up and photos with a hybrid beam (left) and a timber comparison beam (right)



Figure 227: Image of the test set-up

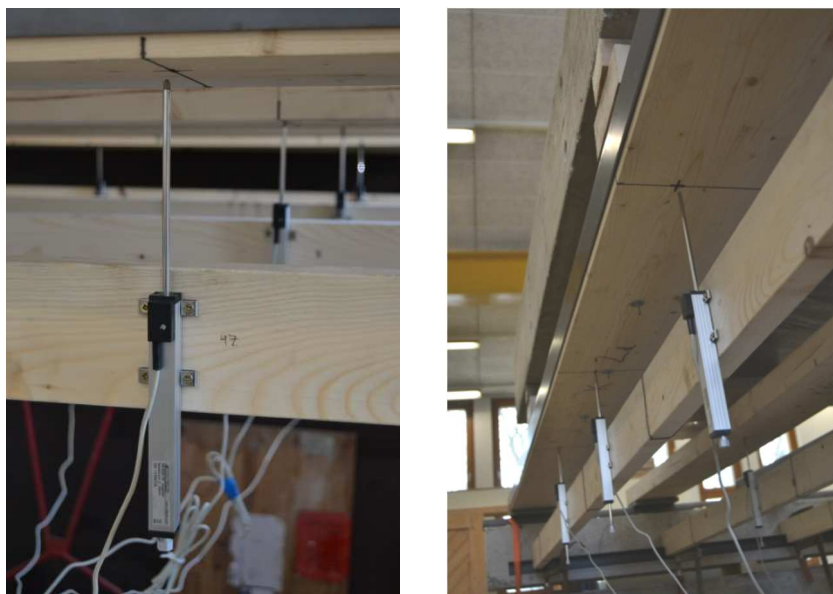


Figure 228: Image of the measuring points



Figure 229: Recording data machine ALMEMO 5690-2

6.7 RESULTS

A graphic showing the deformation behaviour of the four specimens during the one year tested can be seen in *Figure 230*.

Only the creeping deflection of the four specimens is graphed. The air humidity content and temperature of the testing room were always continuously recorded. As it can be seen in *Figure 230*, the air relative humidity exceeded the value of 65% only some days during one year. The temperature of the room was also over 20°C almost the full time, fluctuating between 15 and 30°C.

These testing conditions fulfil therefore the definition of a Service Class 1 following Eurocode 5 (6) : “Service class 1 is characterised by a moisture content in the materials corresponding to a temperature of 20% and the relative humidity of the surrounding air only exceeding 65% for a few weeks per year.”

Moreover, the moisture content of the tested beams was controlled and measured weekly using the electrical resistance method stated in EN 13183-2(233) . The moisture content was found to fluctuate between 9% and 11%, fulfilling also the Eurocode 5 (6) note: “In service class 1 the average moisture content in most softwoods will not exceed 12%”

The fluctuations in the creeping values during time have a direct relation with the atmospheric conditions, especially air relative humidity content.

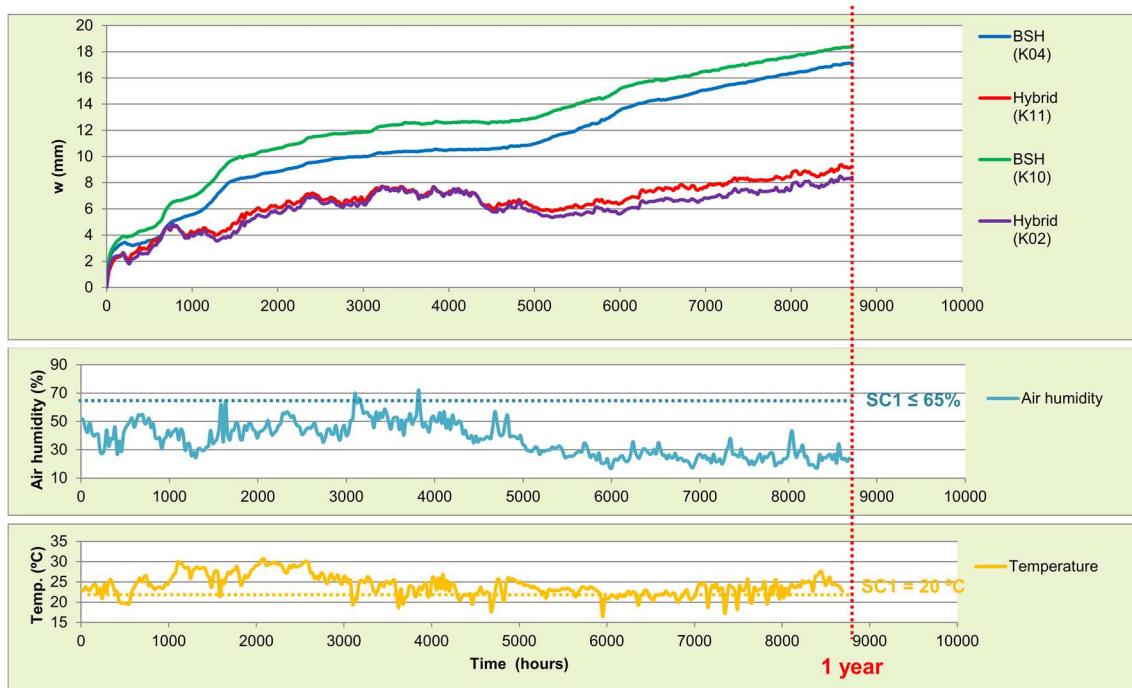


Figure 230: Results of the creeping test after one year

After the initial loading all the beams presented an almost identical instant deflection value very close to the predicted one of 39 mm, as shown in *Table 55* and *Table 56*.

This common instant deformation guarantees that the initial normal stress value in the glulam pieces is the same for the hybrid specimens and the glulam ones.

The graphics showing the progression of the creeping deformation of the pairs of beams to be compared are shown in *Figure 231*.

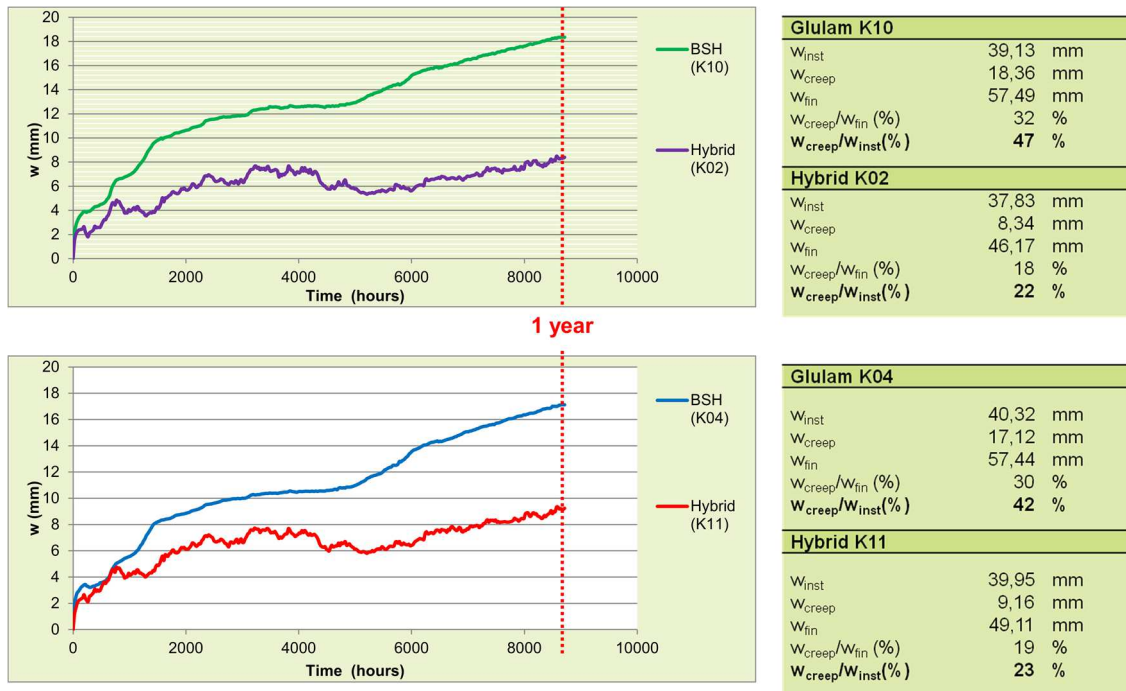


Figure 231: Results of the creeping test after one year. Comparison of pair of beams.

It resulted that after one year of constant loading the glulam specimens experienced a medium value of creeping of 17,74 mm, meanwhile the hybrid ones of only 8,75. The creeping deflection of the hybrid K11 (9,16 mm) was around 54% of the correspondent creeping deflection of its comparison pure-timber K04 (17,12 mm). In the case of the hybrid K02 (8,34 mm) this value was of only 45% of the one experience by its partner beam K10 (18,36 mm). The ratio of creeping deformation to final deformation was 30-32% for the glulam specimens meanwhile only of 18-19% for the hybrid ones. The ratio of creeping deformation to initial deformation was 42-47% for the glulam specimens meanwhile only of 22-23% for the hybrid ones. The most important test results data are summarized in *Table 55* and *Table 56*.

Glulam K04		
Total Load	2,83	kN
w_{inst}	40,32	mm
w_{creep}	17,12	mm
w_{fin}	57,44	mm
$w_{creep}/w_{fin} (\%)$	30	%
$w_{creep}/w_{inst} (\%)$	42	%
Hybrid K11		
Total Load	5,40	kN
w_{inst}	39,95	mm
w_{creep}	9,16	mm
w_{fin}	49,11	mm
$w_{creep}/w_{fin} (\%)$	19	%
$w_{creep}/w_{inst} (\%)$	23	%

Table 55: Results for the pair Glulam K04-Hybrid K11

Glulam K10		
Total Load	2,83	kN
W_{inst}	39,13	mm
W_{creep}	18,36	mm
W_{fin}	57,49	mm
W_{creep}/W_{fin} (%)	32	%
W_{creep}/W_{inst} (%)	47	%
Hybrid K02		
Total Load	5,40	kN
W_{inst}	37,83	mm
W_{creep}	8,34	mm
W_{fin}	46,17	mm
W_{creep}/W_{fin} (%)	18	%
W_{creep}/W_{inst} (%)	22	%

Table 56: Results for the pair Glulam K10-Hybrid K02

6.8 INTERPRETATION AND CONCLUSIONS – LONG TERM LOADING TESTS

In order to analyse, model and interpret the results obtained the method proposed in the norm prEN 1156 (236). Although this norm is proposed for wood-based panels, the creeping factor calculation model proposed is a classic creeping analysis method. This method, although simple, was precise enough for the small number of specimens tested and was used also for other researchers studying the creeping of timber-steel solutions like Nakajima et al (52).

This method defines a creeping factor k_c as the ratio of creep to the initial deformation:

$$k_c = \frac{(a_T - a_0) - (a_1 - a_0)}{a_1 - a_0} = \frac{a_T - a_1}{(a_1 - a_0)}$$

being:

a_T	total deformation, in mm, in Time T, in min
a_1	total deformation, in mm, after 1 min
$a_1 - a_0$	initial elastic deformation, in mm, after 1 min

The test results can be represented in a graphic as the one shown in *Figure 232* and be used for determine the creeping factor k_c

It should be mention that the X axis represents the time as \log_{10} min. That means that a value of 5,72 represents one year, in correspondence to the duration of the gathering of creeping data.

Fitting the line representing the ratio k_c to time (both logarithmically) to the testing data until one year, the values of k_c can be projected for the case of 10 or 50 years loading. On the axis X a value of 6,72 would represent 10 years and a value of 7,42 would represent 50 years.

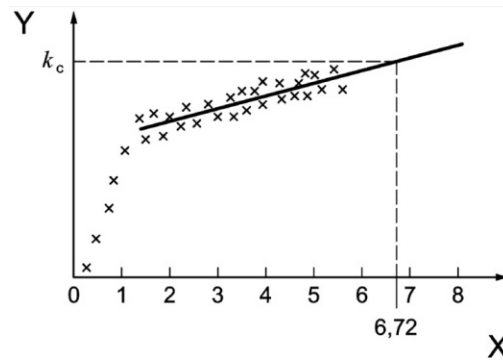


Figure 232: Determination of the creeping factor k_c for ten years using testing data (236)

Being:

X time under load in \log_{10} min
Y \log_{10} from creeping factor k_c

Following this procedure the values of k_c can be found as shown in *Figure 233* for the pair of beams K10 (Glulam) and K02 (Hybrid).

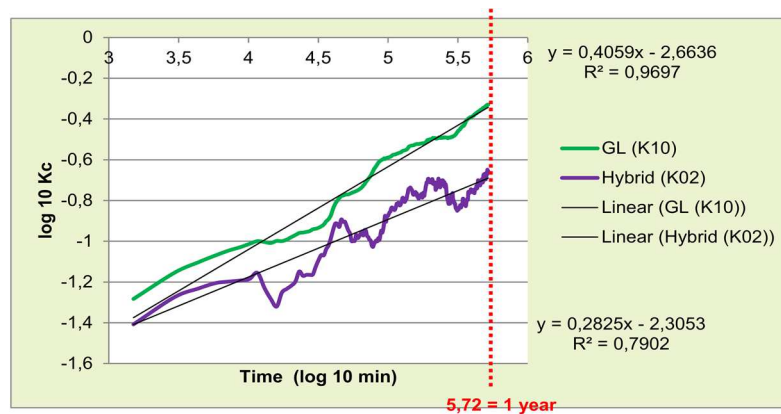


Figure 233: Calculation of the creeping factor k_c for the pair of beams K10 (Glulam) and K02 (Hybrid)

The converted graphic showing the values of k_c can be represented in a not logarithmic axis as shown in *Figure 234*. For the calculation of these curves the middle value of the specimens tested was used. That means, the middle value of both glulam specimens and the middle value of both hybrid specimens.

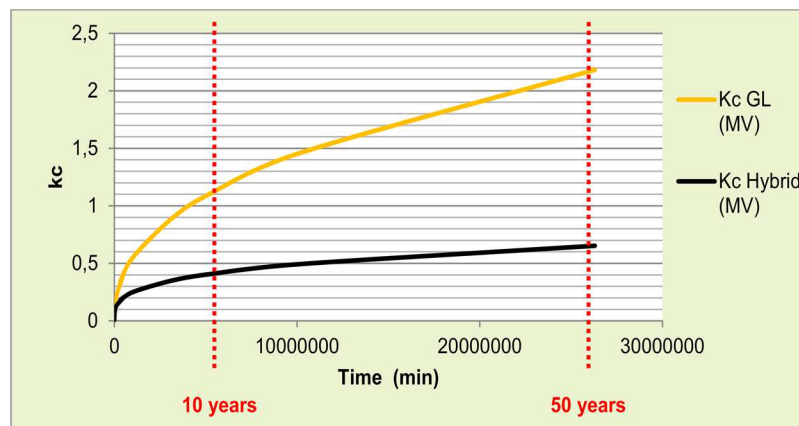


Figure 234: Creeping factor k_c obtained from test results. Middle value of the two specimens tested

Using the k_c values theoretical deformation curves can be drawn, both for absolute creep and relative creep.

In the case of absolute creep the curves are shown in *Figure 235*.

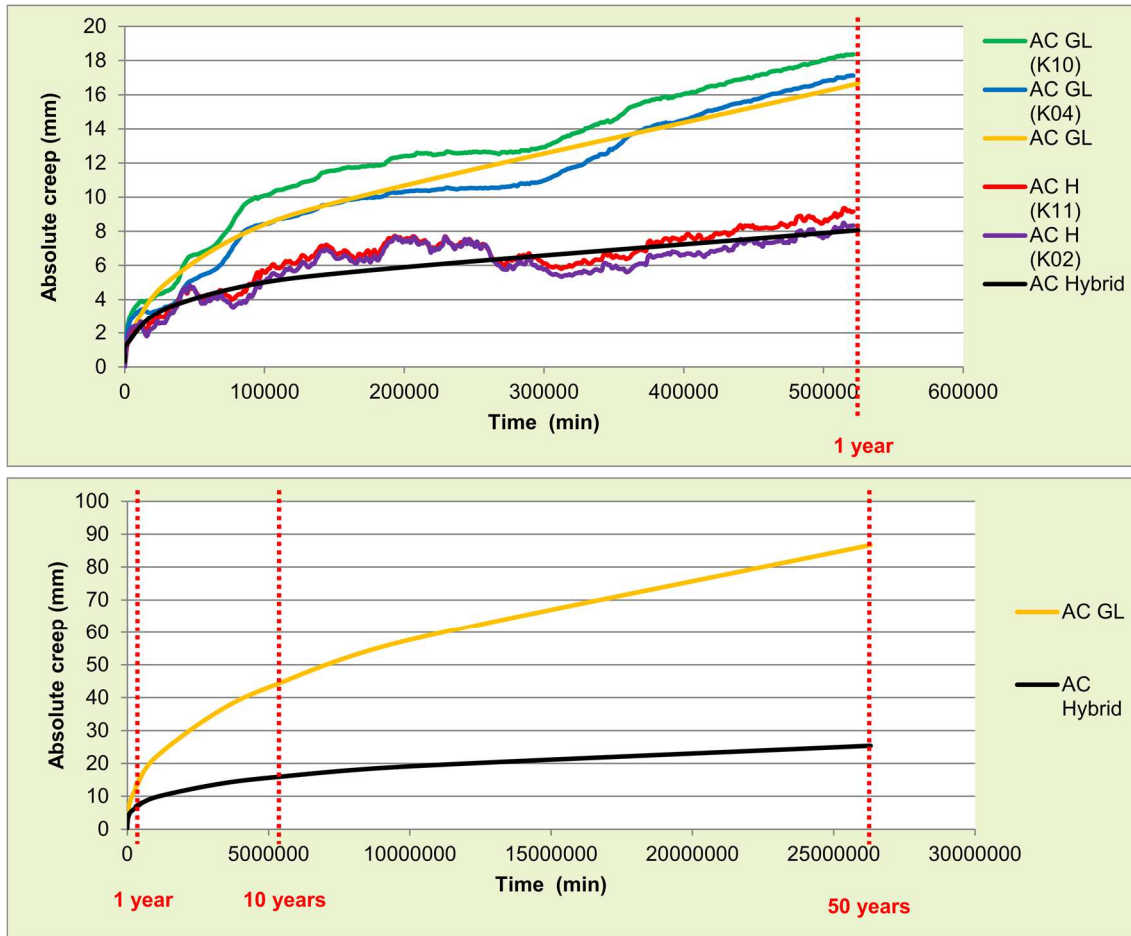


Figure 235: Test results and theory curves of absolute creep for pure glulam and hybrid beams

In the upper part of the *Figure 235* the absolute creep curve for one year obtained from the tests is drawn, and the theory curves determined following the procedure explained are superposed in yellow and black. It can be seen that the fitting of the curve to the real results is quite good.

The complete curve for the calculated absolute creep is represented in the bottom graphic. The calculated numerical values of absolute creep, and the ratio between absolute creep from hybrid to only glulam specimens are shown in *Table 57*.

Year	Absolute creep (mm)		Ratio $w_{\text{hybrid}} / w_{\text{glulam}}$
	Glulam	Hybrid	
1	16,7	8,1	0,48
10	43,9	15,8	0,36
50	86,7	25,4	0,29

Table 57: Estimated absolute creep values for 1, 10 and 50 years

It is found that the absolute creep of a hybrid beam is around 50% of the one experienced by a glulam beam.

After fifty years the absolute creep of a hybrid beam would be around the 30% of the one suffered by an only glulam one.

Studying the problem in terms of relative creep, being the relative creep the ratio from total deformation to initial deformation, the testing results and calculated curves are shown in *Figure 236*.

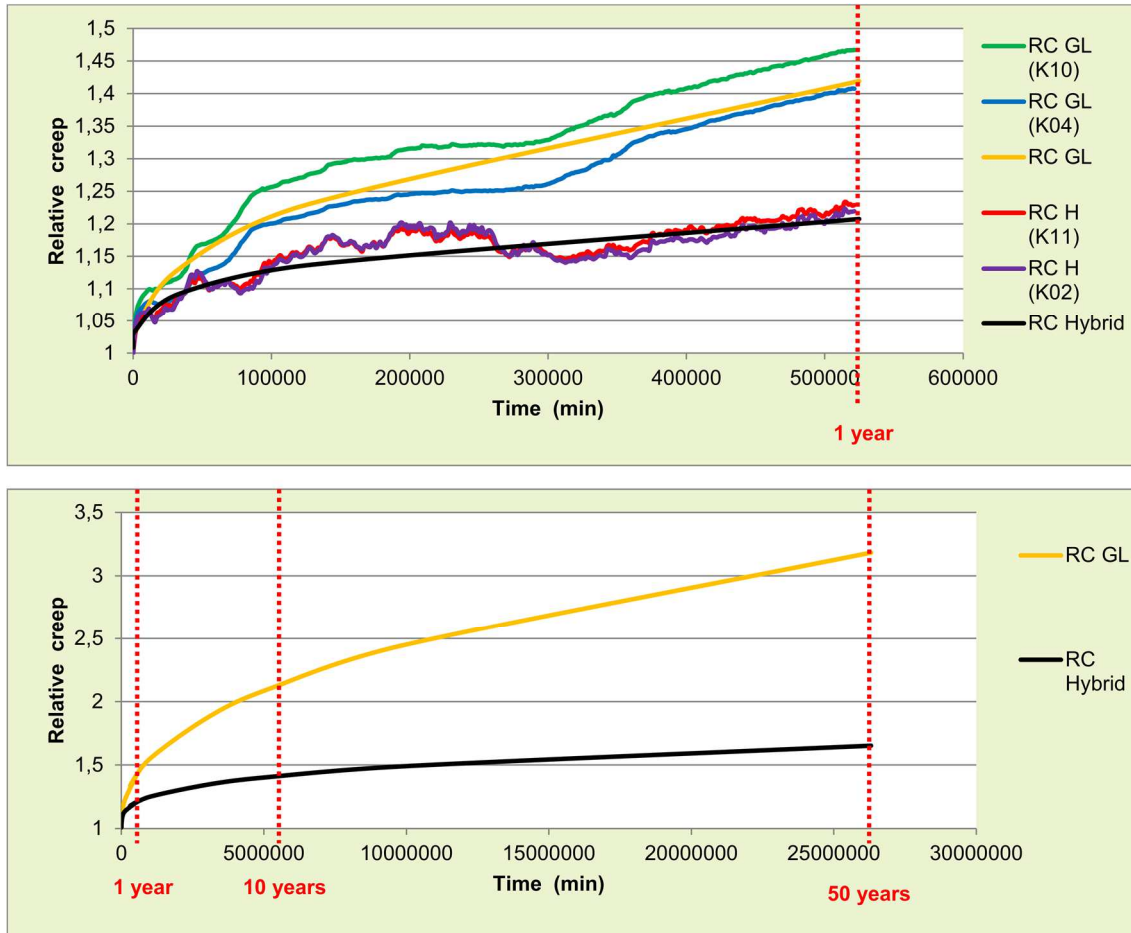


Figure 236: Test results and theory curves of relative creep for pure glulam and hybrid beams

The calculated numerical values of relative creep, and the ratio between absolute creep from hybrid to only glulam specimens are shown in *Table 58*.

Year	Relative creep		Ratio
	Glulam	Hybrid	
			$R_{\text{hybrid}} / R_{\text{glulam}}$
1	1,42	1,21	0,85
10	2,11	1,41	0,67
50	3,18	1,65	0,52

Table 58: Estimated relative creep values for 1, 10 and 50 years

It is found that after one year the relative creep of a hybrid beam is around 85% of the one experienced by a glulam beam. After fifty years this value would be around only 50%.

The comparison of this performance with the calculation procedure proposed in the Eurocode 5 (6), see chapter 4.4.8 and 6.2, it is shown in *Table 59* for the absolute creep values and *Table 60* for the relative creep.

Year	Absolute creep (mm)		Ratio	EC5
	Glulam	Hybrid		$w_{\text{hybrid}} / w_{\text{glulam}}$
50	86,7	25,4	0,29	0,40

Table 59: Comparison of estimated absolute creep following tests and EC5 methods

Year	Relative creep		Ratio	EC5
	Glulam	Hybrid		$w_{\text{hybrid}} / w_{\text{glulam}}$
50	3,18	1,65	0,52	0,40

Table 60: Comparison of estimated relative creep following tests and EC5 methods

The tested beams were calculated following the Eurocode 5 criteria, with the result that the ratio from the final deformation of a hybrid beam to a glulam one has a value of 0,40, considering a coefficient k_{def} of 0,6, both in absolute and relative points of view. It is important to point out that the Eurocode calculation methods only provide the value of the total end deflection, but not the progression of the deformation curve itself.

It can be seen that in comparison with the calculated ratios derived from the test results the Eurocode 5 methods are conservative from an absolute point of view but not conservative in relative terms.

This means that some type of adjustments would be made the Eurocode 5 criteria for the case of hybrid elements.

At this point it is important to emphasize the limits of the research carried out:

- Only two pair of beams were tested, the number of specimens is very reduced.
- Only one initial tension level could be tested, namely 9,95 N/mm²
- The initial deformation of the specimens after loading was very high, around L/100
- The specimens were tested during one year
- The experiment was a “scaled problem test”. A new specific type of hybrid beam was tested, but not the original hybrid beam design itself.

Due to all of this it is not possible to derive strong numerical conclusions from the tests carried out and the results obtained. More detailed research is needed but the behavioural trend was very clear and the advantages of hybrid systems when long-term deflections are relevant could be confirmed. The data and results collected contribute to explain the long term behaviour of hybrid beams and point out a promising performance.

7. FUTURE LINES OF RESEARCH

7.1 JOINT DESIGN, MODELLING AND TESTING

One of the ideas to be explored for the combination of timber and steel in beams is the feasibility of building rigid or semi-rigid joints.

Some approaches on this direction were already made. Several joint solutions were designed, calculated and tested as a continuation of the works gathered in this Doctoral Thesis, being the author part of the researching team. More information can be found in Tavoussi et al (228)

The idea was to use the hybrid cross sections detailed in this Doctoral Thesis without many connection elements. The objectives were the use of timber and steel in a statically equivalent way and not to change the properties of the tested single span beams and the assembly process should remain simple as possible. After considering several concept designs, the system depicted in *Figure 237* was adopted. The hybrid beams are placed inside a stiff knot element and the bending moments are transferred by a “couple of forces” (228).

This connection system was modelled, calculated and tested with two different lever arms of 50 and 80 cm. The connection stiffness obtained from the test results were simulated with spring connections in the calculations models for connecting beams and supports (228).



Figure 237: Example of the moment transmission mechanism for knots between timber-steel hybrid beams and supports (left) and testing of a timber-steel hybrid joint (right) (228)

7.2 FLOOR SYSTEM DESIGN, MODELLING AND TESTING

Timber-steel hybrid beams can be combined with any type of structural floor. But in the particular case of the concrete ones, and due to the possibility of achieving steel-concrete and timber-concrete stiff connections, a new series of structural possibilities and concepts emerge.

Some approaches on that direction were already made. Several timber-steel-concrete slab solutions were designed, calculated and will be tested during the years 2016 and 2017 in the frame of a research project in continuation of the works gathered in this Doctoral Thesis. The author is also part of the researching team. More information can be found in Winter et al (237)



Figure 238: Visualization of a hybrid timber-steel-concrete hybrid ribbed deck prefabricated slab (237)

7.3 FRAME DESIGN, MODELLING AND OPTIMIZATION

After gathering the knowledge and experience needed regarding the structural performance of timber-steel hybrid beams and their combination with semi-rigid joints and concrete structural floors, the next step is the design, analysis and optimization of frames.

A preliminary feasibility study for multi-storey buildings was already carried out (228), although only taking into account the known results for timber-steel beams and semi-rigid joints. The implementation of the structural performance of timber-steel-concrete floors is devised as the next research step.

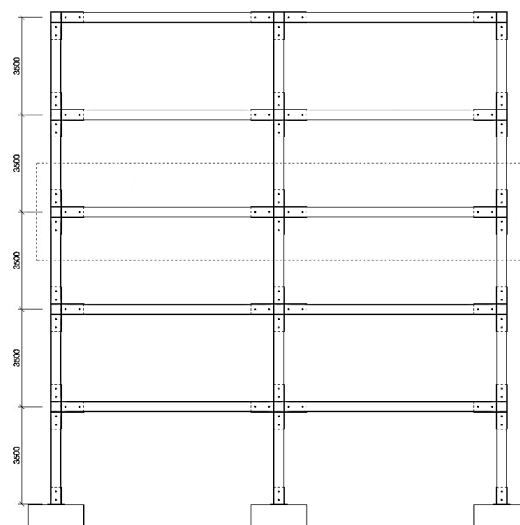


Figure 239: Example of timber-steel hybrid frame system

A three dimensional model of a multi-storey frame construction with a frame spacing of 4,5 metres and two-span beams with six or eight metres per field was analysed according to Eurocode for the case of vertical loads.

Continuous columns were assumed to have the same bending stiffness as the beams and in this case the bending moments at the fixed joints are double as in the middle of the beam. The joint splice was designed to be where the absolute value of the support moment is similar to the moment at the midspan. The implementation in the calculation of the knot elements described in the point 7.1 with springs for the connection between beams and columns made the static calculation of these structures possible.

For an exemplary building located in Vienna a parameter study for different number of storeys was done. Taking into account only the semi-rigid frame performance against horizontal loads, the results showed that frame buildings up to four storeys with a beam span of six metres and a distance between frames of 4,4 metres would be realistic. The reduction of the frame distance to 3 metres would make five storeys possible.

Frame buildings up to five storeys with a beam span of eight metres and a distance between frames of 3,2 metres also seems possible.

The use of additional bracing systems makes possible an increased number of storeys (228).

7.4 ADVANCED FIRE DESIGN, MODELLING AND TESTING

The fire performance of timber-steel structural solutions is a key issue for their practical use. In this work some basic concepts and proofed design rules were introduced, see 4.2.7. The developing of advanced fire design concepts and models and the testing of the solutions adopted are topics of the utmost interest.

Some interesting work was already carried out regarding the performance of timber combined with other materials under fire. The contribution of inner steel elements to the reduction of the charring velocity was studied by Wolfgruber (238) . The contribution of inserted mortar pieces in order to get a self-charring-stop effect was studied by Oka (239) and Oka et al (240).

A group of Japanese researchers studied and tested this concepts, with the assistance of members of the Institute of Structural Design and Timber Engineering of the Technical University of Vienna, and tested the behaviour of similar timber-steel solutions as the one proposed in this work, in a related project designed as a continuation of the works started in this doctoral thesis. More detailed information can be found in Izumi et al (221).

7.5 DETAILED ECONOMICAL EVALUATION AND LIFE CYCLE ASSESSMENT

Although preliminary economical and ecological evaluations were introduced in this work, see 4.7.1, the number of beams tested was limited, as well as the data gathered regarding costs.

A detailed economical evaluation, taking into account the different available technologies, see 4.3.2, as well as the material, fabrication and erection costs is an interesting future research field. The same could be said of a full life cycle evaluation of the solutions proposed.

8. CONCLUSION

8.1 TIMBER-STEEL HYBRID SYSTEMS AS AN ALTERNATIVE FOR TIMBER-BASED MULTI-STOREY BUILDINGS

The technical possibilities for building with timber experienced a big advance in the last years. The development of new timber and timber-based products together with growing environmental concerns is pushing the research and study on timber construction.

One objective is the construction of multi-storey buildings in urban environment. Urban timber and timber-based building proposals are now possible, as many research projects and built examples illustrate.

Most projects propose the use combined used of timber elements with other materials, steel and/or concrete, for elements with specific structural purposes difficult or costly to fulfil with an only-timber solution.

Some examples are the “Life Cycle Tower” project and buildings (241) combining timber beams with concrete floors and edge concrete beams. In “The Case for Tall Wood Buildings” (242) cross laminated plates for floors and walls are combined with steel beams for getting ductility. The “Timber Tower research Project” (243) studied a solution combining cross-laminated timber floors, glulam columns and concrete beams. The tower “HoHo-Wien” (244) combines glulam columns, timber-concrete floors and edge concrete beams.

In all these cases elements made from different materials are combined, but, with the exception of the already well-known timber-concrete floor solution, the materials are not combined in the elements themselves.

Timber-steel elements in general and beams in particular are presented as an alternative for developing a holistic construction concept making the most of the properties from both materials starting at the structural element level. Its application and optimization for their use in multi-storey architectural solutions is the final objective and main application field.

Therefore the conditions for the application of timber-steel structural solutions from an architectural design point of view are one of the main research fields to be studied in depth in the future.



Figure 240: Timber-based multi-storey projects. From left to right: 8+(245), Life Cycle Tower(241), The Case for Tall Wood Buildings (242), Timber Tower Research Project (243), HoHo Wien (244)

LIST OF REFERENCES

1. **Jahan, Selim (Ed.).** *Human Development Report 2015*. New York : United Nations Development Programme, 2015.
2. **Schmidt-Bleek, Friedrich.** *MIPS and Ecological Rucksacks in Designing the Future*. EcoDesign 2001 : 2nd International Symposium on Environmentally Conscious design and Inverse Manufacturing, Tokyo, 2001.
3. —. *The Fossil Makers*. Basel : Birkhauser, 1993.
4. —. *Grüne Lügen*. München : Ludwig Verlag, 2014.
5. **Glos, P.** *Streght grading. Chapter A6 from "STEP 1 - Timber Engineering"*. The Netherlands : Centrum Hout, 1995.
6. **EN1995-1-1:2004.** *Eurocode 5: Design of timber structures - Part 1-1: General - Common rules and rules for buildings*. 2004.
7. **EN1993-1-1:2005.** *Eurocode 3: Design of steel structures - Part 1-1: General rules and rules for buildings*. 2005.
8. **André, Alan.** *Fibres for Strengthenign of Timber Structures (PhD Thesis)*. Lulea : Lulea University of Technology, 2006.
9. **EN13501-1:2007.** *Fire classification of construction products and building elements - Part 1: Classification using data from reaction to tests*. 2007.
10. **Merriam-Webster.** "Malleable" - Merriam-Webster Online Dictionary. Access 21 September 2016.
11. **Kelsey, John (Ed.).** *Fine Wood Working on Bending Wood*. Newtown : The Taunton Press, 1985.
12. **Dinwoodie, J. M.** *Timber: Its nature and behaviour*. New York : E & FN Spon, 2000.
13. **EN338:2009.** *Structural timber - Strength classes*. 2009.
14. **EN14080:2013.** *Timber structures - Glued laminated timber and glued solid timber- Requirements*. 2013.
15. **Block, Philippe, Gengnagel, Christoph and Peters, Stefan.** *Faustformel. Tragwerksentwurf*. München : DVA, 2013.
16. **EN1993-1-2:2005.** *Eurocode 3: Design of steel structures - Part 1-2: General rules - Structural fire design*. 2005.
17. **ISO834:1999.** *Norm ISO 834. Fire-Resistance Tests - Elements of building construction - Part 1. General Requirements*. 1999.
18. **EN1995-1-2:2004.** *Eurocode 5: Design of timber structures - Part 1-2: General - Structural fire design*. 2004.

19. **Ritter, Michael A.** *Timber Bridges. Design, Construction, Inspection and Maintenance.* Washington : U.S. Government, 1990.
20. **Forest Products Laboratory.** *Wood Handbook. Wood as an Engineering Material.* Madison : U.S. Department of Agriculture, Forest service, Forest Products Laboratory, 2010.
21. **EN1992-1-1:2004.** *Eurocode 2: design of concrete structures - Part 1-1: General rules and rules for buidings.* 2004.
22. **Mettem, Christopher.** *Breakthroughs in timber engineering.* London : The Structural Engineer, 2 September, 2003.
23. **OI3-Indikator.** *Leitfaden zur Berechnung von Ökokennzahlen für Gebäude. Version 3.1.* Wien : IBO - Österreichisches Institut für Bauen und Ökologie GmbH, 2016.
24. **IBO.** *IBO - Richtwerte für Baumaterialien, Stand: Juni 2013.* 2013.
25. **SteelBenchmaker(TM).** *Price history - Tables and Charts - SteelBenchmaker Report#250.* September 12, 2016.
26. **ÖSTAT.** *Evolution of prices "Sägerundholz, Fi/Ta, B, Stärkeklasse 2b".* file:///C:/Users/Felipe/Downloads/Preisentwicklung.pdf : s.n., Accesed 12.09.2016.
27. **Teischinger, Alfred.** *Wechselwirksam - Holz und Feuchtigkeit.* Wien : In "Zuschnitt 22: Wasserkontakt", 2006.
28. **Jeska, Simone and Saleh Pascha, Khaled.** *Neue Holzbau Technologien. Materialien, Konstruktionen, Bautechnik, Projekte.* Basel : Birkhäuser, 2015.
29. **Boomsliter, G.P.** *Timber beams reinforced with spiral drive dowels.* Morgantown : West Virginia University Bulletin. October, 1948.
30. **Krueger, G.P.** *Ultimate-strength design of reinforced timber: State of the art.* s.l. : Wood Science 6 (2), 1973.
31. **Bulleit, W.M.** *Reinforcement of wood materials: a review.* Wood and Fiber Science : 16 (3): 391-397, 1984.
32. **Isoda, Hiroshi, et al.** *Case Study of Combination Ways of Steel and Timber in Japanese Buildings.* Whistler : World Conference on Timber Engineering - WCTE 2000, 2000.
33. **Borgin, K.B., Loedolff, G.F. and Saunders, C.R.** *Laminated wood beams reinforced with steel strips.* s.l. : ASCE Journal Structural Division 94 (ST7), 1968.
34. **Krueger, G. P. and Eddy Jr., F.M.** *Ultimate strenght design of reinforced timber: Moment rotation characteristics.* s.l. : Wood Science 6 (4), 1974.
35. **Krueger, G.P. and Sandberg, L.B.** *Ultimate strenght design of reinforced timber. Evaluation of design parameters.* s.l. : Wood Science 6 (4), 1974.

36. **Kobetz, R. W. and Krueger, G.P.** *Ultimate-strength design of reinforced timber: Biaxial stress failure criteria*. s.l. : Wood Science 8 (4), 1976.
37. **Uzielli, G.L.** *Instandsetzung von Holzkonstruktionen - Reparatur und Verstärkung*. STEP 2. Bauteile. Konstruktionen. Details : Fachverlag Holz, 1995.
38. **Hansson, Simon and Karlsson, Kristoffer.** *Moisture-related creep of reinforced timber. Theoretical studies and laboratory tests*. Göteborg : Chalmers University of Technology. Master's Thesis 2007:123, 2007.
39. **Kliger, Robert, Johansson, Marie and Crocetti, Roberto.** *Strengthening timber with CFRP or steel plates - short and long-term performance*. Miyazaki : World Conference on Timber Engineering - WCTE 2008, 2008.
40. **Kliger, Robert I. and André, Alann.** *Enhanced timber properties with FRP composites*. Nicosia : COST Action FP1004 - Innovative Timber Composites - Improving wood with other materials, 2013.
41. **Borri, A. and Corradi, M.** *Strengthening of timber beams with high strength steel cords*. Elsevier : Composites: Part B 42 (2011) 1480-1491, 2011.
42. **Dorey, A.B. and Cheng, J.J.R.** *Development of Composite Glued Laminated Timber*. Edmonton : Minister of Supply and Services Canada, 1996.
43. **Sakamoto, Isao, et al.** *Final Report of a Research and Development Project on Timber-based Hybrid Building Structures*. Lahti : World Conference on Timber Engineering - WCTE 2004, 2004.
44. **González Bravo, Carlos.** *Recuperación de la capacidad mecánica en piezas de madera solicitadas a flexión en estructuras tradicionales operando por la cara superior mediante refuerzos y prótesis metálicas*. Madrid : Escuela Técnica Superior de Arquitectura de Madrid, Tesis Doctoral, 2007.
45. **González-Bravo, Carlos, Arriaga-Martitegui, Francisco and Díez-Barra, Rafael.** *Bending reinforcement of wooden beams with steel cross-sections*. Miyazaki : World Conference on Timber Engineering -WCTE 2008, 2008.
46. **González-Bravo, Carlos.** *Recuperación de forjados de madera*. Madrid : Cercha No. 101, April, 2009.
47. **González-Bravo, Carlos, et al.** *Refuerzo de vigas de madera mediante perfiles metálicos situados en la cara superior*. Madrid : Materiales de la Construcción Vol. 60, 298, 123-135, 2010.
48. **González-Bravo, C., et al.** *Prótesis metálicas para la reparación de cabezas de vigas de madera degradadas*. Madrid : Informes de la Construcción Vol. 63, 521, 37-45, 2011.
49. **Granholm, H.** *Reinforced timber*. Gothenburg : Transactions of Chalmers University of Technology, 1954.

50. **Mark, R.** *Wood-aluminium beams within and beyond the elastic range. Part I: Rectangular sections.* Forest Products Journal : 11 (10): 477-484, 1961.
51. **Isoda, H., et al.** *A new R/D national programm on timber structures in B.R.I, Japan-Research and development on hybrid timber structural system.* Whistler : World Conference on Timber Engineering - WCTE 2000, 2000.
52. **Nakajima, Shiro, et al.** *Creep Performance of hybrid the Timber Beams.* Lahti : World Conference on Timber Engineering - WCTE 2004, 2004.
53. **Kirlin, C.P.** *Experimental and finite-element analysis of stress distributions near the end of reinforcement in partially reinforced glulam.* Oregon : Oregon State University. Master Thesis, 1996.
54. **Shchuko, W.J.** *Investigation on ultimate strength of reinforced wooden beam.* Stroitelstwo and Architektura : No. 2: 24-28, 1969.
55. **Anonymous.** *Gluelam timber beams stiffened with steel.* London : Engineering 198 (5132): 260, 1964.
56. **Lantos, G.** *Reinforced and post-tensioned glue-laminated beams under development at TRADA labs.* London : Civil Engineering and Public Works Review 59 (690), 1964.
57. —. *Test results on mild steel reinforced glulam timber beams.* London : Civil Engineering, November, 1964.
58. **Lantos, G. and Harvey, R.** *Tests on flitch and plank beams.* London : Timber Research and Development Association, 1964.
59. **Lantos, G. and Wellner, G.L.** *Steel reinforced plywood-web box beams.* London : Timber Research and Development Association, 1966.
60. **Dziuba, T.** *Bearing capacity of reinforced wooden beams.* Poznan : Agricultural University of Poznan, 1980.
61. —. *The ultimate strength of wooden beams with tension reinforcement.* Holzforschung und Holzverwertung : Vol. 37 No. 6: 115-119, 1985.
62. **Candowicz, R. and Dziuba, T.** *Ultimate strength of wooden beams with tension reinforcement as a function of random material properties.* Berlin : International Council for Building Research Studies and Documentation - W18A - Timber Structures, 1989.
63. **Bulleit, W.M., Bogue Sandberg, L. and Woods, G.J.** *Steel-Reinforced Glued Laminated Timber.* Journal of Structural Engineering : Vol. 115, No. 2, February, 1989.
64. **Fabris, Alessandro.** *Verstärkung der Biegezugzone von Holzträgern mittels Stahlarmierung.* Tragende Verbundkonstruktionen mit Holz. Zürich : SAH, 1999.

65. **Jorissen, A. and Fragiaco, M.** *Ductility in Timber Structures*. Nelson : International Council for Research and Innovation in Building and Construction - W18 - Timber Structures, 2010.
66. **Lu, Weidong, et al.** *Experimental Study on Bending Creep behaviour of Reinforced Glulam Beam*. Auckland : World Conference on Timber Engineering - WCTE 2012, 2012.
67. **Kaestner, Martin, et al.** *High-Tech timber beam - A high-performance hybrid beam system made of composites and timber*. Quebec City : World Conference on Timber Engineering - WCTE 2014, 2014.
68. **Alam, P.** *The reinforcement of timber for structural applications and repair*. Bath : University of Bath. Doctoral Thesis, 2004.
69. **Sliker, A.** *Reinforced wood laminated beams*. Forest Products Journal : 12 (2): 91-96, 1962.
70. **Lantos, G.** *The flexural behaviour of steel reinforced laminated timber beams*. Wood Science : 2 (3): 136-143, 1970.
71. **Coleman, G.E. and Hurst, H.T.** *Timber structures reinforced with light gage steel*. Forest Products Journal : 24 (7): 45-53, 1974.
72. **Gardner, G.P.** *A Reinforced Glued Laminated Timber System*. London : International TimberEngineering Conference, 3.218-3.225, 1991.
73. **Oiger, K.** *Experimental investigation and analysis of reinforced glulam beams*. Vancouver : International Council for Building Research Studies and Documentation - W18 - Timber Structures, 1997.
74. **Schober, K.U., et al.** *Timber with passive reinforcement*. COST E34 - WG1 : Bonding on Site, 2008.
75. **Shioya, S., et al.** *An innovative hybrid timber structure in Japan: performance of column and beams*. Vienna : World Conference on Timber Engineering - WCTE 2016, 2016.
76. **Uchimura, K., Shioya, S. and Hira, T.** *An innovative hybrid timber structure in Japan: experiments on the long term behaviour in beam*. Vienna : World Conference on Timber Engineering - WCTE 2016, 2016.
77. **Kusumoto, S., et al.** *An innovative hybrid timber structure in Japan: beam-to-beam moment resisting connection*. Vienna : World Conference on Timber Engineering - WCTE 2016, 2016.
78. **Yagi, H., Shioya, S. and Tomiyoshi, E.** *Innovative hybrid timber structures in Japan: bending behaviour of T-shaped CLT-to-hybrid timber composite beam*. Vienna : World Conference on Timber Engineering - WCTE 2016, 2016.
79. **Subic, B., Fajdiga, G. and Lopatic, J.** *Bending of wooden based hybrid beams: experimental analysis*. Vienna : World Conference on Timber Engineering - WCTE 2016, 2016.

80. **Nielsen, J.** *Analysis of timber reinforced with punched metal plate fasteners*. Graz : International Council for Research and Innovation in Building and Construction - W18 - Timber Structures, 1999.
81. **Tanaka, H., Ono, T. and Idota, H.** *Evaluation of Buckling Strength of Hybrid Timber Columns reinforced with Steel Plates and carbon Fiber Sheets*. Portland : World Conference on Timber Engineering - WCTE, 2006.
82. **Dolby, C.M.** *Wooden laminated beams joined with nail-plates*. Tokyo : International Timber Engineering Conference, 1990.
83. **Echavarría, C., Echavarría, B. and Cañola, H.** *Bamboo reinforced glulam beams: an alternative to punched metal plate, GRP and CFRP reinforced glulam beams*. Quebec City : World Conference on Timber Engineering - WCTE, 2014.
84. **Steurer, A.** *Holzkonstruktionen mit Stahl- und Kunststoffverstärkung*. Tragende Verbundkonstruktionen mit Holz. Zürich : SAH, 1999.
85. **Kliger, R., et al.** *Strengthening glulam beams with steel or CFRP plates*. Asia-Pacific Conference on FRP in Structures (APFIS) : International Institute for FRP in Construction, 2007.
86. **Jacob, J. and Garzon Barragán, O.** *Flexural Strengthening of Glued Laminated Timber Beams with Steel and Carbon Fiber Reinforced Polymers*. Göteborg : Chalmers University of Technology. Master's Thesis 2007:28, 2007.
87. **De Melo Moura, J.D., et al.** *Metal reinforcement for pine glulam beams as a strategy to enhance mechanical behaviour*. Miyazaki : World Conference on Timber Engineering - WCTE, 2008.
88. **Jones, R.** *Upgrading of timber members in historic buildings*. Journal of the Institute of Wood Science : Vol. 14 No.4: 192-193, 1997.
89. **Fontana, M.** *Einführung Verbundkonstruktionen mit Holz*. Tragende Verbundkonstruktionen mit Holz. Zürich : SAH, 1999.
90. **Robinson, W.J.** *Space joists in irish timber*. Dublin : International Council for Building Research Studies and Documentation - W18A - Timber Structures, 1987.
91. **Guan, Z. and Gendall, J.** *Finite element modelling of buckling behaviour of steel webbed timber joists*. Miyazaki : World Conference on Timber Engineering - WCTE, 2008.
92. **Nail Web.** *Viga mixta acero-madera*. 2001.
93. **Tilling Timber.** *TecBeam Design Guide*. 2013.
94. **MiTek Holdings, Inc.** *Posi-Joist. Positively engineered for a better floor*. 2013.
95. **Hoyle, R.J.** *Steel-reinforced wood beam design*. Forest Products Journal : Vol. 25 No. 4: 17-23, 1975.

96. **Usuki, S., et al.** *A new timber beam bridge with an orthotropic steel deck*. Whistler : World Conference on Timber Engineering - WCTE, 2000.
97. **Usuki, S., et al.** *Ultimate strength of glulam sandwich beam reinforced by inserted steel ribs*. Proceedings of the 57th JSCE Annual Meeting : I-366, 2002.
98. **Usuki, S., Gotou, T. and Kiss, L.** *Bending capacity of glued-laminated timber stiffened with inserted steel plate*. Journal of Structural Engineering, JSCE : Vol. 49 A: 889-894, 2003.
99. **Kiss, L., Usuki, S. and Sasaki, T.** *Experimental and analytical study on steel deck-glulam beam hybrid bridge behavior*. Journal of Structural Engineering, JSCE : Vol. 51A: 1211-1218, 2005.
100. **Kiss, L., et al.** *Performance of glulam beam-orthotropic steel deck hybrid bridge structure*. Portland : World Conference on Timber Engineering - WCTE, 2006.
101. **Honda, H., Sasaki, T. and Usuki, S.** *Structural Performance of Hybrid Timber Truss highway Bridge*. Portland : World Conference on Timber Engineering, 2006.
102. **Kiss, L., et al.** *Failure test and finite element analysis of timber-steel hybrid bridge*. Miyazaki : World Conference on Timber Engineering - WCTE, 2008.
103. **Gotou, H., et al.** *Estimation of shear modulus by FEM bending simulation of steel-plate-inserted glulam wood beams*. Miyazaki : World Conference on Timber Engineering - WCTE, 2008.
104. **Chida, T., et al.** *Proposal of a square steel tube-timber hybrid bridge and the technologies used for it*. Trentino : World Conference on Timber Engineering - WCTE, 2010.
105. **Alam, P., Ansell, M.P. and Smedley, D.** *Reinforcement of LVL beams with bonded-in plates and rods - Effect on placement of steel and FRP reinforcements on beam strength and stiffness*. Edinburgh : International Council for Research and Innovation in Building and Construction - W18 - Timber Structures, 2004.
106. **Alam, P., Ansell, M. and Smedley, Dave.** *Effects of reinforcement geometry on Strength and Stiffness in Adhesively Bonded Steel-Timber Flexural Beams*. Buildings : 2, 231-244, 2012.
107. **Lawson, R.M., et al.** *Developments of Cold-Formed Steel Sections in Composite Applications for Residential Buildings*. Advances in Structural Engineering : Vol. 11 No. 6, 2008.
108. **Negrão, J., et al.** *Resistência ao fogo de glulam com chapa de reforço interna*. Coimbra : 1º Congresso Ibero-LatinoAmericano da Madeira na Construção, 2011.
109. **Wenighofer, G., Mauritz, R. and Neuhauser, A.** *Novel high performance timber hybrid beam*. Vienna : World Conference on Timber Engineering - WCTE, 2016.
110. **Kumar, V.K., Stern, E.G. and Szabp, T.** *Built-up Composite Beams*. V.P.I. Research Division Wood Research and Construction Laboratory : Report No. 110, 1972.
111. **Stern, E.G. and Kumar, V.K.** *Flitch beams*. Forest Products Journal : 23 (5): 40-47, 1973.

112. **National Association of Home Builders.** *Flitch Plate and Steel I-Beams*. Washington : NAHB, 1981.
113. **DeStefano, J. and MacDonald, J.** *Design guides for flitch plate beams and lally columns*. Connecticut : Structural Engineers Coalition, 1997.
114. **DeStefano, J.** *Flitch Plate Beams. Design Guide*. in Structure Magazine : June, 2007.
115. **Ban, S., Yoshida, A. and Motohasi, S.** *Nagano Olympic Memorial Arena: design and construction*. IABSE reports : Band 79, 1998.
116. **Hart, A. and Fast, P.A.** *Material combinations incorporating wood - recent west coast examples*. Whistler : World Conference on Timber Engineering, 2000.
117. **Alam, P. and Ansell, M.** *The Effects of Varying Nailing density upon the Flexural Properties of Flitch Beams*. Journal of Civil Engineering Research : 2 (1): 7-13, 2012.
118. **Koshihara, M., Isoda, H. and Yusa, S.** *The design and installation of a five-story new timber building in Japan*. 2005.
119. **Isoda, H., Kawai, N. and Koshihara, M.** *Case Study of Combination Ways of Timber and Steel in Japanese Buildings*. Trentino : World Conference on Timber Engineering - WCTE, 2010.
120. **Koshihara, M.** *Contemporary mid-rise timber buildings in Japan 2013*. Quebec City : World Conference on Timber Engineering, 2014.
121. **TRADA.** *Timber frame housing: UK Structural recommendations*. Great Britain : TRADA Technology, 2006.
122. **Gotou, H., et al.** *New type hybrid bridges utilizing stress-laminated decks and steel members*. Auckland : World Conference on Timber Engineering - WCTE, 2012.
123. **MiTek.** *Gang-nail Flitch Beam Manual*. New Zealand : MiTek Holdings, Inc., 2007.
124. **Pryda.** *Pryda Flitch Beam Specification Guide and Design Manual*. New Zealand : Pryda New Zealand, 2013.
125. **Radford, D.W., et al.** *Composite repair of timber structures*. Construction and Building Materials : Vol. 16: 417-425, 2002.
126. **Mark, R.** *Wood-aluminium beams within and beyond the elastic range. Part II: Trapezoidal sections*. Forest Products Journal : 13 (11): 508-516, 1963.
127. **Tharmabala, T. and Bakht, B.** *Steel-Wood Composite Bridges*. Ontario : The Research and Development Branch - Ontario Ministry of Transportation and Communications, 1986.
128. **Bakht, B. and Tharmabala, T.** *Steel-Wood Composite Bridges and their Static Load response*. Canadian Journal of Civil Engineering : 14 (2): 163-170, 1987.
129. **Taylor, R.J. and Ritter, M.A.** *Development of longer span wood bridges*. Toronto : Proceedings of the 3rd International Conference on Short and Medium Span Bridges, 1990.

130. **Krisciunas, R.** *Ontario's Experience With Composite Wood/Steel Bridges*. National Conference on Wood Transportation Structures : U.S. Department of Agriculture, Forest Service, Forest Products Laboratory, 1996.
131. **Ma, Z. and He, M.** *Experimental analysis of timber diaphragm's capacity on transferring horizontal loads in timber-steel hybrid structure*. Auckland : World Conference on Timber Engineering - WCTE, 2012.
132. **He, M., et al.** *Research and application of timber-steel hybrid structures*. Quebec City : World Conference on Timber Engineering - WCTE, 2014.
133. **Loss, C., Piazza, M. and Zandonini, R.** *Experimental tests of cross-laminated timber floors to be used in timber-steel hybrid structures*. Quebec City : World Conference on Timber Engineering - WCTE, 2014.
134. —. *Innovative construction system for sustainable buildings*. Geneva : IABSE Conference - Structural Engineering: Providing Solutions to Global Challenges, 2015.
135. **Hassanieh, A., Valipour, H.R. and Bradford, M.A.** *Experimental and numerical study of steel-timber composite (STC) beams*. Journal of Constructional Steel Research : 122 (2016) 367-378, 2016.
136. **Hassanieh, A., Valipour, H. and Bradford, M.** *Development of timber-steel composite system for large scale construction*. Vienna : World Conference on Timber Engineering - WCTE, 2016.
137. **Keipour, N., Valipour, H.R. and Bradford, M.A.** *Steel-timber versus steel-concrete composite floors: a numerical study*. Vienna : World Conference on Timber Engineering, 2016.
138. **Zimmer, S.E. and Augustin, M.** *Timber-steel-composite - A possibility for hybrid structures of long span timber floors*. Vienna : World Conference on Timber Engineering - WCTE, 2016.
139. **Lim, J., et al.** *Performance evaluation of hybrid beam consisted of timber and steel for guardrail*. Trentino : World Conference on Timber Engineering - WCTE, 2010.
140. **Ito, T., Kambe, W. and Kondo, S.** *An experimental study on resistant mechanism of plywood panel - steel composite timber*. Auckland : World Conference on Timber Engineering - WCTE, 2012.
141. **Kimura, M., et al.** *Experimental study on the behaviour of LVL-steel composite beams*. Tokyo : International Timber Engineering Conference, 1990.
142. **Yamaguchi, N., et al.** *Constructions and Researches after the Project of Developing Hybrid Timber Buildings*. Miyazaki : World Conference on Timber Engineering - WCTE, 2008.
143. **Izumi, B.** *Development of beam elements composed of timber and steel for medium-rise office buildings considering fire safety*. Vienna : Vienna University of Technology - Master Thesis, 2008.

144. **Izumi, B., et al.** *Development of frame structures for multistory buildings with partial bending stiffness using timber steel hybrid members with improved fire resistance.* Miyazaki : World Conference on Timber Engineering -WCTE, 2008.
145. **Peterson, J.L.** *Wood beams prestressed with bonded tension elements.* s.l. : ASCE Journal Structural Division 91 (ST1), 1965.
146. **Turkovsky, S.B. and Lukyanov, E.I.** *Use of Glued-I Bars for Reinforcement of Wood Structures.* London : International Timber Engineering Conference: 3.212-3.217, 1991.
147. **Pletz, E. and de Melo Moura, J.D.** *Experimental evaluation of prestressed timber beams.*
148. **Peterson, J.** *Wood beams prestressed with bonded tension elements.* ASCE Journal of the Structural Division : Vol. 91 No. ST1: 103-119, 1965.
149. **Bohannon, B.** *Prestressing wood members.* Forest Products Journal : 12 (12): 596-602, 1962.
150. —. *Prestressed laminated wood beams.* Madison : U.S. department of Agriculture, Forest Products Laboratory, Forest service, 1964.
151. —. *Time-dependent characteristics of prestressed wood beams.* Madison : U.S. Department of Agriculture, Forest Service, Forest Products Laboratory, 1974.
152. **Mischler, A.** *Verstärkung von Holz/Beton-Verbundträgern mittels vorgespannter Armierung.* Tragende Verbundkonstruktionen mit Holz. Zürich : SAH, 1999.
153. **Negrao, J., Brunner, M. and Lehmann, M.** *Pre-stressing of timber.* COST E34 WG1 : Bonding on Site, 2008.
154. **Negrao, J.** *Prestressing systems for timber beams.* Auckland : World Conference on Timber Engineering - WCTE, 2012.
155. **Sigrist, C. and Lehmann, M.** *Development of a cross laminated, post tensioned bridge deck.* Auckland : World Conference on Timber Engineering - WCTE, 2012.
156. **Leyder, C., et al.** *Field testing on innovative timber structures.* Quebec City : World Conference on Timber Engineering - WCTE, 2014.
157. **Wanniger, F., Frangi, A. and Fragiacomio, M.** *Post-tensioned timber connections, experimental analysis of the long term behavior.* Quebec City : World Conference on Timber Engineering - WCTE, 2014.
158. **Leyder, C.** *ETH house of Natural Resources.* Munich : PhD Colloquium Presentation, 2015.
159. **Wanniger, F.** *Post-tensioned timber frame structures.* Zurich : ETH Zurich - Doctoral Thesis, 2015.
160. **Ogrizovic, J., Wanniger, F. and Frangi, A.** *Post-tensioned timber frames at the ETH house of natural resources.* Vienna : World Conference on Timber Engineering - WCTE, 2016.

161. **Leyder, C., Frangi, A. and Chatzi, E.** *Modal vibration testing of an innovative timber structure*. Vienna : World Conference on Timber Engineering - WCTE, 2016.
162. **Estévez-Cimadevila, J., et al.** *New system of self-tensioning for long-span wooden structural floors*. Vienna : World Conference on Timber Engineering - WCTE, 2016.
163. **Pampanin, S., et al.** *Code provisions for seismic design of multi-storey post-tensioned timber buildings*. Florence : International Council for Research and Innovation in Building and Construction - W18 - Timber Structures, 2006.
164. **Buchanan, A., et al.** *Multi-Storey Prestressed Timber Buildings in New Zealand*. Structural Engineering International : 2, 2008.
165. **Fragiacomo, M. and Davies, M.** *Evaluation of the prestressing losses in timber members prestressed with unbonded tendons*. St. Andrews : International Council for Research and Innovation in Building and Construction - W18 - Timber Structures, 2008.
166. **Davies, M. and Fragiaco, M.** *Long-Term Behaviour of Laminated Veneer Lumber Members Prestressed with Unbonded Tendons*. Miyazaki : World Conference on Timber Engineering - WCTE, 2008.
167. **Iqbal, A., Pampanin, S. and Buchanan, A.** *Seismic Behaviour of Prestressed Timber Columns under Bi-directional Loading*. Miyazaki : World Conference on Timber Engineering, 2008.
168. **Smith, T., et al.** *Design and Construction of Prestressed Timber Buildings for Seismic Areas*. Miyazaki : World Conference on Timber Engineering - WCTE, 2008.
169. **Carradine, D.M., Newcombe, M.P. and Buchanan, A.H.** *Using screws for structural applications in laminated veneer lumber*. Dübendorf - Zürich : International Council for Research and Innovation in Building and Construction - W18 - Timber Structures, 2009.
170. **Newcombe, M.P., et al.** *Simplified design of post-tensioned timber frames*. Nelson : International Council for Research and Innovation in Building and Construction - W18 - Timber Structures, 2010.
171. **van Beerschoten, W., et al.** *The stiffness of beam to column connections in post-tensioned timber frames*. Alghero : International Council for Research and Innovation in Building and Construction - W18 - Timber Structures, 2011.
172. **van Beerschoten, W., et al.** *Failure Criteria for Post-Tensioned Timber Beams*. Växjö : International Council for Research and Innovation in Building and Construction - W18 - Timber Structures, 2012.
173. **van Beerschoten, W., et al.** *Design procedure for long-span post-tensioned timber frames under gravity loading*. Auckland : World Conference on Timber Engineering - WCTE, 2012.
174. **Carradine, D., et al.** *Study of a high performance timber buildings: design, construction and performance*. Auckland : World Conference on Timber Engineering - WCTE, 2012.

175. **Curtain, B., et al.** *Design of Carterton Event Centre: an example of innovative collaboration between architecture and timber engineering*. Auckland : World Conference on Timber Engineering - WCTE, 2012.
176. **Holden, T., et al.** *Innovative structural design of a three storey post-tensioned timber building*. Auckland : World Conference on Timber Engineering - WCTE, 2012.
177. **John, S. and Buchanan, A.H.** *Cost and construction time for a 3-storey post-tensioned timber building compared with concrete and steel buildings*. Auckland : World Conference on Timber Engineering - WCTE, 2012.
178. **Morris, H., Wang, M. and Zhu, X.** *Deformations and loads in an LVL building with 3-storey post-tensioned shear walls*. Auckland : World Conference on Timber Engineering - WCTE, 2012.
179. **Newcombe, M., Pampanin, S. and Buchanan, A.H.** *Governing criteria for the lateral force design of post-tensioned timber buildings*. Auckland : World Conference on Timber Engineering - WCTE, 2012.
180. **Ponzo, F.C., et al.** *Shaking table test of a multistorey post-tensioned glulam building: design and construction*. Auckland : World Conference on Timber Engineering, 2012.
181. **Smith, T., et al.** *Seismic performance of a post-tensioned glue laminated beam to column joint: experimental and numerical results*. Auckland : World Conference on Timber Engineering - WCTE, 2012.
182. **Spellman, P., et al.** *Full-scale fire tests of post-tensioned timber beams*. Auckland : World Conference on Timber Engineering - WCTE, 2012.
183. **Armstrong, T., et al.** *Seismic detailing of post-tensioned timber frames*. Quebec City : World Conference on Timber Engineering - WCTE, 2014.
184. **Buchanan, A.** *Post-tensioned Multi-storey Timber Buildings*. Vancouver : International Wood Symposium, 2014.
185. **Ponzo, F.C., et al.** *Shaking table testing of a multi-storey post-tensioned glulam building: preliminary experimental results*. Quebec City : World Conference on Timber Engineering, 2014.
186. **Sarti, F., Palermo, A. and Pampanin, S.** *Design and testing of post-tensioned timber wall systems*. Quebec City : World Conference on Timber Engineering - WCTE, 2014.
187. **Smith, T., et al.** *Shaking table test of a multi-storey post-tensioned glulam building: numerical modelling*. Quebec City : World Conference on Timber Engineering - WCTE, 2014.
188. **Smith, T., et al.** *Long-term dynamic characteristics of pres-lam structures*. Vienna : World Conference on Timber Engineering - WCTE, 2016.
189. **Granello, G., et al.** *Post-Tensioned LVL Beams: Experimental Results and Numerical Modelling*. Vienna : World Conference on Timber Engineering - WCTE, 2016.

190. **Mostafavi, Mohsen (Ed.).** *Structure as Space. Engineering and Architecture in the Works of Jürg Conzett and His Partners.* London : AA Publications, 2006.
191. **Wacker, J. and Smith, M.** *Standard Plans for Timber Bridge Superstructures.* Madison : U.S. Department of Agriculture, Forest Service, Forest Products Laboratory, 2001.
192. **Crews, K. and Bakoss, S.** *Fundamental Structural Behaviour of "Built-up" Stress Laminated Timber Bridge Decks.* Madison : National Conference on Wood Transportation Structures. U.S. Department of Agriculture, Forest Service, Forest Products Laboratory, 1996.
193. **Crews, K.** *Development of limit states design (LRFE) methods for stress laminated timber "cellular" bridge decks.* Whistler : World Conference on Timber Engineering - WCTE, 2000.
194. —. *Development and application of stress laminated timber bridge decks in Australia.* NZ Timber Design Journal : Issue 2 Volume 10, 2001.
195. —. *An Overview of the Development of Stress Laminated Timber Bridges in Australia.* 2002.
196. —. *Recommended procedures for determination of distribution widths in the design of stress laminated timber plate decks.* Florence : International Council for Research and Innovation in Building and Construction - W18 - Timber Structures, 2006.
197. —. *An Overview of the Development of Stress Laminated Cellular Timber Bridge decks for Short to Medium Span Applications in Australia.*
198. **Cheung, A.B., Lindquist, M. and Calil, C.** *Structural reliability of Stress-Laminated Timber Bridges.* Miyazaki : World Conference on Timber Engineering - WCTE, 2008.
199. **Karlsson, K., Crocetti, R. and Kliger, R.** *Mechanical properties of stress laminated timber decks - experimental study.* Dübendorf - Zürich : International Council for Research and Innovation in Building and Construction - W18 - Timber Structures, 2009.
200. —. *Ultimate limit state load test of stress-laminated-timber deck.* Trentino : World Conference on Timber Engineering, 2010.
201. **Ekholm, K.** *Performance of Stress-Laminated-Timber Bridge Decks.* Gothenburg : Chalmers University of Technology - Doctoral Thesis, 2013.
202. **Ekholm, K. and Kliger, I.R.** *Effect of vertical interlaminar shear slip and butt joints in narrow stress-laminated-timber bridge decks.* Engineering Structures : 72 (2014) 161-170, 2014.
203. **EN1995-2:2004.** *Eurocode 5: Design of timber structures - Part 2: Bridges.* 2004.
204. **Dagher, H.J.** *Advanced engineering wood composites for use in civil engineering.* In "Advanced civil infrastructure materials" : Wu, H.C. (Ed.). Woodhead Publishing Limited, Cambridge, 2006.

205. **Leckie, John.** *Steel and other materials three-part series. Part two: steel and wood.* Advantage Steel : No. 30, Winter, 2007.
206. **Larsen, H.J. and Munch-Andersen, J.** *CIB-W18 Timber Structures - A review of meetings 1 - 43. Part 3: Structures and structural members* : Danish Timber Information, 2011.
207. **SchluderArchitektur ZT GmbH.** *Möglichkeit eines vielgeschossigen Holzbaus im urbanen Raum mit Zielrichtung auf acht oder mehr Geschosse.* Wien : Bundesministerium für Verkehr, Innovation und Technologie, 2008.
208. **Tavoussi, K., Winter, W. and Pixner, T.** *Das erdbebensichere Holzhaus - Forschungsbericht.* Bauingenieur, 85 : p. 129 - 134, 2010.
209. **Hsu, T., et al.** *Study on performance of timber-steel composite beams with different shapes of steel components.* Vienna : World Conference on Timber Engineering - WCTE, 2016.
210. **Eisert, D., Noack, T. and Ruth, J.** *Bewertungsstrategien für hybride Tragwerke.* Weimar : Beiträge zum 37. Forschungskolloquium des DAfStb Bauhaus-Universität Weimar, 1999.
211. **Natterer, J.K.** *A way to sustainable architecture by new technologies for engineered timber structures.* Lahti : World Conference on Timber Engineering - WCTE, 2004.
212. **Kovacic, I.** *Life cycle analysis. Life cycle assessment and life cycle costing. (Class presentations).* Vienna : Industriebau und interdisziplinäre Bauplanung, 2013.
213. **European Union Council.** *EU Council Presidency Conclusions 7224 / 1 / 07.*
214. **Kuklík, P. (Ed.).** *Handbook 1 - Timber Structures.* TEMTIS : Leonardo da Vinci Pilot Projects "Educational Materials for Designing and Testing of Timber Structures- TEMTIS, 2008.
215. **Welser-Profile-GmbH.** *www.welser.com.* Accessed in August 2016.
216. **Stam.** *www.stam.it.* Accessed in December 2016.
217. **Göecke-Umformtechnik.** *www.goecke-umformtechnik.de.* Accessed in August 2016.
218. **OiB-Richtlinie2.** *Brandschutz.* OiB : Österreichisches Institut für Bautechnik, 2011.
219. **CTE.** *Documento Básico SI. Seguridad en caso de incendio.* CTE : Código Técnico de la Edificación, 2009.
220. **EN1993-1-3:2006.** *Eurocode 3: Design of steel structures. Part 1 - 3: General rules - Supplementary rules for cold-formed members and sheeting.* 2009.
221. **Izumi, B., et al.** *Fire performance of timber-cold formed thin steel plate composite beam.* Vienna : World Conference on Timber Engineering - WCTE, 2016.
222. **Timoshenko, S.** *Strength of Materials. Part I. Elementary Theory and Problems.* New York : D. van Nostrand Company, Inc., 1940.
223. **EN1990:2002.** *Eurocode - Basis of structural design.* 2002.

224. **EN1991-1-1.** *Eurocode 1: Actions on structures - Part 1 - 1: General actions - Densities, self-weight, imposed loads for buildings.* 2002.
225. **Blanco, E., Cervera, M. and Suárez, B.** *Análisis matricial de estructuras.* Barcelona : Centro Internacional de Métodos Numéricos en Ingeniería, 2015.
226. **IBO.** *IBO - Richtwerte für Baumaterialien.* Wien : Österreichisches Institut für Bauen und Ökologie GmbH, 2013.
227. **Argüelles, R., et al.** *Estructuras de madera. Bases de cálculo.* Madrid : AITIM, 2013.
228. **Tavoussi, K., et al.** *Semi-rigid joints of timber-steel hybrid beams for multi-storey buildings.* Vienna : World Conference on Timber Engineering - WCTE, 2016.
229. **EN1993-1-5:2006.** *Eurocode 3: Design of steel structures - Part 1-5: General rules - Plated structural elements.* 2006.
230. **EN408:2010.** *Timber structures - Structural timber and glued laminated timber - Determination of some physical and mechanical properties.* 2010.
231. **EN384:2010.** *Structural timber - Determination of characteristic values of mechanical properties and density.* 2010.
232. **Ravenshorst, G. and van de Kuilen, J.** *Relationships between local, global and dynamic modulus of elasticity for soft- and hardwoods.* Dubendorf : International Council for Research and Innovation in Building and Construction - Working Commission W18 - Timber Structures, 2009.
233. **EN13183-2:2002.** *Moisture content of a piece of sawn timber - Part 2: Estimation by electrical resistance method.* 2002.
234. **Kliger, R.** *Determination of creep data for the component parts of stressed-skin panels.* Florence : International Council for Building Research Studies and Documentation - Working Commission W18 - Timber Structures, 1986.
235. —. *Deformation modification factors for calculating built-up wood-based structures.* Oxford : International Council for Building Research Studies and Documentation - Working Commission W18 - Timber Structures, 1991.
236. **prEN1156.** *Wood-based panels - Determination of duration of load and creep factors.* 2011.
237. **Winter, W., et al.** *Development of prefabricated timber-steel-concrete ribbed decks.* Vienna : World Conference on Timber Engineering - WCTE, 2016.
238. **Wolfsgruber, Josef.** *Untersuchung der Prinzipien des Brandverhaltens von Holz-Stahl-Verbundkonstruktionen.* Wien : Technische Universität Wien - Doctoral Thesis, 2011.
239. **Oka, Hideo.** *A study on self-charring-stop of glued laminate timber made of Japanese cedar installing mortar pieces.* Miyazaki : World Conference on Timber Engineering, 2008.

240. **Oka, H., et al.** *A study on self-charring-stop of glued laminate timber made of japanese cedar installing mortar pieces*. Tokyo : Bulletin of Japan Association for Fire Science and Engineering Vol. 58. No.1, 2008.
241. **Kaufmann, H. (Ed.).** *Bauen mit Holz: Wege in die Zukunft*. München : Prestel, 2011.
242. **Green, M., et al.** *The Case for Tall Wood Buildings*. Vancouver : Canadian Wood Council, 2012.
243. **Skidmore, Owings & Merrill, LLP.** *Timber Tower Research Project*. Chicago : Softwood Lumber Board, 2013.
244. **HoHo.** *www.hoho-wien.at*. Accessed August 2016.
245. **proHolz Austria (Ed.).** *Vielgeschossiger Holzbau im urbanen Raum. Dokumentation Forschungsprojekt 8+*. Wien : Zuschnitt Attachment Dezember, 2008.
246. **Winter, Wolfgang, et al.** *Timber-steel hybrid beams for multi-storey buildings*. Auckland : WCTE, 2012.
247. **Gehri, Ernst.** *Grundlagen zum Materialverhalten*. Tragende Verbundkonstruktionen mit Holz. Zürich : SAH, 1999.
248. **Smedley, D., Alam, P. and Ansell, M.P.** *George Street, St. Albans, UK - a case study in the repair of historic timber structures using bonded-in pultruded plates*. Miyazaki : World Conference on Timber Engineering - WCTE, 2008.
249. **Khelifa, M.** *Numerical analysis of damage evolution of 3D timber-steel hybrid beams in bending*. Vienna : World Conference on Timber Engineering - WCTE, 2016.
250. **Carradine, D.M., Newcombe, M.P. and Buchanan, A.H.** *Using screws for structural applications in laminated veneer lumber*. Dübendorf - Zürich : International Council for Research and Innovation in Building and Construction - W18 - Timber Structures, 2009.
251. **Mang, H. and Hofstetter, G.** *Festigkeitslehre*. Wien : Springer, 2000.
252. **WK-Blechtechnik.** *www.pulverbeschichtung.at*. Accessed in August 2016.

LIST OF FIGURES

Figure 1: Tensile strength distribution of structural timber assigned to three grades a, b, c (5) ...	5
Figure 2: Variability, middle and characteristic values of timber, glulam and FRP reinforced glulam (8)	6
Figure 3: Tension-Strain diagrams of different materials. Steel in blue and timber in yellow. (15)	9
Figure 4: Damage resulting from a large building fire. Steel members yielded by the heat are supported by a charred wood beam (19).	12
Figure 5: Evolution of standard steel plates prices from 2001 to 2016 (25).	16
Figure 6: Evolution of spruce and fir sawn timber in Austria from 1995 to 2016 (26)	16
Figure 7: Classification of timber-based hybrid members (32).....	20
Figure 8: Systematic classification of timber-steel combination in beams.	21
Figure 9: Bonded steel strip specimen (33) in Dorey & Cheng (42).....	22
Figure 10: Different strengthening schemes and a reference for creep tests specimens (39).....	23
Figure 11: Distribution of strain, stress and forces in the cross section of a strengthened beam with high steel strength chords (41).	23
Figure 12: Steel cross-section reinforcement in timber sections of 180x200 mm and 130x150 mm (45).	24
Figure 13: Image of hybrid timber members (51).	25
Figure 14: Test specimens type A (52)	25
Figure 15: Geometric arrangement of Dziuba's experiments cited in (68).....	26
Figure 16: Typical beam cross sections in Bulleit (63).....	27
Figure 17: Prototypes of HTTB (left) and tension zone reinforcement with steel and LVL (right) (67)	27
Figure 18: Creep deformation of glulam beams reinforced with steel bars. Specimens: L1- pure glulam beam; L8- 1Ø6 in the compression area; L9 - 1Ø6 in the tensile area; L10 - 1Ø8 in the tensile area (66).	28
Figure 19: Cross sectional arrangement of beams tested by Sliker (69) with laminates of aluminium (in blue) as timber reinforcements cited by Alam (68).	29
Figure 20: Rebar-glulam beam by Gardner (72) cited by Dorey and Cheng (42).....	30
Figure 21: Steel reinforcement systems, Tasbeam® (left) and Aralam® (right) in Schober et al (74)	30
Figure 22: Interface and jointing bars for the moment resisting joints of the RGTSB system (77)	31
Figure 23: The first prototype building, "Samurai", utilizing glulam timber reinforced using deformed steel bars and epoxy resin adhesives (RGTSB)(75).....	31
Figure 24: Test specimens with plate reinforcement by Nielsen (80).....	32
Figure 25: Cross section of column reinforced with steel plates (81).....	33
Figure 26: Wooden laminated beam joined with nail-plates (82)	34
Figure 27: Punched metal plate reinforced glulam beams (83).....	34
Figure 28: Reinforcement configuration with 4x(4mm x 30 mm) steel plates (85).....	35
Figure 29: Tension face reinforcement specimens (68)	36
Figure 30: Geometric parameters and cross-section of reinforced beams (87).....	36
Figure 31: Vertically laminated steel-timber composite beam by Borgin (33). The steel reinforcement comprises 5% of the total cross sectional area. Cited in (68)	37
Figure 32: Geometric arrangement of tests by Jones (88) cited in Alam (68)	38
Figure 33: Compression face reinforcements for the reparation of beams by Alam (68)	38

Figure 34: Out of plane buckling of steel webbed joist with centre restraint (91)	39
Figure 35: TecBeam® (93)	40
Figure 36: Posi-Joist® (94)	40
Figure 37: Nail Web® (92)	40
Figure 38: Vertically laminated steel-timber composite beams by Borgin (33). The steel reinforcement comprises 5% of the total cross sectional area. Cited in Alam (68)	41
Figure 39: The “Steelam” beam form Hoyle (95) is composed from two plates with protruding toothed connectors mechanically sandwiched between two timber members. Cited in Alam (68)	42
Figure 40: Shear fracture of Japanese cedar glulam beam reinforced with steel plates (104)	42
Figure 41: Composite beam reinforcement configurations by Alam et al (106).....	42
Figure 42: Reinforcement configurations studied by Kliger et al (40); (b) and (c)steel, (d) and (e) CFRP	43
Figure 43: Steel-timber joist configurations using T and C section flanges (107).....	43
Figure 44: Reinforced section studied by Negrao et al (108).....	43
Figure 45: Image of the Bouchu Bridge(101) and reinforced beams tested before its construction (103)	44
Figure 46: Vertical laminates of aluminium (in blue) tested by Sliker (69), cited in Alam (68) ..	45
Figure 47: Flitch beam by Kumar et al (110) cited in Dorey & Cheng (42).....	46
Figure 48: “Flitch” beam arrangement with two vertical steel plates and three timber members connected mechanically using nails by Stern & Kumar (111) cited in Alam (68).....	46
Figure 49: Flitch beam arrangement using 18 gage steel by Coleman & Hurst (71), cited in Alam (68)	46
Figure 50: Schematic cross-section of a beam pair showing the arrangement of steel plates and nailing direction (117).....	47
Figure 51: One-box test model (plate) of timber-steel hybrid deck bridge (122)	47
Figure 52: Section of the hanging roof of the Nagano Olympic Memorial Arena (115)	47
Figure 53: Visualization of the Rupert Station in Vancouver (116)	48
Figure 54: Roof system of the Saitama Prefectural Budokan (32).....	48
Figure 55: Kanazawa M Building (2005). Façade, interior view and cross section of the floor beams (120).....	48
Figure 56: “Shear spike” concept by Radford et al (125) cited in Alam (68)	49
Figure 57: Timber-steel hybrid diaphragm by He et al (132)	51
Figure 58: Geometrical outline and four-point bending tests on steel-timber composite beams (136)	52
Figure 59: Dimensions of the cross section of the version I of timber-steel composite plates (138)	52
Figure 60: The concept of composite steel-wood bridge deck (130)	52
Figure 61: Hybrid beam consisting of hollow timber section and inner aluminium or steel pipe (139)	53
Figure 62: Elements of the plywood-steel panel composite (140)	54
Figure 63: “Wood Square” building in Japan (120).....	55
Figure 64: Horizontal lamination of the tensile face of a wooden beam using pre-stressed steel by Peterson (148) cited in Alam (68)	56
Figure 65: Reinforcing anchor bracket by Turkovsky et al (146) cited in Dorey & Cheng (42) ..	56
Figure 66: Proposal of pre-stressed beams by Pletz & de Melo Moura (147)	57
Figure 67: View of a beam reinforced with steel cables showing bearing plates (150).....	59
Figure 68: Halves of tested beam with grooves for steel bars (73)	59

Figure 69: Specimens for adhesion tests (left) and post-tensioned beams (right) (154)	60
Figure 70: Force-multiplying device (left) and its 3D-printer prototype by Estévez Cimadevila et al (162)	60
Figure 71: Longitudinal section of a timber-box beam with straight post-tensioning (left) and draped post-tensioning tendons (right) (172)	60
Figure 72: Pedestrian bridge in Murau, Austria (190)	61
Figure 73: Sketch of the structural solution for the Swiss Re Lobby Roof (190)	61
Figure 74: Several cross sections of the Benau footbridge (190)	61
Figure 75: Expan building in Christchurch (188)	62
Figure 76: lateral view of the post-tensioned frame (left) and draped tendon detailing (right) of the Massey University in Wellington (189)	62
Figure 77: Exterior and frame (left) (183) and view of the post-tensioned frame (right) of the Merrit Building in Christchurch (189)	62
Figure 78: View of the post-tensioned beams of the Diocesan School for girls aquatic centre (189)	63
Figure 79: Trimble Navigation Offices in Christchurch (188)	63
Figure 80: Visualization of the first timber storey of the ETH House of natural Resources. Post-tensioned timber frames made of ash and composite floor of beech-LVL and concrete (156). 63	63
Figure 81: Stress-laminated sawn lumber deck (191)	64
Figure 82: Section detail of the cellular deck utilising Radiata pine flanges and pine LVL webs (195)	65
Figure 83: Typical stress-laminated deck (198)	65
Figure 84: One-box test model with lateral perforated steel plates (122)	65
Figure 85: Summary of amount of existing research and number of built examples. Red: combinations with more than ten references in the state-of-the-art review. Green: number of already built examples using the respective technique.	66
Figure 86: The potential of combination of steel and timber	70
Figure 87: Hybrid construction combining timber and steel beams (207)	71
Figure 88: Sketch of the detail connection between timber-steel beams and supports (207)	72
Figure 89: Anchoring system (left) and test set-up for wall and anchoring system (right) (208)	72
Figure 90: Example of a reinforced timber beam with steel plates	74
Figure 91: Example of a composite timber-steel beam with nailed steel plates	74
Figure 92: Example of a timber- steel hybrid beam	74
Figure 93: Bad hybrid design for bending stiffness. Comparison of glulam-glulam hybrid and composite options	78
Figure 94: Good hybrid design for bending stiffness. Comparison of two glulam-glulam hybrid and composite options	79
Figure 95: System effects diagram following Natterer (211)	79
Figure 96: Frequency distribution of the ultimate strength of glulam and structural timber following P. Kuklík et al (214)	80
Figure 97: System strength factor k_{sys} , for laminated deck plates of solid timber or glued laminated members. From Eurocode 5 (6)	81
Figure 98: Hybrid beam cross-section and detail of cold-formed steel elements	84
Figure 99: Steel plates being deformed between rollers in a continuous process (215)	85
Figure 100: Example of complex cold-formed steel profile manufactured with roll-forming (215)	85
Figure 101: Corrugated sheet steel profile manufactured with roll-forming (216)	85
Figure 102: Image of a steel bending press (217)	86

Figure 103: Image of a big-size cold-formed profile (217).....	86
Figure 104: Production (left) of cold-formed steel profiles manufactured with bending presses (right) (217).....	86
Figure 105: Example of symmetric timber-steel hybrid beam.....	87
Figure 106: Example of asymmetric timber-steel hybrid beam.....	87
Figure 107: Basic structural concept of a timber-steel hybrid beam.....	88
Figure 108: Cross-section design. Step 01 – Structural depth allowable.....	90
Figure 109: Representation of the thermal decomposition of timber by Dinwoodie (12).....	92
Figure 110: Temperature profile for $br > 2 a_0$ following P. Kuklik et al (214).....	92
Figure 111: Reduction factors for stress-strain of carbon steel at elevated temperatures. Eurocode 3 (16).....	93
Figure 112: Reduction factors for carbon steel for stress-strain relationship of cold formed and hot rolled class 4 steel sections at elevated temperatures. Eurocode 3(220).....	93
Figure 113: Temperatures through the cross section of a hybrid beam in function of charring depths.....	94
Figure 114: Definition of residual cross-section and effective cross-section, following Eurocode (18).....	95
Figure 115: Cross-section design. Step 02 – Fire protection strategy.....	96
Figure 116: Diagram of a bending beam by Timoshenko (222).....	97
Figure 117: Timber-steel cross-section and strain (10-3) and stress diagrams.....	98
Figure 118: Stress-strain (·10-3) diagrams of different steel and glulam grades in elastic range.....	99
Figure 119: Structural depth ratio $R=d(t)/d(s)$ for a asymmetric timber-steel hybrid beam.....	99
Figure 120: Strain and stress diagrams for two equivalent symmetric (top) and asymmetric (bottom) timber-steel hybrid cross-sections.....	100
Figure 121: Cross-section design. Step 03 – Combination of materials. Structural depth ratios.....	105
Figure 122: Cross-section design. Step 04 – Total bending stiffness required.....	106
Figure 123: Examples of reduction factor η_{fi} versus load ratio $Q_{k,1} / G_k$	107
Figure 124: Hybrid beam type G before and after 60 minutes fire.....	108
Figure 125: Hybrid beam type H before and after 60 minutes fire.....	108
Figure 126: Hybrid beam type H before and after 60 minutes fire.....	109
Figure 127: Hybrid beam type H before and after 60 minutes fire.....	109
Figure 128: Cross-section design. Step 05 – Balance of bending stiffness. Fire situation.....	110
Figure 129: Influence of the position of grooves for the distribution of shear stresses.....	110
Figure 130: Cross-section design. Step 06 – Verification of shear capacity.....	111
Figure 131: Comparative creeping deflection diagrams of steel, timber and hybrid beams.	112
Figure 132: Initial and final strain and stress diagrams for a timber steel hybrid beam of glulam GL28c and steel S275. Case Study A; Structural depth ratio 1,37; Initial bending stiffness balance 50%-50%.....	116
Figure 133: Initial and final strain and stress diagrams for a timber steel hybrid beam of glulam GL28c and steel S235 allowing partial plasticization. Structural depth ratio 1,28. Initial bending stiffness balance 50%-50%.....	121
Figure 134: Cross-section design. Step 07 – Long term performance. Structural depth ratios.....	121
Figure 135: Summary – cross-section design in seven steps.....	122
Figure 136: Calculation model and positioning of loads for four point bending test with 6 meters span.....	123
Figure 137: Straight bar considering shear flexibility (225).....	123
Figure 138: Simply supported single span beam with uniformly distributed load.....	134

Figure 139: Single span beam with clamped support ends and uniformly distributed load.....	134
Figure 140: Calculation model for a timber-steel hybrid continuous beam with pinned outer supports	135
Figure 141: Calculation model for a timber-steel hybrid continuous beam with fixed outer supports	135
Figure 142: Calculation model for a timber-steel hybrid continuous beam with fixed (steel) and pinned (timber) outer supports	136
Figure 143: Calculation model for a timber-steel hybrid beams inside a structural frame	136
Figure 144: Maximum bending moments – Hybrid Type G, continuous beam with pinned outer supports. $M_s/M_t=1,452$	137
Figure 145: Maximum bending moments – Hybrid Type G, continuous beam with fixed outer supports. $M_s/M_t=1,533$	137
Figure 146: Maximum bending moments – Hybrid Type G, continuous beam with fixed (steel) and pinned (timber) outer supports. $M_s/M_t=1,421$	137
Figure 147: Maximum bending moments – Hybrid Type G, beams inside a structural frame. $M_s/M_t=1,533$	137
Figure 148: Calculation model and positioning of loads for four point bending test with 6 meters span	142
Figure 149: Dimensions of flanges of hybrid beams Type D (left-first testing series) and Type J (right-second testing series)	143
Figure 150: Definition of effective width parameters following EC3 (229).....	143
Figure 151: Type D hybrid beam during assembling	146
Figure 152: Delivery of timber components. First testing series	147
Figure 153: Delivery of steel components, cold formed steel profiles (left) and welded elements (right).....	147
Figure 154: Glulam and steel components for beams before assembling. Beams Type A in the middle of the timber components for the correspondent hybrid beam.....	147
Figure 155: Image of specimens Type C (left: welded steel) and Type D (right: cold-formed steel) from the first testing series	148
Figure 156: Rupture due to a big knot in the specimen B02	149
Figure 157: Four point bending test arrangement	149
Figure 158: Installations of measuring devices and measuring of temperature and timber humidity content.....	150
Figure 159: Characteristics of specimens Type A.....	151
Figure 160: Specimens B02 (left) and assembling of hybrid beams Type B.....	152
Figure 161: Characteristics specimens Type B	152
Figure 162: Results. Stiffness in elastic range for the specimens B01 and B02. Red: calculation - Blue: test.....	153
Figure 163: Load deformation graphics tests B01-B02	154
Figure 164: Specimen C02 after testing (left) and disassembled (right).....	154
Figure 165: Characteristics specimen C01	155
Figure 166: Characteristics specimens C02	155
Figure 167: Results. Stiffness in elastic range for the specimens C01 and C02. Red: calculation - Blue: test.....	156
Figure 168: Load deformation graphics tests C01-C02	157
Figure 169: Assembling of specimen D02 (left) and finished cross section (right).....	157
Figure 170: Characteristics specimens D01 and D03	158
Figure 171: Characteristics specimens D02 and D04	158

Figure 172: Results. Stiffness in elastic range for the specimens D01 to D04. Red: calculation - Blue: test.....	159
Figure 173: Load deformation graphics tests D01-D04.....	160
Figure 174: Hybrid beam D01 after rupture.....	160
Figure 175: Assembling of specimen CLT- Hybrid F02	161
Figure 176: Testing of CLT- Hybrid F01.....	161
Figure 177: Characteristics of specimen CLT01.....	162
Figure 178: Characteristics of specimen E01.....	162
Figure 179: Characteristics of specimen E02.....	163
Figure 180: Results. Stiffness in elastic range for the specimens E01 to E02. Red: calculation - Blue: test.....	163
Figure 181: Load deformation graphics tests E01-E04.....	164
Figure 182: Rupture sequence of a hybrid beam.....	166
Figure 183: Image of specimen D01 after testing and opening of the section	167
Figure 184: Image of specimen D01 after showing local buckling beginning at the upper steel flange and extending to web.....	167
Figure 185: Failure of compression area in specimen Type F	167
Figure 186: Timber components for beams type G (left) and 8 m and 6 m long steel components (right).....	169
Figure 187: Preparation of the supporting details of specimen H04	170
Figure 188: Four point bending test arrangement	170
Figure 189: Four point bending test of steel and glulam components of hybrid beam Type H on their own.....	171
Figure 190: Four point bending test of hybrid Type H	172
Figure 191: Image of specimens type G from the second testing series, with support conditions “Timber(T)” (left) and “Timber+Steel (T+S)” (right)	173
Figure 192: Frontal (left) and lateral (right) images of specimen G05 from the second series, with support conditions “Steel (S)”	173
Figure 193: Filling with steel plates under the loading heads between the steel flange and timber in the case of the supporting condition “steel”	174
Figure 194: Example of faulty finger-joint in the specimen G05	174
Figure 195: Cross-section parameters of hybrid beams Type G	175
Figure 196: Results. Stiffness in elastic range for the specimens G01 to G06. Red: calculation - Blue: test.....	176
Figure 197: Load deformation graphics tests G01-G03	177
Figure 198: Load deformation graphics tests G04-G06.....	178
Figure 199: Cross-section parameters of hybrid beams Type H.....	179
Figure 200: Results. Stiffness in elastic range for the specimens H01 to H06. Red: calculation - Blue: test.....	180
Figure 201: Load deformation graphics tests H01-H03	181
Figure 202: Load deformation graphics tests H04-H06.....	182
Figure 203: Assembling of 8 metres long specimen I02 (left) and ready for testing (right).....	183
Figure 204: Cross-section parameters of hybrid beams Type I.....	184
Figure 205: Results. Stiffness in elastic range for the specimens I01 to I02. Red: calculation - Blue: test.....	184
Figure 206: Load deformation graphics tests I01-I02	185
Figure 207: Support of specimen I01 (left) and shear rupture of the same specimen (right)....	185
Figure 208: Assembling of specimen J02	186

Figure 209: Cross-section parameters of hybrid beams Type J	187
Figure 210: Results. Stiffness in elastic range for the specimens J01 to J02. Red: calculation - Blue: test.....	187
Figure 211: Load deformation graphics tests J01-J02.....	188
Figure 212: predicted timber ruptures of specimen J02 due to faulty finger-joints	188
Figure 213: Rupture pattern of asymmetric timber-steel hybrid beams	189
Figure 214: Image of specimen type I showing local buckling of steel flanges after rupture of timber components	190
Figure 215: Successive timber ruptures in specimen I02.....	191
Figure 216: Hybrid beam H1 after test.....	196
Figure 217: Comparative creeping deflection diagrams of steel, timber and hybrid beams.	197
Figure 218: Conceptual design of the test for a hybrid beam (left) and a timber comparison beam (right).....	200
Figure 219: Vertical connector through glulam and steel for the creeping hybrid beams.	201
Figure 220: Timber specimens to be tested and classified regarding their Young Modulus values.....	203
Figure 221: Three point bending tests for selecting the timber specimens regarding their Young Modulus.....	203
Figure 222: Comparison of the central and bottom face of the beams K01 (rejected due to presence of knots in the middle part and in the proximity to the connecting holes) and K02 (accepted)	204
Figure 223: Image where the warping of the specimen K06 can be observed.....	204
Figure 224: Preparation of the test set-up for the long-term four point bending test.....	206
Figure 225: Test set-up for the long-term four point bending test	206
Figure 226: Test set-up and photos with a hybrid beam (left) and a timber comparison beam (right).....	207
Figure 227: Image of the test set-up	207
Figure 228: Image of the measuring points.....	208
Figure 229: Recording data machine ALMEMO 5690-2	208
Figure 230: Results of the creeping test after one year	209
Figure 231: Results of the creeping test after one year. Comparison of pair of beams.....	210
Figure 232: Determination of the creeping factor k_c for ten years using testing data (236).....	212
Figure 233: Calculation of the creeping factor k_c for the pair of beams K10 (Glulam) and K02 (Hybrid).....	212
Figure 234: Creeping factor k_c obtained from test results. Middle value of the two specimens tested	212
Figure 235: Test results and theory curves of absolute creep for pure glulam and hybrid beams	213
Figure 236: Test results and theory curves of relative creep for pure glulam and hybrid beams	214
Figure 237: Example of the moment transmission mechanism for knots between timber-steel hybrid beams and supports (left) and testing of a timber-steel hybrid joint (right) (228).....	216
Figure 238: Visualization of a hybrid timber-steel-concrete hybrid ribbed deck prefabricated slab (237).....	217
Figure 239: Example of timber-steel hybrid frame system	217
Figure 240: Timber-based multi-storey projects. From left to right: 8+(245), Life Cycle Tower(241), The Case for Tall Wood Buildings (242), Timber Tower Research Project (243), HoHo Wien (244).....	219

LIST OF TABLES

Table 1: Specific performance relative to timber (22)	13
Table 2: Specific performance relative to timber a $k_{mod} = 0,8$ and material security factors γ_M	14
Table 3: The potential of combination of timber and steel in beams.	19
Table 4: Part of the timber-steel specimens reported by Isoda et al (32)	23
Table 5: Values of β_n in function of type of wood and correspondence with structural grading.	95
Table 6: Thickness of protection wood required depending on type of wood and fire duration. 96	
Table 7: Depth ratios calculation for combined glulam; $\gamma_{steel}=1$; $\gamma_{glulam}=1$; $k_{mod}=1$	101
Table 8: Depth ratios calculation for coniferous and deciduous sawn timber; $\gamma_{steel}=1$; $\gamma_{glulam}=1$; $k_{mod}=1$	102
Table 9: Depth ratios calculation for combined glulam; $\gamma_{steel}=1$; $\gamma_{glulam}=1,25$; $k_{mod}=0,8$..	103
Table 10: Depth ratios calculation for coniferous and deciduous sawn timber; $\gamma_{steel}=1$; $\gamma_{timber}=1,3$; $k_{mod}=0,8$	104
Table 11: Case Study A. Depth ratios calculation for combined glulam; $\gamma_{steel}=1$; $\gamma_{glulam}=1,25$; $k_{mod}=0,8$; $k_{def}=0,6$; $\psi_2=1$	118
Table 12: Case Study B. Depth ratios calculation for combined glulam; $\gamma_{steel}=1$; $\gamma_{glulam}=1,25$; $k_{mod}=0,8$; $k_{def}=0,6$; $\psi_2=0,6$	118
Table 13: Case Study A and Case Study B. Depth ratios calculation for sawn timber (softwood)	119
Table 14: Case Study A and Case Study B. Depth ratios calculation for sawn timber (hardwood)	120
Table 15: Study cases for the evaluation of the single span hybrid beams performance	125
Table 16: Comparison between hybrid, steel and glulam performances. Six metres span, total structural depth $L/17$; Category of use A and B1	126
Table 17: Comparison between hybrid, steel and glulam performances. Six metres span, total structural depth $L/17$; Category of use C and D	126
Table 18: Comparison between hybrid, steel and glulam performances. Six metres span, total structural depth $L/20$; Category of use A and B1	127
Table 19: Comparison between hybrid, steel and glulam performances. Six metres span, total structural depth $L/20$; Category of use C and D	127
Table 20: Comparison between hybrid, steel and glulam performances. Eight metres span, total structural depth $L/17$; Category of use A and B1	128
Table 21: Comparison between hybrid, steel and glulam performances. Eight metres span, total structural depth $L/17$; Category of use C and D	128
Table 22: Comparison between hybrid, steel and glulam performances. Eight metres span, total structural depth $L/20$; Category of use A and B1	129
Table 23: Comparison between hybrid, steel and glulam performances. Eight metres span, total structural depth $L/20$; Category of use C and D	129
Table 24: Comparison of kg CO ₂ eq. for equally performing hybrid, steel and glulam beams taking into account a factors of -1,235 kgCO ₂ eq / kg for glulam and +1,188 kg CO ₂ eq / kg for steel	130
Table 25: Ratio of maximum bending moments between and steel and timber M_s/M_t	138
Table 26: Loads for dimensioning of structural elements	141
Table 27: Specimens of the first testing series. The global cross-section dimensions are 160x360 mm for all the specimens.	145

Table 28: Determined global E-Modulus of cross-sections A	151
Table 29: Results tests B01 – B02	153
Table 30: Results and tests C01 – C02.....	156
Table 31: Results tests D01 – D04	159
Table 32: Results Tests E01-E02	164
Table 33: Specimens of the second testing series	168
Table 34: Development of the cross-section geometry	169
Table 35: List of specimens with indication of length of span and support conditions	172
Table 36: Tested E-modulus of timber components and tested moment of inertia of steel elements for hybrid beams Type G	175
Table 37: Results tests G01 – G03	177
Table 38: Results tests G04 – G06	178
Table 39: Tested E-modulus of timber components and tested moment of inertia of steel elements for hybrid beams Type H	179
Table 40: Results tests H01 – H03	181
Table 41: Results tests H04 – H05	182
Table 42: Tested E-modulus of timber components and tested moment of inertia of steel elements for hybrid beams Type I.....	184
Table 43: Results tests I01 – I02	185
Table 44: Tested E-modulus of timber components and tested moment of inertia of steel elements for hybrid beams Type J.....	187
Table 45: Results tests J01 – J02.....	188
Table 46: Summary of test results and statistical evaluation	192
Table 47: Steel prices for the specimens tested – April 2013	194
Table 48: Steel prices for the specimens tested – November 2013.....	194
Table 49: Steel prices for the specimens tested – April 2014	194
Table 50: Cross section properties of hybrid beams for the creeping test.....	202
Table 51: Partial and modification factors	202
Table 52: E-modulus for the selection of glulam beams Type K.....	205
Table 53: Pairs of beams formed for the comparison creeping test	205
Table 54: Loads applied and tension values for the different beams and components	205
Table 55: Results for the pair Glulam K04-Hybrid K11	210
Table 56: Results for the pair Glulam K10-Hybrid K02.....	211
Table 57: Estimated absolute creep values for 1, 10 and 50 years.....	213
Table 58: Estimated relative creep values for 1, 10 and 50 years.....	214
Table 59: Comparison of estimated absolute creep following tests and EC5 methods.....	215
Table 60: Comparison of estimated relative creep following tests and EC5 methods.....	215

Lebenslauf
Felipe Riola Parada

Architekt

Lebenslauf

Felipe Riola Parada

Architekt

Persönliche Angaben

Nachname: Riola Parada
Vorname: Felipe
Nationalität: Spanien
Personalausweis: 32.687.203 V
Geburtsdatum: 10 Juli 1978 (Ferrol - A Coruña; Galicien - Spanien)
Familienstand: Ledig, keine Kinder
Adresse: Goldschlagstrasse 69/6/34 – 1150 Wien - Österreich
Telefonnummer: +43 (0) 664 890 3142
Emailadresse: riola@iti.tuwien.ac.at



Universitäre Ausbildungen:

- | | |
|---|--------------------------|
| -Architekt (Fachrichtung Technologie)
Universität A Coruña. Galicien. Spanien. | A Coruña, Februar 2007 |
| - University Specialist in Design and Calculation of Building Structures
Universität A Coruña. Galicien. Spanien | A Coruña, Oktober 2008 |
| - University Specialist in Design and Calculation of Wood Structures
Universität Santiago de Compostela. Galicien. Spanien. | Santiago, September 2009 |
| - University Expert in Computer-Assisted Advanced Calculation
of Wood Structures
Universität Santiago de Compostela. Galicien. Spanien. | Santiago, Oktober 2010 |

Auszeichnungen

- | | | |
|--|---------------|---------------------|
| - Stiftung Pedro Barrié de la Maza 2010
Grant Programme for Postgraduate Study Abroad | Stipendiat | A Coruña, Juni 2010 |
| - CIS-Madeira Award for the Best Project
of Design and Calculation of Wood Structures | Zweiter Preis | Lugo, Mai 2009 |
| - 2007 ACXT/IDOM International Award for
Architecture Diploma | Annerkennung | Madrid, Jänner 2008 |

Unterricht

- | | |
|--|---------------------|
| - Lehrer: <i>Universitätsassistent am Institut für Architekturwissenschaften</i>
TU Wien. Österreich | Wien, seit 2014 |
| -Lehrer: <i>Master in Structural Wood Engineering</i>
Universität Santiago de Compostela. Galicien. Spanien | Lugo, 2009-2010 |
| - Lehrer: <i>Master in Architecture Rehabilitation</i>
Universität A Coruña. Galicien. Spanien | A Coruña, 2010-2011 |

Artikel und Konferenzen

- | | |
|---|-------------------|
| -World Conference on Timber Engineering 2016
<i>Winter, Tavoussi, Riola Parada, Bradley:</i>
<i>Timber Steel Hybrid Beams for Multi-storey Buildings: Final Report</i>

<i>Riola Parada, Winter, Tavoussi:</i>
<i>Long-term testing of timber-steel hybrid beams</i>

<i>Tavoussi, Winter, Bradley, Riola Parada:</i>
<i>Semi-rigid joints of timber-steel hybrid beams for multi-storey buildings</i>

<i>Winter, Tavoussi, Fadai, Riola Parada, Prašnjak:</i>
<i>Development of prefabricated timber-steel-concrete ribbed decks</i> | Wien, August 2016 |
|---|-------------------|

- PhD Colloquium Munich 2015 München, August 2015
Riola Parada (Invited):
Timber Steel Hybrid Beams for Multi-storey Buildings

- From Knowledge to Innovation. Schweighofer Students Workshop Wien, Juni 2015
Riola Parada (Invited):
Timber-steel hybrid beams for multi-storey buildings:
Design and validation of beams with optimized material properties
thanks to the combination of timber with cold formed steel profiles

in: "Wood Innovation: From Knowledge to Innovation. Schweighofer Students Workshop 2015",
A. Teischinger (Hrg.); Lignovisionen / Universität für Bodenkultur Wien, 30 / Wien (2015), ISSN: 1681-2808.

- World Conference on Timber Engineering 2014 Quebec City, August 2014
Winter, Tavoussi, Pixner, Riola Parada:
Timber Steel Hybrid Beams for Multi-storey Buildings: Design, Calculation, Tests

- Exploring the potential of Hybrid Structures for Sustainable Construction Fribourg, Juni 2014
Tavoussi, Winter, Riola Parada, Pixner:
Timber Steel Hybrid Beams for Multi-storey Buildings:
Design criteria, calculation and tests

- World Conference on Timber Engineering 2012 Auckland, Juli 2012
Winter, Tavoussi, Pixner, Riola Parada:
Timber-steel-hybrid beams for multi-storey buildings

- First Iberian – Latin American Construction with Wood Congress: CIMAD11 Coimbra, Juni 2011
Riola Parada, Guaita Fernández:
Suspension wooden footbridge. Ulla river.

- AITIM Technical Information Bulletin, ISSN 0044-9261; Nummer 265, Jahr 2010 Madrid, Mai/Juni 2010
Riola Parada, Felipe:
Raison d'être of covered wooden footbridges

Beruflicher Werdegang

- als Architekt

Technische Universität Wien	Universitätsassistent	Wien, seit 2014
Desescribir Architekturbüro	Partner	A Coruña, 2007-2010
CreuseCarrasco Architekturbüro.	Mitarbeiter	A Coruña, 1999-2007
Ausgewählte Projekte: <ul style="list-style-type: none">- Fishmarktgebäude und Hafen in Fisterra.- Architekturbürogebäude in A Coruña.- Stiftung Luís Seoane. A Coruña.		Erster Preis. 2007 ENOR Preis. Zweiter Preis. <i>Living with Wood</i> Preis Wettbewerb erster Preis. Erster Preis. 2004 COAG Preis

- als Statiker - Bauingenieur

„Sparkling Science“ Forschungsprojekte	Mitarbeiter	Wien, seit 2012
Projekt 1: „Holzmischbauweise für das verdichtete Bauen im urbanen Raum“ (2012-2015) Projekt 2: „Entwicklung von vorgefertigten Rippendeckensystemen in Hybridverbundbauweise (Holz-Beton-Stahl) für das verdichtete Bauen im urbanen Raum“ (2015-voraussichtlich 2017) Projektleitende Einrichtung: Technische Universität Wien, Institut für Tragwerksplanung und Ingenieurholzbau; o. Univ. Prof. DDI Wolfgang Winter		
PEMADE	Mitarbeiter	Lugo, 2009-2010
2009 begann in die Zusammenarbeit mit PEMADE, „University of Santiago de Compostela Structural Wood Engineering Centre“, hinsichtlich der Entwicklung von statischen Projekten sowie Unterricht.		
Ausgewählte Projekte: <ul style="list-style-type: none">- Holzsteg. Ullafluss in Galicien (Spanien)		Mai 2010
Statiker	Freelance	A Coruña, 2008-2010

EDV

Zeichenprogramme	AutoCAD, CadWork, SketchUp, Photoshop
Berechnung	CypeCAD, Metal 3D, Robot Structural Analysis, RSTAB/RFEM, Ansys, MATLAB
Textverarbeitung/Tabellenkalkulation	Microsoft Office: Microsoft Excel / Microsoft Word / Microsoft Powerpoint

Sprachkenntnisse

Deutsch	_Mündlich und schriftlich	Fortgeschritten	Universität Wien: B2/2 Sehr gut	Dezember 2013
English	_Mündlich und schriftlich	Fortgeschritten	TOEFL iBT: 106/120	September 2010
Spanisch	_Mündlich und schriftlich	Muttersprache		
Galicisch	_Mündlich und schriftlich	Muttersprache		

Wien
Ort

12. Dezember 2016
Datum


Unterschrift